Bacterial adhesion to abiotic surfaces: Atomic force spectroscopy and Monte Carlo simulations

Dissertation
zur Erlangung des Grades
des Doktors der Naturwissenschaften
der Naturwissenschaftlich-Technischen Fakultät II
- Physik und Mechatronik -
der Universität des Saarlandes

von

Nicolas Thewes

Saarbrücken
2016

Tag des Kolloquiums: 29.07.2016

Dekan: Univ.-Prof. Dr.-Ing. G. Frey

Mitglieder des Prüfungsausschusses:

Vorsitzender:	Univ.-Prof. Dr.-Ing. M. Vielhaber
Gutachter:	Univ.-Prof. Dr. rer. nat. K. Jacobs Univ.-Prof. Dr. M. Bischoff Univ.-Prof. Dr. rer. nat. Ch. Ziegler, TU Kaiserslautern
Akademischer Beisitzer:	Dr. Andreas Tschöpe

Kurzzusammenfassung

Ein grundlegendes Verständnis der Adhäsion von Bakterien an abiotischen Substratoberflächen ist von größter Bedeutung für medizinische Belange. Kraftmessungen mit Rasterkraftmikroskopen und Bakteriensonden stellen den modernsten Stand quantitativer Erforschung bakterieller Adhäsion dar. In dieser Arbeit wurde eine einfache und reproduzierbare Methode entwickelt, um Bakteriensonden mit einzelnen Zellen herzustellen. Mit diesen Sonden wurden daraufhin Adhäsionsmechanismen von Bakterien an abiotischen Substratoberflächen untersucht. Um die molekularen Mechanismen der Bakterienadhäsion besser zu verstehen, wurden zudem Monte Carlo Simulationen durchgeführt. Dadurch konnten grundlegende Haftungsmechanismen bestimmt werden: Die Adhäsion von Bakterien beruht auf der Bindung von Zellwandpolymeren, wobei die Stärke der Haftung eines Bakteriums durch die Eigenschaften und die Anzahl der an eine Oberfläche bindenden Polymere bestimmt wird. Zum Beispiel wird die Adhäsion von Bakterien auf hydrophoben Substraten durch thermisch fluktuierende Zellwandproteine hervorgerufen, die in großer Zahl an die Oberfläche binden. Im Gegensatz dazu ist die Adhäsion von Bakterien auf hydrophilen Substraten wesentlich schwächer, aufgrund einer geringeren Anzahl bindender Polymere. Die stark unterschiedliche Adhäsionskraft von Bakterien auf hydrophoben und hydrophilen Oberflächen war die Grundlage der Entwicklung einer neuen Technik zur Messung der Kontaktfläche zwischen Bakterien und Oberflächen.

Abstract

A profound understanding of bacterial adhesion on abiotic substrates is of great importance for health care concerns. Force measurements with an atomic force microscope (AFM) and bacterial probes are the state-of-the art method in quantitative bacterial adhesion research. In this thesis, a simple and reproducible method to produce single bacterial probes was developed and, subsequently, used to investigate bacterial adhesion mechanisms on abiotic surfaces. To deepen the understanding of the molecular mechanisms of bacterial adhesion, Monte Carlo simulations were paired with AFM experiments. By using highly controlled substrates, fundamental mechanisms of bacterial adhesion are revealed: Bacterial adhesion relies on the binding of bacterial surface polymers, and the nature and the amount of bound polymers finally determine the strength of adhesion. On hydrophobic substrates, for instance, bacterial adhesion relies on fast binding of a large number of thermally fluctuating surface proteins. In contrast, on hydrophilic substrates, bacterial adhesion is weak due to a small amount of attaching surface polymers. Thus, the individual adhesion properties of a bacterial cell rely on the interplay of the surface polymers of a cell with a substrate in close proximity. Furthermore, the difference of bacterial adhesion strength to hydrophilic and hydrophobic substrates was utilized to develop a new technique to determine the contact area between a single bacterial cell and surface.

Contents

Abbreviations

AFM atomic force microscope

BSA bovine serum albumin

DLVO Derjaguin-Landau-Verwey-Overbeek

EPS extracellular polymeric substances

Fn fibronectin

FnBP fibronectin binding protein

Fg fibrinogen

H-bond hydrogen bond

IS ionic strength

LapA large adhesion protein A

LPS lipopolysaccharides

MSCRAMM microbial surface components recognizing adhesive matrix molecules

OTS octadecyltrichlorosilane

PBS phosphate-buffered saline

PS polystyrene

QS quorum sensing

RMS root mean square

Si silicon

SMFS single molecule force spectroscopy

TSB tryptic soy broth

vdW van der Waals

WLC worm-like chain

1 Introduction

The growth of bacterial biofilms is an important issue for health care, industrial and environmental concerns [Cos1987, Cos1999, Shi2009a]. The adhesion of bacteria is a crucial step during the formation of biofilms [Hal2004, Kat2004]. Therefore, a comprehensive understanding of the bacterial adhesion process is of elementary importance. In general, the adhesion of bacteria is a highly complex process [Bos1999, Dun2002]. Hence, a simplified system is essential to study the basic mechanisms and interactions governing bacterial adhesion. Considering the effort that is necessary to decrease the complexity of bacterial cells, decreasing the complexity of the corresponding surfaces is a reasonable step. In a bottom-up approach, the knowledge gained in the simplified system may then be applied to more complex i.e. more realistic biological adhesion scenarios.
In this thesis, the adhesion of a non-pathogenic and a pathogenic staphyloccocal species on highly controlled surfaces is investigated using AFM force spectroscopy with bacterial probes. In addition, a theoretical model of the bacterial adhesion process is analyzed using a Monte Carlo algorithm. By combining the experimental and computational approach, fundamental mechanisms governing bacterial adhesion are revealed.

2 Overview and Connectivity

This thesis enfolds four publications published in peer-reviewed journals and additional, yet unpublished manuscripts. The common issue of the presented research is the study of the bacterial adhesion process using bacterial probes in atomic force spectroscopy: *Bacterial cell force spectroscopy.*
In the publication of **Thewes et al. in *Eur. Phys. J. E* 2015** (Addendum I) the bacterial cell force spectroscopy method as well as related problems are described. The study provides the experimental know-how for the later publications by i) detailing the production of bacterial probes, ii) teaching the realization of force spectroscopy experiments with bacterial probes and iii) explaining the way to analyze force/distance curves.
The influence of van der Waals interactions and the hydrophobic interaction on bacterial adhesion is studied in the publication of **Loskill et al. in *Langmuir* 2012** (Addendum II) and in the publication of **Thewes et al. in *Beilstein J. Nanotechnol.* 2014** (Addendum III) using apathogenic *Staphylococcus carnosus*. For the first time, the study in the publication of **Thewes et al. in *Beilstein J. Nanotechnol.* 2014** (Addendum III) describes a long-ranging attraction between a bacterial cell and a hydrophobic substrate upon approach of the bacterium to the substrate. This previously unknown, long-ranging attraction is studied in detail in the publication of **Thewes et al. in *Soft Matter* 2015** (Addendum IV). Besides the experimental approach, simulated force/distance curves that base on a simple model describing bacterial adhesion are introduced in this study.
The fundamental mechanisms that govern the adhesion process of *Staphylococcus aureus* on hydrophilic and hydrophobic substrates are investigated as described in the manuscript in Addendum V. Thereby, genetically modified bacterial cells as well as simulated force/distance curves are applied. Finally, in the manuscript in Addendum VI an AFM-based method is presented that enables for the measurement of the contact radius of cocci bacteria by performing force/distance measurements on tailored substrates that feature a sharp transition between a hydrophilic and a hydrophobic surface section.

The thesis is grouped in five chapters:

- The chapter *Theoretical and Biological Background* introduces the most important biological and theoretical aspects of the thesis.

- The chapter *State of the Art* is a review of previous bacterial adhesion studies with a strong focus on the use of bacterial probes in AFM force spectroscopy.

- The *Material and Methods* chapter describes the substrates and basic techniques used in the thesis at hand. The production of bacterial probes as well as the evaluation of force/distance curves is presented as a shortcut of an attached publication.

- The *Bacterial Adhesion to abiotic Surfaces* chapter presents the results of the thesis as a brief summary of the attached published and unpublished results.

- The chapter *Summary and Outlook* completes the thesis with a recapitulation of the presented work and an illustration of its significance for ongoing and future research projects.

3 Theoretical and Biological Background

3.1 Bacteria

This section introduces the biology of bacterial cells in short. Detailed information about bacteria can be found in numerous text books, e.g. see [Mad1997].

Besides eukaryotes and archaea, bacteria form one out of three domains, the life on earth is classified into. Bacteria are single-celled organisms that do not have a cell nucleus or any other organelles. Their genome is located at a certain region in the cytoplasm, the nucleoid. Throughout evolution, an impressive diversity of bacteria developed. The detailed classification of different bacterial cells relies, nowadays, on molecular biological analysis [Woe1990, Wan2007, Col2009]. However, classic phenotypic methods, like the Gram method, do still have significant relevance [Gra1884, Van1996, Bev2001]: The Gram method classifies bacteria into gram-positive and gram-negative, according to their response to a specific way of staining ('Gram staining') [Gra1884]. The two different colors that appear by a Gram staining, are a result of the two different cell wall structures that bacteria exhibit, see fig. 3.1.

The cell wall of gram-negative bacteria consists of a thin layer of peptidoglycan (PG) followed by an outer membrane. The outer membrane is a phospholipid double layer with embedded proteins and augmented by lipopolysaccharides (LPS). The exact composition of the LPS is strain specific [Mil2005], the fundamental structure, however, is always the same: The lipopolysaccharides share their lipid-group, the lipid A, with the phospholipid double layer. The lipid A is linked to the core-polysaccharide followed by the O-antigen (a second polysaccharide complex). The LPS may be linked to proteins forming a complex outermost lipo-protein layer on gram-negative bacteria.
In contrast, the cell wall of gram-positive bacteria does not have an outer membrane but exhibits a much thicker PG layer as compared to gram-negative cells. Numerous proteinaceous and non-proteinaceous macromolecules are linked covalently or non-covalently to the PG layer of gram-positive bacteria, fulfilling various tasks, such as transport of nutrients or adhesion to (cell) surfaces (adhesins) [Lin2011].
Additionally, gram-negative as well as gram-positive bacteria may express large, usually proteinaceous, surface organelles (e.g. pili or fimbriae) that promote adhesion or provide the cell the ability to move actively.

In this thesis, bacterial adhesion is investigated using two gram-positive bacterial species, *Staphylococcus carnosus* and *Staphylococcus aureus*. While *S. carnosus* is a non-pathogenic bacterium used in meat production [Sch1982], *S. aureus* is an opportunistic pathogen associated with potentially lethal infections [Low1998]. A large number of surface adhesins linked

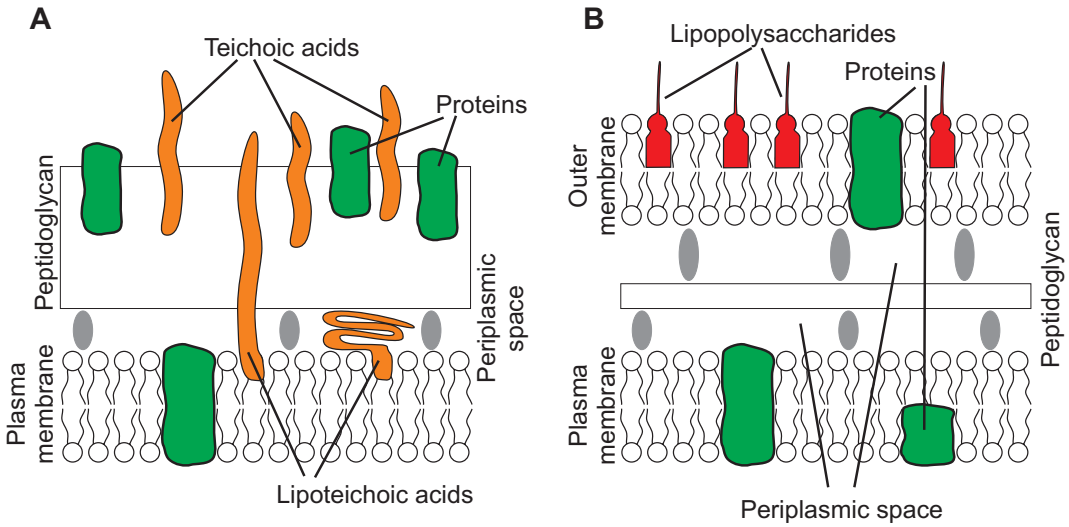

Figure 3.1: Sketch illustrating the cell wall of (A) gram-positive and (B) gram-negative bacteria. Adapted, with permission, from [Los2012a]

to the cell wall of *S. aureus* can be found in literature [Hei2011]. These macromolecules are categorized into three major groups according to their properties [Hei2011]:

- The **covalently-linked proteins** belong to the MSCRAMM (microbial surface components recognizing adhesive matrix molecules) protein family [Cla2006]. At least 20 *S. aureus* genes are known to encode covalently bound surface adhesins, for example the Fibronectin-Binding Proteins A and B (FnBPA and FnBPB) that establish binding to the human extracelluar matrix component fibronectin [Sig1989, Jön1991].

- The **Non-covalently-linked proteins** are bound to the bacterial surface by ionic or hydrophobic interactions (e.g. the autolysin Atl) [Cla2006, Hir2010] or get secreted into the environment to bind back to the bacterium (e.g. the extracellular adherence protein Eap) [Cha2005].

- **Non-proteinaceous adhesins** like the positively charged polysaccharide intercellular adhesin (PIA) that is presumably associated with biofilm formation. As well as the highly negatively charged teichoic acids that are covalently linked to the bacterial cell membrane (lipoteichoic acids) or cell wall (wall teichoic acids) and cause the overall cell charge [Göt2002].

The expression of surface macromolecules depends, in a nontrivial manner, on the growth medium and the bacterial growth phase [Pöh2000, Koh2005, Bec2009, Han2011]. In the case of *S. aureus*, for instance, the MSCRAMM proteins are predominantly expressed in the exponential growth phase, while the expression of secreted proteins increases in stationary phase [Che2004, Dre2011]. In this thesis, bacteria in stationary and exponential growth phase are used for adhesion studies.

Taken as a whole, the bacterial adhesion process is anything but well understood as the range of functions of most bacterial surface adhesins is still largely unknown and as fundamental mechanisms of bacterial adhesion are subject to ongoing research [Lin2011, Agu2015b, Duf2015].

3.2 Relevant forces

3.2.1 Surface forces

There are some standard references concerning the theory of surface forces that have slightly differing thematic priorities [Lec2001, VanOss2006, Isr2011]. This section provides a brief introduction into the field of surface interactions. Thereby, considering the biological background of this thesis, the focus is on the nature of forces in aqueous media.

Steric repulsion

Atoms consist of a core of protons and neutrons as well as an electron shell. Bringing two atoms into close proximity, causes a strong repulsive force, called *steric repulsion*, due to overlapping electron clouds. This repulsion is of quantum mechanical nature and no general equation describing the distance dependency is established. Rather, different empirical equation exist, that incorporate a massive rise in force upon very short distances. An often used potential is the *hard sphere potential* (eq. 3.1) featuring zero force for distances r above a certain threshold σ, reflecting the hard sphere diameter, and infinite repulsion below.

$$w_{steric}(r) = \begin{cases} 0 \text{ if } r \geq \sigma \\ \infty \text{ if } r < \sigma \end{cases} \approx \left(\frac{\sigma}{r}\right)^n \text{ with } n \to \infty \tag{3.1}$$

Another frequently used potential assumes a power-law behavior with an exponent n between 9 and 16 (see eq. 3.2). The *power-law potential* applies as the repulsive part of the common *Lennard-Jones* pair potential $w_{LJ}(r)$, thereby σ denotes the distance where $w_{LJ}(r) = 0$.

$$w_{steric}(r) = \left(\frac{\sigma}{r}\right)^n \text{ with } n \in [9, 16] \tag{3.2}$$

Another force, also called steric repulsion, arises between approaching, polymer covered, surfaces. This force is a consequence of the increasing confinement of the polymers and the consequently decreasing available polymer configurations (see entropic forces in 3.2.2). Theories describing *steric polymer repulsion* are complicated and depend on different parameters like the nature of the surrounding medium (solvent) [Hes1971a, Hes1971b, Vri1976, DeGen1987, Rut1997]. Some approaches present different regimes of exponentially increasing

forces upon approach of two polymer covered surfaces [Dol1974, DeGen1987, Li2007, Isr2011]. Steric polymer interactions may play a role in bacterial adhesion processes, as the surfaces of bacterial cells are covered by a variety of bio-polymers, see section 3.1.

Van der Waals forces

Van der Waals (vdW) forces sum up three related forces arising from the interaction between i) two permanent dipoles (*Keesom interaction*), ii) a permanent dipole and an induced dipole (*Debye interaction*) as well as iii) fluctuating dipoles (*London* or *Dispersion interaction*). For point-like objects (atomes or molecules), all three forces decrease proportional to $\frac{1}{r^6}$, with distance r between the dipols (see eq. 3.3). A generalized approach to vdW forces between molecules, describing all three forces in one theory, was introduced by McLachlan [McL1963c, McL1963a, McL1963b, McL1964]:

$$w_{vdW}(r) = -(C_{keesom} + C_{debye} + C_{london}) \cdot \frac{1}{r^6} = -\frac{C_{vdW}}{r^6} \ . \tag{3.3}$$

Although vdW forces are weak and of short range on a molecular level, their ever-present action generates strong, long-ranging forces on macroscopic scales. Two distinct approaches calculating vdW forces between macroscopic bodies exist:

- The **Hamaker** approach assumes vdW forces to be additive [Ham1937]. Consequently, vdW forces between two bodies calculate by simply summarizing the forces between all atoms or molecules of the two bodies. The problem of this approach is that the assumption of pairwise additivity is not correct [Isr2011].

- To overcome the shortcomings of the Hamaker ansatz, **Lifshitz** introduced a vdW force theory that incorporates macroscopic properties of interacting bodies [Lif1956]. That is, the dielectric functions and the refractive indices.

The medium that surrounds two bodies has major influence on their vdW interactions. This is obvious by imaging that the omnipresent vdW forces act between two interacting bodies, as well as between the bodies and the surrounding medium.
Finally, vdW forces between macroscopic bodies are characterized by equations that depend on the geometries of the interacting bodies and the so called *Hamaker constant*. The Hamaker constant incorporates the chemical and physical nature of the interacting bodies and the surrounding medium. For example, the force between a sphere of material 1 and radius R and a flat surface of material 2 in a medium 3 is given by eq. 3.4.

$$F_{vdW}(r) = -\frac{A_{132}R}{6r^2} \ , \tag{3.4}$$

where A_{132} is the Hamaker constant for material 1 interacting with material 2 through material

3. Lifshitz and Hamaker approach result in the same equations for vdW forces between bodies, the only difference is related to the calculation of the Hamaker constants [Isr2011].
Using a simplified approach based on the Lifshitz theory, the Hamaker constant A_{132} can be written as [Isr2011]:

$$\begin{aligned} A_{132} \approx & \frac{3}{4} k_b T \left(\frac{\epsilon_1 - \epsilon_3}{\epsilon_1 + \epsilon_3} \right) \left(\frac{\epsilon_2 - \epsilon_3}{\epsilon_2 + \epsilon_3} \right) \\ & + \frac{3h\nu_e}{8\sqrt{2}} \frac{(n_1^2 - n_3^2)(n_2^2 - n_3^2)}{(n_1^2 + n_3^2)^{1/2}(n_2^2 + n_3^2)^{1/2}[(n_1^2 + n_3^2)^{1/2} + (n_2^2 + n_3^2)^{1/2}]} \, . \end{aligned} \tag{3.5}$$

With the respective dielectric permittivities ϵ and refractive indices n, the absolute temperature T, the Boltzmann constant k_b. In addition to it, h is the planck constant and ν_e is the main electronic adsorption frequency that is assumed to be equal for all three media. The first summand incorporates the Keesom and Debye contributions, the second includes the dispersion interaction.
Van der Waals forces do exhibit some remarkable properties, see eq. 3.5 and [Isr2011]:

- VdW forces in vacuum are always attractive ($\epsilon_3 = n_3 = 1$).
- VdW forces between two chemically identical objects (Hamaker constant A_{131}) are always attractive, independently of the surrounding medium ($\epsilon_1 = \epsilon_2$ and $n_1 = n_2$).
- There are combinations of materials and surrounding mediums that cause repulsive vdW forces (A_{132} negative). Repulsion occurs if attraction between one body and the surrounding medium is stronger than the attraction between two bodies.
- The distance dependency of vdW forces changes for large distances (above roughly 10 nm) due to the finite propagation speed of electromagnetic fields. This effect of *retardation* causes an increasing decay of vdW forces for large distances.
- Chemically heterogeneous bodies (e.g. biological objects) require the calculation of *effective Hamaker constants*. Different approaches exist, see [Isr1972, Par1973, See2001].

In biological systems, vdW forces do influence, e.g. the adsorption process of proteins on solid substrates as has be shown by ellipsometry [Bel2008] as well as the structure of adsorbed protein films measured by X-ray reflectometry [Häh2012].

Electrostatic forces in liquids: The electrical double layer

Electrostatic interactions in liquid media behave much different compared to simple Coulomb interactions. Surfaces immersed in liquids (e.g. water) exhibit charges due to 'the ionization or dissociation of surface groups' and/or 'the adsorption or binding of ions from solutions'

[Isr2011]. Charged surfaces in liquids attract ions of the opposite charge. These charges are more or less stationary on or close to the surface. The result is the *electrical double layer* with a layer of (weakly) attached ions (*Stern* or *Helmholtz* layer) close to the surface, and a diffusive layer of thermally moving ions further away from the surface. The potential above the Stern layer is accessible in experiments and usually called *Streaming* or *Zeta potential*.
Theoretical descriptions of electrostatic forces in liquids are complex and depend on the types of surfaces and liquids. In general, electrostatical double layer interactions between two bodies decay exponentially and the so-called *Debye length* sets the characteristic length scale.
For example, the electrostatical double layer force between a sphere of radius R and a flat surface, both with similar and constant surface potentials, in electrolyte solution is given by eq. 3.6.

$$F_{DL}(r) = \kappa R Z \exp(-\kappa r) \ , \tag{3.6}$$

where the interaction constant Z (a constant similar to the Hamaker constant) depends in a nontrivial manner on valency and dielectric properties of the solution as well as on the surface potential. The Debye length κ^{-1}, however, depends only on solution properties, i.e. number and valency of ions as well as dielectric permittivity [Isr2011].

A widely used method to study the influence of electrical double layer forces on biophysical processes relies on changing the Debye length by changing the ionic strength of a electrolyte solution [Gra1993, Rot1995]. Thereby, increasing the ionic strength results in a decreased Debye length [Isr2011]. For instance, the adsorption of proteins on solid surfaces was shown to be sensitive to electrical double layer forces [Rot1993, Rot1995].

The DLVO theory

Two bodies in liquid medium interact via van der Waals forces *and* electrostatical double layer forces. Derjaguin and Landau as well as Verwey and Overbeek explained the stability of colloids in solution on the basis of vdW and electrical double layer forces [Der1941b, Ver1947, Ver1948]. Because of that, the combined action of van der Waals and electrostatical double layer force is described by the so-called *DLVO theory*.
For example, the force between a colloid and a surface in solution is given by the sum of eq. 3.4 and eq. 3.6. However, vdW and electrical double layer forces feature fundamental differences: Electrical double layer forces are sensitive to changes in electrolyte concentration (i.e. ionic strength) and pH, yet van der Waals forces are not. Additionally, the different force/distance behavior causes a domination of van der Waals forces at small distances. In the end, the exact treatment of DLVO forces is nontrivial and depends very much on the exact combination of interacting bodies and surrounding conditions [Isr2011].

Hydrogen bonds

Hydrogen atoms that are covalently bound to electronegative atoms, like oxygen or nitrogen, exhibit a high positive charge density because the electron is much closer associated with the electronegative atom. Such hydrogen-containing molecules are able to interact via strong directional coulomb interactions with other electronegative atoms. This type of bonding is named *hydrogen bond* (*H-bond*). The strength of a single hydrogen bond is typically between 5 and $10\,\mathrm{k}_b\mathrm{T}$ [Isr2011]. Liquids that are able to form hydrogen bonds, exhibit an ordering of much larger range compared to non H-bond-forming liquids. This gives rise to additional interactions that are discussed in the next section.

Hydrogen bonds do have major influence on the structure of biological objects, for instance of DNA and proteins. Although, polar amino acids of proteins may form H-bonds on suitable surfaces, the influence of H-bonds on protein adsorption was predicted to be low [Nor1996].

Hydrophobic and hydrophilic interactions

Hydrophobic surfaces are surfaces that are unable to form H-bonds with water, to some extend. As a consequence, the water H-bond network close to hydrophobic surfaces is disturbed and a water depletion zone arises [Mez2006, Mez2010]. The tendency to decrease this zone, in order to increase the energetically favorable water network, causes an attraction between hydrophobic surfaces in water. This attraction is known as *hydrophobic force* [Fra1975, VanOss2006].
The other way around, surfaces that extensively form H-bonds (*hydrophilic* surfaces), tend to separate in water. This *hydrophilic repulsion* is a result of the energetically favorable state, where hydrophilic surfaces are surrounded by water molecules [VanOss2006, Isr2011].
The generalized theory of *acid-base interactions* describes H-bond associated forces. The ability of a material to form H-bonds is expressed by two parameters γ^+ and γ^- that describe the tendency of atoms or surfaces to act as *electron-acceptor* respectively *electron-donor* [VanOss1987, VanOss2006]. Subsequently, different combinations of γ^+ and γ^- parameters of interacting surfaces and mediums result, in the case of water, in hydrophobic attraction or hydrophilic repulsion. Varying degrees of hydrophobicity (hydrophilicity) give rise to attractive (repulsive) forces of different strength. The strength of acid-base interactions between two chemically identical particles 1 in water W may be expressed by the free energy at contact, [VanOss2006]:

$$\begin{aligned} w_{AB} &= -\underbrace{4\sqrt{\gamma_1^+\gamma_1^-}}_{\text{Cohesion of 1}} - \underbrace{4\sqrt{\gamma_W^+\gamma_W^-}}_{\text{Cohesion of water}} + \underbrace{4\sqrt{\gamma_1^+\gamma_W^-}+4\sqrt{\gamma_1^-\gamma_W^+}}_{\text{Adhesion between 1 and water}} \\ &= -4\left(\sqrt{\gamma_1^+}-\sqrt{\gamma_W^+}\right)\left(\sqrt{\gamma_1^-}-\sqrt{\gamma_W^+}\right) \ . \end{aligned} \tag{3.7}$$

Obviously, attraction occurs if the cohesion of water respectively material 1 exceeds the adhesion between both [VanOss2006]. Acid-base interactions in water decay exponentially with

the correlation length of water as characteristic length scale, that is below one nanometer [VanOss2006].

In biological systems, the hydrophobic interaction is of utmost importance. For instance, proteins are able to interact with hydrophobic surfaces via hydrophobic side groups and different studies ruled out a strong influence of the hydrophobic interaction on the adsorption of proteins [Nor1986, Wah1991, Bel2008], as well as on the structure of protein films on solid substrates [Häh2012].

The extended-DLVO theory

Physical phenomena that were not properly explained by classic DLVO theory lead to the generalized description of acid-base interactions [VanOss1986, VanOss1987, VanOss1988, VanOss1990]. The strength of acid-base interactions may exceed classic DLVO forces by orders of magnitude [VanOss1989, Isr2011]. The theory including classic DLVO forces *and* acid-base interactions is called extendend DLVO theory (xDLVO theory) [VanOss1990, VanOss2006]. For example, the total interaction energy between two chemically identical flat plates 1 in a medium 3 can be expressed by the sum of vdW, electrical double layer and acid-base interactions as well as steric repulsion:

$$\begin{aligned} w_{131}^{tot}(l) &= w_{vdW}(l) + w_{Dl}(l) + w_{AB}(l) + w_{steric}(l) \\ &= \frac{-A_{131}}{12\pi l^2} + \left(\frac{\kappa}{2\pi}\right) Z \exp(-\kappa l) + w_{131} \exp(-l/\lambda) + w_{steric}(l) \ . \end{aligned} \tag{3.8}$$

Thereby, l is the distance between the two plates, A and Z are the interaction constants described above. κ^{-1} is the Debye length and λ the correlation length of molecules in the respective medium. w_{131} is a parameter describing the strength of the acid-base interactions and evolves out of eq. 3.7 by inserting the parameters of medium 3 instead of water and taking into account the equilibrium distance between the two plates [VanOss2006]. For a variety of systems, the interaction parameters are accessible experimentally, e.g. via contact angle and streaming-potential measurements. For reasons of shortness, this introduction into xDLVO theory is in simplified terms. For an in depth description of xDLVO theory and related experimental procedures, the reader is referred to the textbooks by Israelachvili and Van Oss [VanOss2006, Isr2011].

In biological systems, theoretical descriptions are much more complicated due to the complex and heterogeneous nature of the interacting objects. Hence, in most biological systems, simple expressions like eq. 3.8 do not exist.

3.2.2 Entropic forces

A fundamental quantity of statistical physics is *entropy*. Entropy links the macroscopic state of a system to its microstates. Given a closed system is in thermodynamic equilibrium, then the probability to find the system in a specific microstate is equal for all microstates. As a consequence, a system tends to be in the macrostate that is represented by most microstates. A common example is the position of a fixed number of ideal gas particles in a box at a given energy. The probability of a state with all particles in one corner and the probability of a particular state where all particles are roughly equally distributed in the box, is the same. However, because much more states with more or less equally distributed particles exist, the state with all particles in one corner will virtually not occur.
Therefore, bringing a system into a macroscopic state that is represented by only few microstates will cause a force that drives the system into a more probable macrostate, i.e. a state that exhibits more available mircostates. If all microstates of the system are equal in terms of energy, this force is not caused by energy minimization. Rather, the force is linked to the maximization of the system's entropy and thus called *entropic force*.
The permanent switching between different microscopic states is caused by the thermal energy of a system. Therefore, the persistent change of a system's state is called *thermal fluctuations*.
Entropic forces are a common phenomenon in polymer physics. For an ideal linear polymer chain (ideal means no correlations between faraway monomers, see section 3.3), the macroscopic state can be characterized by its end-to-end vector [Rub2003]. The microscopic state of the chain is given by realizations of a random walk with a step size corresponding to the bond length. Hence, the most probable macroscopic state of the polymer will be end-to-end vector zero, because most realizations of the random walk (that may be identified as microstates) result in end-to-end vector zero (note, that this does not mean that the most probable end-to-end *distance* is zero). In contrast, it is obvious that a fully elongated macroscopic state has only one realization respectively microstate, that is all monomers in parallel. In consequence, an entropic force tears the polymer chain into coiled states.
For end-to-end vectors with a small but non-zero length, the entropic *restoring* force in a ideal polymer chain is proportional to the elongation, see section 3.3 and [Rub2003]. Hence, the chain behaves like an *entropic spring*. The respective spring constant decreases with number and length of the monomers whereas it increases with temperature (in contrast to Hookean springs, where the restoring force is of energetic origin and decreases with temperature). The influence of the temperature on entropic forces can be understood in terms of thermal fluctuations: At zero temperature, thermal fluctuations are absent and so are entropic forces.
This thesis investigates the adhesion of bacterial cells. Bacterial cells are covered by a variety of polymers. Although these polymers are not ideal, entropic forces influence their conformation.

3.3 Ideal polymers

The theoretical treatment of polymers relies on *ideal polymers*. Ideal polymers assume the absence of long-ranging correlations between monomers. This section provides a brief introduction into the physics of ideal polymers. For in depth information on polymer physics the

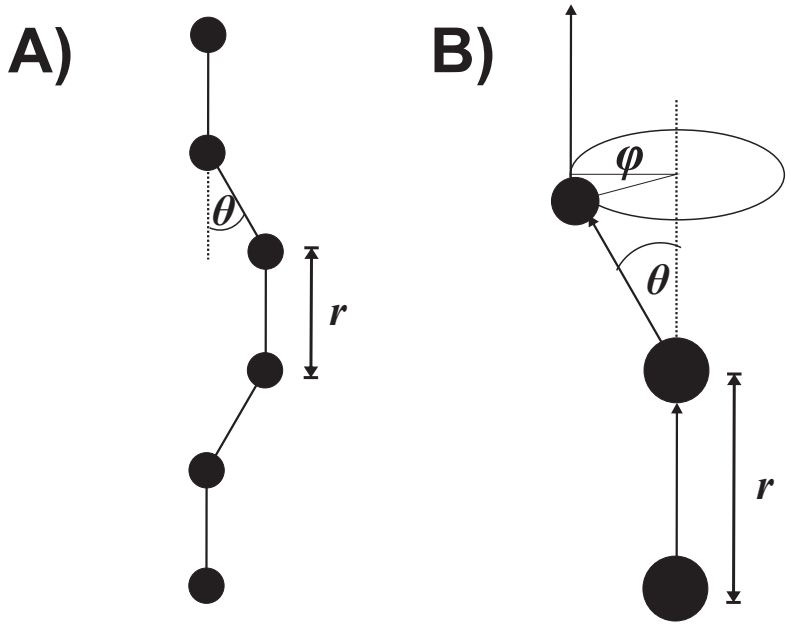

Figure 3.2: Sketch of the basic structure of a simple polymer chain. A sequence of monomers with a distance r (bond length) and a bond angle θ between two neighboring monomers A). The torsion angle φ depicts the rotation of the bond vector between two monomers B). Sketch is motivated by fig. 2.1 in the textbook of M. Rubinstein and R. H. Colby [Rub2003].

reader is referred to specific literature such as the textbooks by M. Doi or M. Rubinstein [Doi1988, Rub2003].
The structure of a simple polymer is defined by the bond length between two monomers, r, as well as two angles, the bond angle θ and the torsion angle φ, see fig. 3.2. The spatial expansion of a polymer chain can be characterized by the square radius of gyration that is defined as the sum over the square of all distance vectors between each two monomers [Rub2003]:

$$R_g^2 = \frac{1}{n^2} \sum_{i=1}^{n} \sum_{j=i}^{n} \left(\vec{R}_i - \vec{R}_j \right)^2 \ , \tag{3.9}$$

where $\vec{R}_i$ denotes the position vector of monomer i and n is the number of monomers in the polymer chain.

The theory of ideal polymers describes basic properties of polymer chains irrespective of the exact nature of a chain. A so-called *equivalent freely jointed chain* describes a real polymer by an hypothetical simple chain of the same maximum length M (*contour length*) but with N freely jointed bonds of an effective length b, called *Kuhn length* [Rub2003]. The square radius of gyration of an ideal linear polymer chain is $Nb^2/6$ [Rub2003].
Different ideal chain models, that base on the equivalent freely jointed chain nomenclature, exist [Doi1988, Rub2003]. In the *freely rotating chain model* all torsion angles of a chain are equally likely, i.e. the angle φ does not influence the potential energy of the polymer chain;

bond length and bond angle have constant values. A special case of the freely rotating chain is the *worm-like chain* (WLC) model that represents a good approximation for stiff polymers with small bond angles θ.
An important task of ideal polymer chain models is the calculation of the force that a polymer chain sets against stretching. For small extensions l, ideal polymers behave like elastic springs, see equation 3.10. However, contrary to Hookean springs, the restoring force is of entropic origin (see section 3.2). Thus, ideal polymers at small extension are called entropic springs [Rub2003].

$$f(l) = \frac{3k_bT}{Nb^2}l = \frac{3k_bT}{Mb}l \ , \tag{3.10}$$

where k_b is the Boltzmann constant, T the absolute temperature and M respectively b the mechanical properties of the ideal chain. More complex expressions describe the force/extension behavior of ideal chains at large stretches. For worm-like chains, the force/extension function cannot be derived analytically. However, Marko and Siggia derived an approximation that is asymptotically exact in the limit of small ($\frac{fb}{k_bT} \ll 1$) and large ($\frac{fb}{k_bT} \gg 1$) forces, see eq. 3.11 [Mar1995]. Between the two limits, the approximation differs less than 10 % from the numerically derived, exact solution of the WLC model [Mar1995].

$$f(l) = \frac{k_bT}{b} \cdot \left(\frac{2l}{M} + 0.5 \left(\frac{M}{M-l} \right)^2 - 0.5 \right) \ . \tag{3.11}$$

Force measurement instruments of high sensitivity such as optical tweezers or atomic force microscopes, enable the validation of ideal polymer models against experimental data [Mar1995, Des2002, Neu2008]. Equation 3.11 is widely used to model force/extension data of DNA and proteins [Mar1995, Rie1997b, Oes2000, Low2001, ElK2014].
In this thesis, Hook's law and the worm-like chain model (eq. 3.10 and 3.11) were incorporated in numerical simulations to model bacterial surface polymer mechanics during bacterial adhesion, see the publication of **Thewes et al. in *Soft Matter* 2015** (Addendum IV) and the manuscript in Addendum V.

3.4 Monte Carlo simulation

This section provides a brief introduction into the numerical computer simulation method called *Monte Carlo* [Met1949]. In depth information can be found in various textbooks [New1999, Fre2001, Lan2014]. The section presupposes the knowledge of some fundamental concepts of statistical mechanics.

Computer simulations in physics are basically related to problems of statistical physics and here usually of statistical mechanics. Statistical mechanics aims to investigate macroscopic properties of many-particle systems based on a view of the microscopic states. Many particle

systems are usually not analytically accessible due to the high number of degrees of freedom, for example, solving the 10^{23} equations of motion for one mole of gas particles is not possible. Statistical mechanics circumvents this problem by accessing the system statistically, i.e. by investigating the probability of a system to be in a certain microstate. Given the statistical properties of a system are known, average values of important quantities may be calculated. These average values correspond to macroscopic properties of the system that might be measured in an experiment.
The function $A(\mathbf{x})$ shall describe the value of a quantity A in the case that a system is in state $\mathbf{x}$ ($\mathbf{x}$ is a vector whose dimension corresponds to the system's degree of freedom), then the average of the quantity is given by:

$$\langle A \rangle = \int \mathbf{dx}\, p(\mathbf{x}) A(\mathbf{x}) \ . \tag{3.12}$$

Where $p(\mathbf{x})$ is the probability density of the system's states and the integration runs over the whole phase space.
The aim of statistical mechanics is to gain the function $p(\mathbf{x})$ and, given a system with N particles is in a volume V at temperature T, the probability distribution is in principle known. In such systems, the probability for a certain state to occur is linked to its energy and can be expressed in terms of the *Boltzmann factor*:

$$p(\mathbf{x}) \propto \exp(-H(\mathbf{x})/k_b T) = \exp(-\beta H(\mathbf{x})) \ , \tag{3.13}$$

where $H(\mathbf{x})$ is the system's *Hamiltonian*, k_b the *Boltzmann constant*, T the temperature and $\beta = 1/k_b T$. Hence, the average of A is:

$$\langle A \rangle = \frac{\int \mathbf{dx}\, A(\mathbf{x}) \exp(-\beta H(\mathbf{x}))}{\int \mathbf{dx}\, \exp(-\beta H(\mathbf{x}))} = \frac{\int \mathbf{dx}\, A(\mathbf{x}) \exp(-\beta H(\mathbf{x}))}{Z} \ , \tag{3.14}$$

with the partition function Z summing up the Boltzmann factors over the whole phase space. By splitting the Hamiltonian into kinetic and potential energy, equation 3.14 can be further simplified. The kinetic energy is of quadratic order in terms of the respective coordinate (the momentum) and, hence, the kinetic energy part of the Hamiltonian is usually solvable analytically, see *Maxwell-Boltzmann distribution*. By dropping the kinetic energy term, equation 3.15 remains:

$$\langle A \rangle = \frac{\int \mathbf{dr}\, A(\mathbf{r}) \exp(-\beta U(\mathbf{r}))}{\int \mathbf{dr}\, \exp(-\beta U(\mathbf{r}))} \ , \tag{3.15}$$

where $\mathbf{r}$ is a vector describing only the coordinates of the system and $U(\mathbf{r})$ is the potential energy of the system in state $\mathbf{r}$. To access all needed averages, it is 'simply' necessary to solve the integrals in equation 3.15.

At this point, the *Monte Carlo method* enters the stage, by providing a possibility to solve integrals numerically. In the most simple Monte Carlo approach the integral is evaluated by calculating the integrand on randomly chosen points of the phase space where each point appears with the same probability [Met1949]. That means, generating a random state $\mathbf{r}'$ of the system, calculating the value $A(\mathbf{r}')$ as well as the energy $U(\mathbf{r}')$ and finally $\exp(-\beta U(\mathbf{r}'))$ to give the configuration $\mathbf{r}'$ a statistical weight [Met1953]. The problem of this brute force method is that for a lot of systems, randomly chosen points will most of the time have a tiny weight. The consequence is an enormous amount of time to reach a reasonable approximation of the integral.
An alternative is, instead of choosing points randomly with equal probability and weighting them afterwards, to generate points directly with a probability according to their statistical weight $\exp(-\beta U(\mathbf{r}))$ [Met1953]. This approach is called *importance sampling*.
In 1953, Metropolis et al. introduced an importance sampling algorithm that produces states according to the Boltzmann distribution [Met1953]. The algorithm starts by generating a system in state $\mathbf{r}_0$ with energy $U(\mathbf{r}_0)$. Next, one particle of the system is chosen randomly and moved by a small randomly chosen vector $\mathbf{dr}$. The move results in new configuration of the system $\mathbf{r}_1$. Subsequently, the difference in energy ΔU between old and new state is calculated, $\Delta U = U(\mathbf{r}_1) - U(\mathbf{r}_0)$. Now, the move from state $\mathbf{r}_0$ to $\mathbf{r}_1$ is allowed with the probability

$$P(\mathbf{r}_0 \to \mathbf{r}_1) = \min(1, \exp(-\beta \Delta U)) \ . \tag{3.16}$$

Given the move was accepted, a new move to state $\mathbf{r}_2$ will be ruled out according to the presented rules. Otherwise, the next move starts again at $\mathbf{r}_0$. Finally, the quantity of interest A is simply calculated by [Met1953]:

$$\langle A \rangle = \frac{1}{M} \sum_{j=1}^{M} A_j \ , \tag{3.17}$$

where A_j is the value of the quantity A after the $j-$th move.

The essential idea of the *Metropolis algorithm* gets obvious by the following consideration: Equation 3.15 can be written as:

$$\langle A \rangle = \int d\mathbf{r} \, A(\mathbf{r}) \frac{\exp(-\beta U(\mathbf{r}))}{Z} \ . \tag{3.18}$$

The probability distribution of states $\mathbf{r}$ in an ensemble of systems is $P(\mathbf{r}) = \frac{\exp(-\beta U(\mathbf{r}))}{Z}$. Unfortunately, for large systems the partition function Z cannot be calculated and so can't $P(\mathbf{r})$. However, the relative probability of two states $\mathbf{r}_0$ and $\mathbf{r}_1$ to occur in an ensemble can be calculated:

$$\frac{P(\mathbf{r}_0)}{P(\mathbf{r}_1)} = \frac{\exp(-\beta U(\mathbf{r}_0))}{\exp(-\beta U(\mathbf{r}_1))} = \exp(-\beta(U(\mathbf{r}_1) - U(\mathbf{r}_0))) = \exp(-\beta \Delta U) \ . \tag{3.19}$$

That way, the metropolis algorithm generates states with a probability that fits their statistical weight by moving between two states according to the respective relative probability in the Boltzmann distribution, see equation 3.16. Finally, because the different states occur with the right statistical weight, the unweighted average of all generated states (eq. 3.17) gives the solution of the integral in equation 3.15.

4 State of the Art

4.1 Introduction

Bacteria adhere to virtually every surface, which may be a welcome (e.g. in a sewage plant) or a dangerous phenomenon (e.g. in hospitals). Therefore, the mechanisms that constitute the bacterial adhesion properties are in the scope of scientific research for decades, e.g. [Mea1971, Wil1972, Gib1975, Bus1987]. A variety of experimental setups were applied to disclose the bacterial adhesion process, e.g. reviewed by Bos et al. [Bos1999]. A widely used device is the parallel plate flow chamber, that enables to investigate adsorption and desorption of bacterial cells on various substrates [Mei1992, Pal1995, Bus2006].
However, quantifying the bacterial adhesion process in terms of force and distance was not possible until the invention of the atomic force microscope (AFM) in 1986 [Bin1986] and its later application in bacterial adhesion research [Duf2003, Gab2007, Dor2010]. A review of the publications using AFM to study bacterial adhesion (*AFM bacterial force spectroscopy*) is presented in the following.

Different approaches have been used to study bacterial adhesion by AFM. The most fundamental and easiest method is to measure the force between the AFM tip and an immobilized bacterial cell [Fan2000, Cam2000]. Early studies using AFM in bacterial adhesion research applied this method [Fan2000, Cam2000, Con2001, Cam2002, Abu2002, Vel2002, Abu2003c, Abu2003a, Vad2003]. However, although this method is a straightforward application of the AFM force spectroscopy mode, it is restricted to the adhesion between bacteria and silicon or silicon nitride.
The second and more complex technique relies on *bacterial probes*. Thereby, bacterial cells are immobilized directly on an AFM cantilever to measure the force acting between bacteria and surfaces, see section 5.4 and [Raz1998, Low2001, Kan2009]. Although this approach has been used by different researchers from the beginning of AFM bacterial force spectroscopy on, it was often limited by two shortcomings besides the complex preparation, i) the number of adhering bacteria was uncontrolled, therefore limiting the results to qualitative statements [Ong1999, Low2000, Agu2015b], and, even more important, ii) the intactness of the immobilized bacterial cell(s) was not guaranteed [Raz1998, Vadgue2004, Kan2009]. The second point is a general problem when performing AFM with bacterial cells [Vadgue2004, Mey2010].

Both approaches improved in the course of time: AFM tips were decorated with special macromolecules to investigate the binding mechanisms and distribution of specific adhesion macromolecules on the bacterial cell [Duf2008, Bea2014c]. This method is called *chemical force spectroscopy* and can be a form of *single molecule force spectroscopy* (SMFS) [Rie1997a, Cla2000, Tri2013]. Studies using chemical force spectroscopy will not be detailed here since it is beyond

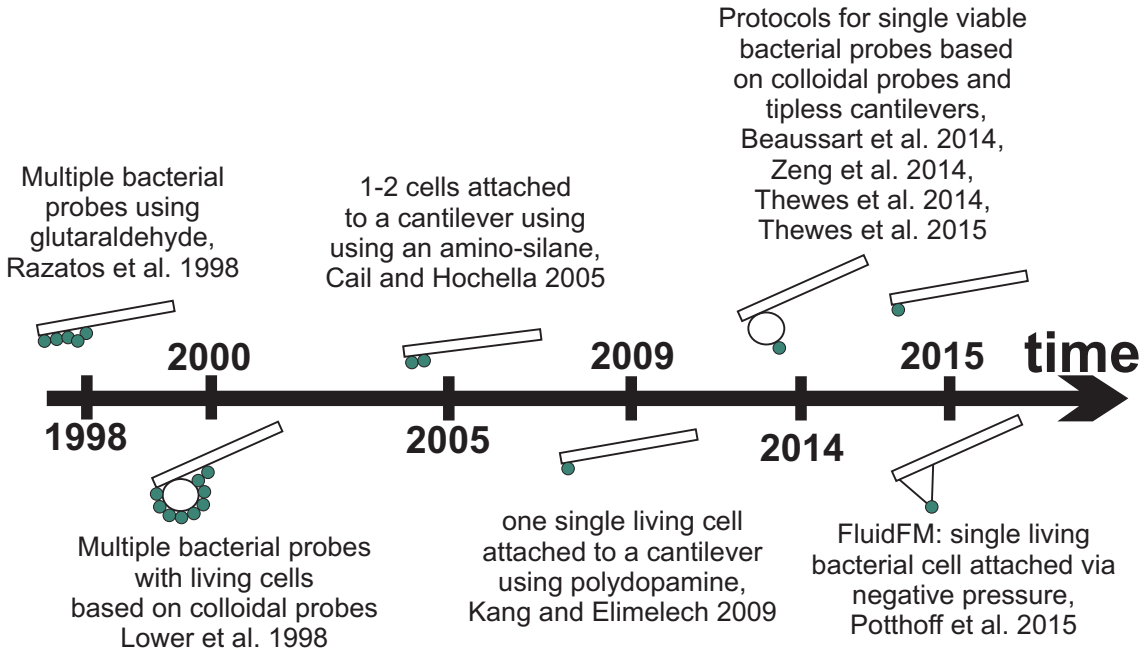

Figure 4.1: Sketch of the most important steps during the development of single bacterial probes.

the scope of this review.
In this work, emphasis lies on bacterial probes in particular on *single* bacterial probes with one living bacterial cell attached to an AFM cantilever. For details of the preparation of bacterial probes as well as technical aspects of force spectroscopy with bacterial probes, the reader is referred to section 5.4 and the publication of **Thewes et al. in *Eur. Phys. J. E* 2015** (Addendum I). Figure 4.1 illustrates the crucial steps towards the establishment of single bacterial probes. Razatos et al. were the first to attach bacterial cells directly to AFM cantilevers, yet, as they used glutaraldehyde (which changes the nature of bacterial cell wall proteins) to immobilize the cells, the translation of their results to in vivo situations is uncertain [Raz1998, Vadgue2004]. Preserving the viability of bacterial cells was a key feature of the colloidal probe based bacterial probes developed by Lower et al., however, the uncontrolled number of interacting bacterial cells caused problems concerning the measurement of absolute force values [Low2000]. Cail and Hochella used amino-silane coated cantilevers to attach one or two bacterial cells to an AFM cantilever [Cai2005]. Finally, in 2009, Kang and Elimelech presented the first bacterial probe with a single living cell attached [Kan2009]. They used polydopamine to immobilize the cells on AFM cantilevers and proofed the viability of the cells by live/dead staining after immobilization. In subsequent years, different protocols that teach the reliable production of single bacterial probes emerged [Bea2014b, Zen2014], including our own protocol [The2014, The2015a]. The latest development in the field of bacterial probes is a method to immobilize cells without bio-chemical glues [Pot2015]. Rather, single bacterial cells are fixed by negative pressure using a tool called FluidFM [Gui2014].

4.2 Forces in bacterial adhesion

A fundamental question of bacterial adhesion research concerned the forces driving the attachment of bacterial cells [Bus1987, Bos1999, Hor2010]. In principle, the answer is clear, as the interaction between two bodies is dominated by well-known forces: van der Waals forces, electrostatic forces, hydrogen-bonding, hydrophobic interaction and steric repulsion [Bus1987, Bos1999, Lec2001, VanOss2006]. These forces condense into the extended DLVO (xDLVO) theory [Der1941a, Ver1948, VanOss1986, VanOss2006].
A brief introduction into the nature of xDLVO forces is given in section 3.2. However, bacterial adhesion is more complex due to the presence of various macromolecules on the bacterial cell surface. The macromolecular contribution to bacterial adhesion forces lead to the classification of *non-specific* and *specific forces*. According to a definition by Busscher, non-specific forces account for the interactions between a surface and the bacterial cell body (described by xDLVO theory), whereas specific forces denote the binding of bacterial macromolecules [Bus1987, Bos1999]. In a slightly different definition specific interactions account only for the binding of two macromolecules i.e. between a receptor and a ligand, whereas other sources of macromolecular binding, e.g. protein binding on hydrophobic surfaces, are called non-specific [Dup2010].
Finally, the complexity of the bacterial adhesion process hampers theoretical predictions [Hor2010]. Therefore, the origin of bacterial adhesion forces with regard to xDLVO forces *and* the contribution of surface macromolecules was studied extensively using AFM. The next paragraphs review the studies concerning the influence of xDLVO forces. The role of surface macromolecules in bacterial adhesion will be reviewed in section 4.4.

4.2.1 Van der Waals forces

The theory of van der Waals forces was introduced in section 3.2.1 and it was indicated, that several studies revealed an influence of van der Waals forces on protein adsorption. Furthermore, the force between colloids and interfaces was shown to be well predicted by DLVO-theory [Duc1992].
In a naive first approach, a bacterium may be modeled as a sphere covered with a variety of proteins and hence, it seems reasonable, that van der Waals forces influence bacterial adhesion. Loskill et al. used multiple bacterial probes (of *Staphylococcus carnosus*) and tailored, silicon-based, substrates to evidence a direct influence of van der Waals forces on bacterial adhesion. The outcome of the study is illustrated in more detail in section 6.

4.2.2 Electrical double layer forces

Electrical double layer forces were introduced in section 3.2.1. Bacterial cells in aqueous solutions exhibit charges due to ionization of amino groups ($NH_3^+ \Leftrightarrow NH_2 + H^+$), carboxyl groups ($COOH \Leftrightarrow COO^- + H^+$) and phosphate groups ($HPO_4 \Leftrightarrow PO_4^- + H^+$) [Poo2002]. Hence, the charging of bacterial cells is pH depended in a non-trivial manner, as the distribution of the

respective surface groups may be specific to strains or individual cells [Poo2002]. Nevertheless, studying the influence of electrical double layer forces on bacterial adhesion relies on i) changing the pH of the surrounding medium to change surface charging or, ii) as has been indicated in section 3.2.1 for the example of protein adsorption, on changing the ionic strength (IS) of the surrounding medium to change the Debey length.
The exact effects of changing IS and pH are complex and usually not predictable quantitatively. However, in general, increasing IS decreases the range of electrical double layer interactions by decreasing the Debye length [Lec2001, Isr2011]. Electrophoretic mobility measurements with four different bacterial species (*E. coli, S. epidermidis, S. mitis, L. acidophilus*) indicated that increasing the pH results in a decreased streaming potential of bacterial cells [Bas1999]. A lot of force spectroscopy studies investigated the influence of electrical double layer forces on bacterial adhesion by changing IS and pH [Raz1998, Low2000, Vel2002, Han2003, Abu2003a, Cai2005, She2007, She2008, Kan2009, Cha2010, Das2011b] and the outcome of some of these studies will be detailed in the following:

Lower and co-workers used bacteria-coated beads attached to an AFM cantilever to explore the adhesion of living *E. coli* cells on three mineral surfaces with different isoelectric points [Low2000]. Differences in the approach parts of the measured force/distance curves were explained, qualitatively, by different electrostatic interactions. Decreasing ranges of repulsive forces for increasing IS supported these findings. Upon retraction of the bacterial probes from the mineral surfaces, the authors found attractive forces on positively charged surfaces, in accordance with electrostatics. The attractive forces decreased with increasing IS. Thereby, the retraction curves always exhibited extended rupture events indicating the involvement of surface polymers. On a negatively charged surface, repulsion was measured for low ionic strength, whereas strong attraction was measured for high ionic strength. While surface electrostatics are not able to explain this attraction, Lower et al. concluded that surface macromolecules tethered to the surface via hydrogen bonds or locally attractive electrostatic interactions [Low2000].
Cail and Hochella Jr. investigated the adhesion of *Enterococcus faecalis* to glass at different pH and IS [Cai2005]. Adhesion forces showed negative correlation to pH and positive correlation to IS, which is in qualitative agreement with DLVO predictions. However, DLVO theory was not able to describe neither the strength of the measured forces nor the length scales [Cai2005].
Chandraprabha et al. measured force/distance profiles between a silicon nitride AFM tip and immobilized *Acidithiobacillus ferrooxidans* cells [Cha2010]. The influence of changing IS (decreasing repulsion for increasing IS) as well as pH (increasing repulsion for increasing pH) on the approach curves was modeled using a steric model for grafted polymers and compared to DLVO predictions. Whereas the polymer model agreed well with the experimental data, DLVO theory could only explain the qualitative behavior but failed again in explaining strength and length scales of the measured forces. Removing the LPS layer (see section 3.1) by chemical treatment decreased repulsive forces upon approach of an AFM tip to a bacterial cell. The authors concluded that the approach is dominated by steric repulsion of bacterial surface polymers. Upon retraction, theoretical prediction derived from DLVO theory agreed qualitatively with experimental force/distance curves concerning changes of IS and pH. Removal of the LPS layer decreased adhesion forces significantly. Taking these findings together, the authors concluded that the adhesion force is governed by the binding of specific adhesins and this binding might be influenced by electrostatic forces [Cha2010].
Sheng and co-workers investigated the combined effect of different electrostatics and surface hydrophobicity using four different metal surfaces and bacterial probes of two different bacterial

species (*Desulfovibrio desulfuricans* and a Pseudomonas species) [She2007]. The measurements showed increasing adhesion for increasing surface hydrophobicity as well as for increasing electrostatic attraction (higher positiv streaming potential). These results qualitatively agreed with the extended DLVO approach [She2007].
In a similar study, Sheng et al. investigated the adhesion of three different bacterial species (*Desulfovibrio desulfuricans*, *Desulfovibrio singaporenus* and a Pseudomonas sp.) to stainless steel in deionized water, artificial seawater and artificial seawater enriched with nutrients [She2008]. For all three species, adhesion was highest in artificial seawater due to the combination of a high water contact angle of stainless steel in artificial seawater of 85° (compared to 85 ° and 60 ° in deionized water and enriched artificial seawater) and a high zeta potential of 1364.4 mV (compared to 6.8 mV and 1356.4 mV in deionized water and enriched artificial seawater). Hence, a combination of hydrophobicity and strong electrostatic attraction was the origin of high adhesion forces on stainless steel in artificial seawater. The authors also studied the influence of the pH on bacterial adhesion. For all species under investigation, adhesion was highest near their isoelectric point at pH 3, decreased for higher pH values up to pH 7 and rose again up to pH 9. These results do not correspond to predictions of DLVO electrostatics and the authors speculated that other forces different from electrostatic ones influence bacterial adhesion [She2008].
However, in both studies by Sheng et al. glutaraldehyde was used to immobilize bacteria on AFM cantilevers [She2007, She2008], hence the translation of the results to real situations is doubtful, as glutaraldehyde significantly changes bacterial surface properties [Vadgue2004, Kan2009].

4.2.3 Hydrophobic interaction

The studies by Sheng et al. already indicated that surface hydrophobicity, usually characterized by water contact angle measurements, influences bacterial adhesion [She2007, She2008]. The theory of hydrophobic interactions was introduced in section 3.2.1. Several other studies illuminated the influence of the hydrophobic interaction on bacterial adhesion [Ong1999, Eme2006, Bok2008, Bea2013, ElK2013, Bea2014b, The2014]. Beaussart et al. for instance used single cell force spectroscopy based on colloidal probes to study the adhesion of *Lactobacillus plantarum* [Bea2013]. Adhesion forces as well as rupture lengths were measured on hydrophilic and hydrophobic substrates. Adhesion forces on the hydrophobic substrates were higher and retraction curves showed multiple peaks. This was attributed to the extensive binding of surface proteins via hydrophobic side groups, which is in accordance with studies on the influence of hydrophobicity on protein adsorption [Nor1986, Wah1991, Bel2008]. In contrast, on the hydrophilic substrates Beaussart and co-workers measured adhesion forces that were smaller and accompanied by only a single or few peaks in the force/distance curves. The adhesion events were, according to the authors, due the the binding of glycopolymers. No differences between hydrophobic and hydrophilic substrates were found concerning rupture lengths [Bea2013].
Using the same single cell force spectroscopy method, El-Kirat-Chatel et al. investigated the adhesion of *Pseudomonas fluorescens* on hydrophilic and hydrophobic substrates, with a focus on the large adhesion protein A (LapA) [ElK2013]. They found similar adhesion forces on hydrophilic and hydrophobic surfaces using a wild type strain. The binding probability, however, was larger on the hydrophobic surface. LapA deficient mutants exhibited significantly lower

adhesion forces on both surfaces, proofing the important role of the adhesin. In contrast to adhesion forces, rupture lengths were larger on the hydrophilic surface and characteristic polymer stretching signals in the force/distance curves were different compared to the hydrophobic surface. This points towards a different binding mechanism respectively binding patch between LapA molecules and hydrophobic respectively hydrophilic surfaces [ElK2013].
In another study, Beaussart and co-workers used *Pseudomonas aeruginosa* to investigate the role of the hydrophobic interaction if adhesion is mainly mediated by Pili [Bea2014b]. Single cell force spectroscopy measurements revealed, also in this case, a strong influence of the hydrophobic interaction.

Finally, it is proven, that the hydrophobic interaction enhances bacterial adhesion by mediating binding of bacterial surface proteins or proteinaceous structures.

In this thesis, fundamental adhesion mechanisms of bacteria are studied by investigating bacterial adhesion to substrates that feature different surface hydrophobicities, see chap. 6.

4.2.4 Hydrogen bonds

The nature of H-bonds was introduced in section 3.2.1. Although Norde predicted that H-bonds will not contribute significantly to protein adsorption [Nor1996], different authors speculated that H-bond formation is an important contributor to polymer tethering during bacterial adhesion on hydrophilic substrates [Low2000, Ata2008, vanderMei2008, Bok2008, Mei2009a, Str2010, Das2011a].
Van der Mei et al. for instance claimed that specific adhesion between mouth colonizing bacteria and saliva coated substrates relies on H-bond formation [vanderMei2008]. Strauss and co-workers found larger adhesion forces between AFM silicon nitride tips and *E. coli* cells, the longer the O-antigen region of the cell was. This result was attributed to the enlarged area available for H-bond formation [Str2010].
In an attempt to quantify the contribution of H-bonds to overall bacterial adhesion forces, Abu-Lail and Camesano adapted a method, called *Poisson analysis*, that was originally developed to elucidate the binding between AFM tips and gold or mica surfaces [Wil1996, Abu2006]. Later on, the Poisson analysis was applied by additional researchers to investigate the binding properties of bacterial cells [Bok2008, Mei2009a, Das2011b, Agu2015a].
However, besides open question concerning the applicability of the Poisson analysis in heterogeneous systems like bacterial cells, the Poisson analysis itself was considered basically wrong as is completely ignores the dynamic nature of bond rupture [Eva1997, Wil2003, Sul2006].

Finally, while the involvement of H-bonds in the bacterial adhesion process seems reasonable as proteins do exhibit strong polar side groups, experimental evidences concerning H-bond formation during bacterial adhesion are still rare.

In this thesis, the influence of H-bond formation on bacterial adhesion to hydrophilic substrates is revealed by combining single cell force spectroscopy and computer simulations, see chap. 6.

4.2.5 Summary

The reviewed research comprehensively showed that the forces incorporated in the xDLVO theory indeed influence bacterial adhesion processes. However, the studies also show that quantitative predictions by the DLVO theory fail to describe the bacterial adhesion process. The reason for this is, as most of the studies state, the significant influence of bacterial surface polymers on the adhesion process, i.e. the contribution of specific interactions. Yet, a theoretical model describing bacterial adhesion in accordance with experimental results is lacking.
In the thesis at hand, a simple model describing bacterial adhesion as *solely* mediated by surface polymers is introduced, analyzed by Monte Carlo simulations and compared to experimental data, see chap. 6.

4.3 The influence of the bacterium/surface contact time on bacterial adhesion

The adhesion strength between a bacterium and a substrate increases for prolonged contact times. This effect is called *bond strengthening* and has been examined well, using AFM force spectroscopy [Vadgue2004, vanderMei2008, Bok2008, Mei2009a, Mei2009c, Mei2011, Das2011b, Ovc2013a, Her2013, Bea2013, Zen2014, Pot2015].
Vadillo-Rodriguez et al. were the first that studied the influence of the contact time on the adhesion of bacteria [Vadgue2004]. They measured adhesion forces between *Streptococcus thermophilus* and a silicon nitride AFM tip for contact times between 10 s and 200 s. Adhesion forces increased for increasing contact times. The authors stated that bond strengthening with residence time was due to larger amounts of *extracellar polymeric substance* (EPS) molecules tethering to the tip during contact [Vadgue2004].
Aguayo et al. used multiple bacterial probes to investigate the adhesion between *S. aureus* and titan [Agu2015b]. They found increasing binding frequencies, increasing adhesion forces and energies for increasing surface contact times.
Boks and co-workers measured the influence of surface delay times on hydrophilic and silanized (hydrophobized) glass [Bok2008] using multiple bacterial probes of different *S. epidermidis* strains. On hydrophilic glass, adhesion became stronger for increasing contact times reaching a saturation value withing one minute of contact, no influence of a surface delay was measured on hydrophobized glass. However, Boks et al. did not find an influence of the surface hydrophobicity on adhesion forces at all, which is in contrast to most other studies on the influence of surface hydrophobicity [Bea2013, Als2013, Sul2015].
Van der Mei et al. studied the bond strengthening of mouth colonizing bacteria on saliva and bovine serum albumin (BSA) coated glass using multiple bacterial probes [vanderMei2008]. The authors claimed that due to the adaption of the adhesion mechanisms of mouth bacteria to the oral environment the adhesion to saliva is of specific nature, whereas on BSA unspecific adhesion takes place. Following this argumentation, the authors stated that bond-strengthening on saliva is due to additional bonds forming between bacterium and surface; bond strengthening on BSA, however, is - according to the authors - due to the removal of interfacial water resulting in closer contact between bacterium and surface.

Alsteens et al. also propose a mechanism of bond strengthening that relies on the formation of additional bonds between a bacterium and a surface with prolonged contact [Als2013].
Hence, two mechanisms explaining the effect of bond strengthening occur in literature [vanderMei2008, Als2013].

4.4 The role of bacterial surface polymers in adhesion

Bacteria adapted to natural habitats by expressing surface polymers specifically designed to enforce adhesion to all kinds of surfaces [Lin2011], see section 3.1. The studies reviewed so far, revealed that the surface polymers play a key role during the bacterial adhesion process and cause the failure of classic theoretical models (like the DLVO theory). Hence, the importance of bacterial surface polymers is a focus of bacterial adhesion research.

4.4.1 The LPS of gram negative bacteria

The outermost layer of gram-negative bacteria is a lipid double layer, followed by polysaccharides, forming a lipopolysaccharide (LPS) layer, see section 3.1. While the exact structure of this layer is strain specific the fundamental sequence is not: The so called lipid A is followed by the core-polysaccharide and a strain specific o-antigen.
The influence of the LPS layer on the adhesion properties of *Escherichia coli* was studied extensively [Raz1998, Ong1999, Vel2002, Abu2003b, Bur2003, Str2009, Str2010]:

Razatos et al. performed force/distance curves with an AFM silicon nitride tip and *E. coli* mutants exhibiting LPS molecules with core-polysaccharides of different length [Raz1998]. They found that the force upon approach of an AFM tip to bacterial cells is sensitive to the length of the LPS core-polysaccharide. However, as glutaraldehyde was used to immobilize bacterial cells [Raz1998], other authors questioned these results [Vel2002, Bur2003].
In the following, Burks and co-workers tried to reproduce the results of Razatos et al. using the exact same experimental procedure and the two *E. coli* mutant strains of Razatos et. al that exhibit the largest difference in LPS core-polysaccharide length (D21 and D21f2). The measurements were performed on cells immobilized with and without glutaraldehyde [Bur2003]. The study reproduced the results of Razatos et al. as they found an influence of the LPS length on the adhesion between glutaraldehyde-fixed cells and AFM tips. However, the experiments without glutaraldehyde-fixed cells did not show any influence of the LPS length on the forces acting between tip and bacterium upon approach [Bur2003].
While Velegol et al. as well as Burks et al. exclusively evaluated the approach parts of force/distance curves between bacteria differing in LPS lengths [Vel2002, Bur2003], further studies also investigated the retraction parts, i.e. the adhesion forces [Abu2003b, Str2009].
Strauss et al. investigated the influence of the LPS length of different *E. coli* strains on the adhesion forces to silicon nitride AFM tips [Str2009]. The length of the LPS was measured for each individual bacterial cell using a steric repulsion model to fit the approach parts of force/distance curves. Control strains without the O-antigen had a significantly shorter LPS and showed no correlation between LPS length and adhesion force. In contrast, strains that

express the O-antigen had longer LPS molecules and showed a linear correlation between LPS lengths and adhesion forces. The authors claimed that higher adhesion forces for larger O-antigen regions are due to the enlarged area available for the development of hydrogen bonds to an AFM tip [Str2009].
Abu-Lail and Camesano used a different approach to investigate the influence of the LPS layer on the adhesion of *E. coli* [Abu2003b]. Instead of using mutants with truncated LPS molecules, they used the full LPS expressing *E. coli* strain JM109 and removed the surface polymer layer chemically. The results of this study also indicated that the LPS layer enforces adhesion to silicon nitride. Electrostatic forces seemed to play a minor role as the ionic strength showed no influence on adhesion forces. Upon approach of an AFM tip to a bacterium, repulsive forces were measured. Range and strength of the forces decreased after polymer removal, indicating a steric polymer origin of the repulsion rather than an electrostatic one. Thus, approach curves were comprehensively described by a polymer brush model [Cam2000] and DLVO theory failed to predict repulsion on approach or adhesion on retraction [Abu2003b].

Besides *E. coli*, studies concerning the importance of the LPS layer of gram-negative *Pseudomonas aeruginosa* have been performed as well [Ata2007, Ata2008, Lau2009b, Lau2009a, Iva2011]. Also these studies reported no trivial correlation between LPS structure and adhesion properties. While Atabek et al. found a positive influence of the LPS length on adhesion forces and rupture distances between an AFM silicon nitride tip and *P. aeruginosa* cells [Ata2007], Ivanov and co-workers measured no correlation between LPS length and adhesion forces [Iva2011].
The adhesion between *P. aeruginosa* and BSA seems to favor short LPS molecules with truncated o-antigen structure as was investigated by Atabek and co-workers [Ata2008]. According to the authors, the increased contact between the LPS core-polysaccharide and the protein layer might favor the formation of hydrogen bonds.
Bacterial probes produced by growth of a whole biofilm on a bead attached to an AFM cantilever were used by Lau and co-workers. They found stronger adhesion between glass and *P. aeruginosa* for mutant strains exhibiting a truncated LPS layer [Lau2009b, Lau2009a].
Finally, the reviewed studies revealed no trivial connection between the LPS structure and the adhesion properties of gram-negative bacteria.

4.4.2 Bacterial adhesion in the human oral environment

The human oral cavity is colonized by a variety of bacterial species [Nyv1987, Nyv1992, Dia2006]. Some of the species cause caries [Nyv1990, Xu2007], hence, multiple studies investigated their adhesive properties using AFM force spectroscopy [Xu2007, Bus2007, Cro2007, vanderMei2008, Mei2009a, Mei2009c, Mei2009b, Wes2013, Agu2015a, Sul2015]. Adhesion processes in the human mouth are complex due to a salivary film that forms on objects entering the mouth, a so-called *conditioning film* [Han1997].
Van der Mei et al. compared the adhesion forces of several mouth colonizing bacterial species to saliva and BSA coated glass using multiple bacterial probes [vanderMei2008]. All investigated strains showed higher adhesion forces to the saliva coated surface, most likely due to specific receptor-ligand binding between bacterial adhesins and their salivary counterparts [vanderMei2008].

In contrast, some studies revealed protective effects of salivary conditioning films. Adhesion forces of diverse mouth colonizing species to stainless steel, orthodontic adhesive, orthodontic composites and bovine enamel, investigated with multiple bacterial probes, decreased after the adsorption of saliva [Mei2009c, Mei2009b, Mei2011].
The human mouth colonizer *Streptococcus mutans* is a common cause of dental caries [Ham1980]. *Antigen I/II*, also known as *surface adhesin P1*, is a surface protein of *S. mutans* that mediates binding to salivary glycoproteins [Lee1989, Bow1991, Oho1998, Hei2015]. Xu et al. measured the adhesion between saliva coated AFM cantilevers and *S. mutans* cells with (wild type) and without (mutant) antigen I/II [Xu2007]. The force spectroscopy data revealed, that the wild type cells that express antigen I/II adhered significantly stronger compared to mutant cells, at pH 6.8. The difference was absent at pH 5.8. The authors concluded that i) the specific binding between antigen I/II and saliva enhances the adhesion of *S. mutans* and ii) this specific binding is of electrostatic nature [Xu2007].
In a more detailed study, Sullan et al. investigated the role of the surface adhesin P1 of *S. mutans* upon adhesion to the glycoprotein *salivary agglutinin* (SAG) [Sul2015]. Single molecule force spectroscopy (SMFS) experiments revealed characteristic binding properties of single P1-SAG complexes. These measurements showed that the two SAG binding domains of P1 bind equally strong and with similar probabilities to SAG. Adhesion measurements with single P1 molecules on hydrophobic surfaces indicated a strong influence of the hydrophobic interaction. Subsequently, single cell force measurements with *S. mutans* cells on SAG coated substrates showed large adhesion forces and rupture distances due to the actions of several P1-SAG bonds. A comparison between the rupture force of a single P1-SAG complex and the adhesion force of an entire *S. mutans* cell revealed the involvement of roughly ten P1 molecules. Based on the shapes of the force/distance curves the authors speculated about cooperative effects that additionally influence the adhesion on the level of an entire cell [Sul2015].
While the P1 based adhesion of *S. mutans* is a sucrose-independent adhesion pathway, other mechanisms exist that depend on the availability of sucrose [Sul2015]. Cross et al. investigated the adhesion of a *S. mutans* wild type strain as well as mutants that lack different glucosyltransferases, in the absence and presence of sucrose [Cro2007]. The mutant strains were not able to produce glucan surface polymers out of sucrose. Investigating the adhesion between an AFM tip and the wild type revealed an increasing adhesion force in the presence of sucrose. The adhesive strength of the mutants indicated no correlation to the availability of sucrose in general, but was more complex in detail. One out of five mutants under investigation showed slightly increasing adhesion forces in the presence of sucrose. The authors concluded that the glucan surface polymer synthesis out of sucrose follows complex pathways, that have to be addressed in further studies [Cro2007].

The above studies show that bacterial adhesion in the oral cavity is largely defined by the presence of saliva and the subsequent specific binding between salivary macromolecules and bacterial adhesins. However, the influence of a salivary film may be positive or negative depending on the surface that serves as comparison [vanderMei2008, Mei2009c, Mei2009b, Mei2011]. Hence, a fundamental problem of adhesion studies investigating bacterial adhesion in the human mouth is the availability of controlled surfaces that enable to study fundamental mechanisms of bacterial adhesion in oral environments without abandoning too much biological relevance [Zei2013].

4.4.3 Bacterial adhesion to human extracellular substances

Staphylococcal species produce adhesins like SdrG or the FnBPs that belong to the family of microbial surface components recognizing adhesive matrix molecules (MSCRAMMs), see section 3.1 and [Cla2006, Hei2011]. These proteins are covalently bound to the bacterial cell wall. *Staphylococcus aureus* and its relative *Staphylococcus epidermidis* are colonizers of the human skin and opportunistic pathogens that are common causes of implant associated infections [Low1998, Len2003, Vuo2002, Ott2009]. Hence, the interaction between these bacterial species and components of the human extracellular matrix, such as fibrinogen (Fg) and fibronectin (Fn) is of utmost importance.
The role of the staphylococcal adhesin SdrG for the adhesion of *S. epidermidis* to Fg was extensively studied [Her2013, Her2014, Van2015]. Single cell force spectroscopy measurements using a wild type and a mutant strain lacking the proteinaceous surface adhesin SdrG revealed the importance of the adhesin for the adhesion of *S. epidermidis* to fibrinogen [Her2013]. A single SdrG-Fg bond is remarkably strong (about 2 nN) as has been shown by SMFS measurements [Her2014] and the adhesion strength of a specific *S. epidermidis* cell to Fg-coated substrates seems to be related to the density of SdrG molecules on the cell surface [Van2015].
The interaction between Fn and *S. aureus* has been studied using Fn-decorated AFM tips [Xu2007, Mit2008, Low2010]. Mitchell et al. measured force/distance curves on two different *S. aureus* wild type strains (Newbould and CF07) as well as their respective sigB mutant [Mit2008]. SigB is a global regulator and positively correlated with the expression of *S. aureus* fibronectin binding protein A (FnBPA) [Bis2004, Ent2005]. Both wild type strains showed similar binding forces to the Fn tip (around 1100(500) pN) but large differences in binding affinity. The newbold sigB mutant was almost non-adherend to Fn, whereas the CF07 mutant was still able to bind Fn with low affinity. The authors concluded that different strains feature natural differences in FnBP expression resulting in different adhesion affinities to Fn, furthermore they speculated that the different Fn affinity of the sigB mutants might be a hint to additional, strain-depended, regulation pathways [Mit2008].
Interestingly, Yongsunthon et al. found significantly higher binding affinities between Fn coated AFM tips and *S. aureus* isolates of infected cardiac prosthesis compared to isolates from healthy human subjects [Yon2007]. This difference might be related to different activities of SigB [Ino2006, Moi2006, Mit2008].
Homophilic FnBPA (FnBPA to FnBPA) bonds play a major role for the formation of *S. aureus* biofilms as revealed by Herman-Bausier and co-workers [Her2015]. Thereby, a single FnBPA-FnBPA bond exhibits a strength of around 125 pN (the force varies depending on the applied loading rate) as was shown with SMFS [Yon2007].
Busscher et al. investigated the role of the surface adhesin antigen I/II (adhesin P1) for the adhesion of the human mouth colonizing bacterium *Streptococcus mutans* (see section 4.4.2) to laminin (a component of the extracellular matrix) [Bus2007]. Force spectroscopy measurements with laminin coated tips revealed significantly lower adhesion force to antigen I/II deficiant *S. mutans* mutants compared to wild type cells.
Pseudomonas aeruginosa is a gram-negative opportunistic pathogen that causes severe infections in the human body [VanDel1998, Dri2007]. Strauss et al. used multiple bacterial probes to measure the adhesion force between *P. aeruginosa* and fetal bovine serum (FBS) or Fn coated surfaces [Str2009]. They found much stronger adhesion to the Fn as compared to FBS-coated surfaces. The large difference was explained by strong specific interactions between the bacteria

and Fn-coated surfaces compared to the FBS-coated surfaces.

Non-proteinaceous adhesins like wall teichoic acids and lipoteichoic acids are widely spread among bacterial species [Lin2011]. Additionally, some bacteria exhibit large proteinaceous filaments, called pili, that interact with host cells or surfaces [Cra2004, Tel2006, Kli2010].
While so far no force spectroscopy studies have been reported to clarify the role of teichoic acids in bacterial adhesion, researchers revealed the importance of pili for the adhesion of *Lactobacillus rhamnosus GG* as well as of *Lactococcus lactis* to mucin [Le2013, Sul2014].

4.4.4 Bacterial adhesion to eukaryotic cells

Pseudomonas aeruginosa is a common cause of lung inflammation (pneumonia)
[Oli2000, Dav2000]. Beaussard et al. investigated the role of type IV pili during the adhesion of *P. aeruginosa* to pneumocyte cells using single cell force spectroscopy and single molecule force spectroscopy (SMFS) [Bea2014a]. The SMFS measurements enabled to identify and characterize the force/distance signal related to the stretching of pili during single cell force/distance curves. The importance of the hydrophobic interaction was revealed by comparing force/distance curves on pneumocyte cells and hydrophobic substrates. The authors concluded that type IV pili largely contribute to the overall adhesion strength of *P. aeruginosa* to pneumocyte cell due to a strong binding and a large rupture length, giving rise to high adhesion energies [Bea2014a].
In a study that might be of direct medical importance, Liu and co-workers investigated the anti-adhesive potential of cranberry juice concerning the adhesion of P-fimbriated and non-fimbriated *E. coli* cells to uroepithelial cells [Liu2010]. *E. coli* cells are responsible for most urinary tract infections. Fimbriae are pili-like structures that are expressed by gram-negtive cells, like *E. coli*, to attach in host environments [Con1996]. Using cell force spectroscopy, Liu et al. revealed that adhesion forces strongly decrease if the fimbriated cells are incubated in cranberry juice solution, while no effect was measured for non-fimriated cells. The authors concluded that the proanthocyanidin (PAC, an ingredient of cranberry juice) is able to block specific binding between fimbriae and uroepithelial cells [Liu2010].

The fungus *Candida albicans* is a common human pathogen that is frequently isolated in combination with pathogenic bacteria. Interactions between *C. albicans* and pathogenic bacteria might influence the development of infections. Hence, studying these interactions is of high clinical importance [Shi2009b, Pel2010, Mor2010].
C. albicans is able to grow in different morphologies, i.e. in yeast and in hyphae morphology [Odd1988, Sud2004]. The pathogenic bacterium *P. aeruginosa* is one species occurring in combination with *C. albicans* infections [War2006, Bra2008]. *P. aeruginosa* may kill *C. albicans* cells in hyphae morphology while it does neither adhere to nor kill the fungus in yeast morphology [Hog2002, Bra2008]. Interestingly, *P. aeruginosa* expresses a quorum sensing (QS) molecule that strongly increases the tendency of *C. albicans* to grow in yeast morphology [Ker1999, Hog2004].
Ovchinnikova et al. investigated the interaction between *C. albicans* and a wild type strain of *P. aeruginosa* as well as a mutant lacking the mentioned QS molecule [Ovc2012b]. Force

spectroscopy experiments using multiple bacterial probes revealed significantly lower adhesion forces between *P. aeruginosa* wild type cells and *C. albicans* cells in yeast morphology compared to the hyphae state. However, QS mutant cells exhibited low adhesion forces to *C. albicans* cells in hyphae state as well. The authors stated that the QS molecule triggering the formation of adhering resistant *C. albicans* yeast morphology might also trigger the expression of specific surface adhesins of *P. aeruginosa* [Ovc2012b].
In a second study, Ovchinnikova and co-workers investigated the role of chitin-binding protein (CbpD) of *P. aeruginosa* for the adhesion to *C. albicans* [Ovc2013a]. Via force/distance measurements using *P. aeruginosa* wild type cells and blocking the CbpD adhesin (with N-acetylglucosamine) or by using CbpD mutant cells the important role of the protein was identified: In both cases where CbpD was unable to mediate binding, adhesion forces reduced significantly. However, substantial adhesion forces were still present, showing the influence of further binding mechanisms [Ovc2013a].

Besides *P. aeruginosa*, staphylococcal species are frequently isolated in the context of *C. albicans* infections [Dou2003, Shi2009b].
The interaction between *S. aureus* (strain NCTC8325-4) and *C. albicans* was the issue of a multiple bacterial probe study by Ovchinnikova et al. [Ovc2013b]. They investigated the adhesion of *S. aureus* to *C. albicans* hyphae in the presence of model proteins, either in whole fetal bovine serum (FBS) solution or in single protein solution containing only one ingredient of FBS, namely BSA, apo-transferrin or fibronection. The results strongly indicate a competing adsorption of proteins in the presence of whole FBS solution: The adhesion force between the two organisms was unaffected by the adsorption of proteins from FBS as well as in the presence of fibronectin only, whereas the adsorption of BSA or apo-transferrin alone decreased adhesion forces to the hyphal surface. The authors explained the results as follows: BSA and apo-transferrin are rather small proteins, consequently their adsorption to a surface is faster compared to larger fibronectin proteins. However, fibronectin is, depending on the surface interactions of the respective proteins, able to replace the firstly adsorbed smaller proteins. The experiments suggest that on the hyphal surface fibronectin replaces the smaller proteins giving rise to an unaffected adhesion force [Ovc2013b].
Another study by Ovchinnikova et al. investigated the adhesion of *S. aureus* along the hyphae form of *C. albicans* [Ovc2012a]. Fluorescence microscopy images revealed an increased number of adhering bacteria in the middle and at the tip of the hyphae, i.e. the regions that are further afar from the former yeast cell. Subsequent force/distance measurements conducted with two different *C. albicans* strains using multiple bacterial probes revealed stronger adhesion forces at the middle and tip regions. The authors stated that this adhesion behavior might be due to surface proteins of the Als family that are specifically present at the respective regions of the *C. albicans* hyphae. Following this argumentation, differences in adhesion values between the two tested *C. albicans* strains for the same hyphae regions may be related to different amounts of Als proteins expressed by the strains [Ovc2012a]. This hypothesis was proven by a follow up study using *C. albicans* mutant cells lacking the Als3 surface adhesin [Pet2012].
The importance of Als-adhesins could be a general feature of the adhesion between *staphylococci* and *C. albicans* as also the adhesion of *S. epidermidis* to *C. albicans* was shown to be positively correlated with the presence Als1 and Als3 [Bea2013].

4.4.5 Other specific surface adhesins and their function in the bacterial adhesion process

Numerous other studies investigated the importance of specific proteinaceous and non-proteinaceous, covalently bound and secreted adhesins for the adhesion capabilities of different bacteria [Low2001, Han2003, Waa2005, Bus2008, Das2011b, Iva2012].
Ivanov et al. found that the adhesion of *Pseudomansa fluorescence* strain Pf0-1 to an AFM silicon nitride tip is largely influenced by the amount of the surface bound large adhesion protein A (LapA) on a bacterial cell surface [Iva2012].
Waar et al. revealed the importance of the adhesin *aggregation substance* (AGG) for the cell-cell adhesion of *E. faecalis* by using multiple bacterial probes and comparing the adhesion of wild type and AGG mutant strains [Waa2005].
Lower et al. investigated how bacteria actively react to their environment and adapt their adhesion properties [Low2001]. The adhesion of the metal reducing bacterium *Shewanella oneidensis* to goethite was measured using multiple bacterial probes. For longer contact times, adhesion forces increased under anaerobic conditions while no effect of the contact time was measured under aerobic conditions. The increasing adhesion forces were accompanied by force/distance curves exhibiting characteristic protein extension signals that might belong to a putative iron reductase present on the bacterial surface under anaerobic conditions. The authors concluded that the combination of anaerobic conditions and long contact times lead to an active response of the bacterium to its environmental situation [Low2001].
Secreted adhesins are part of the EPS of bacterial organisms [Las2002]. Busscher et al. investigated the adhesion between different carbon particles and gram-negative *Raoultella terrigena* [Bus2008]. They found a significantly decreasing number of adhesion events upon removing the EPS-layer biochemically which reveals a direct influence of the amount of EPS on the adhesion of *Raoultella terrigena*.
Extracellular DNA (eDNA) is expressed by some organisms as a part of the EPS [Fle2010]. Das et al. studied the role of eDNA for different adhesion scenarios of *S. mutants* [Das2011a, Das2011b]. They found that in general eDNA enhances bacterial adhesion, most likely by increasing the number of available binding sites between a bacterium and a surface. However, a detailed description was more complex as differences occurred depending on type of surface, ionic strength and surface delay times [Das2011a, Das2011b].

4.4.6 Summary

Using a variety of adhesin deficient mutants and host factor providing surfaces the reviewed studies revealed how well-equipped bacteria are concerning adhesion in their habitat. Thereby, surface adhesins play a key role by forming strong specific bonds. At the same time, the extensive macromolecular binding during bacterial adhesion may explain the deviations between experimental results and theoretical predictions, at least phenomenologically, see section 4.2.

4.5 Prevention of bacterial adhesion

The fundamental motivation of bacterial adhesion research is usually its prevention [Hor2010]. Tuning the surface roughness to change the contact area between a bacterium and a surface is a possibility to influence bacterial adhesion [Tay1998, Eme2006, Zha2011].
Zhang et al. measured adhesion forces between multiple bacterial probes (of *E. coli* cells) and surfaces covered with nanoparticles of different sizes. They found an increasing adhesion force for decreasing particle size. Unfortunately, the authors did not relate adhesion forces to common quantities characterizing surface roughness (e.g. rms-roughness) [Zha2011].
Besides tuning the surface roughness, another promising approach towards the control of bacterial adhesion is tuning the substrate chemistry to control interaction forces. In the oral environment, fluoridation is a long-known method to decrease caries susceptibility [Dea1938, Lev1982]. Loskill et al. investigated the effect of fluoridation on the adhesion of mouth colonizing bacteria [Los2013]. They found decreasing adhesion forces on fluoridated artificial teeth compared to non-fluoridated ones. Hence, one pathway that explains the caries reduction due to fluoridation is the formation of unfavorable adhesion condition for oral bacteria by the uptake of fluorine into teeth material [Los2013].
Instead of changing the chemistry of an existing surface, producing a new surface with less favorable adhesion conditions is a popular method. A promising technique is the formation of polymer brushes. A polymer brush coating is a dense layer of polymers standing upright next to each other with one side attached to a surface [Mil1991]. Polymer brush covered surfaces withstand protein adsorption and decrease bacterial adhesion [Jeo1991, Par1998, Raz2000, Mus2012, Wan2012, Rod2015].
Wang et al. combined the effects of surface roughness and polymer brushes [Wan2011, Wan2012] by producing surfaces covered with polymer brush micro-bollards on different length scales. For inter-bollard spacings in the range of $1\,\mu$m (which is the typical diameter of coccal bacteria like *S. aureus* or *S. epidermidis*) they found decreased bacterial adhesion, while adhesion and spreading of mammalian cells was almost unaffected.
Rodriguez-Emmenegger and co-workers used single cell force spectroscopy to study the adhesion of *Yersinia pseudotuberculosis* on different polymer brush coatings as compared to glass and polystyrene (PS) [Rod2015]. Using one and the same bacterial probe (to eliminate fluctuations due to cell-cell variations) they found strong reductions in bacterial adhesion strength on the polymer brush coated surfaces. The two best anti-adhesive surfaces provided less than one percent of the adhesion strength (force and energy) of glass or PS. Thereby, the anti-adhesive behavior was in good agreement to the anti-fouling behavior (the tendency to withstand protein coverage). This lead to speculations of the authors about a close connection between 'protein-adhesion' and bacterial adhesion. In other words, the bacteria can not attach to polymer brushes, because their surface polymers, in particular the proteinaceous, cannot [Rod2015].
As a consequence, non-proteinaceous adhesins might be able to outsmart the anti-adhesive properties of polymer brush coatings [Zen2015]. Using single cell force spectroscopy Zeng et al. revealed that S. epidermidis strain 1457 adhesion to titan is not affected by the presence of a polymer-brush layer, while mutant cells of the *S. epidermidis* strain that lack eDNA or cell wall polysaccharides were strongly affected [Zen2015]. By increasing the polymer brush density, the authors were able achieve a reduction in adhesion forces also for the wild type cells. Thus, low density polymer brushes have shown to be ineffective against bacterial strains expressing large amounts of non-proteinaceous adhesins. The underlying mechanism could be the penetration

and subsequent release of the polymer brush by the non-proteinaceous adhesins. However, this mechanism seems to be ineffective against polymer brushes featuring higher surface densities [Zen2015].

4.6 Concluding remarks and outlook

Bacterial cell force spectroscopy lead to an unprecedented understanding of bacterial adhesion [Duf2015, Agu2015b]. Quantitative results as well as insights into nanomechanical processes governing bacterial adhesion became possible [Duf2015, Agu2015b]. However, a lot of studies lack reproducibility, due to harsh treatment of the bacterial cells resulting in non-viable cells or due to incomplete information about experimental parameters [Bur2003, Vadgue2004, Kan2009]. The introduction of single cell force spectroscopy using viable bacterial cells might solve this problems [Kan2009]. Unfortunately, the technique is still an experimental niche and much remains to do: Considering that *S. aureus* alone expresses at least 21 covalently bound proteinaceous adhesins shows how spars our knowledge about the role of bacterial adhesins still is [Lin2011]. Also a theoretical model describing bacterial adhesion of different species on different surfaces is not within sight and adhesion resistant surfaces do only exist in laboratories so far. In the end, today's research only scratched the surface of the bacterial adhesion prowess.
However, the supreme discipline of bacterial cell force spectroscopy using single viable cells is on the rise, including new technological approaches like FluidFM [Bea2014b, Zen2014, Pot2015, The2015b]. In the end, bacterial adhesion research might experience golden days as sophisticated techniques are available, a lot of preliminary work has been done while many important questions still await answers.

5 Material and Methods

5.1 Substrates

Highly controlled abiotic (i.e. without any biological substances) substrates pave the way to a fundamental understanding of bacterial adhesion mechanisms. Here, monocrystalline silicon (Si) wafers featuring a native silicon oxide (SiO_2) layer of 1.7(2) nm (the number in the brackets depicts the uncertainty of the last digit) or a thermally grown SiO_2-layer of 150(2) nm are the basis of very hydrophilic and, with an additional functionalization, strongly hydrophobic substrates. Preparation and properties of all substrates are detailed in the **publication of Loskill et al. in *Langmuir* 2012 (Addendum II)** and the **publication of Thewes et al. in *Beilstein J. Nanotechnol.* 2014 (Addendum III)**.
Briefly, Si wafers were thoroughly cleaned to obtain zero degree water contact angle hydrophilic substrates. Thereby, a surface energy of 64(1) mJ/m^2 was achieved for the Si wafers with a native SiO_2-layer, the (rms) surface roughness was determined (by AFM) to 0.09(2) nm and the streaming potential of these types of surfaces was measured to be -104.4(1) mV at pH 7.3 [Bel2008]. The surface properties of the Si wafers with a thick (150 nm) SiO_2-layer do not differ significantly, see the **publication of Loskill et al. in *Langmuir* 2012 (Addendum II)**.
To obtain equally smooth hydrophobic substrates, Si wafers were covered with a self-assembled monolayer (SAM) of octadecyltrichlorosilane (OTS) molecules according to a standard protocol [Les2015]. These CH_3-terminated surfaces feature a receding water contact angle of 107(2)° with a very low hysteresis of 4°, which demonstrates their high quality. The surface energy was determined to 24(1) mJ/m^2 and a streaming potential of -80.0(1) mV at pH 7.3 was measured on these type of hydrophobic surfaces [Les2015]. OTS wafers that base on Si wafers with a native or thick SiO_2-layer do not exhibit significant differences concerning the surface properties, as detailed in the **publication of Loskill et al. in *Langmuir* 2012 (Addendum II)**.
All substrates enable the investigation of the bacterial adhesion process with controlled surface interactions and high reproducibility. As a consequence, variations concerning the adhesion of one cell on various substrates are directly related to variations of the physical interactions. The other way around, variations between different bacterial cells on one and the same substrate reveal cell-specific properties.

5.2 Bacterial strains and growth conditions

In this thesis, the non-pathogenic staphylococcal species *Staphylococcus carnosus* (strain TM300) and the opportunistic pathogenic *Staphylococcus aureus* (strain SA113) were used to study bacterial adhesion. The genome of *S. carnosus* strain, TM300, has been decoded and lacks large amounts of the adhesion factors expressed in *S. aureus* [Ros2009, Ros2010]. *S. aureus* strain SA113 is a biofilm-forming laboratory strain that serves as a platform to study cell wall linked macromolecules of this species [Max1986, Pes1999, Wei2005, Bur2013]. Accordingly, three mutant strains of *S. aureus* strain SA113, that exhibit changes in the cell wall macromolecular structure were used in this thesis. A description of the mutant cells is given in the **manuscript in Addendum V**.
All species were grown on blood-agar and for the study in the **publication of Loskill et al. in *Langmuir* 2012 (Addendum II)** cells were grown in 5 ml Mueller Hinton broth for 24 hours at 37 °C to obtain stationary phase cells. For all other studies in the thesis at hand, an overnight culture was seeded in tryptic soy broth (TSB) medium the day before each experiment. Bacteria were grown at 37 °C and 150 rpm. The next morning, 40 μl of the overnight culture were transferred into 4 ml of fresh TSB medium and incubated for another 2.5 hours to obtain exponential phase cells. Afterwards, 0.5 ml of the bacterial solution were diluted using 0.5 ml PBS (pH 7.3, ionic strength 0.1728 mol/l at 20 °C) and subsequently, washed four times, using 1 ml PBS each, to remove extracellular material. Finally, bacteria were used to prepare bacterial probes, see section 5.4.

5.3 Atomic Force Spectroscopy

The *atomic force microscope* (AFM) is a scanning probe microscopy technique that uses intermolecular forces to measure surface profiles [Bin1986, Bin1987]. Detailed information about the AFM are compiled in various textbooks [Sar1991, Bhu2004, Sam2006, Eat2010] and review articles [Qua1994, But2005, Seo2007]. Additional to the investigation of surface topographies, the AFM is capable to quantify surface properties like elasticity or adhesion with nm spatial and pN force resolution:
In *force spectroscopy mode*, the AFM tip is lowered to and retracted from a surface at constant (x,y)-position. Thereby, cantilever deflection is monitored as a function of the expansion of the piezo-motor controlling the movement in z-direction. Subsequently, the raw data may be processed into *force/distance curves* that display the force between tip and surface as a function of their separating distance. A force/distance curve is strongly influenced by various internal and external parameters. For a detailed (theoretical) description of force/distance curves, the reader is referred to the literature mentioned in the beginning.
A general strength of the AFM is its undemanding nature concerning surrounding medium and sample preparation. Hence, the AFM was identified as a very suitable tool in biological research [Han1998, Duf2003]. Using chemically modified AFM tips or even biological objects attached to an AFM cantilever instead of a tip, AFM is a powerful technique to study biological adhesion [Cla2000, Hör2003, Dup2010, Duf2013, Duf2015, Agu2015b]. In this thesis, atomic force spectroscopy with bacterial cells attached to an AFM cantilever - *bacterial cell force spectroscopy* -

is the method of choice to study bacterial adhesion.

5.4 Bacterial probes and force/distance curves

Bacterial cell force spectroscopy relies on bacterial probes. Bacterial probes are AFM cantilevers with a single bacterial cell or a cluster of bacterial cells attached in order to investigate bacterial adhesion properties. The history of bacterial probes has been introduced in section 4.1. Different techniques to produce bacterial probes exist in literature [Low2001, Bea2014b, Zen2014, Pot2015] including our own [Los2012b, The2014, The2015a]. *Bacterial cluster probes* are easier in production and result in better statistics per probe, however, no quantitative measurements are possible as the number of cells that interact with a surface is unknown. Hence, experimental values measured with different multiple bacterial probes are not comparable. *Single bacterial probes* are complex in terms of production, but enable for a quantitative characterization of the bacterial adhesion process. Fundamental requirements of bacterial probes are detailed in the **publication of Thewes et al. in *Eur. Phys. J. E* 2015 (Addendum I)** as well as protocols to produce bacterial cluster probes and single bacterial probes with one single, living, bacterial cell.

The outcome of bacterial cell force spectroscopy measurements are force/distance curves. Besides a step by step recipe to produce bacterial probes, the **publication of Thewes et al. in *Eur. Phys. J. E* 2015 (Addendum I)** details the evaluation of force/distance curves with bacterial probes. Several important quantities in a force/distance curve that characterize the bacterial adhesion process are sketched in fig. 5.1 and are described briefly in the following:

The approach part is characterized by the distance between bacterium and surface where attractive forces start acting - the *snap-in distance* - as well as the maximum attractive force during approach - the *snap-in force*. It is worth noting here (and will be described in detail in chap. 6) that the studies in this thesis are the first that recognized and investigated the bacterial snap-in processes systematically.
The retraction part is mainly characterized by the maximum force acting between bacterium and surface - taken as *adhesion force* - as well as by the work necessary to completely separate bacterium and surface - the *adhesion energy* - that is calculated by integrating the area above the retraction part of a force/distance curve. In addition, the distance where the bacterium loses contact to the surface can be evaluated, and is referred to as the *rupture length*.

In this thesis, bacterial probes are an essential tool to study the nature of bacterial adhesion processes and these probes are produced according to the protocols in the **publication of Thewes et al. in *Eur. Phys. J. E* 2015 (Addendum I)**.

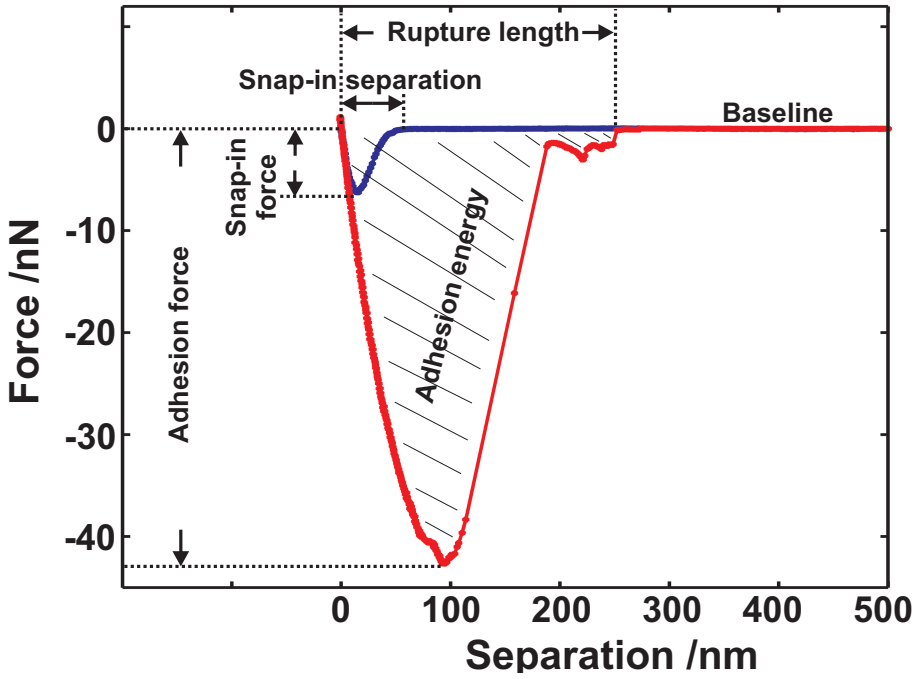

Figure 5.1: Representative force/distance curve of a single bacterial probe as well as basic quantities characterizing the bacterial adhesion process. The approach (retraction) part of the force/distance curve is shown in blue (red). The curve depicts the adhesion between a single *S. aureus* cell and a hydrophobized Si wafer in PBS buffer. Note the density of data points as well as the extend of the snap-in event in the approach part of the force/distance curve.

6 Results: Bacterial Adhesion to abiotic Surfaces

Today, there exists nor a comprehensive understanding of the bacterial adhesion process in general neither of bacterial adhesion to abiotic surfaces in particular. Accordingly, the construction of a theoretical model describing bacterial adhesion is an objective of current research.
As detailed in chap. 4 and section 5.4, bacterial cell force spectroscopy enables the quantitative study of bacterial adhesion to various surfaces. The influence of xDLVO forces on bacterial adhesion is an important issue of bacterial cell force spectroscopy studies, see section 4.2. Thereby, xDLVO theory is in most cases able to qualitatively corroborate the force spectroscopy results, while quantitative predictions always fail due to the complex nature of the bacterial adhesion process, see section 3.1 and chap. 4. Besides electrostatic forces, acid-base interactions and van der Waals (vdW) forces constitute the most important forces considered in xDLVO theory, see section 3.2.

Studying the influence of vdW forces with multiple bacterial probes. VdW forces are sensitive to a materials polarizability. Hence, the vdW potential of a silicon (Si) substrate is tunable by tuning its SiO_2-layer thickness. It was shown that vdW forces influence the adsorption of proteins [Bel2008] and to investigate if bacterial adhesion is also affected by vdW forces, adhesion forces of *S. carnosus* cells to Si substrates with a SiO_2-layer thickness of 2 nm and 150 nm were measured by bacterial cell force spectroscopy. The results that are compiled in the **publication of Loskill et al. in *Langmuir* 2012 (Addendum II)** reveal two times higher adhesion forces of *S. carnosus* cells to Si substrates with the thin SiO_2-layer as compared to Si substrates with the thick SiO_2-layer. Because both Si substrates feature the same short-range interactions, these measurements evidence a direct influence of vdW forces on bacterial adhesion. The force spectroscopy results were supported by macroscopic adsorption measurements and were qualitatively corroborated by theoretical modeling using DLVO theory and incorporating the different Hamaker constants of the substrates with thin and thick Si-oxide layer.
Additionally, the influence of vdW forces on a pair of substrates that exhibit very low surface energies was measured by adding a hydrophobic monolayer (octadecyltrichlorosilane, OTS) onto the Si wafers. Also on hydrophobic substrates force spectroscopy measurements reveal an influence of vdW forces on bacterial adhesion. However, a direct comparison between the force measurements on the hydrophilic Si substrates and the hydrophobic OTS substrates is not possible, because multiple bacterial probes were used to achieve the results in the **publication of Loskill et al. in *Langmuir* 2012 (Addendum II)**.

Studying bacterial adhesion on hydrophobic substrates using single bacterial probes. The influence of the hydrophobic interaction (see section 3.2.1) on the adhesion of staphylocci was investigated by single cell force spectroscopy. Therefor, hydrophilic Si wafers and hydrophobic OTS wafers (both with a thin SiO_2-layer) were probed with one and the same bacterial cell. These experiments reveal that *S. carnosus* cells (note that the cells in this study, where cultured differently compared to the cells used to study the influence of vdW forces, see section 5.2) adhere at least one order of magnitude stronger to hydrophobic OTS substrates than to hydrophilic Si substrates. This means that - if present - the hydrophobic interaction is the key factor defining the strength of bacterial adhesion.
Further measurements with single bacterial probes reveal that the bacterial adhesion process on hydrophobic substrates is very robust: Consecutive force/distance curves measured with one bacterial probe do almost not differ in the basic quantities that are described in section 5.4.
In contrast, these quantities may exhibit large differences for force/distance curves of different cells, even of one bacterial culture, i.e. bacterial cells behave like 'individuals'.
The approach parts of force/distance curves between single *S. carnosus* cells and OTS substrates show a long-ranging attraction between cell and substrate ('bacterial snap-in'). This attraction is of much longer range than xDLVO forces could explain!

All these results are written down in the **publication of Thewes et al. in *Beilstein J. Nanotechnol.* 2014 (Addendum III)** and in order to understand the details of the experimental findings a simple model was introduced. In this model, bacterial adhesion is solely caused by the tethering of bacterial surface polymers and these polymers behave like elastic springs. Subsequently, the experimental results may be explained in terms of the model: i) Strong adhesion forces on hydrophobic substrates are caused by the excessive binding of bacterial cell wall polymers (proteins) via the hydrophobic interaction. On hydrophilic substrates protein binding is almost absent, hence, adhesion forces are low. ii) The robustness of the bacterial adhesion process on hydrophobic substrates is a result of a large number of proteins that tether to the surface, thus suppressing stochastic fluctuations. iii) The individuality of bacterial cells is a result of differences of surface macromolecules (in mechanical properties and number) between bacterial cells. iv) The long-ranging attraction upon approach of a bacterium to a hydrophobic surface is caused by cell wall proteins that tether to the surface and subsequently pull the cell to the surface.

To conclude, the most important result of the **publication of Thewes et al. in *Beilstein J. Nanotechnol.* 2014 (Addendum III)** is a new model describing bacterial adhesion. By assuming that the contact between a bacterial cell and a surface is exclusively generated by tethered macromolecules, the influence of xDLVO forces and the failing of xDLVO theory in describing the bacterial adhesion process (see chap. 4) are satisfied at the same time: While xDLVO forces cause the binding of macromolecules yielding the influence of xDLVO forces, the consecutive stretching and detaching of those causes the break down of xDLVO theory in regard to bacterial adhesion.

Attachment mechanisms of *Staphylococci*. The long-ranging attraction between single *S. carnosus* cells and hydrophobic surfaces was investigated for the first time in the thesis at hand and the **publication of Thewes et al. in *Beilstein J. Nanotechnol.* 2014 (Addendum III)** provides the first description of the bacterial snap-in process in literature. Although a

mechanism to explain the bacterial snap-in was proposed, further details of this process were obscure.
To gain a fundamental understanding of the bacterial snap-in process, single cell force spectroscopy measurements with pathogenic *Staphylococcus aureus* and hydrophobic OTS substrates were conducted. These experiments were accompanied by Monte Carlo simulations of the model that has been introduced in the preceding paragraph and that is detailed in the **publication of Thewes et al. in *Beilstein J. Nanotechnol.* 2014 (Addendum III)**.
The results of this approach, that combines experimental and computational expertise, are compiled in the **publication of Thewes et al. in *Soft Matter* 2015 (Addendum IV)**.
Experimental data revealed snap-in distances of more than 50 nm between single *S. aureus* cells and hydrophobic OTS surfaces. To clarify the origin of the snap-in, force/distance curves were conducted where the approach of the cell was stopped during the attractive part of the approach curve (see negative portion of the approach curve in fig. 5.1) and the cell was subsequently retracted from the surface. For this method, we coined the term 'partitioned' force/distance curves in order to stress that it is possible to measure a full force/distance curve also part by part. Note that this study is the first describing these kind of force/distance measurements. By retracting the cell during the snap-in process and before full contact is achieved, the partitioned force/distance curves enable the investigation of the nature of the contact that causes the attraction upon approach of a bacterial cell to a hydrophobic substrate. That way, partitioned force/distance curves with single *S. aureus* cells adhering to OTS substrates proofed the macromolecular origin of the snap-in process: The approach was stopped at different stages of the snap-in process and partitioned force/distance curves testing only the very beginning of the snap-in already showed the consecutive stretching and rupturing of bacterial surface macromolecules upon retraction.

Furthermore, a comparison between experimental and simulated full and partitioned force/-distance curves revealed that the contact formation of bacterial cells relies on the binding of thermally fluctuating cell wall macromolecules of different stiffness. These macromolecules bind to a surface in close proximity and pull the bacterium to the surface. For details of these findings, the reader is referred to the **publication of Thewes et al. in *Soft Matter* 2015 (Addendum IV)**.
In order to investigate the nature of the contact-forming macromolecules more closely, *S. aureus* cells were treated with glutaraldehyde or protease. Both reagents modify the cell wall proteins by crosslinking proteins (glutaraldehyde) or cutting peptide bonds (protease) and that way, both reagents decrease the protein dynamics. Thus, if cell wall proteins cause the snap-in process, glutaraldehyde as well as protease should decrease the extend of this process. Finally, force/distance measurements with single bacterial cells before and after protein-modifying treatments reveal that indeed bacterial cell wall proteins cause the long-ranging attraction during bacterial contact formation.

To summarize, the presented research project provides the first combination of experimental and computational approaches (using the introduced model) to investigate bacterial adhesion. This powerful combination revealed and explained a to date unknown attachment mechanism that enables bacterial cells to attach to surfaces 'beyond the range of classic surface forces', see the **publication of Thewes et al. in *Soft Matter* 2015 (Addendum IV)**.

The adhesion of *Staphylococcus aureus* to abiotic substrates. The results that have been presented so far, revealed the importance of the hydrophobic interaction for staphylococcal adhesion and clarified the contact formation process of *staphylococci* on hydrophobic substrates. What has not been studied in detail, yet, is the large difference that force/distance measurements exhibited that were performed with single bacterial cells on hydrophobic and hydrophilic substrates, see the **publication of Thewes et al. in *Beilstein J. Nanotechnol.* 2014 (Addendum III)**. In order to investigate the origin of these differences and to deduce general mechanisms of bacterial adhesion on abiotic substrates, the adhesion of *S. aureus* was studied on hydrophilic and hydrophobized Si wafers. Thereby, single cell force spectroscopy was combined with genetic tools and accompanied by computer simulations of an improved version of the model used in the **publication of Thewes et al. in *Soft Matter* 2015 (Addendum IV)**. The results of this approach are particularized in the **manuscript in Addendum V** and are briefly presented in the following:

A comparison between experimental and simulated force/distance curves reveals fundamental differences of bacterial adhesion mechanisms on hydrophilic and hydrophobic substrates: On hydrophobic substrates, bacterial adhesion is mediated by a large number of bacterial surface polymers (proteins) that attach the substrate surface via the hydrophobic interaction. The result is a large adhesion force and very stable force/distance curves (in terms of the basic quantities described in section 5.4). In contrast, on hydrophilic substrates, only few bacterial surface polymers tether to the substrate surface with a binding energy that is higher compared to hydrophobic substrates. As van der Waals and electrostatic interactions are usually an order of magnitude smaller than the hydrophobic interaction, it was concluded that polymer tethering on hydrophilic substrates bases on hydrogen bond formation. Yet, on hydrophilic substrates, the low amount of tethering polymers results in small adhesion forces and force/distance curves with strongly fluctuating shapes.
Hence, by comparing experimental and simulated force/distance curves it is possible to evidence that the difference between bacterial adhesion on hydrophilic and hydrophobic substrates is mainly a result of the different numbers of cell wall macromolecules that tether to the surfaces during the time of contact.
In general, the number of cell wall polymers that attach to a substrate in certain time interval, is given by (if no detachment occurs in the respective time interval) the product of the attachment rate and the number of polymers available to attach. Therefore, two reasons are identified that may explain the smaller number of tethering surface polymers on hydrophilic substrates compared to hydrophobic ones: i) Bacterial surface polymers that are able to form hydrogen bonds with hydrophilic substrates are less numerous on the bacterial cell surface than those that tether to hydrophobic substrates, ii) the formation of hydrogen bonds leads to a decreased attachment rate compared to the attachment of polymers on hydrophobic substrates.

Furthermore, single cell force spectroscopy measurements using *S. aureus* wild type and mutant cells as well as cells of apathogenic *S. carnosus* revealed the following results:

- Pathogenic *S. aureus* cells adhere much stronger to hydrophilic and to hydrophobic substrates compared to apathogenic *S. carnosus* cells.

- Surface proteins that are covalently bound to the bacterial cell wall are much more im-

portant for the adhesion to hydrophobic substrates than for the adhesion to hydrophilic substrates.

- The bacterial surface polymers that mediate adhesion to hydrophobic substrates are, at least partially, different polymers than that mediating adhesion to hydrophilic substrates.

- The cell surface charge influences bacterial adhesion to hydrophilic substrates, yet not to hydrophobic substrates.

- Changes of the cell wall teichoic acids decrease adhesion forces to hydrophobic substrates.

To infer, the findings that were illustrated in this paragraph elucidated fundamental mechanisms that govern the adhesion of *Staphylococcus aureus* on abiotic substrates, see the **manuscript in Addendum V**. The results give strong evidences that it is possible to describe the bacterial adhesion process by solely taking into account the cell wall polymers that tether to a surface and, hence, corroborate the model introduced in this thesis.

The interaction area of cocci bacteria. In the experimental series reported before, the interaction strength between bacteria and different substrates was investigated. Yet, the size of the contact area that is actually probed by performing force/distance curves with a single bacterial cell on a solid substrate remained unclear and no measurements of this area are described in literature to date. In this section, a method to measure the contact area of bacteria directly is described. This method relies on the huge difference in adhesion forces of bacteria (e.g. of *S. carnosus*) on hydrophilic and hydrophobic substrates (see section 4.2 and the **publication of Thewes et al. in *Beilstein J. Nanotechnol.* 2014 (Addendum III)** as well as the **manuscript in Addendum V**).

The first and most crucial experimental step was to produce a substrate, that features a very sharp transition zone (width of less than 20 nm) between a hydrophilic and a hydrophobic surface area with a negligible high step (≈ 2 nm) as compared to a bacterial cell. Adhesion forces of a single bacterial cell, measured by force/distance curves, are very small on the hydrophilic part of the substrate and much higher on the hydrophobic part. Intermediate adhesion forces are revealed by force/distance measurements on the transition zone, where parts of the bacterial cell probe the hydrophilic and the hydrophobic surface area. By moving a single bacterial cell (attached to an AFM cantilever) in small steps across the transition zone and by determining the adhesion force with a force/distance curve in each step, the radius of the contact area is accessible. Therefor, the adhesion force measured at each point is plotted against the position of the bacterial probe. By inspecting the progression of adhesion forces between the low force values on the hydrophilic and the high forces on the hydrophobic surface area, the radius of the contact area is determined. Besides the adhesion forces, also the progression of adhesion energies may be utilized to determine the contact radius. In general, the experimental procedure is similar to displacement measurement of a light point on a segmented photodiode.

The method as well as results of a first series of measurements are detailed in the **manuscript in Addendum VI**. The results provide a proof of concept and reveal contact radii between 20 nm and 250 nm for different *S. carnosus* cells. Hence, the individuality of bacterial cells

that showed up in adhesion forces (see the **publication of Thewes et al. in *Beilstein J. Nanotechnol.* 2014 (Addendum III)**), also shows up in the contact radius. Contact radii determined according to the progression of adhesion forces can differ from the radii determined according to the adhesion energy progression. This difference can be attributed to molecular details of the bacterium/surface contact, see the **manuscript in Addendum VI**. Thus, the method to measure bacterial contact radii might reveal molecular details of the assembly of bacterial surface polymers. However, further measurements will be necessary at this point.
To understand details of the experimental results, the experimental procedure to measure the contact radius of a bacterial cell was modeled using the approach described in the preceding paragraph and that is detailed in the **manuscript in Addendum V**. First results reveal large differences between the contact radius of a model bacterial cell and its 'real' counterpart. As the model assumes equally distributed surface polymers this might be a hint towards a formation of adhesion clusters on the bacterial surface.

Finally, the method to measure the contact radius of a single bacterial cell yields promising data. However, further effort will be necessary to improve the experimental setup, produce experimental data and interpret the data in combination with the simulation approach.

7 Summary and Outlook

The bacterial adhesion process in general is significantly more complex than adhesion scenarios involving only abiotic, 'bare' materials. In this thesis, however, fundamental mechanisms of bacterial adhesion were to be studied and the use of abiotic surfaces decreased the complexity of the process, since the properties of those surfaces are well-controlled and highly reproducible. Nevertheless, also in nature, bacteria might interact with similar abiotic surfaces, e.g. on implants or catheters.

The method of choice to study bacterial adhesion was AFM cell force spectroscopy paired with Monte Carlo simulations. The key result of this work is that the bacterial adhesion process can be attributed exclusively to the interaction between bacterial surface polymers and a substrate. In consequence, to comprehend bacterial adhesion, a basic understanding of bacterial surface polymer mechanics and polymer/surface interactions is of utmost importance.

Probing clusters of bacteria that adhered to substrates with identical surface properties (roughness, chemical composition, surface energy), yet different chemical compositions of the subsurface revealed differences in adhesion force. Since all other parameters were held constant, only differences in vdW forces can be responsible for this. The results are in accordance with those of proteins and polymer films on the mentioned substrates.

To reveal further details of the bacterial adhesion process and especially of the role of the cell wall macromolecules, the experimental setup to study bacterial adhesion was improved in order to be able to characterize bacterial adhesion in a quantitative way on a single cell level. Finally, a protocol was drawn up to attach single bacterial cells to AFM cantilevers in a reproducible way with relatively high throughput.

Subsequently, single cell force spectroscopy was used to measure adhesion of single bacterial cells on hydrophilic Si wafers and hydrophobized Si wafers. Upon approach of a cell to hydrophobic substrates, a long-ranging attractive force was measured (for *S. carnosus* and *S. aureus* cells) that was absent on hydrophilic substrates. This attraction ('bacterial snap-in') that was described for the first time in this thesis, was of much longer range ($> 50\,\mathrm{nm}$) than classic surface forces could explain.
Upon retraction, adhesion forces were much larger on hydrophobic substrates as compared to hydrophilic substrates. Furthermore, the shape of force/distance curves captured with one and the same cell on both substrates exhibited significant differences.
These results called for a model to capture the molecular details of the experimental outcome: In the model, a bacterial cell is idealized as an inelastic sphere that is covered by elastic polymers with different mechanical properties. This model was analyzed using Monte Carlo simulations and these simulations evidenced that the simple model is able to capture basic

experimental observations:

A comparison between experimental and simulated force/distance curves revealed that the bacterial snap-in is a result of thermally fluctuating cell wall proteins of different stiffness that attach to a surface in close proximity and subsequently pull the bacterial cell to the surface.

Experiments and simulations also revealed that the huge difference in bacterial adhesion to hydrophilic and hydrophobic substrates is a result of different numbers of tethering bacterial surface polymers. On hydrophobic substrates large amounts of cell wall polymers (proteins) bind to the surface via the hydrophobic interaction. In contrast, on hydrophilic substrates cell wall polymers tether less numerous and binding relies on the formation of hydrogen bonds.

By performing single cell force spectroscopy with *S. aureus* mutant cells that exhibit changes in the cell wall polymer composition it was shown that covalently bound cell wall proteins are much more important for the adhesion on hydrophobic than on hydrophilic substrates. Furthermore, a comparison between wild type and mutant cells revealed that the bacterial surface charge influences adhesion to hydrophilic substrates, yet not to hydrophobic ones.

As a further refinement to understand bacterial adhesion, a method was introduced to determine the contact area between a bacterial cell and a substrate directly. Therefor, a substrate that features a very sharp transition ($< 20\,\mathrm{nm}$) between a very hydrophilic and a strongly hydrophobic surface area was produced. Subsequently, a single bacterial probe was moved stepwise across the transition zone and a force/distance curve was performed at each point. This procedure allows for the determination of the contact radius of the cell by inspecting the progression of the adhesion forces during the pathway from the hydrophilic to the hydrophobic surface area. A proof of concept is given and demonstrates the big potential of the technique, in particular by adding simulated force/distance curves. Yet, further improvements of the technique as well as additional measurements are necessary.

This work investigated fundamental binding properties of staphylococcal cells on abiotic substrates. Direct follow-up studies should address the role of teichoic acids in staphylococcal adhesion to abiotic substrates by using single cell force spectroscopy.
Furthermore, the model should be improved in order to capture more complex polymer binding scenarios.
An important future step will be to translate the results of this thesis to i) other bacterial species and ii) to adhesion processes involving more complex biotic substrates.
The translation to different bacterial species is rather straightforward as bacterial cells in general exhibit surface polymers 'designed' to fulfill adhesion tasks. The translation in the second case requires greater efforts. On biotic substrates the tethering of bacterial surface polymers is more complex due the possible macromolecular nature of the adhesion partner, however, the general result that the number of tethering polymers is a major parameter controlling the strength of adhesion, will still be valid. Nevertheless, additional complexity may result out of more complex binding potentials between bacterial surface polymers and other macromolecules.

To conclude, bacterial cell force spectroscopy turns out to be a powerful tool to study bacterial adhesion. By coupling the experimental results with numerical simulations, the results can be

comprehended on a molecular level. In turn, predictions of the simulations can give hints of how to change experimental parameters. In the future, this will be more and more important when moving to biotic surfaces.

Bibliography

[Agu2015a] S. Aguayo, N. Donos, D. Spratt, and L. Bozec, *Nanoadhesion of Staphylococcus aureus onto Titanium Implant Surfaces*, Journal of dental research **94** (2015) 1078–1084. ↑4.2.4, 4.4.2

[Agu2015b] S. Aguayo, N. Donos, D. Spratt, and L. Bozec, *Single-bacterium nanomechanics in biomedicine: unravelling the dynamics of bacterial cells*, Nanotechnology **26** (2015) 062001. ↑3.1, 4.1, 4.3, 4.6, 5.3

[Abu2002] N. I. Abu-Lail and T. A. Camesano, *Elasticity of Pseudomonas putida KT2442 surface polymers probed with single-molecule force microscopy*, Langmuir **18** (2002) 4071–4081. ↑4.1

[Abu2003a] N. I. Abu-Lail and T. A. Camesano, *Role of Ionic Strength on the Relationship of Biopolymer Conformation, DLVO Contributions, and Steric Interactions to Bioadhesion of Pseudomonas putida KT2442*, Biomacromolecules **4** (2003) 1000–1012. ↑4.1, 4.2.2

[Abu2003b] N. I. Abu-Lail and T. A. Camesano, *Role of lipopolysaccharides in the adhesion, retention, and transport of Escherichia coli JM109*, Environmental science & technology **37** (2003) 2173–2183. ↑4.4.1

[Abu2003c] N. Abu-Lail and T. Camesano, *Polysaccharide properties probed with atomic force microscopy*, Journal of Microscopy **212** (2003) 217–238. ↑4.1

[Abu2006] N. I. Abu-Lail and T. A. Camesano, *Specific and Nonspecific Interaction Forces Between Escherichia coli and Silicon Nitride, Determined by Poisson Statistical Analysis*, Langmuir **22** (2006) 7296–7301. ↑4.2.4

[Als2013] D. Alsteens, A. Beaussart, S. Derclaye, S. El-Kirat-Chatel, H. R. Park, P. N. Lipke, and Y. F. Dufrêne, *Single-cell force spectroscopy of Als-mediated fungal adhesion*, Analytical Methods **5** (2013) 3657–3662. ↑4.3

[Ata2007] A. Atabek and T. A. Camesano, *Atomic force microscopy study of the effect of lipopolysaccharides and extracellular polymers on adhesion of Pseudomonas aeruginosa*, Journal of bacteriology **189** (2007) 8503–8509. ↑4.4.1

[Ata2008] A. Atabek, Y. Liu, P. A. Pinzón-Arango, and T. A. Camesano, *Importance of LPS structure on protein interactions with Pseudomonas aeruginosa*, Colloids and Surfaces B: Biointerfaces **67** (2008) 115–121. ↑4.2.4, 4.4.1

[Bas1999] A. Baszkin and W. Norde, *Physical chemistry of biological interfaces*, CRC Press, 1999. ↑4.2.2

[Bea2013] A. Beaussart, S. El-Kirat-Chatel, P. Herman, D. Alsteens, J. Mahillon, P. Hols, and Y. F. Dufrêne, *Single-cell force spectroscopy of probiotic bacteria*, Biophysical journal **104** (2013) 1886–1892. ↑4.2.3, 4.3, 4.4.4

[Bea2014a] A. Beaussart, A. E. Baker, S. L. Kuchma, S. El-Kirat-Chatel, G. A. O'Toole, and Y. F. Dufrêne, *Nanoscale adhesion forces of Pseudomonas aeruginosa type IV pili*, ACS nano **8** (2014) 10723–10733. ↑4.4.4

[Bea2014b] A. Beaussart, S. El-Kirat-Chatel, R. M. A. Sullan, D. Alsteens, P. Herman, S. Derclaye, and Y. F. Dufrêne, *Quantifying the forces guiding microbial cell adhesion using single-cell force spectroscopy*, Nature protocols **9** (2014) 1049–1055. ↑4.1, 4.2.3, 4.6, 5.4

[Bea2014c] A. Beaussart, C. Péchoux, P. Trieu-Cuot, P. Hols, M.-Y. Mistou, and Y. F. Dufrêne, *Molecular mapping of the cell wall polysaccharides of the human pathogen Streptococcus agalactiae*, Nanoscale **6** (2014) 14820–14827. ↑4.1

[Bec2009] D. Becher, K. Hempel, S. Sievers, D. Zühlke, J. Pané-Farré, A. Otto, S. Fuchs, D. Albrecht, J. Bernhardt, and S. Engelmann, *A proteomic view of an important human pathogen - towards the quantification of the entire Staphylococcus aureus proteome*, PLoS One **4** (2009) e8176. ↑3.1

[Bel2008] M. Bellion, L. Santen, H. Mantz, H. Hähl, A. Quinn, A. Nagel, C. Gilow, C. Weitenberg, Y. Schmitt, and K. Jacobs, *Protein adsorption on tailored substrates: long-range forces and conformational changes*, Journal of Physics: Condensed Matter **20** (2008) 404226. ↑3.2.1, 3.2.1, 4.2.3, 5.1, 6

[Bev2001] T. J. Beveridge, *Use of the Gram stain in microbiology*, Biotechnic & Histochemistry **76** (2001) 111–118. ↑3.1

[Bhu2004] Bhushan (Hrsg.), *Handbook of nanotechnology*, Springer, 2004. ↑5.3

[Bin1986] G. Binnig, C. F. Quate, and Ch. Gerber, *Atomic Force Microscope*, Phys. Rev. Lett. **56** (1986) 930–933. ↑4.1, 5.3

[Bin1987] G. Binnig, Ch. Gerber, E. Stoll, T. R. Albrecht, and C. F. Quate, *Atomic resolution with atomic force microscope*, Surface Science **189-190** (1987) 1 –6. ↑5.3

[Bis2004] M. Bischoff, P. Dunman, J. Kormanec, D. Macapagal, E. Murphy, W. Mounts, B. Berger-Bächi, and S. Projan, *Microarray-based analysis of the Staphylococcus aureus σB regulon*, Journal of Bacteriology **186** (2004) 4085–4099. ↑4.4.3

[Bok2008] N. P. Boks, H. J. Busscher, H. C. van der Mei, and W. Norde, *Bond-Strengthening in Staphylococcal Adhesion to Hydrophilic and Hydrophobic Surfaces Using Atomic Force Microscopy*, Langmuir **24** (2008) 12990–12994. ↑4.2.3, 4.2.4, 4.3

[Bos1999] R. Bos, H. C. van der Mei, and H. J. Busscher, *Physico-chemistry of initial microbial adhesive interactions - its mechanisms and methods for study*, FEMS Microbiology Reviews **23** (1999) 179–230. ↑1, 4.1, 4.2

[Bow1991] W. Bowen, K. Schilling, E. Giertsen, S. Pearson, S. Lee, A. Bleiweis, and D. Beeman, *Role of a cell surface-associated protein in adherence and dental caries.*, Infection and immunity **59** (1991) 4606–4609. ↑4.4.2

[Bra2008] A. Brand, J. D. Barnes, K. S. Mackenzie, F. C. Odds, and N. A. Gow, *Cell wall glycans and soluble factors determine the interactions between the hyphae of Candida albicans and Pseudomonas aeruginosa*, FEMS microbiology letters **287** (2008) 48–55. ↑4.4.4

[Bur2003] G. A. Burks, S. B. Velegol, E. Paramonova, B. E. Lindenmuth, J. D. Feick, and B. E. Logan,

Macroscopic and nanoscale measurements of the adhesion of bacteria with varying outer layer surface composition, Langmuir **19** (2003) 2366–2371. ↑4.4.1, 4.6

[Bur2013] S. Bur, K. T. Preissner, M. Herrmann, and M. Bischoff, *The Staphylococcus aureus extracellular adherence protein promotes bacterial internalization by keratinocytes independent of fibronectin-binding proteins*, Journal of Investigative Dermatology **133** (2013) 2004–2012. ↑5.2

[Bus1987] H. J. Busscher and A. H. Weerkamp, *Specific and non-specific interactions in bacterial adhesion to solid substrata*, {FEMS} Microbiology Letters **46** (1987) 165 –173. ↑4.1, 4.2

[Bus2006] H. J. Busscher and H. C. van der Mei, *Microbial adhesion in flow displacement systems*, Clinical microbiology reviews **19** (2006) 127–141. ↑4.1

[Bus2007] H. J. Busscher, B. van de Belt-Gritter, R. J. Dijkstra, W. Norde, F. C. Petersen, A. A. Scheie, and H. C. van der Mei, *Intermolecular forces and enthalpies in the adhesion of Streptococcus mutans and an antigen I/II-deficient mutant to laminin films*, Journal of bacteriology **189** (2007) 2988–2995. ↑4.4.2, 4.4.3

[Bus2008] H. J. Busscher, R. J. B. Dijkstra, D. E. Langworthy, D. I. Collias, D. W. Bjorkquist, M. D. Mitchell, and H. C. V. der Mei, *Interaction forces between waterborne bacteria and activated carbon particles*, Journal of Colloid and Interface Science **322** (2008) 351 –357. ↑4.4.5

[But2005] H.-J. Butt, B. Cappella, and M. Kappl, *Force measurements with the atomic force microscope: Technique, interpretation and applications*, Surface science reports **59** (2005) 1–152. ↑5.3

[Cai2005] T. L. Cail and M. F. H. Jr., *The effects of solution chemistry on the sticking efficiencies of viable Enterococcus faecalis: An atomic force microscopy and modeling study*, Geochimica et Cosmochimica Acta **69** (2005) 2959 –2969. ↑4.1, 4.2.2

[Cam2000] T. A. Camesano and B. E. Logan, *Probing Bacterial Electrosteric Interactions Using Atomic Force Microscopy*, Environmental Science & Technology **34** (2000) 3354–3362. ↑4.1, 4.4.1

[Cam2002] T. A. Camesano and N. I. Abu-Lail, *Heterogeneity in bacterial surface polysaccharides, probed on a single-molecule basis*, Biomacromolecules **3** (2002) 661–667. ↑4.1

[Cha2005] T. Chavakis, K. Wiechmann, K. T. Preissner, and M. Herrmann, *Staphylococcus aureus interactions with the endothelium*, Thromb Haemost **94** (2005) 278–285. ↑3.1

[Cha2010] M. N. Chandraprabha, P. Somasundaran, and K. A. Natarajan, *Modeling and analysis of nanoscale interaction forces between Acidithiobacillus ferrooxidans and AFM tip*, Colloids and Surfaces B: Biointerfaces **75** (2010) 310 –318. ↑4.2.2

[Che2004] A. L. Cheung, A. S. Bayer, G. Zhang, H. Gresham, and Y.-Q. Xiong, *Regulation of virulence determinants in vitro and in vivo in Staphylococcus aureus*, FEMS Immunology & Medical Microbiology **40** (2004) 1–9. ↑3.1

[Cla2006] S. R. Clarke and S. J. Foster, *Surface adhesins of staphylococcus aureus*, 2006, pp. 187 –224. ↑3.1, 4.4.3

[Col2009] J. R. Cole, Q. Wang, E. Cardenas, J. Fish, B. Chai, R. J. Farris, A. Kulam-Syed-Mohideen, D. M. McGarrell, T. Marsh, and G. M. Garrity, *The Ribosomal Database Project: improved alignments and new tools for rRNA analysis*, Nucleic acids research **37** (2009) D141–D145. ↑3.1

[Con1996] I. Connell, W. Agace, P. Klemm, M. Schembri, S. Mărild, and C. Svanborg, *Type 1 fimbrial expression enhances Escherichia coli virulence for the urinary tract*, Proceedings of the National Academy of Sciences **93** (1996) 9827–9832. ↑4.4.4

[Con2001] R. F. Considine, C. J. Drummond, and D. R. Dixon, *Force of interaction between a biocolloid and an inorganic oxide: complexity of surface deformation, roughness, and brushlike behavior*, Langmuir **17** (2001) 6325–6335. ↑4.1

[Cos1987] J. W. Costerton, K. J. Cheng, G. G. Geesey, T. I. Ladd, J. C. Nickel, M. Dasgupta, and T. J. Marrie, *Bacterial Biofilms in Nature and Disease*, Annual Review of Microbiology **41** (1987) 435–464. ↑1

[Cos1999] J. W. Costerton, P. S. Stewart, and E. P. Greenberg, *Bacterial Biofilms: A Common Cause of Persistent Infections*, Science **284** (1999) 1318–1322. ↑1

[Cra2004] L. Craig, M. E. Pique, and J. A. Tainer, *Type IV pilus structure and bacterial pathogenicity*, Nature Reviews Microbiology **2** (2004) 363–378. ↑4.4.3

[Cro2007] S. E. Cross, J. Kreth, L. Zhu, R. Sullivan, W. Shi, F. Qi, and J. K. Gimzewski, *Nanomechanical properties of glucans and associated cell-surface adhesion of Streptococcus mutans probed by atomic force microscopy under in situ conditions*, Microbiology **153** (2007) 3124–3132. ↑4.4.2

[Cla2000] H. Clausen-Schaumann, M. Seitz, R. Krautbauer, and H. E. Gaub, *Force spectroscopy with single bio-molecules*, Current opinion in chemical biology **4** (2000) 524–530. ↑4.1, 5.3

[Das2011a] T. Das, B. P. Krom, H. C. van der Mei, H. J. Busscher, and P. K. Sharma, *DNA-mediated bacterial aggregation is dictated by acid–base interactions*, Soft Matter **7** (2011) 2927–2935. ↑4.2.4, 4.4.5

[Das2011b] T. Das, P. K. Sharma, B. P. Krom, H. C. van der Mei, and H. J. Busscher, *Role of eDNA on the adhesion forces between Streptococcus mutans and substratum surfaces: influence of ionic strength and substratum hydrophobicity*, Langmuir **27** (2011) 10113–10118. ↑4.2.2, 4.2.4, 4.3, 4.4.5

[Dav2000] M. E. Davey and G. A. O'toole, *Microbial biofilms: from ecology to molecular genetics*, Microbiology and molecular biology reviews **64** (2000) 847–867. ↑4.4.4

[Dea1938] H. T. Dean, *Endemic fluorosis and its relation to dental caries*, US Government Printing Office, 1938. ↑4.5

[Der1941a] B. Derjaguin, *Theory of the stability of strongly charged lyophobic sols and the adhesion of strongly charged particles in solutions of electrolytes*, Acta Physicochim. USSR **14** (1941) 633–662. ↑4.2

[Der1941b] B. Derjaguin and L. Landau, *The theory of stability of highly charged lyophobic sols and coalescence of highly charged particles in electrolyte solutions*, Acta Physicochim. URSS **14** (1941) 633–52. ↑3.2.1

[Des2002] M.-N. Dessinges, B. Maier, Y. Zhang, M. Peliti, D. Bensimon, and V. Croquette, *Stretching single stranded DNA, a model polyelectrolyte*, Physical review letters **89** (2002) 248102. ↑3.3

[DeGen1987] P. De Gennes, *Polymers at an interface; a simplified view*, Advances in Colloid and Interface Science **27** (1987) 189–209. ↑3.2.1

[Dia2006] P. I. Diaz, N. I. Chalmers, A. H. Rickard, C. Kong, C. L. Milburn, R. J. Palmer, and P. E. Kolenbrander, *Molecular characterization of subject-specific oral microflora during initial colonization of enamel*, Applied and environmental microbiology **72** (2006) 2837–2848. ↑4.4.2

[Doi1988] M. Doi and S. F. Edwards, *The theory of polymer dynamics*, Band 73, Oxford University Press, 1988. ↑3.3, 3.3

[Dol1974] A. Dolan and S. Edwards, *Theory of the stabilization of colloids by adsorbed polymer*, Proceedings of the royal society of london a: Mathematical, physical and engineering sciences, 1974, pp. 509–516. ↑3.2.1

[Dor2010] L. S. Dorobantu and M. R. Gray, *Application of atomic force microscopy in bacterial research*, Scanning **32** (2010) 74–96. ↑4.1

[Dou2003] L. J. Douglas, *Candida biofilms and their role in infection*, Trends in microbiology **11** (2003) 30–36. ↑4.4.4

[Dre2011] A. Dreisbach, J. M. van Dijl, and G. Buist, *The cell surface proteome of Staphylococcus aureus*, Proteomics **11** (2011) 3154–3168. ↑3.1

[Dri2007] J. A. Driscoll, S. L. Brody, and M. H. Kollef, *The epidemiology, pathogenesis and treatment of Pseudomonas aeruginosa infections*, Drugs **67** (2007) 351–368. ↑4.4.3

[Duc1992] W. A. Ducker, T. J. Senden, and R. M. Pashley, *Measurement of forces in liquids using a force microscope*, Langmuir **8** (1992) 1831–1836. ↑4.2.1

[Duf2003] Y. F. Dufrêne, *Recent progress in the application of atomic force microscopy imaging and force spectroscopy to microbiology*, Current Opinion in Microbiology **6** (2003) 317 –323. ↑4.1, 5.3

[Duf2008] Y. F. Dufrêne, *Atomic force microscopy and chemical force microscopy of microbial cells*, Nature protocols **3** (2008) 1132–1138. ↑4.1

[Duf2013] Y. F. Dufrêne and A. E. Pelling, *Force nanoscopy of cell mechanics and cell adhesion*, Nanoscale **5** (2013) 4094–4104. ↑5.3

[Duf2015] Y. F. Dufrene, *Sticky microbes: forces in microbial cell adhesion*, Trends in microbiology (2015). ↑3.1, 4.6, 5.3

[Dun2002] W. M. Dunne, *Bacterial Adhesion: Seen Any Good Biofilms Lately?*, Clinical Microbiology Reviews **15** (2002) 155–166. ↑1

[Dup2010] V. Dupres, D. Alsteens, G. Andre, and Y. F. Dufrêne, *Microbial nanoscopy: a closer look at microbial cell surfaces*, Trends in Microbiology **18** (2010) 397 –405. ↑4.2, 5.3

[Eat2010] P. Eaton and P. West, *Atomic force microscopy*, Oxford Univ. Press, 2010. ↑5.3

[ElK2013] S. El-Kirat-Chatel, A. Beaussart, C. D. Boyd, G. A. O'Toole, and Y. F. Dufrêne, *Single-cell and single-molecule analysis deciphers the localization, adhesion, and mechanics of the biofilm adhesin LapA*, ACS chemical biology **9** (2013) 485–494. ↑4.2.3

[ElK2014] S. El-Kirat-Chatel, C. D. Boyd, G. A. O'Toole, and Y. F. Dufrêne, *Single-molecule analysis of Pseudomonas fluorescens footprints*, ACS nano **8** (2014) 1690–1698. ↑3.3

[Eme2006] Emerson, T. S. Bergstrom, Y. Liu, E. R. Soto, C. A. Brown, W. G. McGimpsey, and T. A. Camesano, *Microscale Correlation between Surface Chemistry, Texture, and the Adhesive Strength of Staphylococcus epidermidis*, Langmuir **22** (2006) 11311–11321. ↑4.2.3, 4.5

[Ent2005] J.-M. Entenza, P. Moreillon, M. M. Senn, J. Kormanec, P. M. Dunman, B. Berger-Bächi, S. Projan, and M. Bischoff, *Role of σB in the expression of Staphylococcus aureus cell wall adhesins ClfA and FnbA and contribution to infectivity in a rat model of experimental endocarditis*, Infection and immunity **73** (2005) 990–998. ↑4.4.3

[Eva1997] E. Evans and K. Ritchie, *Dynamic strength of molecular adhesion bonds*, Biophysical Journal **72** (1997) 1541 –1555. ↑4.2.4

[Fan2000] H. H. P. Fang, K.-Y. Chan, and L.-C. Xu, *Quantification of bacterial adhesion forces using atomic force microscopy (AFM)*, Journal of Microbiological Methods **40** (2000) 89–97. ↑4.1

[Fle2010] H.-C. Flemming and J. Wingender, *The biofilm matrix*, Nature Reviews Microbiology **8** (2010) 623–633. ↑4.4.5

[Fra1975] F. Franks, *The hydrophobic interaction*, Water a comprehensive treatise, 1975, pp. 1–94. ↑3.2.1

[Fre2001] D. Frenkel and B. Smit, *Understanding molecular simulation: from algorithms to applications*, Band 1, Academic press, 2001. ↑3.4

[Gab2007] F. Gaboriaud and Y. F. Dufrêne, *Atomic force microscopy of microbial cells: Application to nanomechanical properties, surface forces and molecular recognition forces*, Colloids and Surfaces B: Biointerfaces **54** (2007) 10 –19. ↑4.1

[Gui2014] O. Guillaume-Gentil, E. Potthoff, D. Ossola, C. M. Franz, T. Zambelli, and J. A. Vorholt, *Force-controlled manipulation of single cells: from AFM to FluidFM*, Trends in biotechnology **32** (2014) 381–388. ↑4.1

[Gib1975] R. Gibbons and J. Houte, *Bacterial adherence in oral microbial ecology*, Annual Reviews in Microbiology **29** (1975) 19–42. ↑4.1

[Gra1884] H. C. J. Gram and C. Friedlaender, *Ueber die isolirte färbung der schizomyceten: in schnitt-und trockenpräparaten*, Theodor Fischer's medicinischer Buchhandlung, 1884. ↑3.1

[Gra1993] A. Grabbe and R. G. Horn, *Double-layer and hydration forces measured between silica sheets subjected to various surface treatments*, Journal of colloid and interface science **157** (1993) 375–383. ↑3.2.1

[Göt2002] F. Götz, *Staphylococcus and biofilms*, Molecular Microbiology **43** (2002) 1367–1378. ↑3.1

[Häh2012] H. Hähl, F. Evers, S. Grandthyll, M. Paulus, C. Sternemann, P. Loskill, M. Lessel, A. K. Husecken, T. Brenner, M. Tolan, and K. Jacobs, *Subsurface influence on the structure of protein adsorbates as revealed by in situ X-ray reflectivity*, Langmuir **28** (2012) 7747–7756. ↑3.2.1, 3.2.1

[Ham1937] H. C. Hamaker, *The London-van der Waals attraction between spherical particles*, Physica **4** (1937) 1058 –1072. ↑3.2.1

[Ham1980] S. Hamada and H. D. Slade, *Biology, immunology, and cariogenicity of Streptococcus mutans.*, Microbiological reviews **44** (1980) 331. ↑4.4.2

[Han1997] M. Hannig, *Transmission electron microscopic study of in vivo pellicle formation on dental restorative materials*, European journal of oral sciences **105** (1997) 422–433. ↑4.4.2

[Han1998] H. G. Hansma and L. Pietrasanta, *Atomic force microscopy and other scanning probe microscopies*, Current Opinion in Chemical Biology **2** (1998) 579 –584. ↑5.3

[Han2003] A. Hanna, M. Berg, V. Stout, and A. Razatos, *Role of capsular colanic acid in adhesion of uropathogenic Escherichia coli*, Applied and environmental microbiology **69** (2003) 4474–4481. ↑4.2.2, 4.4.5

[Han2011] V. Hancock, I. L. Witsø, and P. Klemm, *Biofilm formation as a function of adhesin, growth medium, substratum and strain type*, International Journal of Medical Microbiology **301** (2011) 570–576. ↑3.1

[Her2015] P. Herman-Bausier, S. El-Kirat-Chatel, T. J. Foster, J. A. Geoghegan, and Y. F. Dufrêne, *Staphylococcus aureus Fibronectin-Binding Protein A Mediates Cell-Cell Adhesion through Low-Affinity Homophilic Bonds*, mBio **6** (2015) e00413–15. ↑4.4.3

[Hei2011] Heilmann, *Kapitel 7* in *Bacterial adhesion* (D. Linke and A. Goldman, Hrsg.), Springer, 2011. ↑3.1, 4.4.3

[Hei2015] K. P. Heim, R. M. A. Sullan, P. J. Crowley, S. El-Kirat-Chatel, A. Beaussart, W. Tang, R. Besingi, Y. F. Dufrene, and L. J. Brady, *Identification of a Supramolecular Functional Architecture of Streptococcus mutans Adhesin P1 on the Bacterial Cell Surface*, Journal of Biological Chemistry **290** (2015) 9002–9019. ↑4.4.2

[Her2013] P. Herman, S. El-Kirat-Chatel, A. Beaussart, J. A. Geoghegan, T. Vanzieleghem, T. J. Foster, P. Hols, J. Mahillon, and Y. F. Dufre ne, *Forces driving the attachment of Staphylococcus epidermidis to fibrinogen-coated surfaces*, Langmuir **29** (2013) 13018–13022. ↑4.3, 4.4.3

[Her2014] P. Herman, S. El-Kirat-Chatel, A. Beaussart, J. A. Geoghegan, T. J. Foster, and Y. F. Dufrêne, *The binding force of the staphylococcal adhesin SdrG is remarkably strong*, Molecular microbiology **93** (2014) 356–368. ↑4.4.3

[Hes1971a] F. T. Hesselink, *Theory of the stabilization of dispersions by adsorbed macromolecules. I. Statistics of the change of some configurational properties of adsorbed macromolecules on the approach of an impenetrable interface*, The Journal of Physical Chemistry **75** (1971) 65–71. ↑3.2.1

[Hes1971b] F. T. Hesselink, A. Vrij, and J. T. G. Overbeek, *Theory of the stabilization of dispersions by adsorbed macromolecules. II. Interaction between two flat particles*, The Journal of Physical Chemistry **75** (1971) 2094–2103. ↑3.2.1

[Hir2010] N. Hirschhausen, T. Schlesier, M. A. Schmidt, F. Götz, G. Peters, and C. Heilmann, *A novel staphylococcal internalization mechanism involves the major autolysin Atl and heat shock cognate protein Hsc70 as host cell receptor*, Cellular microbiology **12** (2010) 1746–1764. ↑3.1

[Hog2002] D. A. Hogan and R. Kolter, *Pseudomonas-Candida interactions: an ecological role for virulence factors*, Science **296** (2002) 2229–2232. ↑4.4.4

[Hog2004] D. A. Hogan, Å. Vik, and R. Kolter, *A Pseudomonas aeruginosa quorum-sensing molecule influences Candida albicans morphology*, Molecular microbiology **54** (2004) 1212–1223. ↑4.4.4

[Hör2003] J. Hörber and M. Miles, *Scanning probe evolution in biology*, Science **302** (2003) 1002–1005. ↑5.3

[Hor2010] K. Hori and S. Matsumoto, *Bacterial adhesion: From mechanism to control*, Biochemical Engineering Journal **48** (2010) 424 –434. ↑4.2, 4.5

[Hal2004] L. Hall-Stoodley, J. W. Costerton, and P. Stoodley, *Bacterial biofilms: from the Natural environment to infectious diseases*, Nat Rev Micro **2** (2004) 95–108. ↑1

[Ino2006] Y. Inose, S. L. Takeshita, T. Hidaka, M. Higashide, A. Maruyama, H. Hayashi, K. Morikawa, and T. Ohta, *Genetic characterization of the natural SigB variants found in clinical isolates of Staphylococcus aureus*, The Journal of general and applied microbiology **52** (2006) 259–271. ↑4.4.3

[Isr1972] J. N. Israelachvili, *The Calculation of Van Der Waals Dispersion Forces between Macroscopic Bodies*, Proceedings of the Royal Society of London. A. Mathematical and Physical Sciences **331** (1972) 39–55. ↑3.2.1

[Isr2011] J. N. Israelachvili, *Intermolecular and surface forces* (J. N. Israelachvili, Hrsg.), Academic Press, 2011. ↑3.2.1, 3.2.1, 3.2.1, 3.2.1, 3.2.1, 3.2.1, 3.2.1, 3.2.1, 3.2.1, 3.2.1, 3.2.1, 3.2.1, 4.2.2

[Iva2011] I. E. Ivanov, E. N. Kintz, L. A. Porter, J. B. Goldberg, N. A. Burnham, and T. A. Camesano, *Relating the physical properties of Pseudomonas aeruginosa lipopolysaccharides to virulence by atomic force microscopy*, Journal of bacteriology **193** (2011) 1259–1266. ↑4.4.1

[Iva2012] I. E. Ivanov, C. D. Boyd, P. D. Newell, M. E. Schwartz, L. Turnbull, M. S. Johnson, C. B. Whitchurch, G. A. O'Toole, and T. A. Camesano, *Atomic force and super-resolution microscopy support a role for LapA as a cell-surface biofilm adhesin of Pseudomonas fluorescens*, Research in microbiology **163** (2012) 685–691. ↑4.4.5

[Jeo1991] S. Jeon, J. Lee, J. Andrade, and P. De Gennes, *Protein-surface interactions in the presence of polyethylene oxide: I. Simplified theory*, Journal of Colloid and Interface Science **142** (1991) 149–158. ↑4.5

[Jön1991] K. Jönsson, C. Signäs, H.-P. Müller, and M. Lindberg, *Two different genes encode fibronectin binding proteins in Staphylococcus aureus*, European Journal of Biochemistry **202** (1991) 1041–1048. ↑3.1

[Kan2009] S. Kang and M. Elimelech, *Bioinspired Single Bacterial Cell Force Spectroscopy*, Langmuir **25** (2009) 9656–9659. ↑4.1, 4.1, 4.2.2, 4.6

[Kat2004] M. Katsikogianni and Y. F. Missirlis, *Concise review of mechanisms of bacterial adhesion to biomaterials and of techniques used in estimating bacteriamaterial interactions*, European Cells and Materials **8** (2004) 37–57. ↑1

[Ker1999] J. Kerr, G. Taylor, A. Rutman, N. Høiby, P. Cole, and R. Wilson, *Pseudomonas aeruginosa pyocyanin and 1-hydroxyphenazine inhibit fungal growth.*, Journal of clinical pathology **52** (1999) 385–387. ↑4.4.4

[Kli2010] K. A. Kline, K. W. Dodson, M. G. Caparon, and S. J. Hultgren, *A tale of two pili: assembly and function of pili in bacteria*, Trends in microbiology **18** (2010) 224–232. ↑4.4.3

[Koh2005] C. Kohler, S. Wolff, D. Albrecht, S. Fuchs, D. Becher, K. Büttner, S. Engelmann, and M.

Hecker, *Proteome analyses of Staphylococcus aureus in growing and non-growing cells: a physiological approach*, International journal of medical microbiology **295** (2005) 547–565. ↑3.1

[Lan2014] D. P. Landau and K. Binder, *A guide to monte carlo simulations in statistical physics*, Cambridge university press, 2014. ↑3.4

[Las2002] C. S. Laspidou and B. E. Rittmann, *A unified theory for extracellular polymeric substances, soluble microbial products, and active and inert biomass*, Water Research **36** (2002) 2711–2720. ↑4.4.5

[Lau2009a] P. C. Lau, J. R. Dutcher, T. J. Beveridge, and J. S. Lam, *Absolute quantitation of bacterial biofilm adhesion and viscoelasticity by microbead force spectroscopy*, Biophysical journal **96** (2009) 2935–2948. ↑4.4.1

[Lau2009b] P. C. Lau, T. Lindhout, T. J. Beveridge, J. R. Dutcher, and J. S. Lam, *Differential lipopolysaccharide core capping leads to quantitative and correlated modifications of mechanical and structural properties in Pseudomonas aeruginosa biofilms*, Journal of bacteriology **191** (2009) 6618–6631. ↑4.4.1

[Le2013] D. T. L. Le, T.-L. Tran, M.-P. Duviau, M. Meyrand, Y. Guerardel, M. Castelain, P. Loubiere, M.-P. Chapot-Chartier, E. Dague, and M. Mercier-Bonin, *Unraveling the role of surface mucus-binding protein and pili in muco-adhesion of Lactococcus lactis* (2013). ↑4.4.3

[Lec2001] D. Leckband and J. Israelachvili, *Intermolecular forces in biology*, Quarterly reviews of biophysics **34** (2001) 105–267. ↑3.2.1, 4.2, 4.2.2

[Lee1989] S. Lee, A. Progulske-Fox, G. Erdos, D. Piacentini, G. Ayakawa, P. Crowley, and A. Bleiweis, *Construction and characterization of isogenic mutants of Streptococcus mutans deficient in major surface protein antigen P1 (I/II).*, Infection and immunity **57** (1989) 3306–3313. ↑4.4.2

[Len2003] J. R. Lentino, *Prosthetic joint infections: bane of orthopedists, challenge for infectious disease specialists*, Clinical Infectious Diseases **36** (2003) 1157–1161. ↑4.4.3

[Les2015] M. Lessel, O. Bäumchen, M. Klos, H. Hähl, R. Fetzer, M. Paulus, R. Seemann, and K. Jacobs, *Self-assembled silane monolayers: an efficient step-by-step recipe for high-quality, low energy surfaces*, Surface and Interface Analysis **47** (2015) 557–564. ↑5.1

[Lev1982] D. H. Leverett, *Fluorides and the changing prevalence of dental caries*, Science **217** (1982) 26–30. ↑4.5

[Li2007] F. Li and F. Pincet, *Confinement free energy of surfaces bearing end-grafted polymers in the mushroom regime and local measurement of the polymer density*, Langmuir **23** (2007) 12541–12548. ↑3.2.1

[Lif1956] E. M. Lifshitz, *The theory of molecular attractive forces between solids*, Soviet Phys. JETP **2** (1956) 73–83. ↑3.2.1

[Lin2011] D. Linke and A. Goldman (Hrsg.), *Bacterial adhesion*, Springer, 2011. ↑3.1, 4.4, 4.4.3, 4.6

[Liu2010] Y. Liu, P. A. Pinzón-Arango, A. M. Gallardo-Moreno, and T. A. Camesano, *Direct adhesion force measurements between E. coli and human uroepithelial cells in cranberry juice cocktail*, Molecular nutrition & food research **54** (2010) 1744–1752. ↑4.4.4

[Los2012a] P. Loskill, *Unraveling the impact of subsurface and surface properties of a material on biological adhesion - a multi-scale approach*, Dissertation, 2012. ↑3.1

[Los2012b] P. Loskill, H. Hähl, N. Thewes, C. T. Kreis, M. Bischoff, M. Herrmann, and K. Jacobs, *Influence of the Subsurface Composition of a Material on the Adhesion of Staphylococci*, Langmuir **28** (2012) 7242–7248. ↑5.4

[Los2013] P. Loskill, C. Zeitz, S. Grandthyll, N. Thewes, F. Mu ller, M. Bischoff, M. Herrmann, and K. Jacobs, *Reduced adhesion of oral bacteria on hydroxyapatite by fluoride treatment*, Langmuir **29** (2013) 5528–5533. ↑4.5

[Low1998] F. D. Lowy, *Staphylococcus aureus infections*, New England Journal of Medicine **339** (1998) 520–532. ↑3.1, 4.4.3

[Low2000] S. K. Lower, C. J. Tadanier, and M. F. H. Jr., *Measuring interfacial and adhesion forces between bacteria and mineral surfaces with biological force microscopy*, Geochimica et Cosmochimica Acta **64** (2000) 3133 –3139. ↑4.1, 4.1, 4.2.2, 4.2.4

[Low2001] S. K. Lower, M. F. Hochella, and T. J. Beveridge, *Bacterial Recognition of Mineral Surfaces: Nanoscale Interactions Between Shewanella and FeOOH*, Science **292** (2001) 1360–1363. ↑3.3, 4.1, 4.4.5, 5.4

[Low2010] S. K. Lower, R. Yongsunthon, N. N. Casillas-Ituarte, E. S. Taylor, A. C. DiBartola, B. H. Lower, T. J. Beveridge, A. W. Buck, and V. G. Fowler, *A tactile response in Staphylococcus aureus*, Biophysical journal **99** (2010) 2803–2811. ↑4.4.3

[Mad1997] M. T. Madigan, J. M. Martinko, J. Parker, and T. D. Brock, *Biology of microorganisms*, Band 985, prentice hall Upper Saddle River, NJ, 1997. ↑3.1

[Mar1995] J. F. Marko and E. D. Siggia, *Stretching dna*, Macromolecules **28** (1995) 8759–8770. ↑3.3, 3.3

[Max1986] I. Maxe, C. Ryden, T. Wadström, and K. Rubin, *Specific attachment of Staphylococcus aureus to immobilized fibronectin.*, Infection and immunity **54** (1986) 695–704. ↑5.2

[McL1963a] A. McLachlan, *Retarded dispersion forces between molecules*, Proceedings of the royal society of london a: Mathematical, physical and engineering sciences, 1963, pp. 387–401. ↑3.2.1

[McL1963b] A. McLachlan, *Retarded dispersion forces in dielectrics at finite temperatures*, Proceedings of the royal society of london a: Mathematical, physical and engineering sciences, 1963, pp. 80–90. ↑3.2.1

[McL1963c] A. McLachlan, *Three-body dispersion forces*, Molecular Physics **6** (1963) 423–427. ↑3.2.1

[McL1964] A. McLachlan, *Van der Waals forces between an atom and a surface*, Molecular Physics **7** (1964) 381–388. ↑3.2.1

[Mea1971] P. Meadows, *The attachment of bacteria to solid surfaces*, Archiv für Mikrobiologie **75** (1971) 374–381. ↑4.1

[Mei1992] J. Meinders, H. Van der Mei, and H. Busscher, *In situ enumeration of bacterial adhesion in a parallel plate flow chamber-elimination or in focus flowing bacteria from the analysis*, Journal of microbiological methods **16** (1992) 119–124. ↑4.1

[Mei2009a] L. Mei, Y. Ren, H. J. Busscher, Y. Chen, and H. C. van der Mei, *Poisson Analysis of Streptococcal Bond-strengthening on Saliva-coated Enamel*, Journal of Dental Research **88** (2009) 841–845. ↑4.2.4, 4.3, 4.4.2

[Mei2009b] L. Mei, H. J. Busscher, H. C. Van Der Mei, Y. Chen, J. De Vries, and Y. Ren, *Oral bacterial adhesion forces to biomaterial surfaces constituting the bracket–adhesive–enamel junction in orthodontic treatment*, European journal of oral sciences **117** (2009) 419–426. ↑4.4.2

[Mei2009c] L. Mei, H. C. van der Mei, Y. Ren, W. Norde, and H. J. Busscher, *Poisson analysis of streptococcal bond strengthening on stainless steel with and without a salivary conditioning film*, Langmuir **25** (2009) 6227–6231. ↑4.3, 4.4.2

[Mei2011] L. Mei, H. J. Busscher, H. C. van der Mei, and Y. Ren, *Influence of surface roughness on streptococcal adhesion forces to composite resins*, Dental materials **27** (2011) 770–778. ↑4.3, 4.4.2

[Met1949] N. Metropolis and S. Ulam, *The monte carlo method*, Journal of the American statistical association **44** (1949) 335–341. ↑3.4, 3.4

[Met1953] N. Metropolis, A. W. Rosenbluth, M. N. Rosenbluth, A. H. Teller, and E. Teller, *Equation of state calculations by fast computing machines*, The journal of chemical physics **21** (1953) 1087–1092. ↑3.4, 3.4

[Mey2010] R. L. Meyer, X. Zhou, L. Tang, A. Arpanaei, P. Kingshott, and F. Besenbacher, *Immobilisation of living bacteria for AFM imaging under physiological conditions*, Ultramicroscopy **110** (2010) 1349–1357. ↑4.1

[Mez2006] M. Mezger, H. Reichert, S. Schöder, J. Okasinski, H. Schröder, H. Dosch, D. Palms, J. Ralston, and V. Honkimäki, *High-resolution in situ x-ray study of the hydrophobic gap at the water–octadecyl-trichlorosilane interface*, Proceedings of the National Academy of Sciences **103** (2006) 18401–18404. ↑3.2.1

[Mez2010] M. Mezger, F. Sedlmeier, D. Horinek, H. Reichert, D. Pontoni, and H. Dosch, *On the origin of the hydrophobic water gap: an X-ray reflectivity and MD simulation study*, Journal of the American Chemical Society **132** (2010) 6735–6741. ↑3.2.1

[Mil1991] S. Milner, *Polymer brushes*, Science **251** (1991) 905–914. ↑4.5

[Mil2005] S. I. Miller, R. K. Ernst, and M. W. Bader, *LPS, TLR4 and infectious disease diversity*, Nature Reviews Microbiology **3** (2005) 36–46. ↑3.1

[Mit2008] G. Mitchell, C.-A. Lamontagne, E. Brouillette, G. Grondin, B. G. Talbot, M. Grandbois, and F. Malouin, *Staphylococcus aureus SigB activity promotes a strong fibronectin–bacterium interaction which may sustain host tissue colonization by small-colony variants isolated from cystic fibrosis patients*, Molecular microbiology **70** (2008) 1540–1555. ↑4.4.3

[Moi2006] H. Moisan, E. Brouillette, C. L. Jacob, P. Langlois-Bégin, S. Michaud, and F. Malouin, *Transcription of virulence factors in Staphylococcus aureus small-colony variants isolated from cystic fibrosis patients is influenced by SigB*, Journal of bacteriology **188** (2006) 64–76. ↑4.4.3

[Mor2010] D. K. Morales and D. A. Hogan, *Candida albicans interactions with bacteria in the context of human health and disease* (2010). ↑4.4.4

[Mus2012] A. K. Muszanska, M. R. Nejadnik, Y. Chen, E. R. van den Heuvel, H. J. Busscher, H. C. van der Mei, and W. Norde, *Bacterial Adhesion Forces with Substratum Surfaces and the Susceptibility of Biofilms to Antibiotics*, Antimicrobial Agents and Chemotherapy **56** (2012) 4961–4964. ↑4.5

[Neu2008] K. C. Neuman and A. Nagy, *Single-molecule force spectroscopy: optical tweezers, magnetic tweezers and atomic force microscopy*, Nature methods **5** (2008) 491. ↑3.3

[New1999] M. Newman and G. Barkema, *Monte carlo methods in statistical physics chapter 1-4*, Oxford University Press: New York, USA, 1999. ↑3.4

[Nor1986] W. Norde, *Adsorption of proteins from solution at the solid-liquid interface*, Advances in colloid and interface science **25** (1986) 267–340. ↑3.2.1, 4.2.3

[Nor1996] W. Norde, *Driving forces for protein adsorption at solid surfaces*, Macromolecular symposia, 1996, pp. 5–18. ↑3.2.1, 4.2.4

[Nyv1987] B. Nyvad and M. Kilian, *Microbiology of the early colonization of human enamel and root surfaces in vivo*, European Journal of Oral Sciences **95** (1987) 369–380. ↑4.4.2

[Nyv1990] B. Nyvad and M. Kilian, *Comparison of the initial streptococcal microflora on dental enamel in caries-active and in caries-inactive individuals*, Caries research **24** (1990) 267–272. ↑4.4.2

[Nyv1992] B. Nyvad, *Microbial colonization of human tooth surfaces.*, APMIS. Supplementum **32** (1992) 1–45. ↑4.4.2

[Odd1988] F. C. Odds et al., *Candida and candidosis: a review and bibliography*, Bailliere Tindall, 1988. ↑4.4.4

[Oes2000] F. Oesterhelt, D. Oesterhelt, M. Pfeiffer, A. Engel, H. Gaub, and D. Müller, *Unfolding pathways of individual bacteriorhodopsins*, Science **288** (2000) 143–146. ↑3.3

[Oho1998] T. Oho, H. Yu, Y. Yamashita, and T. Koga, *Binding of Salivary Glycoprotein-Secretory Immunoglobulin A Complex to the Surface Protein Antigen ofStreptococcus mutans*, Infection and immunity **66** (1998) 115–121. ↑4.4.2

[Oli2000] A. Oliver, R. Cantón, P. Campo, F. Baquero, and J. Blázquez, *High frequency of hypermutable Pseudomonas aeruginosa in cystic fibrosis lung infection*, Science **288** (2000) 1251–1253. ↑4.4.4

[Ong1999] Y.-L. Ong, A. Razatos, G. Georgiou, and M. M. Sharma, *Adhesion Forces between E. c oli Bacteria and Biomaterial Surfaces*, Langmuir **15** (1999) 2719–2725. ↑4.1, 4.2.3, 4.4.1

[Ott2009] M. Otto, *Staphylococcus epidermidis - the 'accidental' pathogen*, Nature Reviews Microbiology **7** (2009) 555–567. ↑4.4.3

[Ovc2012a] E. S. Ovchinnikova, B. P. Krom, H. J. Busscher, and H. C. van der Mei, *Evaluation of adhesion forces of Staphylococcus aureus along the length of Candida albicans hyphae*, BMC Microbiology **12** (2012). ↑4.4.4

[Ovc2012b] E. S. Ovchinnikova, B. P. Krom, H. C. van der Mei, and H. J. Busscher, *Force microscopic and thermodynamic analysis of the adhesion between Pseudomonas aeruginosa and Candida albicans*, Soft Matter **8** (2012) 6454–6461. ↑4.4.4

[Ovc2013a] E. S. Ovchinnikova, B. P. Krom, A. K. Harapanahalli, H. J. Busscher, and H. C. van der Mei, *Surface Thermodynamic and Adhesion Force Evaluation of the Role of Chitin-Binding Protein in the Physical Interaction between Pseudomonas aeruginosa and Candida albicans*, Langmuir **29** (2013) 4823–4829. ↑4.3, 4.4.4

[Ovc2013b] E. S. Ovchinnikova, H. C. van der Mei, B. P. Krom, and H. J. Busscher, *Exchange of adsorbed serum proteins during adhesion of Staphylococcus aureus to an abiotic surface and Candida albicans hyphae - An AFM study*, Colloids and Surfaces B: Biointerfaces **110** (2013) 45 –50. ↑4.4.4

[Pal1995] R. J. Palmer and D. E. Caldwell, *A flowcell for the study of plaque removal and regrowth*, Journal of microbiological methods **24** (1995) 171–182. ↑4.1

[Par1973] V. A. Parsegian and B. W. Ninham, *Van der waals forces in many-layered structures: generalizations of the lifshitz result for two semi-infinite media*, Journal of theoretical biology **38** (1973) 101–109. ↑3.2.1

[Par1998] K. D. Park, Y. S. Kim, D. K. Han, Y. H. Kim, E. H. B. Lee, H. Suh, and K. S. Choi, *Bacterial adhesion on PEG modified polyurethane surfaces*, Biomaterials **19** (1998) 851–859. ↑4.5

[Pöh2000] P. Pöhlmann-Dietze, M. Ulrich, K. B. Kiser, G. Döring, J. C. Lee, J.-M. Fournier, K. Botzenhart, and C. Wolz, *Adherence of Staphylococcus aureus to endothelial cells: influence of capsular polysaccharide, global regulatoragr, and bacterial growth phase*, Infection and immunity **68** (2000) 4865–4871. ↑3.1

[Pel2010] A. Y. Peleg, D. A. Hogan, and E. Mylonakis, *Medically important bacterial–fungal interactions*, Nature reviews microbiology **8** (2010) 340–349. ↑4.4.4

[Pes1999] A. Peschel, M. Otto, R. W. Jack, H. Kalbacher, G. Jung, and F. Götz, *Inactivation of the dlt Operon inStaphylococcus aureus Confers Sensitivity to Defensins, Protegrins, and Other Antimicrobial Peptides*, Journal of Biological Chemistry **274** (1999) 8405–8410. ↑5.2

[Pet2012] B. M. Peters, E. S. Ovchinnikova, B. P. Krom, L. M. Schlecht, H. Zhou, L. L. Hoyer, H. J. Busscher, H. C. van der Mei, M. A. Jabra-Rizk, and M. E. Shirtliff, *Staphylococcus aureus adherence to Candida albicans hyphae is mediated by the hyphal adhesin Als3p*, Microbiology **158** (2012) 2975–2986. ↑4.4.4

[Poo2002] A. T. Poortinga, R. Bos, W. Norde, and H. J. Busscher, *Electric double layer interactions in bacterial adhesion to surfaces*, Surface Science Reports **47** (2002) 1–32. ↑4.2.2

[Pot2015] E. Potthoff, D. Ossola, T. Zambelli, and J. A. Vorholt, *Bacterial adhesion force quantification by fluidic force microscopy*, Nanoscale **7** (2015) 4070–4079. ↑4.1, 4.3, 4.6, 5.4

[Qua1994] C. Quate, *The AFM as a tool for surface imaging*, Surface Science **299** (1994) 980–995. ↑5.3

[Raz1998] A. Razatos, Y.-L. Ong, M. M. Sharma, and G. Georgiou, *Molecular determinants of bacterial adhesion monitored by atomic force microscopy*, Proceedings of the National Academy of Sciences **95** (1998) 11059–11064. ↑4.1, 4.1, 4.2.2, 4.4.1

[Raz2000] A. Razatos, Y.-L. Ong, F. Boulay, D. L. Elbert, J. A. Hubbell, M. M. Sharma, and G. Georgiou, *Force measurements between bacteria and poly (ethylene glycol)-coated surfaces*, Langmuir **16** (2000) 9155–9158. ↑4.5

[Rod2015] C. Rodriguez-Emmenegger, S. Janel, A. de los Santos Pereira, M. Bruns, and F. Lafont, *Quantifying bacterial adhesion on antifouling polymer brushes via single-cell force spectroscopy*, Polymer Chemistry (2015). ↑4.5

[Rie1997a] M. Rief, F. Oesterhelt, B. Heymann, and H. E. Gaub, *Single Molecule Force Spectroscopy on Polysaccharides by Atomic Force Microscopy*, Science **275** (1997) 1295–1297. ↑4.1

[Rie1997b] M. Rief, M. Gautel, F. Oesterhelt, J. M. Fernandez, and H. E. Gaub, *Reversible unfolding of individual titin immunoglobulin domains by AFM*, Science **276** (1997) 1109–1112. ↑3.3

[Ros2009] R. Rosenstein, C. Nerz, L. Biswas, A. Resch, G. Raddatz, S. C. Schuster, and F. Götz, *Genome analysis of the meat starter culture bacterium Staphylococcus carnosus TM300*, Applied and environmental microbiology **75** (2009) 811–822. ↑5.2

[Ros2010] R. Rosenstein and F. Götz, *Genomic differences between the food-grade Staphylococcus carnosus and pathogenic staphylococcal species*, International Journal of Medical Microbiology **300** (2010) 104–108. ↑5.2

[Rot1993] C. M. Roth and A. M. Lenhoff, *Electrostatic and van der Waals contributions to protein adsorption: computation of equilibrium constants*, Langmuir **9** (1993) 962–972. ↑3.2.1

[Rot1995] C. M. Roth and A. M. Lenhoff, *Electrostatic and van der Waals contributions to protein adsorption: comparison of theory and experiment*, Langmuir **11** (1995) 3500–3509. ↑3.2.1

[Rub2003] M. Rubinstein and R. H. Colby, *Polymer physics*, OUP Oxford, 2003. ↑3.2.2, 3.2, 3.3, 3.3

[Rut1997] M. Ruths, J. N. Israelachvili, and H. J. Ploehn, *Effects of Time and Compression on the Interactions of Adsorbed Polystyrene Layers in a Near-ϑ Solvent*, Macromolecules **30** (1997) 3329–3339. ↑3.2.1

[Sam2006] P. Samorì, *Scanning probe microscopies beyond imaging: manipulation of molecules and nanostructures*, John Wiley & Sons, 2006. ↑5.3

[Sar1991] D. Sarid, *Scanning force microscopy*, Oxford University Press, 1991. ↑5.3

[Sch1982] K. H. Schleifer and U. Fischer, *Description of a New Species of the Genus Staphylococcus: Staphylococcus carnosus*, International Journal of Systematic Bacteriology **32** (1982) 153–156. ↑3.1

[See2001] R. Seemann, S. Herminghaus, and K. Jacobs, *Dewetting Patterns and Molecular Forces: A Reconciliation*, Phys. Rev. Lett. **86** (2001) 5534–5537. ↑3.2.1

[Seo2007] Y. Seo and W. Jhe, *Atomic force microscopy and spectroscopy*, Rep. Prog. Phys. (2007). ↑5.3

[She2007] X. Sheng, Y. Peng Ting, and S. O. Pehkonen, *Force measurements of bacterial adhesion on metals using a cell probe atomic force microscope*, Journal of Colloid and Interface Science **310** (2007) 661 –669. ↑4.2.2, 4.2.3

[She2008] X. Sheng, Y. P. Ting, and S. O. Pehkonen, *The influence of ionic strength, nutrients and pH on bacterial adhesion to metals*, Journal of Colloid and Interface Science **321** (2008) 256 –264. ↑4.2.2, 4.2.3

[Shi2009a] X. Shi and X. Zhu, *Biofilm formation and food safety in food industries*, Trends in Food Science & Technology **20** (2009) 407–413. ↑1

[Shi2009b] M. E. Shirtliff, B. M. Peters, and M. A. Jabra-Rizk, *Cross-kingdom interactions: Candida albicans and bacteria*, FEMS microbiology letters **299** (2009) 1–8. ↑4.4.4

[Sig1989] C. Signäs, G. Raucci, K. Jönsson, P.-E. Lindgren, G. Anantharamaiah, M. Höök, and M. Lindberg, *Nucleotide sequence of the gene for a fibronectin-binding protein from Staphylococcus aureus: use of this peptide sequence in the synthesis of biologically active peptides*, Proceedings of the National Academy of Sciences **86** (1989) 699–703. ↑3.1

[Str2009] J. Strauss, N. A. Burnham, and T. A. Camesano, *Atomic force microscopy study of the role of LPS O-antigen on adhesion of E. coli*, Journal of Molecular Recognition **22** (2009) 347–355. ↑4.4.1, 4.4.3

[Str2010] J. Strauss, A. Kadilak, C. Cronin, C. M. Mello, and T. A. Camesano, *Binding, inactivation, and adhesion forces between antimicrobial peptide cecropin P1 and pathogenic E. coli*, Colloids and Surfaces B: Biointerfaces **75** (2010) 156–164. ↑4.2.4, 4.4.1

[Sud2004] P. Sudbery, N. Gow, and J. Berman, *The distinct morphogenic states of Candida albicans*, Trends in microbiology **12** (2004) 317–324. ↑4.4.4

[Sul2006] T. Sulchek, R. W. Friddle, and A. Noy, *Strength of multiple parallel biological bonds*, Biophysical journal **90** (2006) 4686–4691. ↑4.2.4

[Sul2014] R. M. A. Sullan, A. Beaussart, P. Tripathi, S. Derclaye, S. El-Kirat-Chatel, J. K. Li, Y.-J. Schneider, J. Vanderleyden, S. Lebeer, and Y. F. Dufrêne, *Single-cell force spectroscopy of pili-mediated adhesion*, Nanoscale **6** (2014) 1134–1143. ↑4.4.3

[Sul2015] R. M. A. Sullan, J. K. Li, P. J. Crowley, L. J. Brady, and Y. F. Dufrêne, *Binding Forces of Streptococcus mutans P1 Adhesin*, ACS nano **9** (2015) 1448–1460. ↑4.3, 4.4.2

[Tay1998] R. L. Taylor, J. Verran, G. C. Lees, and A. P. WARD, *The influence of substratum topography on bacterial adhesion to polymethyl methacrylate*, Journal of Materials Science: Materials in Medicine **9** (1998) 17–22. ↑4.5

[Tel2006] J. L. Telford, M. A. Barocchi, I. Margarit, R. Rappuoli, and G. Grandi, *Pili in gram-positive pathogens*, Nature Reviews Microbiology **4** (2006) 509–519. ↑4.4.3

[The2014] N. Thewes, P. Loskill, P. Jung, H. Peisker, M. Bischoff, M. Herrmann, and K. Jacobs, *Hydrophobic interaction governs unspecific adhesion of staphylococci: a single cell force spectroscopy study*, Beilstein journal of nanotechnology **5** (2014) 1501–1512. ↑4.1, 4.2.3, 5.4

[The2015a] N. Thewes, P. Loskill, C. Spengler, S. Hümbert, M. Bischoff, and K. Jacobs, *A detailed guideline for the fabrication of single bacterial probes used for atomic force spectroscopy*, The European Physical Journal E **38** (2015) 1–9. ↑4.1, 5.4

[The2015b] N. Thewes, A. Thewes, P. Loskill, H. Peisker, M. Bischoff, M. Herrmann, L. Santen, and K. Jacobs, *Stochastic binding of Staphylococcus aureus to hydrophobic surfaces*, Soft matter **11** (2015) 8913–8919. ↑4.6

[Tri2013] P. Tripathi, A. Beaussart, D. Alsteens, V. Dupres, I. Claes, I. Von Ossowski, W. M. De Vos, A. Palva, S. Lebeer, and J. Vanderleyden, *Adhesion and nanomechanics of pili from the probiotic Lactobacillus rhamnosus GG*, ACS Nano **7** (2013) 3685–3697. ↑4.1

[Van1996] P. Vandamme, B. Pot, M. Gillis, P. De Vos, K. Kersters, and J. Swings, *Polyphasic taxonomy,*

a consensus approach to bacterial systematics., Microbiological reviews **60** (1996) 407–438. ↑3.1

[Van2015] T. Vanzieleghem, P. Herman-Bausier, Y. F. Dufrene, and J. Mahillon, *Staphylococcus epidermidis Affinity for Fibrinogen-Coated Surfaces Correlates with the Abundance of the SdrG Adhesin on the Cell Surface*, Langmuir **31** (2015) 4713–4721. ↑4.4.3

[VanDel1998] C. Van Delden and B. H. Iglewski, *Cell-to-cell signaling and Pseudomonas aeruginosa infections.*, Emerging infectious diseases **4** (1998) 551. ↑4.4.3

[vanderMei2008] H. C. van der Mei, M. Rustema-Abbing, J. de Vries, and H. J. Busscher, *Bond strengthening in oral bacterial adhesion to salivary conditioning films*, Applied and environmental microbiology **74** (2008) 5511–5515. ↑4.2.4, 4.3, 4.4.2

[Vel2002] S. B. Velegol and B. E. Logan, *Contributions of bacterial surface polymers, electrostatics, and cell elasticity to the shape of AFM force curves*, Langmuir **18** (2002) 5256–5262. ↑4.1, 4.2.2, 4.4.1

[Ver1947] E. J. W. Verwey, *Theory of the Stability of Lyophobic Colloids.*, The Journal of Physical and Colloid Chemistry **51** (1947) 631–636. ↑3.2.1

[Ver1948] E. J. Verwey, J. Th. G. Overbeek, and K. van Nes, *Theory of the stability of lyophobic colloids: The interaction of sol particles having an electric double layer*, Elsevier Pub. Co., 1948. ↑3.2.1, 4.2

[VanOss1986] C. Van Oss, R. Good, and M. Chaudhury, *The role of van der Waals forces and hydrogen bonds in "hydrophobic interactions" between biopolymers and low energy surfaces*, Journal of colloid and Interface Science **111** (1986) 378–390. ↑3.2.1, 4.2

[VanOss1987] C. Van Oss, M. Chaudhury, and R. Good, *Monopolar surfaces*, Advances in colloid and interface science **28** (1987) 35–64. ↑3.2.1, 3.2.1

[VanOss1988] C. Van Oss, R. Good, and M. Chaudhury, *Additive and nonadditive surface tension components and the interpretation of contact angles*, Langmuir **4** (1988) 884–891. ↑3.2.1

[VanOss1989] C. J. Van Oss, *Energetics of cell-cell and cell-biopolymer interactions*, Cell biophysics **14** (1989) 1–16. ↑3.2.1

[VanOss1990] C. Van Oss, R. Giese, and P. M. Costanzo, *DLVO and non-DLVO interactions in hectorite*, Clays Clay Miner **38** (1990) 151–159. ↑3.2.1

[VanOss2006] C. J. Van Oss, *Interfacial forces in aqueous media*, CRC press, 2006. ↑3.2.1, 3.2.1, 3.2.1, 3.2.1, 3.2.1, 4.2

[Vad2003] V. Vadillo-Rodríguez, H. J. Busscher, W. Norde, J. de Vries, and H. C. van der Mei, *On relations between microscopic and macroscopic physicochemical properties of bacterial cell surfaces: an AFM study on Streptococcus mitis strains*, Langmuir **19** (2003) 2372–2377. ↑4.1

[Vadgue2004] V. Vadillo-Rodrı guez, H. J. Busscher, W. Norde, J. de Vries, and H. C. van der Mei, *Atomic force microscopic corroboration of bond aging for adhesion of Streptococcus thermophilus to solid substrata*, Journal of colloid and interface science **278** (2004) 251–254. ↑4.1, 4.1, 4.2.2, 4.3, 4.6

[Vri1976] A. Vrij, *Polymers at interfaces and the interactions in colloidal dispersions*, Pure and Applied Chemistry **48** (1976) 471–483. ↑3.2.1

[Vuo2002] C. Vuong and M. Otto, *Staphylococcus epidermidis infections*, Microbes and infection **4** (2002) 481–489. ↑4.4.3

[Waa2005] K. Waar, H. C. van der Mei, H. J. Harmsen, J. de Vries, J. Atema-Smit, J. E. Degener, and H. J. Busscher, *Atomic force microscopy study on specificity and non-specificity of interaction forces between Enterococcus faecalis cells with and without aggregation substance*, Microbiology **151** (2005) 2459–2464. ↑4.4.5

[Wah1991] M. Wahlgren and T. Arnebrant, *Protein adsorption to solid surfaces*, Trends in biotechnology **9** (1991) 201–208. ↑3.2.1, 4.2.3

[Wan2007] Q. Wang, G. M. Garrity, J. M. Tiedje, and J. R. Cole, *Naive Bayesian classifier for rapid assignment of rRNA sequences into the new bacterial taxonomy*, Applied and environmental microbiology **73** (2007) 5261–5267. ↑3.1

[Wan2011] Y. Wang, G. Subbiahdoss, J. Swartjes, H. C. van der Mei, H. J. Busscher, and M. Libera, *Length-Scale Mediated Differential Adhesion of Mammalian Cells and Microbes*, Advanced Functional Materials **21** (2011) 3916–3923. ↑4.5

[Wan2012] Y. Wang, G. Subbiahdoss, J. de Vries, M. Libera, van der Mei H C, and B. H. J, *Effect of adsorbed fibronectin on the differential adhesion of osteoblast-like cells and Staphylococcus aureus with and without fibronectin-binding proteins*, Biofouling **28** (2012). ↑4.5

[War2006] M. J. Wargo and D. A. Hogan, *Fungal - bacterial interactions: a mixed bag of mingling microbes*, Current opinion in microbiology **9** (2006) 359–364. ↑4.4.4

[Wei2005] C. Weidenmaier, A. Peschel, Y.-Q. Xiong, S. A. Kristian, K. Dietz, M. R. Yeaman, and A. S. Bayer, *Lack of wall teichoic acids in Staphylococcus aureus leads to reduced interactions with endothelial cells and to attenuated virulence in a rabbit model of endocarditis*, Journal of infectious diseases **191** (2005) 1771–1777. ↑5.2

[Wes2013] S. W. Wessel, Y. Chen, A. Maitra, E. R. van den Heuvel, A. M. Slomp, H. J. Busscher, and H. C. van der Mei, *Adhesion Forces and Composition of Planktonic and Adhering Oral Microbiomes*, Journal of Dental Research (2013). ↑4.4.2

[Wil1972] R. Williams and R. Gibbons, *Inhibition of bacterial adherence by secretory immunoglobulin A: a mechanism of antigen disposal*, Science **177** (1972) 697–699. ↑4.1

[Wil1996] J. M. Williams, T. Han, and T. P. Beebe, *Determination of single-bond forces from contact force variances in atomic force microscopy*, Langmuir **12** (1996) 1291–1295. ↑4.2.4

[Wil2003] P. M. Williams, *Analytical descriptions of dynamic force spectroscopy: behaviour of multiple connections*, Analytica Chimica Acta **479** (2003) 107–115. ↑4.2.4

[Woe1990] C. R. Woese, O. Kandler, and M. L. Wheelis, *Towards a natural system of organisms: proposal for the domains Archaea, Bacteria, and Eucarya.*, Proceedings of the National Academy of Sciences **87** (1990) 4576–4579. ↑3.1

[Xu2007] C.-P. Xu, B. van de Belt-Gritter, R. J. Dijkstra, W. Norde, H. C. van der Mei, and H. J. Busscher, *Interaction forces between salivary proteins and Streptococcus mutans with and without antigen I/II*, Langmuir **23** (2007) 9423–9428. ↑4.4.2, 4.4.3

[Yon2007] R. Yongsunthon, V. G. Fowler, B. H. Lower, F. P. Vellano, E. Alexander, L. B. Reller, G. R. Corey, and S. K. Lower, *Correlation between fundamental binding forces and clinical prognosis of Staphylococcus aureus infections of medical implants*, Langmuir **23** (2007) 2289–2292. ↑4.4.3

[Zei2013] C. Zeitz, *Zahnhartgewebe im fokus: In vitro-untersuchungen zur biokompatibilität von fluorierten und nichtfluorierten hydroxylapatit-modelloberflächen*, Dissertation, 2013. ↑4.4.2

[Zen2014] G. Zeng, T. Mu ller, and R. L. Meyer, *Single-cell force spectroscopy of bacteria enabled by naturally derived proteins*, Langmuir **30** (2014) 4019–4025. ↑4.1, 4.3, 4.6, 5.4

[Zen2015] G. Zeng, R. Ogaki, and R. L. Meyer, *Non-proteinaceous bacterial adhesins challenge the antifouling properties of polymer brush coatings*, Acta biomaterialia (2015). ↑4.5

[Zha2011] W. Zhang, A. G. Stack, and Y. Chen, *Interaction force measurement between E. coli cells and nanoparticles immobilized surfaces by using AFM*, Colloids and Surfaces B: Biointerfaces **82** (2011) 316–324. ↑4.5

Publications and Manuscripts

Addendum I - A detailed guideline for the fabrication of single bacterial probes used for atomic force spectroscopy

Authors: N. Thewes[1], P. Loskill[1], C. Spengler[1], S. Hümbert[1], M. Bischoff[2], and K. Jacobs[1]

[1] Department of Experimental Physics, Saarland University, 66041 Saarbrücken, Germany.
[2] The Institute of Medical Microbiology and Hygiene, Saarland University, 66421 Homburg/Saar, Germany.

Reprint with permission of Springer.
Eur. Phys. J. E (2015) **38**: 140.
(http://dx.doi.org/10.1140/epje/i2015-15140-2)

Author contributions:
The fabrication of 'bacterial probes' was developed by N. Thewes for single bacterial cells and the bacterial cluster probes were developed by P. Loskill and S. Hümbert. Protocols were drawn up by N. Thewes and C. Spengler. Experimental results were achieved by N. Thewes. The article was written by N. Thewes, C. Spengler, M. Bischoff and K.Jacobs. Scientific work was directed by M. Bischoff and K. Jacobs.

Abstract - The atomic force microscope (AFM) evolved as a standard device in modern microbiological research. However, its capability as a sophisticated force sensor is not used to its full capacity. The AFM turns into a unique tool for quantitative adhesion research in bacteriology by using 'bacterial probes'. Thereby, bacterial probes are AFM cantilevers that provide a single bacterium or a cluster of bacteria as the contact-forming object. We present a step-by-step protocol for preparing bacterial probes, performing force spectroscopy experiments and processing force spectroscopy data. Additionally, we provide a general insight into the field of bacterial cell force spectroscopy.

Eur. Phys. J. E (2015) **38**: 140
DOI 10.1140/epje/i2015-15140-2

THE EUROPEAN PHYSICAL JOURNAL E

Tips and Tricks

A detailed guideline for the fabrication of single bacterial probes used for atomic force spectroscopy

Nicolas Thewes[1], Peter Loskill[1,a], Christian Spengler[1], Sebastian Hümbert[1], Markus Bischoff[2], and Karin Jacobs[1,b]

[1] Experimental Physics, Campus E2 9, Saarland University, D-66123 Saarbrücken, Germany
[2] Institute of Medical Microbiology and Hygiene, Saarland University, D-66421 Homburg/Saar, Germany

Received 3 July 2015 and Received in final form 28 September 2015
Published online: 28 December 2015 –

Abstract. The atomic force microscope (AFM) evolved as a standard device in modern microbiological research. However, its capability as a sophisticated force sensor is not used to its full capacity. The AFM turns into a unique tool for quantitative adhesion research in bacteriology by using "bacterial probes". Thereby, bacterial probes are AFM cantilevers that provide a single bacterium or a cluster of bacteria as the contact-forming object. We present a step-by-step protocol for preparing bacterial probes, performing force spectroscopy experiments and processing force spectroscopy data. Additionally, we provide a general insight into the field of bacterial cell force spectroscopy.

1 Introduction

Infectious biofilms on implants or catheters cause serious medical problems that may lead to major medical intervention [1,2]. One key step in the development of a biofilm is the adhesion of bacteria to these medical devices. However, a fundamental understanding of the basic processes governing bacterial adhesion is still lacking [3]. Atomic force microscope (AFM) used in force spectroscopy mode is a promising technique to close this gap in knowledge. By attaching a single bacterium or a cluster of bacteria to an AFM cantilever, so called "bacterial probes" can be prepared, which allow studying the adhesion process of bacteria with nanometer spatial and piconewton force resolution [4–7].

This paper details a protocol for the fabrication of bacterial probes, both with a cluster of bacteria ("bacterial cluster probe", fig. 1a) or one single bacterium ("single bacterial probe", fig. 1b). Further, a detailed description of how to measure and process force spectroscopy data ("force/distance curves", fig. 1c) with bacterial probes will be given.

2 Bacterial cell force spectroscopy

Single cell force spectroscopy (SCFS) is a well-established method for the characterization of adhesive properties of eukaryotic cells [9–12]. The concept of bacterial cell force spectroscopy is the logical continuation of SCFC to prokaryotic cells.

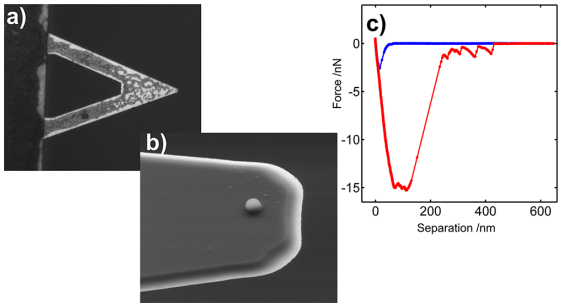

Fig. 1. a) "Bacterial cluster probe", tipless cantilever covered with a large number of bacteria, b) "single bacterial probe", tipless cantilever with one single bacterial cell attached, c) representative force/distance curve taken with a single *S. aureus* cell adhering to a hydrophobized Si wafer in PBS buffer (for preparation of the hydrophobic substrate see ref. [8]). Approach (retraction) curve in blue (red).

To perform AFM force spectroscopy experiments with bacterial probes, a single bacterium or a cluster of bacteria has to be immobilized on an AFM cantilever. For the immobilization, two parameters are of major importance, namely the geometry of the AFM tip and the selection of an appropriate glue, *i.e.* a glue that binds the bacteria strong enough to the cantilever to perform force measurements, without changing the properties of the bacterial cells.

[a] *Present address:* Dept. of Bioengineering and California Institute for Quantitative Biosciences (QB3), University of California at Berkeley, Berkeley, California 94720, USA.
[b] e-mail: k.jacobs@physik.uni-saarland.de

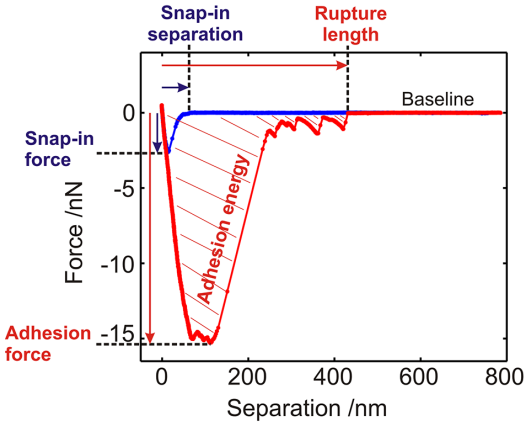

Fig. 2. Representative force/distance curve taken with a single *S. aureus* cell adhering on a hydrophobized Si wafer in PBS buffer. Approach (retraction) curve in blue (red). Fundamental measurands that characterize the bacterial adhesion process are highlighted.

The outcome of AFM force spectroscopy measurements with bacterial probes are called force/distance curves. Thereby, the force acting on the bacterium (attached to an AFM cantilever), is monitored as the cantilever (and the bacterium) is approached to the surface, pressed onto it with a certain maximum force (called "force trigger"), and retracted from the surface. Figure 1c and fig. 2 show a representative force/distance curve taken with a *Staphylococcus aureus* single bacterial probe; the approach and retraction curves are shown in blue and red, respectively. Force/distance curves allow to quantify bacterial adhesion by several means (cf. fig. 2): The range of attractive forces upon approach can be measured ("snap-in separation"), additionally the "snap-in force" is a measure for the strength of the attractive forces. During retraction, the lowest point of the curve determines the adhesion force of the bacterium and the distance where the adhesive contact is lost defines the "rupture length". Integrating over the area above the retraction curve provides the adhesion energy. Further quantitative parameters such as the separation of the adhesion peak, or the number and depth of secondary peaks can be evaluated depending on the experimental goal. Thus, AFM force spectroscopy with bacterial probes is a unique tool to gain access into bacterial adhesion in a quantitative manner.

2.1 Tip geometries

Various tip geometries can be used as a basis for bacterial probes. To implement experiments enabling both a large number of repetitions required in biological experiments and a large degree of control of experimental parameters, the number of immobilized bacteria needs to be controlled while keeping the preparation procedure as simple as possible. The most advanced bacterial probes feature one single immobilized bacterium (single bacterial probe) as this is the most precise way to characterize bacterial adhesion [7,13]. However, bacterial probes with a larger number of immobilized bacteria (bacterial cluster probes) may be used, as their preparation is less complex and time consuming [14,6]. When using bacterial cluster probes, on the one hand only measurements with the same bacterial probe are comparable, on the other hand the overall larger adhesion force and the averaging over many individual adhesion events can lead to better statistics of the measurements.

The most common tip geometry is the absence of a tip [5,15–18]. These so-called tipless cantilevers feature a large and accessible contact area. Functionalization with a glue and fixation of bacteria are straightforward in the case of tipless cantilevers.

Further typical tip geometries utilized as a basis for bacterial probes are spherical probes [19–21] and pyramidal tips [22–24]. Both spherical probes and pyramidal tips offer only a small contact area to the bacteria due to the curved and pointed geometry. Therefore, a high adhesive strength of the glue holding the bacteria onto the cantilevers is necessary. Moreover, it is challenging to place single bacteria at a specific spot, the apex of the tip or the topmost part of the sphere.

Here we detail a protocol using tipless cantilevers which possesses ease of use and, while using "single bacterial probes", ensures the comparability of different bacterial probes.

2.2 Immobilization methods

As mentioned above, the selection of the best suited glue is challenging due to two major requirements: On the one hand, bacteria have to be attached to the cantilever by a force that exceeds the adhesion force to the substrate under study. On the other hand, the viability and the properties of the bacterial cell wall that is not in contact with the cantilever should not be affected.

Various types of glues based on different binding mechanisms have been presented in the literature:

- Positively charged polymer coatings such as polyethyleneimine (PEI) [22,25] and poly-L-lysine (PLL) [16, 26] can be used, since the surfaces of both the bacterium and the cantilever, are negatively charged at a physiological *p*H. However, the effectivity of the electrostatic immobilization may decrease depending on the concentration of electrolytes.
- By using aminosilanes, -thiols [20,27], or (poly)dopamine (PDA) [28,5], the cantilevers can be functionalized with amino groups that can form strong, unspecific, covalent bonds with carboxyl groups that are accessible in the bacterial cell wall. Covalent binding between carboxyl and amino groups may be enhanced by 1-Ethyl-3-(3-dimethylaminopropyl)-carbodiimide/N-hydroxysuccinimide (EDC/NHS) treatment [29,30].

– Specific linkage can be achieved by coating the cantilevers with proteins serving as ligands for components of the bacterial cell wall (*i.e.* fibronectin-fibronectin binding proteins) [31,32]. Similarly, a commercially available cell adhesive protein derived from *Mytilus edulisi* (Cell-Tak^{TM}) was reported to be a suitable glue to immobilize bacterial cells [30,33].

Although approaches such as the use of regular glue (*e.g.* glass adhesive) have also been reported in the literature [15,34], a satisfactory fulfillment of the second requirement, the prevention of any alteration of the bacterium, is highly doubtful. The same is true for procedures involving a crosslinking via glutaraldehyde or formaldehyde [25,22], which are known to have an effect on the surface properties of the entire bacterium [35,36].

To immobilize bacterial cells, our protocol utilizes a polydopamin coating of AFM cantilevers that is inspired by a work by Lee *et al.* [37]. This coating combines ease of use with biological compatibility and durability [5,7,13].

2.3 Bacterial cluster force spectroscopy

The small size of bacterial cells makes their handling challenging, yet measuring the adhesion of bacterial cell clusters using "bacterial cluster probes" circumvents this problem [14,6]: These bacterial probes are much easier to produce, but lead to less controlled and less quantitative experimental results as the number of bacteria and the area of contact interacting with the respective surface is largely unknown. When comparing the adhesion to different surfaces, this problem can be handled by performing consecutive measurements on the surfaces of interest with the identical bacterial probe. The result, however, will always be a relative one, since absolute force values cannot be measured with this kind of probe. A comparison between different bacterial probes or different bacterial species is not possible [6]. Bacterial cluster probes are usually based on tipless cantilevers [18,6], some studies, however, describe the use of spherical tips [19] or even normal cantilevers, where the tip is covered with bacteria [23,14]. Another interesting approach is the application of an entire bacterial biofilm to a glass sphere attached to an AFM cantilever [38,39]. Regardless of the exact procedure, all of these bacterial cluster probes lack a certain level of control.

2.4 Single bacterial cell force spectroscopy

The problem of measuring adhesion in an absolute manner can be solved by controlling the number of adhering bacteria, at best by using only one bacterium ("single bacterial probes"). However, the accurate attachment of a single bacterium to an AFM cantilever is fairly impossible without adequate technical equipment, *e.g.* an AFM with an integrated inverted microscope [7,21] or a micromanipulation system [5,13]. The use of a single bacterial probe results in a highly controlled experiment in terms of the load applied to the bacterium and the measured quantities, in particular the adhesion force. In addition, the viability of the characterized single bacterium can be checked by subsequent live/dead staining.

3 Experimental protocol

3.1 Fundamentals

3.1.1 AFM

We use a Bioscope Catalyst (Bruker-Nano, Santa Barbara, Ca, USA) for AFM bacterial cell force spectroscopy. Yet, the protocol detailed here does not require any special AFM model, except for the possibility of recording force/distance curves.

The following components are part of our AFM system:

1. BioScope Catalyst head ("head")
2. Nanoscope V controller ("controller")
3. BioScope Catalyst Electronics Interface Box ("E-Box")
4. BioScope Catalyst baseplate with sample holder plate ("sample holder")
5. EasyAlign for infrared laser alignment ("alignment station")
6. Joystick for controlling x, y, z motors
7. Nanoscope Software (version 8.15) ("software")
8. Probe holder for measurement in liquid
9. Mount for the probe holder while changing cantilever
10. Magnetic sample substrate clamps

3.1.2 Micromanipulation system

The components of our micromanipulation system are:

1. Inverted fluorescence light microscope Leica DMIL LED Flou
2. Micromanipulator Narishige MOM 202D
3. A homemade aluminum arm with a hole on its upper end (fig. 3a)
4. A small cross of PMMA that can be inserted into the aluminum arm (fig. 3b)
5. Double-sided adhesive tape

3.1.3 Cantilevers

The adhesion forces of bacteria can vary over a huge range of forces, from below 100 pN to several tenths of nN. Hence, some experience is necessary to identify the right cantilever spring constant, since stiff cantilevers allow the

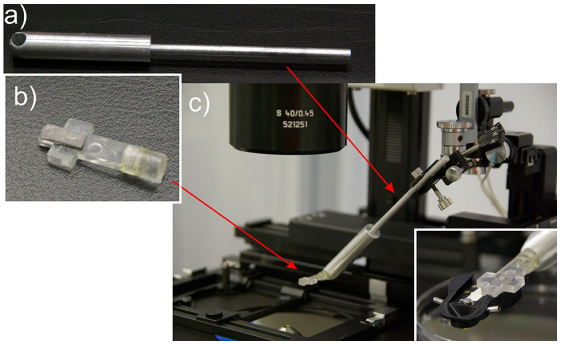

Fig. 3. a) Aluminium micromanipulation arm with a hole to insert the PMMA cross, b) PMMA cross with a small piece of double-sided adhesive tape, c) manipulation arm with PMMA cross inserted into the micromanipulator. The inset shows the cantilever holder attached to the PMMA cross.

measurement of higher forces but reduce the experimental resolution in terms of force. We use spring constants between 0.03 and 0.5 N/m depending on the expected forces during the adhesion process.

3.2 The protocol

3.2.1 Functionalization of the cantilever

This method of cantilever-functionalization is inspired by a publication by Lee *et al.* [37].

1. Take out as many cantilevers as you plan to use in today's experiment, and put them into a clean glass petri dish. The cantilever coating should be freshly prepared each day.
2. Cantilevers are cleaned in an air-plasma for 30 seconds, to get rid of any organic residues.
3. From now on, we perform every step under class 100 (less than 100 particles/ft^3) clean room conditions to reduce the risk of cantilever contamination (clean room conditions are helpful, yet might not be necessary).
4. Prepare a solution of 4 mg/ml dopamin hydrochloride (Sigma-Aldrich) in TRIS/HCL-Buffer (Sigma-Aldrich, 10 mMolar, *p*H 7.9 at 22 °C).
5. Dip the cantilevers vertically into the dopamin solution and store them for about one hour in the refrigerator.
6. Take the cantilevers out of the solution and rinse them carefully with ultrapure water (0.055 μS/cm at 26 °C).
7. Dry the cantilevers under vacuum (approx. 1 mbar) for about 15 minutes or under a laminar flow bench for at least one hour.
8. Proceed with the calibration of the cantilever.

3.2.2 Preparation of the substratum

The surface preparation very much depends on the type of substratum. Therefore, this issue is not detailed here. However, some fundamentals have to be obeyed irrespective of the exact surface: The surface has to be clean and inert concerning the used buffer solution and it must be fixed within the liquid cell (a petri dish or something similar) in order to prevent unwanted motion of the substratum. If using glue for fixation, it must not contaminate the buffer and should not dissolve. We use polystyrene of high molecular weight (780 kg/mol) dissolved in chloroform (in a concentration of 40-50 mg/ml), which works well in combination with polystyrene petri dishes. The chloroform evaporates fast and the residual polymer melt is a ideal non-dissolving glue.

3.2.3 Calibration of the cantilever

The calibration of the cantilever is a crucial step in AFM force spectroscopy. In order to be able to apply exact force values, calibration should be done before bacterial force spectroscopy measurements. If the single bacterium is attached using the AFM piezo drive, no difficulties will occur during this step (the protocol is the same) [21]. However, this protocol describes the attachment of a single bacterium via an external micromanipulation system. Therefore, the cantilever has to be removed from the AFM head after calibration. This step could result in a change of the deflection sensitivity since the laser spot has to be refocused after the reassembly of the cantilever into the AFM head. Yet, experience has shown that the deflection sensitivity does not change significantly if i) the laser position on the cantilever matches the position during calibration, which should be controlled by eye and ii) the laser sum is almost identical to before. In the following, we give step-by-step instructions for calibrating an AFM cantilever:

1. Check that AFM, computer, controller, and other AFM electronic devices as well as all necessary components of the optical microscope are turned on. Depending on the instruments, it may take a significant amount of time until *e.g.* thermal drifts have equilibrated.
2. Prepare everything for a contact mode experiment in liquid.
3. For the calibration of the cantilever, a hard (indeformable) sample should be used to determine the deflection sensitivity.
4. Insert the functionalized cantilever carefully into the cantilever holder that enables measurements in liquid and cover it with a droplet of liquid (*e.g.* PBS) to avoid contamination.
5. Integrate the cantilever holder into the AFM head.
6. Align the laser spot on the back of the cantilever maximising the sum of the voltage signal on the photodiode.

7. Place the cantilever over the hard sample surface to calibrate it.
8. Approach the surface to a distance of about 100 μm manually.
9. Give the AFM/cantilever some time to equilibrate, until a constant signal on the photodiode is reached.
10. Enter the deflection setpoint to approach the surface.
11. Start the approach.
12. As soon as the cantilever reaches the surface, change into ramp mode.
13. Give values for ramp rate (ramp size). Common values are between 0.5 and 1.5 Hz (600 to 1000 nm).
14. Enter an approximate spring constant to perform the calibration force/distance curve. Usually, the value indicated by the manufacturer is sufficient at this point.
15. Enter a force trigger of 3–8 nN (depending on the cantilever stiffness) and record one single force/distance curve.
16. To get a reliable value for the deflection sensitivity, a large, undisturbed, linear part in the contact regime of the force/distance curve is necessary. If the force curve does not exhibit an appropriate linear part, try a larger force trigger.
17. The deflection sensitivity is determined by calculating the inverse of the slope of the force/distance curve in the contact regime (this is usually implemented in the AFM software).
18. Update the deflection sensitivity.
19. Retract the cantilever from the surface.
20. To prepare for thermal tune, the influence of the surface must be excluded. Therefore, enlarge the distance between the surface and the cantilever. It should be at least 50 μm.
21. Perform a thermal tune to determine the cantilever spring constant (details should be checked in the user manual of the respective AFM).
22. Update the spring constant and retract the cantilever completely.
23. Remove the cantilever holder (with cantilever) from the AFM. Care should be taken to maintain a small amount of liquid on the cantilever holder covering the cantilever to avoid contamination of the cantilever.
24. Go on with "attachment of bacteria".

3.2.4 Attachment of bacteria

In the following, we describe two different methods for attaching bacteria to a functionalized cantilever: i) A rather simple method to produce a bacterial probe with a cluster of attached bacteria, and ii) a more complex preparation for the attachment of a single bacterial cell to a tipless cantilever is detailed.

Bacterial cluster probe

1. Place the functionalized tipless cantilever on a hydrophobic surface. The side intended to carry the bacteria faces upwards.
2. Cover the cantilever with a droplet of bacterial solution ($\approx$ 60 μl) and leave it in the refrigerator (to reduce Brownian motion) for at least one hour.
3. Remove the bacterial solution and rinse the cantilever carefully with PBS buffer to get rid of poorly attached bacteria.
4. By optical microscopy, verify that bacteria are attached close enough to the free end of the cantilever (not further away than roughly three bacterial diameters[1] to safely exclude cantilever/substrate interactions), while the cantilever stays in liquid the whole time. Ideally, this step is done using reflection optical microscopy. Alternatively, a transmission optical microscope can be used after integrating the cantilever into the cantilever holder for measurements in liquid and using a set-up similar to the one described in the section "single bacterial probe".
5. Integrate the cantilever into the probe holder for measurements in liquid and mount it to the AFM head.
6. Cover the cantilever immediately with a droplet of PBS to avoid drying.

Single bacterial probe

For the attachment of a single bacterium to a functionalized cantilever, a micromanipulation system is used. Stress due to capillary forces or drying should be avoided by maintaining bacterium as well as cantilever in liquid/buffer during the entire preparation procedure.

1. Put a plastic petri dish on the microscope of the micromanipulator.
2. Place a tiny droplet ($\approx$ 1 μl) of bacterial solution on the petri dish.
3. Give the bacteria some minutes to sediment on the petri dish, without complete drying.
4. Insert the manipulation arm into the micromanipulator (cf. figs. 3a and c).
5. Put a small piece of the double-sided adhesive tape on the PMMA-cross (cf. fig. 3b).
6. Fix the cantilever holder with the cantilever and the covering droplet (resulting from the calibration step) on the PMMA-cross (cf. inset to fig. 3c)[2].
7. Insert the PMMA-cross with the cantilever holder into the aluminum arm (cf. fig. 3c).

[1] The cantilever is usually tilted by an angle α in the AFM, the upper limit of the distance l between the bacteria (with diameter d) and the free end of the cantilever can be calculated as $l = d/\sin(\alpha)$.

[2] The exact procedure of integrating the cantilever holder into the micromanipulator might differ, depending on type and design of the cantilever holder.

8. Place a droplet of PBS-buffer ($\approx 20\,\mu$l) on the tiny droplet covering the pre-attached bacteria.
9. Use a 10× objective/10× eyepiece of the microscope to bring the cantilever directly over the droplet and lower it into the droplet of bacterial solution.
10. Focus onto the bacteria lying on the petri dish and approach the cantilever to the surface until it is almost in focus.
11. Change to 40× or higher objective and use the precision control to place the cantilever straight above a single bacterium.
12. Lower the cantilever onto the single bacterial cell and press it gently (the pressure can be controlled by watching the light reflection off the cantilever, which should change only slightly) onto the bacterium.
13. Pull the cantilever immediately away from the surface again. Focus onto the cantilever to confirm the attachment of a single bacterial cell close enough to the free end of the cantilever (cf. bacterial cluster probe).
14. If the bacterium did not attach, repeat step 10 to 13.
15. Retract the cantilever from the surface and out of the droplet. Ensure that a small amount of buffer remains at the probe holder covering the cantilever. As the cantilever has to be covered by liquid the whole time, some more liquid might be added if the cantilever starts drying out.
16. Confirm again the attachment of the single bacterium close enough to the free end of the cantilever (see above). If the bacterium has detached, start again with step 8.
17. Remove the probe holder from the micromanipulator and insert it into the AFM head.
18. Go on with section "Force distance measurements with a bacterial probe".

3.3 Force distance measurements with a bacterial probe

1. Place the bacterial probe right above the surface on which the adhesion will be measured. At best, the droplet covering the cantilever and the liquid covering the surface do not touch at this step.
2. Use the AFM step motor to lower the cantilever towards the surface. Stop the movement about $100\,\mu$m above the surface. Crashing the cantilever into the surface will at best only detach bacteria, but may destroy the cantilever.
3. Check the experimental parameters: AFM in "contact mode", set scan size to zero, choose a "deflection setpoint" that ensures a force of less than 1 nN.
4. Start the approach.
5. As soon as the approach is finished, change into force spectroscopy mode, this will retract the bacterium from the surface.
6. Set the parameter values for the force/distance measurements:
   - Define the total distance the piezo moves during the force/distance curve (this value may be called "ramp size"). The value for the ramp size depends on the expected rupture length (see above), common values for the ramp size are around $1\,\mu$m.
   - Define the number of data points while approaching/retracting, which constitutes —in combination with the ramp size— the z-resolution of the curve. The z-resolution should be at least one point per nm.
   - Define the number of full force/distance curves per second ("ramp rate"). In combination with the ramp size, the ramp rate defines the tip velocity. Typical values are between 0.5 and 1.5 Hz.
   - Define the speed of the piezo movement in z-direction. This defines in combination with the ramp size - the ramp rate.
   - Define the so called "trigger threshold" (this is the force value at which the cantilever/bacterium approach is stopped). Typical values are less than 0.5 nN.
   - Define a time span between stopping the approach and starting the retraction of the cantilever, *i.e.* a time of contact between bacterium and surface (this value is called "surface delay").
   - A second timespan may be defined that delays the start of a force/distance curve after full retraction of the preceding one.
7. Perform one single force/distance curve with the above-defined parameters.
8. Investigating the shape of the force/distance curve will help to decide whether the bacterium is still attached to the cantilever (cf. fig. 3 of ref. [13]) or not. However, as the shape of the force/distance curve depends on the combination of surface and bacterium, this may require some experience. If the bacterium becomes detached, attach a new one.
9. Run a number of force/distance measurements with one set of parameters. Take care that the same spot of the substratum is not probed twice to exclude influences of potential residues originating from preceding approaches. Some AFM offer an automatic realization of a number of force/distance curves on different spots.
10. Conduct additional sets of force/distance curves while changing the experimental parameters according to the respective experimental goal.
11. Take care that the last series of force/distance curves for a bacterial probe reproduce the parameters of the first series. That way, changes of the bacterial adhe-

sion properties due to the force measurements can be identified. The number of maximum force/distance curves per bacterial probe is usually limited due to fading effects (*i.e.* the adhesion strength of the bacterium may decrease due to repeated pull-off events, possibly by losing surface adhesins) or loss of the bacterium/bacteria. The influence of fading effects depends on the respective bacterium/surface combination, however, at least 100-150 curves per bacterial probe are usually possible.

12. If all measurements are finished, retract the cantilever from the surface.
13. In the case of single cell measurements, the existence of the single bacterium can be confirmed optically.
14. If the AFM is linked to an integrated inverse microscope, the presence of the single bacterium on the cantilever can be checked directly. Otherwise, the cantilever has to be removed from the AFM and reintegrated into the inverse microscope linked to the micromanipulator:
    (a) Use the motors to retract the cantilever as far as possible from the surface.
    (b) Remove the cantilever holder (with cantilever) from the AFM. It is important that some liquid (buffer) remains that covers the bacterial probe. This avoids losing the bacterium by capillary forces and prevents it from drying out. If the droplet covering the cantilever is tiny, add a small amount of buffer ($\approx 10\,\mu$l) with the pipette.
    (c) Insert holder and cantilever into the microscope set-up (specified in paragraph "Single bacterial probe").
    (d) Use the microscope to confirm the attachment of the single bacterium.
15. The cantilever may be reused by detaching the single bacterium and attaching a new one:
    (a) Put a plastic petri dish on the inverted microscope linked to the micromanipulator.
    (b) Use the 10× objective to approach the cantilever with the single bacterium towards the surface of the petri dish and stop a few micrometers before.
    (c) Use the 40× objective and carefully press the bacterium onto the surface until a slight deflection of the cantilever can be seen by a change in the cantilever light reflection.
    (d) Pulling the cantilever backwards over the surface (in the xy plane) will shear the bacterium off the cantilever.
    (e) Retract the cantilever from the surface. Make sure that a small amount of liquid remains on the petri dish covering the bacterium. The viability of this bacterium can then be checked by a live/dead stain in the following.
    (f) Repeat the "single bacterium probe" steps to attach a new bacterium.

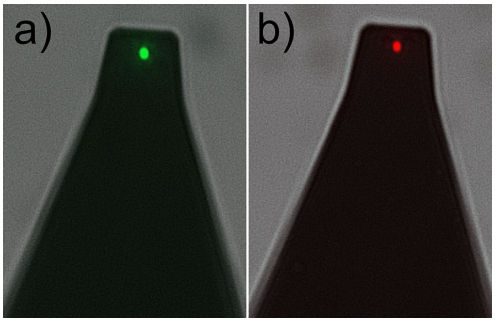

Fig. 4. a) Viable *Staphylococcus carnosus* cell attached to a tipless AFM cantilever. Staining was applied after one hundred force/distance curves. b) Ethanol-killed *S. carnosus* cell attached to a tipless AFM cantilever. Live/dead staining was performed as described in chapt. 3.4.

3.4 Viability of bacteria

The viability of the bacterium/bacteria either attached to the cantilever or the one sheared off on a petri dish (see previous paragraph) can be checked via a live/dead stain. However, as the shearing process may harm sensitive bacterial cell types, we recommend testing the viability directly on the cantilever.

1. Focus the fluorescence microscope on the bacterium lying on the petri dish or fixed to the cantilever.
2. Add a small amount of live/dead stain (*e.g.* Life Technologies GmbH, Germany) (about $20\,\mu$l) to the buffer covering the bacterium.
3. Shade all the surrounding light to avoid photobleaching and wait for ten minutes.
4. Verify the viability of the bacterium used in the force measurements by means of its color (cf. fig. 4).

3.5 Data calibration

The basic data recorded by the AFM during a force spectroscopy experiment are the voltage applied to the piezo controlling the movement in z-direction (z-piezo) and the voltage signal on the photodiode, quantifying the shift of the laser spot reflected from the back of the cantilever. A "height sensor" may give a second measure for the z-position of the cantilever. Based on the calibration, these outputs are then presented as a force *vs.* z-position curve. This is usually done automatically, nevertheless, we will go through it here:

1. The AFM internal calibration of the z-piezo converts the applied voltage into the dilatation of the piezo. However, users should be aware that the z-position is always a relative measure between the starting point and the actual position.

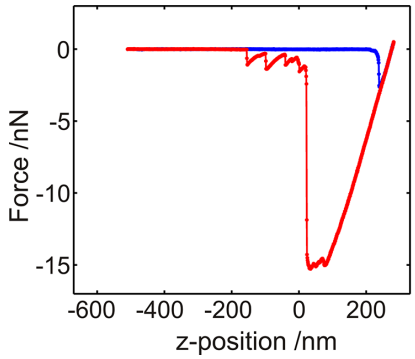

Fig. 5. Force/distance curve plotted as force *vs.* z-position after baseline correction. Approach (retraction) curve is shown in blue (red).

2. Two steps are performed to convert the voltage signal from the photodiode into the actual force exerted on the cantilever:
   - The deflection of the cantilever "d" in nm can be obtained by multiplying the voltage signal by the deflection sensitivity (see calibration of cantilever).
   - The force on the cantilever "F" in nN can be calculated by applying Hooke's law ($F = k \cdot d$), with the spring constant "k" of the cantilever (see calibration of cantilever).
3. Since the output of the photodiode is a relative measure, the baseline of the force distance curve — representing the zero-force part before/after contact— is often shifted along the y-axis. By applying an offset correction, the baseline can be brought in line with the x-axis (cf. fig. 5)

These three steps result in a calibrated force/distance curve in the form of a force *vs.* z-position plot (cf. fig. 5). For most subsequent analysis steps, however, the force *vs.* z-position representation is not ideal and rather a force "F" *vs.* separation "s" plot is required. One of the main disadvantages of AFM in general is that it lacks the ability to directly measure the separation between probe and surface since the system basically reports solely the z-position of the cantilever mount. Yet, if the point of zero separation *i.e.* the point of contact "z_0" between probe and surface can be accurately determined in the force/distance curve, it is possible to convert the z-position to the actual separation. In the case of a bacterium adhering to a hard surface, the point of contact can be assumed to be the point at which force is again zero after the snap-in event (cf. fig. 6a). To convert the force *vs.* z-position plot then into a force *vs.* separation plot, the following two steps are required (cf. fig. 6):

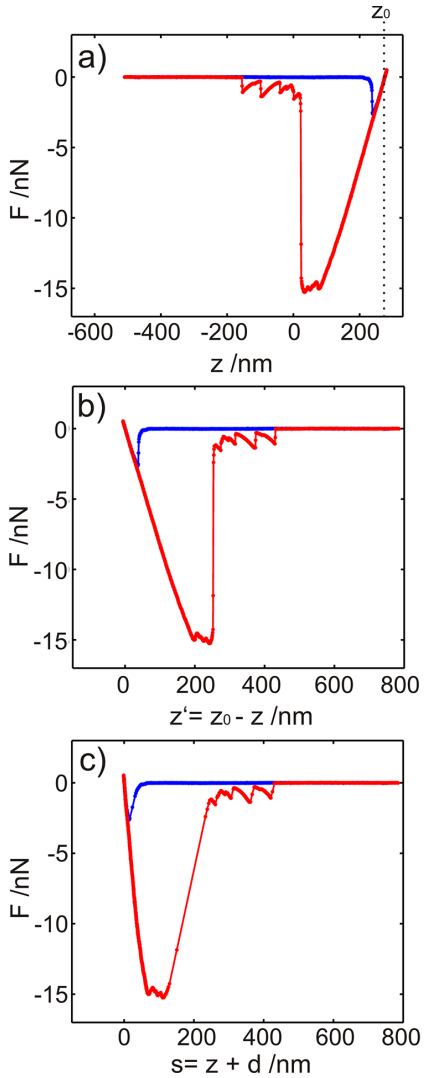

Fig. 6. Work steps for calculating a force (F) *vs.* separation (s) curve. a) Starting with a baseline-corrected force (F) *vs.* z-position (z) curve, b) a force (F) *vs.* z-position (z') curve with the respective point of contact is calculated and c) subsequently transformed into the force (F) *vs.* separation (s) curve.

1. Define the contact point z_0, in our case this is the point of zero force after the snap-in (cf. fig. 6a). Shift the force/distance curve along the x-axis by calculating $z' = z_0 - z$ (cf. fig. 6b).
2. The separation between the bacterium and the substrate surface is calculated by adding the deflection d to the shifted z-position z' (cf. fig. 6c).

The calculation can be done simultaneously for both approach and retraction part of the force/distance curve.

4 Conclusion

Here we present a simple and reproducible procedure to fabricate viable bacterial probes and to perform bacterial cell force spectroscopy measurements. The protocols presented describe the fabrication of both bacterial cluster probes, as well as single bacterial probes, in detail. Our approach allows for measurements with high precision and high throughput and features a simplicity with regards to applicability and equipment availability, which may pave the way for bacterial cell force spectroscopy as a standard technique in modern bacterial adhesion research.

This work was supported by the Deutsche Forschungsgemeinschaft (DFG) within the collaborative research center SFB 1027 and the research training group GRK 1276 (N.T.). M.B. was supported by the grant of the German Ministry for Education and Research 01Kl1301B.

References

1. A.E. Khoury, K. Lam, B. Ellis, J.W. Costerton, ASAIO J. **38**, M174 (1992).
2. J.W. Costerton, P.S. Stewart, E.P. Greenberg, Science **284**, 1318 (1999).
3. K. Hori, S. Matsumoto, Biochem. Engin. J. **48**, 424 (2010) ISSN 1369-703X, invited Review Issue 2010.
4. Y. Seo, W. Jhe, Rep. Prog. Phys. **71**, 016101 (2008).
5. S. Kang, M. Elimelech, Langmuir **25**, 9656 (2009).
6. P. Loskill, H. Haehl, N. Thewes, C.T. Kreis, M. Bischoff, M. Herrmann, K. Jacobs, Langmuir **28**, 7242 (2012).
7. A. Beaussart, S. El-Kirat-Chatel, P. Herman, D. Alsteens, J. Mahillon, P. Hols, Y. Dufrêne, Biophys. J. **104**, 1886 (2013).
8. M. Lessel, O. Bäumchen, M. Klos, H. Hähl, R. Fetzer, M. Paulus, R. Seemann, K. Jacobs, Surf. Interface Anal. **47**, 557 (2015).
9. M. Benoit, D. Gabriel, G. Gerisch, H.E. Gaub, Nat. Cell Biol. **2**, 313 (2000).
10. M. Benoit, H.E. Gaub, Cells Tissues Organs **172**, 174 (2002).
11. P.H. Puech, K. Poole, D. Knebel, D.J. Muller, Ultramicroscopy **106**, 637 (2006).
12. J. Helenius, C.P. Heisenberg, H.E. Gaub, D.J. Muller, J. Cell Sci. **121**, 1785 (2008).
13. N. Thewes, P. Loskill, P. Jung, H. Peisker, M. Bischoff, M. Herrmann, K. Jacobs, Beilstein J. Nanotechnol. **5**, 1501 (2014).
14. X. Sheng, Y. Peng Ting, S.O. Pehkonen, J. Colloid Interface Sci. **310**, 661 (2007).
15. W.R. Bowen, R.W. Lovitt, C.J. Wright, J. Colloid Interface Sci. **237**, 54 (2001).
16. N.P. Boks, H.J. Busscher, H.C. van der Mei, W. Norde, Langmuir **24**, 12990 (2008).
17. L. Mei, Y. Ren, H.J. Busscher, Y. Chen, H.C. van der Mei, J. Dental Res. **88**, 841 (2009).
18. W. Zhang, A.G. Stack, Y. Chen, Colloids Surf. B: Biointerfaces **82**, 316 (2011).
19. S.K. Lower, C.J. Tadanier, M.F.H. Jr., Geochim. Cosmochim. Acta **64**, 3133 (2000).
20. S.K. Lower, M.F. Hochella, T.J. Beveridge, Science **292**, 1360 (2001).
21. A. Beaussart, S. El-Kirat-Chatel, R.M.A. Sullan, D. Alsteens, P. Herman, S. Derclaye, Y.F. Dufrêne, Nat. Protocols **9**, 1049 (2014).
22. A. Razatos, Y.L. Ong, M.M. Sharma, G. Georgiou, Proc. Natl. Acad. Sci. U.S.A. **95**, 11059 (1998).
23. R.J. Emerson IV, T.S. Bergstrom, Y. Liu, E.R. Soto, C.A. Brown, W.G. McGimpsey, T.A. Camesano, Langmuir **22**, 11311 (2006).
24. T. Cao, H. Tang, X. Liang, A. Wang, G.W. Auner, S.O. Salley, K. Ng, Biotechnol. Bioengin. **94**, 167 (2006).
25. Y.L. Ong, A. Razatos, G. Georgiou, M.M. Sharma, Langmuir **15**, 2719 (1999).
26. W. Qu, H.J. Busscher, J.M. Hooymans, H.C. Van der Mei, J. Colloid Interface Sci. **358**, 430 (2011).
27. A.L. Neal, T.L. Bank, M.F. Hochella, K.M. Rosso, Geochem. Trans. **6**, 77 (2005).
28. H. Lee, J. Rho, P.B. Messersmith, Adv. Mater. **21**, 431 (2009).
29. E. Velzenberger, I. Pezron, G. Legeay, M.D. Nagel, K.E. Kirat, Langmuir **24**, 11734 (2008).
30. R.L. Meyer, X. Zhou, L. Tang, A. Arpanaei, P. Kingshott, F. Besenbacher, Ultramicroscopy **110**, 1349 (2010).
31. P. Kuusela, Nature **276**, 718 (1978).
32. A.W. Buck, V.G. Fowler Jr., R. Yongsunthon, J. Liu, A.C. DiBartola, Y.A. Que, P. Moreillon, S.K. Lower, Langmuir **26**, 10764 (2010).
33. G. Zeng, T. Mu ller, R.L. Meyer, Langmuir **30**, 4019 (2014).
34. W.R. Bowen, A.S. Fenton, R.W. Lovitt, C.J. Wright, Biotechnol. Bioengin. **79**, 170 (2002).
35. S.B. Velegol, B.E. Logan, Langmuir **18**, 5256 (2002).
36. G.A. Burks, S.B. Velegol, E. Paramonova, B.E. Lindenmuth, J.D. Feick, B.E. Logan, Langmuir **19**, 2366 (2003).
37. H. Lee, S.M. Dellatore, W.M. Miller, P.B. Messersmith, Science **318**, 426 (2007).
38. P.C. Lau, J.R. Dutcher, T.J. Beveridge, J.S. Lam, Biophys. J **96**, 2935 (2009).
39. P.C. Lau, T. Lindhout, T.J. Beveridge, J.R. Dutcher, J.S. Lam, J. Bacteriol. **191**, 6618 (2009).

Addendum II - The Influence of the subsurface composition of a Material on the Adhesion of *Staphylococci*

Authors: P. Loskill[1], H. Hähl[1], N. Thewes[1], C. T. Kreis[1], M. Bischoff[2], M. Herrmann[2], and K. Jacobs[1]

[1] Department of Experimental Physics, Saarland University, 66041 Saarbrücken, Germany.
[2] The Institute of Medical Microbiology and Hygiene, Saarland University, 66421 Homburg/Saar, Germany.

Reprinted with permission from Loskill et al.,
Langmuir **28**, 7242–7248 (2012).

(`http://dx.doi.org/10.1021/la3004323`)

Author contributions:
Experiments were conceived and designed by P. Loskill, H. Hähl, M. Bischoff, M. Herrmann, and K. Jacobs. AFM experiments were performed by P. Loskill and N. Thewes. Flow chamber experiments were performed by C. T. Kreis. Data was analyzed by P. Loskill. The article was written by P. Loskill and K. Jacobs. Research was directed by M. Herrmann and K. Jacobs.

Abstract - Controlling the interface between bacteria and solid materials has become an important task in biomedical science. For a fundamental and comprehensive understanding of adhesion it is necessary to seek quantitative information about the involved interactions. Most studies concentrate on the modification of the surface (chemical composition, hydrophobicity or topography), neglecting, however, the influence of the bulk material, which always contributes to the overall interaction via van der Waals forces. In this study, we applied AFM force spectroscopy and flow chamber experiments to probe the adhesion of S. carnosus to a set of tailored Si wafers, allowing for a separation of short- and long-range forces. We provide experimental evidence that the subsurface composition of a substrate influences bacterial adhesion. A coarse estimation of the strength of the van der Waals forces via the involved Hamaker constants substantiates the experimental results. The results demonstrate that the uppermost layer is not solely responsible for the strength of adhesion. Rather, for all kinds of adhesion studies, it is equally important to consider the contribution of the subsurface.

Langmuir

Article

pubs.acs.org/Langmuir

Influence of the Subsurface Composition of a Material on the Adhesion of *Staphylococci*

Peter Loskill,[†] Hendrik Hähl,[†] Nicolas Thewes,[†] Christian Titus Kreis,[†] Markus Bischoff,[‡] Mathias Herrmann,[‡] and Karin Jacobs*[,†]

[†]Department of Experimental Physics, Saarland University, Saarbrücken, 66041, Germany

[‡]The Institute of Medical Microbiology and Hygiene, Saarland University, Homburg/Saar, 66421, Germany

ABSTRACT: Controlling the interface between bacteria and solid materials has become an important task in biomedical science. For a fundamental and comprehensive understanding of adhesion it is necessary to seek quantitative information about the involved interactions. Most studies concentrate on the modification of the surface (chemical composition, hydrophobicity, or topography) neglecting, however, the influence of the bulk material, which always contributes to the overall interaction via van der Waals forces. In this study, we applied AFM force spectroscopy and flow chamber experiments to probe the adhesion of *Staphylococcus carnosus* to a set of tailored Si wafers, allowing for a separation of short- and long-range forces. We provide experimental evidence that the subsurface composition of a substrate influences bacterial adhesion. A coarse estimation of the strength of the van der Waals forces via the involved Hamaker constants substantiates the experimental results. The results demonstrate that the uppermost layer is not solely responsible for the strength of adhesion. Rather, for all kinds of adhesion studies, it is equally important to consider the contribution of the subsurface.

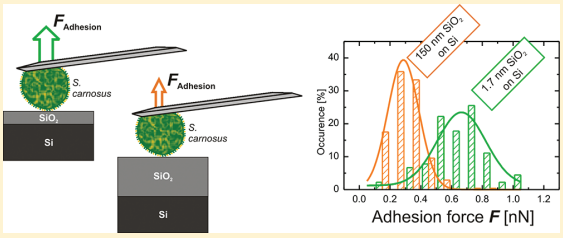

INTRODUCTION

Adhesion and adsorption of proteins and bacteria onto inorganic surfaces is crucial in various biomedical fields, such as biofilm formation or DNA arrays.[1,2] Thus, it has become an important task to control the interface between organic (macro)molecules and solid materials. The relevant interactions can be tuned by modifying the substrates: Most studies concentrate on the modification of the surface chemistry, the hydrophobicity, or the topography. That way, the short-range interactions are tuned.[3,4] The composition beneath the surface, however, is mostly overlooked and thereby long-range interactions are disregarded. Previous studies focusing on polymer dewetting[5,6] and liquid nanodroplets[7] showed an effect of differences in long-range van der Waals (vdW) interactions. These differences had been provoked by a variation of the subsurface composition. Similar observations have been reported for biological systems such as the adhesion of geckos[8] and the adsorption of proteins.[9]

Bacterial adhesion is mediated by proteins.[10] Hence, an influence of van der Waals interactions on the bacterial adhesion is also expected. Previous studies, however, were not able to separate parameters influencing short-range, electrostatic, and van der Waals interactions independently.[11,12] Yet, for a comprehensive understanding of the bacterial adhesion process it is necessary to seek quantitative information about the contributions of the involved interactions. In this study, we are able to tune van der Waals forces separately from other forces by using a set of tailored silicon wafers (Figure 1A): The set consists of wafers with a native oxide layer ["type N", d = 1.7(2) nm] and wafers with a thermally grown thick oxide layer ["type T", d = 150(2) nm]. Another pair of wafers with different surface properties was obtained by hydrophobizing the naturally hydrophilic wafers. Short-range interactions do not depend on the thickness of the silicon dioxide layer, whereas long-range vdW interactions do.[13,14]

The adhesion onto synthetic surfaces and the formation of biofilms is a key factor for the pathogenesis of bacteria from multiple different species.[1,15] Some species of the *Staphylococcus* genus, for instance, are known to adhere strongly to surfaces and are capable of forming biofilms[16] that are extremely resistant to removal and to antimicrobial drugs.[17] Here, we were interested in the unspecific interactions acting between a bacterium and a surface. Therefore, we concentrated on *Staphylococcus carnosus* strain TM300, an apathogenic member of the genus *Staphylococcus* and an important organism in food manufacturing, which usually serves as host organism for gene cloning.[18]

To characterize the adsorption of microorganisms to surfaces, typically parallel plate flow chambers are used.[19] In this macroscopic approach, adsorption, adhesion, and desorption effects are indistinguishable. In the past decades, some new tools have been introduced that allow for a quantitative study of bacterial adhesion, e.g., atomic force microscope (AFM).[20] Using the force spectroscopy mode of an AFM it is possible to

Received: January 30, 2012
Revised: March 2, 2012
Published: April 4, 2012

Langmuir Article

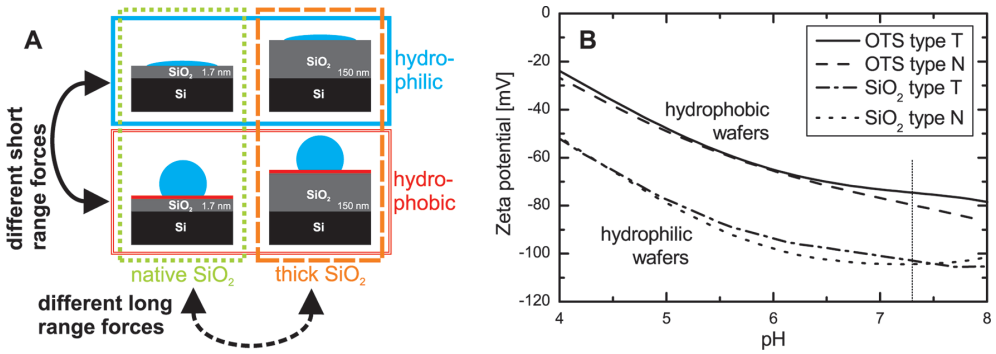

Figure 1. (A) Model substrates based on silicon wafers with different thicknesses of oxide layers that allow for a separation of effects due to short- and long-range forces. Short-range interactions are tuned by a silanization of the wafers that renders them hydrophobic. The blue droplet illustrates the different water contact angles. (B) Zeta potentials of hydrophobic and hydrophilic type T and N wafers as function of pH, giving insight into the strength of electrostatic interactions. Since the zeta potentials are indistinguishable for type T and N wafers with the same surface chemistry, differences in SiO_2 layer thickness are irrelevant for the electrostatic interactions.

probe a wide range of forces in a biologically relevant magnitude (pN to μN). A direct method to characterize bacterial adhesion onto various substrates is to use AFM probes that are covered with bacteria ("bacterial probes").[4,11,21] In this study, we used AFM force spectroscopy with bacterial probes to investigate the adhesion of *S. carnosus* (TM300) to the set of tailored silicon wafers. Since bacteria in an already adhered state (bacterial probes) might react differently as compared to bacteria in planktonic state, we also performed macroscopic flow chamber experiments with the same set of Si wafers.

MATERIALS AND METHODS

Preparation of the Substrates. The silicon wafers with the native [type N, d = 1.7(2) nm] silicon oxide layer were purchased from Wacker Siltronic AG (Burghausen, Germany) and the ones with the thick thermally grown layer [type T, d = 150(2) nm] were from Silchem (Freiberg, Germany). The substrates were cleaned by immersing them for 30 min in fresh 1:1 H_2SO_4 (conc)/H_2O_2 (30%) solution. To remove residues of the acids, the wafers were put in boiling deionized water for 90 min, the water being changed four times in between. The hydrophobic substrates were obtained by functionalizing the cleaned wafers using a liquid phase preparation of self-assembling silane molecules with a CH_3 tailgroup (octadecyltrichlorosilane, OTS, purchased from Sigma-Aldrich) following standard procedures.[22] The produced OTS surfaces feature a thickness of ≈2.6 nm, an rms roughness below 0.2 nm, and an uniform coverage, indicating a homogeneous, dense, upright, all-trans configuration of the molecules. All types of substrates were characterized by AFM, ellipsometry, zeta potential, and contact angle measurements (Figure 1B and Table 1).

Bacteria. We took stationary phase cells for the experiments. *S. carnosus* strain TM300 was cultured from blood agar plates in 5 mL of Mueller Hinton broth for 24 h at 37 °C. To remove extracellular material, bacteria were washed once with 1 mL of NaCl solution (0.9% w/v) and twice with phosphate-buffered saline (PBS, pH 7.3), each with 1 mL. Finally, the bacteria were resuspended in 300 μL of PBS and stored at 4 °C (for typically 2 h and a maximum of 48 h).

Table 1. Parameters of the Model Substrates: Root Mean Square (rms) Roughness, Advancing (adv) and Receding (rec) Contact Angles Θ of Water, and the Surface Energy γ

d_{SiO_2} (nm)	surface	rms (nm)	Θ_{adv} (deg)	Θ_{rec} (deg)	γ (mJ/m^2)
151(1)	hydrophobic	0.15(2)	112(1)	108(4)	24(1)
1.7(3)	hydrophobic	0.12(2)	111(1)	107(2)	24(1)
151(1)	hydrophilic	0.13(3)	5(2)	compl wetting	63(1)
1.7(3)	hydrophilic	0.09(2)	7(2)	compl wetting	64(1)

Preparation of Bacterial Probes. To immobilize bacteria onto tipless cantilevers we used poly-L-lysine, PLL (MP Biomedicals, Solon, OH), a polymer with positively charged side chains. Since the surfaces of both the bacterium and the cantilever are negatively charged in buffer (pH 7.3), PLL forms an adhesive interlayer.[23] Prior to the preparation procedure, the cantilevers were cleaned by treating them with an air plasma. The PLL coating was then applied by immersing the AFM cantilever in a droplet of poly-L-lysine solution (0.1 mg/mL) for 1 h. Subsequently, the cantilevers were carefully rinsed with PBS and placed in a droplet of bacteria solution for 1 h at 4 °C. To remove unbound bacteria, the probes were rinsed with PBS buffer. All probes used in this study were prepared immediately before the experiments.

AFM-Force Measurements. Experiments were conducted in PBS (pH 7.3) at room temperature with a Bioscope Catalyst (Bruker, Santa Barbara, CA). Each experiment consists of at least five series of 100 single force/distance curves. Every cantilever was calibrated using the thermal tune technique.[24] To avoid systematic errors due to local irregularities of the surface, every measurement was done on a different spot on a grid with separations of 5 μm. Single force measurements were carried out using a z-range of 1 μm, a scan rate of 1 Hz, and a relative force trigger of 1 nN. Adhesion forces were evaluated with the Nanoscope software (Bruker, Santa Barbara, CA) by calculating the difference between the adhesion peak[25] and the baseline for every single curve.[26] All single values on each substrate were fitted using a Gaussian curve. Displayed error bars describe the standard deviation.

Bacterial Probes. The bacterial probes were based on tipless cantilevers (PNP-TR-TL, Nanoworld, NeuchÃćtel, Switzerland) onto which bacteria were allowed to adsorb (Figure 2). The restricting issue of this type of probe is the comparability of serial measurements due to the uncertainty of the number of bacteria that are in contact with the substrate's surface. Therefore, it is not possible to compare measurements with different cantilevers. Measurements with the same cantilever on different substrates, however, are comparable as long as the integrity of the bacterial probe can be granted by, for example, an optical control or control measurements. We therefore always carried out the experiments on a type T and a type N wafer with the identical AFM probe. Within one experiment, consecutive series of force/distance measurements were taken alternately on the type N and T substrates, ending always on the substrate that has been probed first.

Flow Chamber Measurements. Bacteria solution of different concentrations was pumped through a custom parallel flow chamber system with dimensions 2 × 1.6 × 3 cm^3, chosen to guarantee a

Langmuir Article

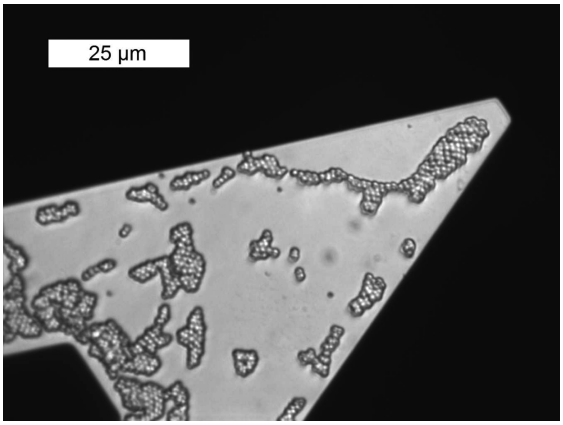

Figure 2. Optical microscopy image of *S. carnosus* immobilized by poly-L-lysine on a tipless cantilever.

uniform flow profile.[27] Measurements on type T and N substrates were always carried out using the same bacteria solution and in random order. The images were taken with a CCD-camera (Pixelfly, PCO, Kelheim, Germany), through a light microscope (Axiophot, Zeiss, Oberkochen, Germany) at a frame rate of 0.1 Hz. The number of adhering bacteria was determined using image analysis software (Image Pro Plus, Media Cybernetics, Bethesda, MD).

RESULTS

To determine whether the subsurface composition has an effect on bacterial adhesion, AFM force spectroscopy experiments with bacterial probes were carried out on all four wafer types. To distinguish from effects due to the surface chemistry, we compare the results of the two hydrophilic substrates and of the two hydrophobic substrates separately.

AFM Force Spectroscopy on Hydrophilic Substrates. Force/distance measurements on the two hydrophilic wafer types (Figure 3A) reveal a higher adhesion force on the type N than on the type T wafers. The distribution of the determined adhesion forces on the hydrophilic SiO_2 surfaces is shown in Figure 3B in the form of a histogram. We determined an average adhesion force on the hydrophilic type N wafer of F_N = 0.65(18)[28] nN and on the type T wafer of F_T = 0.30(10) nN. The integrity of the bacterial probes (detaching bacteria or other probe alteration) is controlled by two means:

(i) optical microscopy prior to and after the experiment;
(ii) control measurements, where consecutive series of force/distance measurements were taken alternately on the type N and type T substrates, ending always on the substrate that has been probed first.

In this case, (i) no detaching of bacteria was observed and (ii) the comparison of the force distribution of the different series is shown in Figure 3C,D. The means of each single series on type T wafers (I, III, V) and on type N wafers (II, IV) are identical within the experimental error.

AFM Force Spectroscopy on Hydrophobic Substrates. The determined adhesion forces on the hydrophobic substrates exhibit the same trend. The identical type of measurements including the test of the integrity of the bacterial probes was performed on the hydrophobic OTS-coated wafers. The force/distance curves (Figure 4A) resemble the ones on the hydrophilic wafers, whereby the bacterial probes stayed also intact. The average adhesion force (Figure 4B) on the hydrophobic type N wafer is F_N = 5.2(10) nN and on the type T wafer is F_T = 3.2(12) nN. Experiments with different bacterial probes lead to different absolute values (due to different densities of the bacterial layer), but the ratio is always similar (Figure 4C). The average forces on the hydrophobic substrates, however, are about one magnitude higher than the corresponding forces on the hydrophilic wafers. This

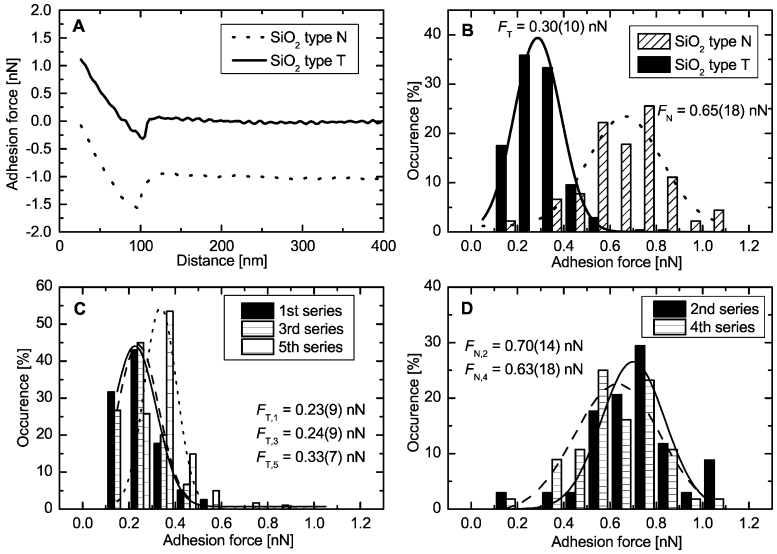

Figure 3. Results of AFM force spectroscopy experiments on bare hydrophilic substrates: (A) Retract parts of two typical force/distance measurements between a bacterial probe and a type N and a type T wafer, respectively. For a clearer display, the curve on the type N wafer is shifted by −1 nN. (B) Distribution of the determined adhesion forces. (C, D) Data of part B are shown as separated series. Odd series were performed on type T (C) and even series on type N wafers (D).

dx.doi.org/10.1021/la3004323 | Langmuir 2012, 28, 7242−7248

Langmuir Article

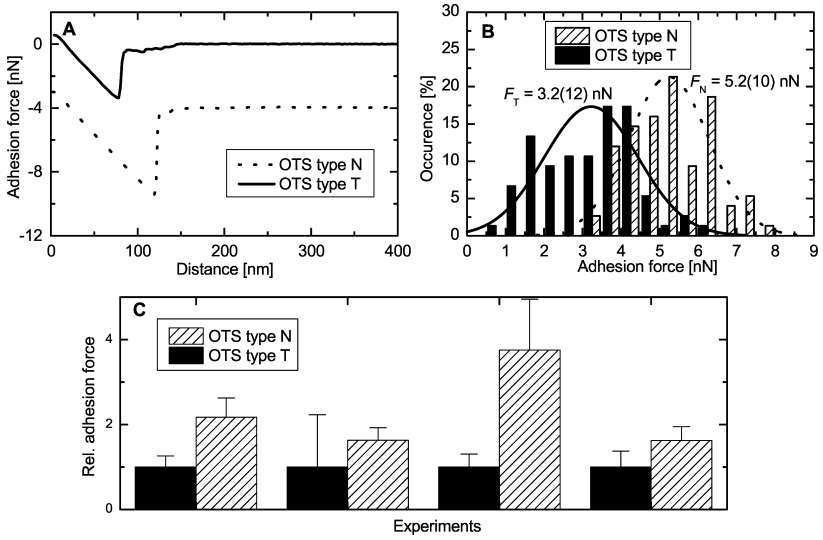

Figure 4. Results of AFM force spectroscopy experiments on hydrophobic substrates: (A) Retract parts of two typical force/distance measurements between a bacterial probe and a type N and a type T wafer, respectively. For a clearer display, the curve on the type N wafer is shifted by −4 nN. (B) Distribution of the determined adhesion forces. (C) Average force values (scaled with F_T) of multiple experiments with different cantilevers.

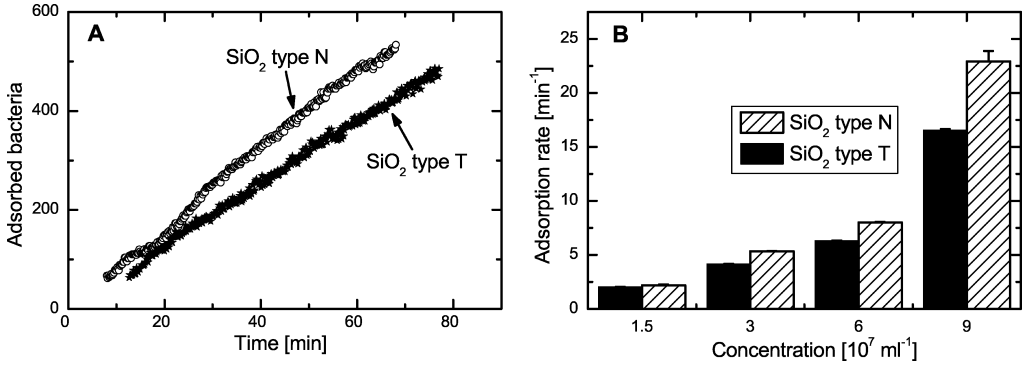

Figure 5. Results of the flow chamber experiments on the hydrophilic substrates: (A) number of the adsorbed bacteria in the field of view on type N and on type T wafers. (B) Adsorption rates of multiple experiments with different concentrations of the bacteria solution.

comparison supports the findings of previous studies, namely that increased hydrophobicity typically boosts adhesion.

Flow Chamber Experiments. Macroscopic adsorption experiments corroborate the results of the microscopic adhesion measurements. Using a custom-built parallel plate flow chamber setup, the growth of the number of bacteria adsorbed to the set of substrates was determined for multiple concentrations. The number of adsorbed bacteria grows faster on the type N than on the type T wafers (Figure 5A). The adsorption rates, i.e., the slopes of linear fits, are always higher on the type N than on the type T substrates independent of the concentration (Figure 5B).

DISCUSSION

The force spectroscopy results show that on both the hydrophilic and the hydrophobic wafers the bacterial adhesion force to the native SiO_2 layer is about twice as high as to the thick SiO_2 layer. Since the measurements were taken with the identical cantilever, the determined forces are reliable. This difference in adhesion forces is also observed for the adsorption of planktonic bacteria, as shown by the parallel plate flow chamber experiments. The surface properties that specifically influence the short-range interactions, e.g., hydrophobicity, roughness, and surface energy (Table 1), are independent of the thickness of the oxide layer. Hence, the difference in adhesion cannot be attributed to short-range forces. Also an effect of electrostatic interactions can be excluded for the explanation of the different adhesion forces, since the zeta potentials (Figure 1B) are identical within the experimental error on type T and N wafers. Therefore, only differences in van der Waals forces can explain the results. van der Waals forces are present in every system and cannot be completely shielded.[13,14,29] Often, vdW interactions are disregarded since they decrease proportional to d^{-6} with distance d, which yet is only correct for two interacting pointlike objects such as single atoms or molecules. For two macroscopic bodies, however, one obtains a lower exponent:[13,14] the nonretarded free energy between, for example, a sphere of radius R and a semifinite half-space is

dx.doi.org/10.1021/la3004323 | *Langmuir* 2012, 28, 7242−7248

Langmuir Article

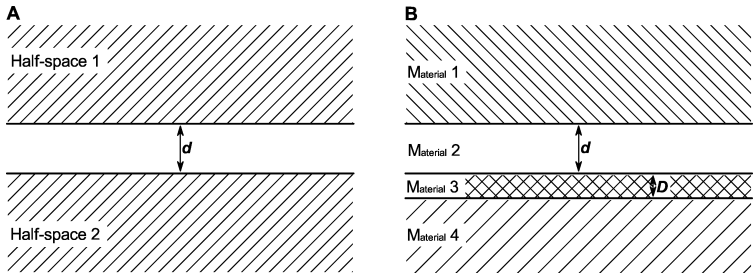

Figure 6. Schemes of two model systems: (A) interaction between two semifinite half-spaces and (B) interaction between a uniform material and a coated material.

$$W_{\mathrm{vdW}} = -R\frac{A}{6d} \tag{1}$$

and between two semifinite half-spaces (Figure 6A) is

$$w_{\mathrm{vdW}} = -\frac{A}{12\pi d^2} \tag{2}$$

per unit area, where A is the Hamaker constant of the system. It can be derived from the optical properties of the involved materials using the Lifschitz approach.[30] In the following we present a rough theoretical description of the system under study.

In principle, a bacterium can be described as a sphere of radius R consisting of two main components: the cytoplasm and the cell wall. Since the cytoplasm consists mainly of water, it has almost the same optical properties as the medium. The cell wall merely differs in its composition and consequently in its optical properties from the surrounding medium.[31] For small separations $d \ll R$, we use eq 2 and describe the system by three layers, namely, the cell wall, medium (buffer), and the substrate. In this study, the substrate is not a uniform bulk material but consists of multiple layers. In general, the vdW energy for a system (Figure 6B) consisting of a uniform half-space (M1), a medium (M2), and a half-space (M4) coated with a layer (M3) of thickness D can be calculated by[14,32]

$$w_{\mathrm{vdW}} = -\frac{1}{12\pi}\left(\frac{A_{12-32}}{d^2} + \frac{A_{12-43}}{(d+D)^2}\right) \tag{3}$$

where A_{12-32} (as well as A_{12-43}) are the Hamaker constants describing the interactions between the two interfaces M1/M2 and M2/M3 (as well as M1/M2 and M3/M4). In the system under study, the interacting interfaces are cell wall/buffer and buffer/silicon dioxide as well as cell wall/buffer and silicon dioxide/silicon. Since the cell wall features a nonuniform composition and barely accessible optical properties, we are not able to give exact theoretical values for the Hamaker constants. Nevertheless, as the polarizability of silicon dioxide (n = 1.46, ε = 3.9) is smaller than that of silicon (n = 4.13, ε = 11.8), we expect $A_{12-43} > 0$.[33] For this case, the second term in eq 3 increases the strength of the overall vdW interactions yet converges to zero for high layer thicknesses D (as on the type T substrates).

Hence, even without a comprehensive quantitative calculation, the experimental results can already be qualitatively explained by the fact that the bacterium on the type N wafer is "closer" to the strongly attractive Si bulk than if placed on a type T wafer. In other words, due to the stronger van der Waals attraction of the silicon, the bacteria experience higher adhesion forces on the wafers with a thin oxide layer. On the hydrophobic set of silicon wafers, the identical argumentation holds true, yet the contribution of an additional layer (the silane monolayer) has to be taken into account in a similar way as presented above for the oxide layer. Moreover, the results can be applied to clinical situations, where bacterial adhesion is preceded or accompanied by an adsorption of proteins, which may form a so-called conditioning layer.[34] This layer changes the surface properties of the substrate. Yet, since the thickness of the layer is usually on a nanometer scale, the unspecific adhesion forces will still be affected by the composition of the subsurface material. (The condition layer then acts like the OTS layer on the type N and T wafers.)

■ CONCLUSIONS

We have demonstrated that bacterial adhesion is influenced by the subsurface composition of a substrate. The reason for this is the strength of the vdW forces, which is given by (a) the type of geometry of two interacting objects (atom/atom or sphere/sphere), (b) their separation, (c) the composition of a stratified substrate, and (d) the polarizabilities of the involved materials. Keeping surface properties of the substrates constant, the influence of the van der Waals forces were probed by varying the subsurface composition. On Si wafers with different oxide layer thicknesses, the adhesion of *S. carnosus* was found to be about a factor of 2 stronger on the wafers with the thin oxide layer, no matter if covered by a molecular-sized hydrophobic layer or not. Consequently, for all types of adhesion studies, e.g., for the development of antibacterial substrates, it is important to characterize not only the surface properties but also the subsurface composition and to consider this in the analysis of the data. Particularly, thin coatings that promise to be antibacterial will have different effects depending on the underlying substrate! The effects could also explain inconsistent results of previous studies due to the different bulk substrates used.

■ AUTHOR INFORMATION

Corresponding Author

*E-mail: k.jacobs@physik.uni-saarland.de.

Notes

The authors declare no competing financial interest.

■ ACKNOWLEDGMENTS

This work was supported by the German Science Foundation under grant numbers GRK 1276 and INST 256/305-1 FUGG, by the German Federal Ministry for Education and Science grant 01 KI 1009E (Skin Staph), and by funds of the Federal

Langmuir Article

State of Saarland. We thank K. Hilgert for the help with handling the bacteria and R. Zimmermann for the zeta potential measurements.

REFERENCES

(1) (a) Costerton, J. W.; Stewart, P. S.; Greenberg, E. P. Bacterial biofilms: A common cause of persistent infections. *Science* **1999**, *284*, 1318−1322. (b) Costerton, J. W.; Cheng, K. J.; Geesey, G. G.; Ladd, T. I.; Nickel, J. C.; Dasgupta, M.; Marrie, T. J. Bacterial biofilms in nature and disease. *Annu. Rev. Microbiol.* **1987**, *41*, 435−464.

(2) Ramsay, G. DNA chips: State-of-the-art. *Nat. Biotechnol.* **1998**, *16*, 40−44.

(3) (a) Bowen, W. R.; Fenton, A. S.; Lovitt, R. W.; Wright, C. J. The measurement of *Bacillus mycoides* spore adhesion using atomic force microscopy, simple counting methods, and a spinning disk technique. *Biotechnol. Bioeng.* **2002**, *79*, 170−179. (b) Speranza, G.; Gottardi, G.; Pederzolli, C.; Lunelli, L.; Canteri, R.; Pasquardini, L.; Carli, E.; Lui, A.; Maniglio, D.; Brugnara, M.; Anderle, M. Role of chemical interactions in bacterial adhesion to polymer surfaces. *Biomaterials* **2004**, *25*, 2029−2037. (c) Tang, H.; Cao, T.; Liang, X.; Wang, A.; Salley, S. O.; Mcallister, J.; Ng, K. Y. S. Influence of silicone surface roughness and hydrophobicity on adhesion and colonization of *Staphylococcus epidermidis*. *J. Biomed. Mater. Res., Part A* **2009**, *88A*, 454−463. (d) Lamour, G.; Eftekhari-Bafrooei, A.; Borguet, E.; Soues, S.; Hamraoui, A. Neuronal adhesion and differentiation driven by nanoscale surface free-energy gradients. *Biomaterials* **2010**, *31*, 3762−3771.

(4) Emerson, R. J.; Bergstrom, T. S.; Liu, Y.; Soto, E. R.; Brown, C. A.; McGimpsey, W. G.; Camesano, T. A. Microscale correlation between surface chemistry, texture, and the adhesive strength of *Staphylococcus epidermidis*. *Langmuir* **2006**, *22*, 11311−11321.

(5) (a) Herminghaus, S.; Jacobs, K.; Mecke, K.; Bischof, J.; Fery, A.; Ibn-Elhaj, M.; Schlagowski, S. Spinodal dewetting in liquid crystal and liquid metal films. *Science* **1998**, *282*, 916−919. (b) Oron, A. Three-dimensional nonlinear dynamics of thin liquid films. *Phys. Rev. Lett.* **2000**, *85*, 2108−2111.

(6) Seemann, R.; Herminghaus, S.; Jacobs, K. Dewetting patterns and molecular forces: A reconciliation. *Phys. Rev. Lett.* **2001**, *86*, 5534−5537.

(7) Rauscher, M.; Dietrich, S. Nano-droplets on structured substrates. *Soft Matter* **2009**, *5*, 2997−3001.

(8) Loskill, P.; Puthoff, J. B.; Wilkinson, M.; Mecke, K.; Jacobs, K.; Autumn, K. Adhesion of gecko setae reflects nanoscale differences in subsurface energy. Submitted

(9) (a) Quinn, A.; Mantz, H.; Jacobs, K.; Bellion, M.; Santen, L. Protein adsorption kinetics in different surface potentials. *EPL* **2008**, *81*, 56003. (b) Bellion, M.; Santen, L.; Mantz, H.; Hähl, H.; Quinn, A.; Nagel, A. M.; Gilow, C.; Weitenberg, C.; Schmitt, Y.; Jacobs, K. Protein adsorption on tailored substrates: Long-range forces and conformational changes. *J. Phys.: Condens. Matter* **2008**, *20*, 404226. (c) Hähl, H.; Evers, F.; Grandthyll, S.; Paulus, M.; Sternemann, C.; Loskill, P.; Lessel, M.; Hüsecken, A. K.; Brenner, T.; Tolan, M.; Jacobs, K. Subsurface influence on the structure of protein adsorbates revealed by in situ X-ray reflectivity. Submitted

(10) Koebnik, R.; Locher, K. P.; van Gelder, P. Structure and function of bacterial outer membrane proteins: Barrels in a nutshell. *Mol. Microbiol.* **2000**, *37*, 239−253.

(11) (a) Ong, Y.-L.; Razatos, A.; Georgiou, G.; Sharma, M. M. Adhesion forces between *E. coli* bacteria and biomaterial surfaces. *Langmuir* **1999**, *15*, 2719−2725. (b) Stevens, M. J.; Donato, L. J.; Lower, S. K.; Sahai, N. Oxide-dependent adhesion of the Jurkat line of T lymphocytes. *Langmuir* **2009**, *25*, 6270−6278.

(12) Liu, C.; Zhao, Q. Influence of surface-energy components of Ni−P−TiO_2−PTFE nanocomposite coatings on bacterial adhesion. *Langmuir* **2011**, *27*, 9512−9519.

(13) Israelachvili, J. N. *Intermolecular and Surface Forces*, 2nd ed.; Academic Press: London, 1991.

(14) Parsegian, V. A. *Van der Waals forces*, 1st ed.; Cambridge University Press: New York, 2006.

(15) (a) Gristina, A. G. Biomaterial-centered infection: Microbial adhesion versus tissue integration. *Science* **1987**, *237*, 1588−1595. (b) Gristina, A. G.; Hobgood, C. D.; Webb, L. X.; Myrvik, Q. N. Adhesive colonization of biomaterials and antibiotic resistance. *Biomaterials* **1987**, *8*, 423−426.

(16) Götz, F. *Staphylococcus* and biofilms. *Mol. Microbiol.* **2002**, *43*, 1367−1378.

(17) (a) Lewis, K. Persister cells, dormancy and infectious disease. *Nat. Rev. Microbiol.* **2007**, *5*, 48−56. (b) Fux, C. A.; Costerton, J. W.; Stewart, P. S.; Stoodley, P. Survival strategies of infectious biofilms. *Trends Microbiol.* **2005**, *13*, 34−40.

(18) (a) Schleifer, K. H.; Fischer, U. Description of a New Species of the Genus *Staphylococcus*: *Staphylococcus carnosus*. *Int. J. Syst. Bacteriol.* **1982**, *32*, 153−156. (b) Götz, F. *Staphylococcus carnosus*: A new host organism for gene cloning and protein production. *J. Appl. Bacteriol.* **1990**, *69*, S49−S53.

(19) Harraghy, N.; Seiler, S.; Jacobs, K.; Hannig, M.; Menger, M.; Herrmann, M. Advances in in vitro and in vivo models for studying the staphylococcal factors involved in implant infections. *Int. J. Artif. Organs* **2006**, *29*, 368−378.

(20) Dufrene, Y. F. Atomic force microscopy, a powerful tool in microbiology. *J. Bacteriol.* **2002**, *184*, 5205−5213.

(21) (a) Razatos, A.; Ong, Y.-L.; Sharma, M. M.; Georgiou, G. Molecular determinants of bacterial adhesion monitored by atomic force microscopy. *Proc. Natl. Acad. Sci. U. S. A.* **1998**, *95*, 11059−11064. (b) Lower, S. K.; Tadanier, C. J.; Hochella, M. F. Measuring interfacial and adhesion forces between bacteria and mineral surfaces with biological force microscopy. *Geochim. Cosmochim. Acta* **2000**, *64*, 3133−3139.

(22) (a) Brzoska, J. B.; Azouz, I. B.; Rondelez, F. Silanization of solid substrates: A step toward reproducibility. *Langmuir* **1994**, *10*, 4367−4373. (b) Wasserman, S. R.; Whitesides, G. M.; Tidswell, I. M.; Ocko, B. M.; Pershan, P. S. Axe, J. D. The structure of self-assembled monolayers of alkylsiloxanes on silicon: A comparison of results from ellipsometry and low-angle X-ray reflectivity. *J. Am. Chem. Soc.* **1989**, *111*, 5852−5861.

(23) (a) Voet, D.; Voet, J. *Biochemistry*; John Wiley & Sons: New York, 1995. (b) West, J. K.; Latour, R. A.; Hench, L. L. Molecular modeling study of adsorption of poly-L-lysine onto silica glass. *J. Biomed. Mater. Res., Part A* **1997**, *37*, 585−591.

(24) Hutter, J. L.; Bechhoefer, J. Calibration of atomic-force microscope tips. *Rev. Sci. Instrum.* **1993**, *64*, 1868−1873.

(25) In the event of multiple adhesion peaks, the most pronounced one was evaluated.

(26) Carpick, R. W.; Batteas, J.; de Boer, M. P. Scanning probe studies of nanoscale adhesion between solids in the presence of liquids and monolayer films. In *Handbook of Nanotechnology*; Bhushan, B., Ed.; Springer Verlag: Berlin, 2007; pp 951−979.

(27) (a) van Wagenen, R. A.; Andrade, J. D. Flat plate streaming potential investigations: Hydrodynamics and electrokinetic equivalency. *J. Colloid Interface Sci.* **1980**, *76*, 305−314. (b) Bowen, B. D. Streaming potential in the hydrodynamic entrance region of cylindrical and rectangular capillaries. *J. Colloid Interface Sci.* **1985**, *106*, 367−376.

(28) The number in brackets gives the error bar of the last digit.

(29) French, R. H. Long range interactions in nanoscale science. *Rev. Mod. Phys.* **2010**, *82*, 1887−1944.

(30) Dzyaloshinskii, I. E.; Lifshitz, E. M.; Pitaevskii, L. P. The general theory of van der Waals forces. *Adv. Phys.* **1961**, *10*, 165−209.

(31) Nir, S.; Andersen, M. Van der Waals interactions between cell surfaces. *J. Membr. Biol.* **1977**, *31*, 1−18.

(32) Parsegian, V. A.; Ninham, B. W. Van der Waals forces in many-layered structures: Generalizations of the Lifshitz result for two semi-infinite media. *J. Theor. Biol.* **1973**, *38*, 101−109.

(33) Technically, the sign of A_{12-43} also depends on the polarizabilities of the cell wall and the buffer. Yet, a probe object featuring a lower polarizability than the medium would experience a repulsive vdW interaction.

(34) Characklis, W. G.; Cooksey, K. E. Biofilms and microbial fouling. *Adv. Appl. Microbiol.* **1983**, *29*, 93−138.

Addendum III - Hydrophobic interaction governs unspecific adhesion of staphylococci: a single cell force spectroscopy study

Authors: N. Thewes[1], P. Loskill[1], P. Jung[2], H. Peisker[1], M. Bischoff[2], M. Herrmann[2], and K. Jacobs[1]

[1] Department of Experimental Physics, Saarland University, 66041 Saarbrücken, Germany.
[2] The Institute of Medical Microbiology and Hygiene, Saarland University, 66421 Homburg/Saar, Germany.

Beilstein J. Nanotechnol. **5**, 1501–1512 (2014).
(http://dx.doi.org/10.3762/bjnano.5.163)

Author contributions:
Experiments were conceived and designed by N. Thewes and K. Jacobs. AFM experiments were performed by N. Thewes. Data was analyzed by N. Thewes. The article was written by N. Thewes, P. Loskill, P. Jung, P. Peisker, M. Bischof and K. Jacobs. Research was directed by M. Bischoff, M. Herrmann and K. Jacobs.

Abstract - Unspecific adhesion of bacteria is usually the first step in the formation of biofilms on abiotic surfaces, yet it is unclear up to now which forces are governing this process. Alongside long-ranged van der Waals and electrostatic forces, short-ranged hydrophobic interaction plays an important role. To characterize the forces involved during approach and retraction of an individual bacterium to and from a surface, single cell force spectroscopy is applied: A single cell of the apathogenic species *Staphylococcus carnosus* isolate TM300 is used as bacterial probe. With the exact same bacterium, hydrophobic and hydrophilic surfaces can be probed and compared. We find that as far as 50 nm from the surface, attractive forces can already be recorded, an indication of the involvement of long-ranged forces. Yet, comparing the surfaces of different surface energy, our results corroborate the model that large, bacterial cell wall proteins are responsible for adhesion, and that their interplay with the short-ranged hydrophobic interaction of the involved surfaces is mainly responsible for adhesion. The ostensibly long range of the attraction is a result of the large size of the cell wall proteins, searching for contact via hydrophobic interaction. The model also explains the strong (weak) adhesion of *S. carnosus* to hydrophobic (hydrophilic) surfaces.

BEILSTEIN JOURNAL OF NANOTECHNOLOGY

Hydrophobic interaction governs unspecific adhesion of staphylococci: a single cell force spectroscopy study

Nicolas Thewes[1], Peter Loskill[1,2], Philipp Jung[3], Henrik Peisker[3], Markus Bischoff[3], Mathias Herrmann[3] and Karin Jacobs[*1]

Full Research Paper

Open Access

Address:
[1]Experimental Physics, Campus E2 9, Saarland University, D-66123 Saarbrücken, Germany, [2]Present address: Dept. of Bioengineering and California Institute for Quantitative Biosciences (QB3), University of California at Berkeley, Berkeley, California 94720, USA and [3]Institute of Medical Microbiology and Hygiene, Saarland University, D-66421 Homburg/Saar, Germany

Email:
Karin Jacobs[*] - k.jacobs@physik.uni-saarland.de

* Corresponding author

Keywords:
atomic force microscopy (AFM); force spectroscopy; hydrophobic interaction; single cell; *Staphylococcus carnosus*

Beilstein J. Nanotechnol. **2014,** *5,* 1501–1512.
doi:10.3762/bjnano.5.163

Received: 21 March 2014
Accepted: 12 August 2014
Published: 10 September 2014

This article is part of the Thematic Series "Biological and bioinspired adhesion and friction".

Guest Editor: S. N. Gorb

Abstract

Unspecific adhesion of bacteria is usually the first step in the formation of biofilms on abiotic surfaces, yet it is unclear up to now which forces are governing this process. Alongside long-ranged van der Waals and electrostatic forces, short-ranged hydrophobic interaction plays an important role. To characterize the forces involved during approach and retraction of an individual bacterium to and from a surface, single cell force spectroscopy is applied: A single cell of the apathogenic species *Staphylococcus carnosus* isolate TM300 is used as bacterial probe. With the exact same bacterium, hydrophobic and hydrophilic surfaces can be probed and compared. We find that as far as 50 nm from the surface, attractive forces can already be recorded, an indication of the involvement of long-ranged forces. Yet, comparing the surfaces of different surface energy, our results corroborate the model that large, bacterial cell wall proteins are responsible for adhesion, and that their interplay with the short-ranged hydrophobic interaction of the involved surfaces is mainly responsible for adhesion. The ostensibly long range of the attraction is a result of the large size of the cell wall proteins, searching for contact via hydrophobic interaction. The model also explains the strong (weak) adhesion of *S. carnosus* to hydrophobic (hydrophilic) surfaces.

Introduction

Members of the genus *Staphylococcus* are known to form extremely resistant biofilms, some of which can cause severe infectious diseases [1]. *Staphylococcus carnosus* is an apathogenic member of that genus and has been described first in the early 1980s [2]. The name *Staphylococcus carnosus* reflects its important role in meat production as it reduces nitrate to nitrite and prevents food rancidity by producing the anti-oxidant enzymes catalase and superoxide dismutase [3].

Beilstein J. Nanotechnol. **2014,** *5,* 1501–1512.

Only recently, the genome of *S. carnosus* strain TM300 has been decoded [4,5]. In contrast to pathogenic staphylococcal species, such as *S. aureus* and *S. epidermidis*, the genome of *S. carnosus* lacks significant amounts of mobile genetic elements, and is poor in repetitive DNA sequences that are thought to facilitate the plasticity of genomes by allowing for enhanced genomic diversification due to recombinational events [5]. Although the *S. carnosus* genome encodes some homologues of adhesion factors found in *S. aureus*, it lacks the majority of adhesive molecules of its pathogenic relative that are thought to be important for the ability of the pathogen to colonize and invade its mammal hosts (reviewed in [1]). Due to its apathogenic properties, and its ability to be transformed with and to express virulence factors of pathogenic staphylococcal species ([6,7]), the strain TM300 is an ideal tool to study the properties of a single virulence factor and its impact on infectivity in this otherwise apathogenic species. Besides this, it has been shown that the survival of bacteria in a food industry environment is strongly related to their efficiency to adhere on abiotic surfaces [8-10]. Therefore, and because adhesion is the first step of the formation of biofilms, the characterization of bacterial adhesion forces has gained increasing importance in recent years [11].

In general, the adhesion of bacteria to a surface is determined by the nature of the bacterium, the surrounding medium, the surface chemistry, and the material composition reflecting the influence of the main interacting forces [12,13]: van der Waals forces, hydrophobic interaction and electrostatic forces. In addition, specific interactions amplify bacterial adhesion whenever corresponding binding partners are available. The adhesion process of microorganisms, such as *S. carnosus*, is usually characterized by using flow chambers [14]. Although flow chamber studies reproduce the natural adsorption process of microorganisms out of fluid flow, it is hard to determine quantitative adhesion force values. The outcome usually results from multiple parallel processes, such as adsorption, desorption, and adhesion. Moreover, results obtained from flow chamber experiments depend on the exact flow conditions of the used chamber [15]. In the last decade, a more quantitative method for measuring bacterial adhesion forces has been introduced: single-cell force spectroscopy is a special mode of an atomic force microscope (AFM) [16] and is optimized to investigate adhesion forces [17,18] of single bacterial cells in a very controlled manner: By using AFM-cantilevers functionalized with single bacteria, "bacterial probes", force/distance measurements are conducted. To date, single cell force spectroscopy is mostly used for exploring specific adhesion [19]. It is the aim of this study to characterize the unspecific adhesion mechanisms of *Staphylococci*, by using *S. carnosus* as an example, and to clarify the range of the attractive interaction of the cells to surfaces. We use abiotic surfaces in order to rule out effects due to specific interactions and to concentrate on the unspecific interactions of *S. carnosus* to surfaces of variable surface energy. As a unique feature of our study, we are able to probe different surfaces with the exact same bacterial cell. Thereby, we are able to demonstrate the importance of the hydrophobic interaction on the bacterial adhesion process. Moreover, we can measure the adhesion forces that are mediated by bacterial cell wall proteins (and further cell wall components) and test their dependency on the 'adhesion history' the cell has experienced before.

Experimental

Preparation of the substrates

The hydrophilic substrates used in this study are silicon wafers with a native silicon oxide layer (d = 1.7(2) nm) (the number in parentheses denotes the error of the last digit) purchased from Siltronic AG (Burghausen, Germany). In order to remove dirt, the silicon wafers were first immersed for 30 min in fresh 1:1 H_2SO_4 (conc.)/H_2O_2 (30%) solution, then in boiling deionized water for 90 min, during which the water was changed at least four times. Following a standard protocol, these hydrophilic surfaces can be rendered hydrophobic by the self-assembly of a monolayer of silane molecules (octadecyltrichlorosilane, OTS, Sigma-Aldrich), featuring a CH_3-tailgroup [20,21]. As has been shown in [21] by perfoming AFM, X-ray reflectometry, ellipsometry, and contact angle measurements, this protocol enables the preparation of a self-assembled monolayer (SAM) with a thickness of about 2.6 nm and an *rms* roughness below 0.2 nm. In [21] it was shown that the SAM is hydrophobic, homogeneous, dense, upright and in all-trans configuration. The contact angles, surface roughnesses and surface energies for hydrophilic and hydrophobic wafers are given in Table 1 and streaming potential measurements reveal that both surfaces are negatively

Table 1: Parameters of the model substrates: Root mean square (*rms*) roughness, advancing (adv) and receding (rec) contact angles Θ of water, surface energy γ (values taken from [21]) and surface charge as revealed by streaming potential measurements at pH 7.3 [22].

surface	*rms* (nm)	Θ_{adv}	Θ_{rec}	γ (mJ/m^2)	streaming potential (mV)
hydrophilic	0.09(2)	7(2)°	compl. wetting	64(1)	−104.4(1)
hydrophobic	0.12(2)	111(1)°	107(2)°	24(1)	−80.0(1)

Beilstein J. Nanotechnol. 2014, 5, 1501–1512.

charged at the used pH of 7.3 (Table 1). For this study, OTS surfaces of the same batch as in [21] have been used. Prior to the AFM force spectroscopy experiments with bacterial cells, both types of surfaces were immersed in PBS buffer.

Bacteria

For the experiments, freshly prepared exponential phase *S. carnosus* strain TM300 cells were used [4]. The bacteria were cultured on blood agar plates and transferred into 5 mL of TSB medium for 24 h at 37 °C. Before the experiments, 100 µL were transferred into 4 mL fresh TSB medium and cultured for 2.5 h at 37 °C and 150 rpm. To remove extracellular material, the bacteria were washed four times with phosphate-buffered saline (PBS, pH 7.3, ionic strength 0.1728 mol/L at 20 °C), each with 1 mL. Then, the bacteria were either used immediately or stored less than two hours at 4 °C. For the preparation of the bacterial AFM probes, bacterial solution was again diluted 1:6.

Preparation of the bacterial probes

Bacterial probes are based on tipless cantilevers (MLCT-O, Bruker, Billerica, MA, USA) with a nominal spring constant of 0.03 N/m. After the cantilevers were cleaned in an air plasma, they were vertically immersed into a solution of 4 mg/mL dopamine hydrochloride (99%, Sigma-Aldrich) in 10 mM TRIS-buffer (pH 7.9 at 22 °C) and kept at 4 °C in the fridge for 50 min. The cantilevers were then carefully rinsed in deionized water to remove unbound dopamine and dried under a laminar flow bench for at least one hour. The poly(dopamine)-covered cantilever was then inserted into the Bioscope Catalyst cantilever holder for measurements in liquids (Bruker, Billerica, MA, USA), mounted onto the AFM. Subsequently, it was calibrated in liquid by using the thermal tune technique [23], which allows for the calculation of the individual spring constant of the cantilever.

Afterwards, holder and cantilever were placed into a micromanipulation system (Narishige Group, Japan). The cantilever thereby is in the horizontal position with the functionalized side facing down. By using the micromanipulator, holder and cantilever were lowered and the cantilever dipped into a droplet of diluted bacterial solution (see above), which was previously placed on a polystyrene petri dish. Under the inspection of an inverted optical microscope, the cantilever was placed on top of an isolated bacterium, briefly and carefully tapped onto the cell, and immediately pulled back again. In order to keep the applied force low, the deflection of the cantilever was monitored by the light reflection off the cantilever and kept constant during motion. Care was taken to position the bacterium as close as possible to the end of the cantilever (not further away than two bacterial diameters) to safely exclude cantilever/substrate interactions.

The successful fixation of a single bacterium at the front end of the cantilever was confirmed with the inverted microscope, c.f. Figure 1. Subsequently, cantilever (and holder) were withdrawn from the bacterial solution, whereby a droplet clings to the cantilever, preventing the bacterium from drying. Cantilever and holder were then carefully transferred to the AFM and immediately immersed into the PBS filled petri dish containing the hydrophilic and hydrophobic substrates.

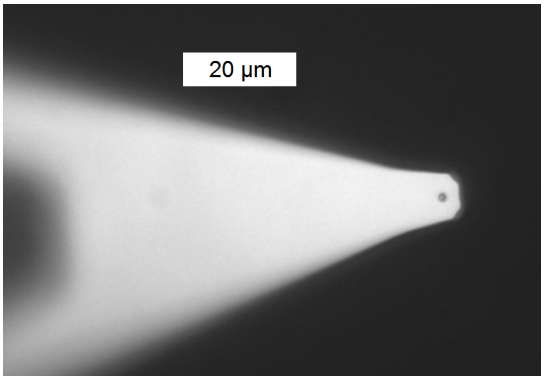

Figure 1: Optical image of a single *S. carnosus* bacterium immobilized by (poly)dopamine on a tipless cantilever.

Single cell force spectroscopy measurements

Single cell force spectroscopy measurements were performed by using a Bioscope Catalyst (Bruker, Billerica, MA, USA). The deflection of the cantilever is recorded during the approach and retraction of the bacterial probe to and from the surface. The deflection data was converted into force values by means of the spring constant of the cantilever, determined as described above. The approach is performed until a certain repulsive force is reached ("force trigger"), typically 150 pN in this study, if not indicated otherwise. Experiments were performed in 6 mL PBS at 20 °C and with tip velocities between 400 nm/s and 2400 nm/s over a total distance of typically 800 nm. (It is important to note here that the tip velocity describes the velocity of the piezo drive that controls the z-movement of the cantilever, which, however, is not necessarily identical with the velocity of the bacterium, especially at retraction.)

For each parameter set, at least 30 force/distance curves were recorded, each on a different surface spot to avoid systematic errors due to local irregularities of the surface or contamination due to preceding adhesion events. If two surfaces were to be compared, the first set of 30 force/distance curves was taken on one surface followed by a series of 30 curves on the second surface, then again 30 on the first surface. By doing this, we took control of the reproducibility of the measurements and can

Beilstein J. Nanotechnol. **2014,** *5,* 1501–1512.

rule out systematic errors like the degradation of the bacterial probe.

A typical force curve is shown in Figure 2. Upon approach, a jump-to-contact ("snap-in") event can be observed, followed by a steep rise of the force, indicating bacterium/surface contact. Since the exact contact formation and mechanics between the bacterial surface and the solid substrate is unclear, it is hard to make predictions on the shape of the force/distance curve. Upon retraction, the force/distance curve exhibits first the same steep slope as upon approach, yet, due to adhesive forces, a deep global minimum is recorded. Further retraction provokes a loss of contact ("jump-off contact"). In the repulsive regime (F > 0), a force of 150 pN is not enough to deform the bacterium: With a force trigger of 150 nN, only an indentation of ca. 10 nm is reached (cf. Figure 2). Therefore, very likely, only components of the cell wall are elastically deformed.

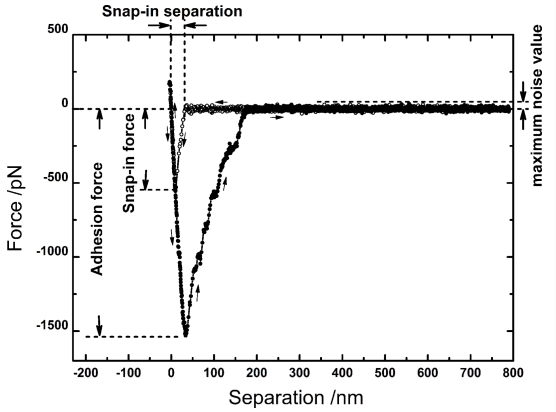

Figure 2: Typical force/distance curve, taken with a single *S. carnosus* probe on an OTS-covered (hydrophobic) Si wafer. By analyzing the curve, the adhesion force, the "snap-in force" and the "snap-in separation" can be obtained, the description of the latter is given in the text. The arrows indicate the direction of motion of the piezo drive.

Three general measures allow for a comparison of the adhesion process: Inspecting the approach curve, the "snap-in" event is characterized by the depth of the global minimum, called "snap-in force" and by the "snap-in separation", defined as the separation at which the deflection reaches 150% of the maximum baseline noise value (typically between 30 and 50 pN), c.f. Figure 2. The snap-in separation serves as a hands-on measure for the determination of the width of the snap-in event. Distances are measured relative to the point of zero force [24]. From the retraction curve, the adhesion force is taken as the depth of the global minimum [24]. Since in some cases, the overall adhesion force decreased after more than about 150 force/distance curves (possibly due to stress applied by the large number of adhesion events), the number of force/distance curves per bacterium was always kept below 150. The bacterium was never "lost" during the experiments, it was safely secured to the cantilever.

As a control for the specificity of force/distance curves for bacterial adhesion and to demonstrate that the cantilever does not influence bacterial adhesion, several experiments have been performed with a bare, (poly)dopamin-coated cantilever: Figure 3 displays the difference between the cantilever adhesion signal of the bare (poly)dopamin-coated cantilever (Figure 3A), and the very same cantilever with the bacterial cell attached (Figure 3B). Reversely, after a force/distance curve with an attached bacterium (Figure 3C), the bacterium was removed (by pressing it very hard to a solid substrate followed by shearing it off with a micromanipulator) and another force/distance curve of only the cantilever was recorded (Figure 3D). Clearly, the force/distance curves without bacterium exhibit (nearly) no snap-in event, and during retraction, only a small adhesion peak occurs and the further retraction curve is smooth without the characteristic jumps in the case of an attached bacterium.

Results and Discussion

First, we will concentrate on the robustness of single cell force microscopy. Each individual *S. carnosus* probe achieves a characteristic force/distance curve that can be reproduced numerous times (Figure 4). Differences from curve to curve occur occasionally (about 4 out of 30), yet span mostly only over one section of the retraction curve, otherwise reproducing the rest of the curve. This holds true even if a set of 60 force/distance curves on a hydrophobic wafer is interrupted by the recording of a set of 30 curves on a hydrophilic wafer: The first 30 curves on the hydrophobic wafer are shown in (Figure 4A), the second set of 30 curves is displayed in (Figure 4B), the curves on the hydrophilic wafer are not shown, since they do not differ from those shown in (Figure 7B). The characteristic features of the first set of curves on the hydrophobic wafer is perfectly reproduced by the second set, though in between, the surface energy of the adhesion partner (the hydrophilic surface) was reduced by a factor of three (c.f. Table 1). Hence, as the shape of the force/distance curves is that robust (surviving 150 contact events and surviving even a change of the type of substrate), these results already demonstrate that force/distance measurements are characteristic for the individual bacterial probe and are therefore most suitable to characterize bacterial adhesion.

Next, we explore the influence of the AFM force spectroscopy parameters on the force/distance curves. The tip (or rather the piezo drive) velocity was varied between 400 nm/s and 2400 nm/s, yet no significant influence on the adhesion force

Beilstein J. Nanotechnol. **2014,** *5*, 1501–1512.

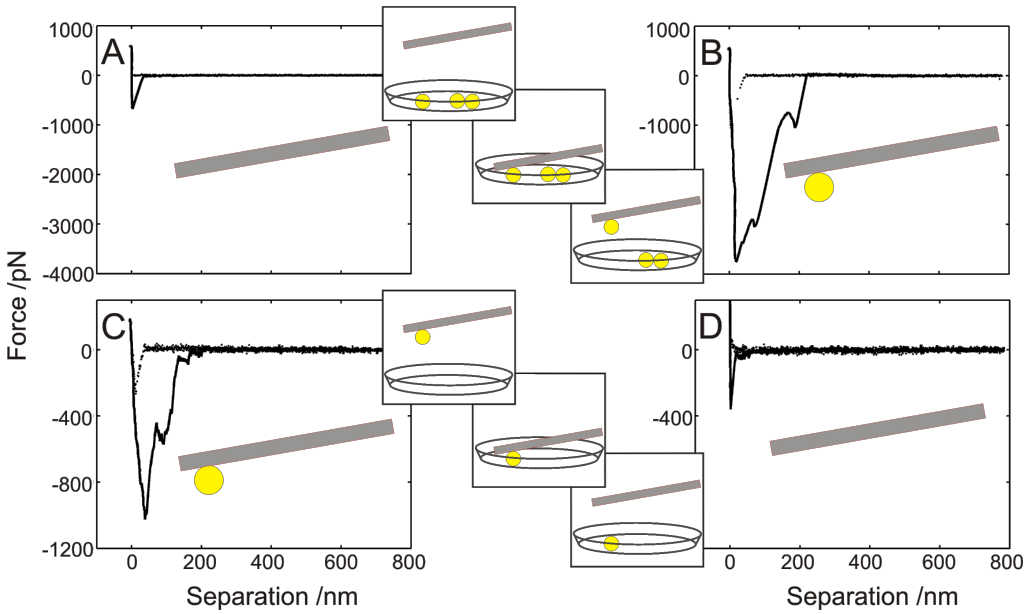

Figure 3: Test of artifacts of AFM force/distance curve with and without bacterium, each taken under the same conditions: (A) Bare (poly)dopamin-coated cantilever force/distance curve. (B) The same cantilever as in (A), yet after attachment of a bacterium. (C) A second cantilever with bacterium and its characteristic force/distance curve. (D) Force/distance curve after detaching the bacterium of the experiment shown in (C).

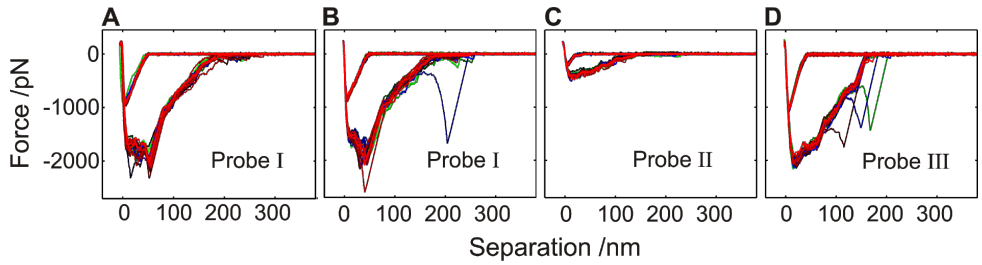

Figure 4: A–D: Overlay of 30 force/distance curves of three individual *S. carnosus* probes I, II and III on hydrophobic Si wafers, each with a force trigger of 150 pN. Between the experimental series shown in A and B, a set of 30 force/distance curves was taken with the identical bacterial probe on a hydrophilic Si wafer (not shown), yet the characteristic form of the second set of force/distance curves did not change significantly.

was recorded (Figure 5A). By varying the tip velocity, we implicitly varied the time the bacterium is enabled to gain contact to the surface. Within the range probed, the contact time (estimated to be of the order of a fraction of a second) does not influence the adhesion force. The snap-in separation, however, decreases with increasing tip velocity (Figure 5B), as does the snap-in force (Figure 5C), which is a first indication to a time-dependent contact-process, which will be detailed in the following. For further measurements, a tip velocity of 800 nm/s is used, since for that speed, one force/distance curve of 800 nm ramp size takes 0.5 Hz, which is a convenient frequency and corresponds to frequencies used in other studies [25].

Increasing the force trigger results in a slight increase of the adhesion force (Figure 6A), whereas the snap-in separation as well as the snap-in force remained constant (Figure 6B and Figure 6C). In the following, the lowest force trigger of 150 pN was used in order to mimic the natural adhesion process of the bacterium in planktonic state.

With the parameters for single cell force spectroscopy as detailed above, we can now specify the large differences in the adhesion of *S. carnosus* to hydrophobic and to hydrophilic surfaces, c.f. Figure 7A and Figure 7B: On the hydrophobic surface, a clear snap-in event is detectable, followed by a large

Beilstein J. Nanotechnol. **2014,** *5,* 1501–1512.

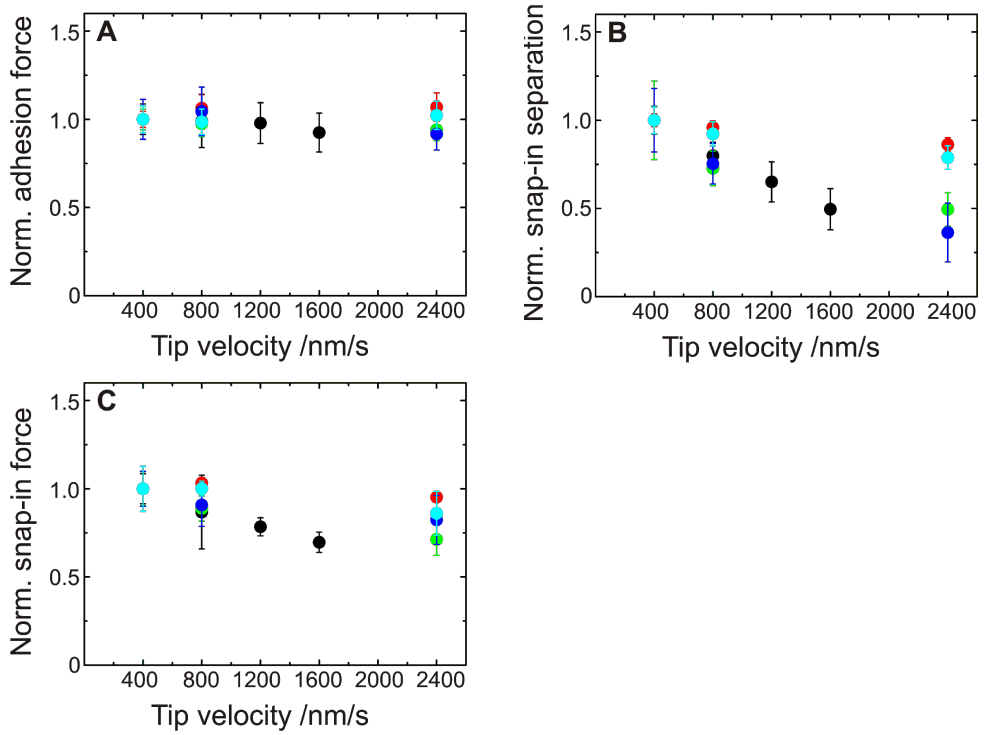

Figure 5: Influence of the tip velocity on the adhesion of *S. carnosus* shown for five different cells. For each bacterium, values for adhesion force (A), snap-in separation (B) and snap-in force (C) are shown. The values are normalized to the value of the measurement with the lowest tip velocity (400 nm/s). Different colors represent different bacterial probes.

adhesive peak upon retraction. On the hydrophilic surface, however, neither of the two can be recorded. It is important to note that the two curves depicted in Figure 7A and Figure 7B were taken under identical external conditions (temperature, buffer), the same AFM force spectroscopy parameters (force trigger, tip velocity) and, most significantly, were recorded with the same bacterium. Figure 7C demonstrates the individual adhesive properties of different bacteria. Gray bars comprise data of the exact same bacterial probe on the two different surfaces. The data of Figure 7A and Figure 7B are taken from the set of curves summarized in bar I.

Obviously, the adhesive mechanism of *S. carnosus* on hydrophobic OTS surface differs strongly from that on a hydrophilic Si wafer, as the adhesion of *S. carnosus* to hydrophilic Si wafers is barely resolvable. From force spectroscopy measurements with multiple bacteria as AFM probes (30–50 bacteria), we learned that on hydrophilic silicon oxide surfaces, the adhesion force is roughly an order of magnitude lower than on OTS-Si wafers [13]. Hence, the adhesion force of a single bacterium on a hydrophilic surface is expected to be below the experimental resolution (about 50 pN), which explains the present results.

What is the difference of bacterial adhesion to hydrophilic or hydrophobic surfaces? Adhesion is the sum of all forces between the interacting partners. In our case, van der Waals and electrostatic forces as well as forces due to the hydrophobic interaction are involved [26]. Since hydrophilic and hydrophobic Si wafers differ in composition only by a 2.6 nm thin OTS-monolayer on the surface, the van der Waals forces are nearly identical [13,27]. Forces due to electrostatic interactions between the negatively charged bacterium and the two types of wafer surfaces, which are both negatively charged (Table 1), are repulsive. Since the streaming potential is 20% more negative on the hydrophilic Si wafer, different electrostatic interactions give rise to a difference of adhesion forces of only a factor of 1.2, yet we record differences in the range of factors 10 to 40 (Figure 7C). Therefore, we hypothesize that the adhesion of *S. carnosus* is governed by hydrophobic interaction.

Inspecting the snap-off event in more detail, not only the large extent is striking but also the reproducible, stepwise reduction of the recorded force (see Figure 4). This is a strong indication of a reversible fold-and-stretch mechanism of the involved macromolecules. It is known that the bacterial surface is covered by a variety of proteinaceous and non-proteinaceous

Beilstein J. Nanotechnol. 2014, 5, 1501–1512.

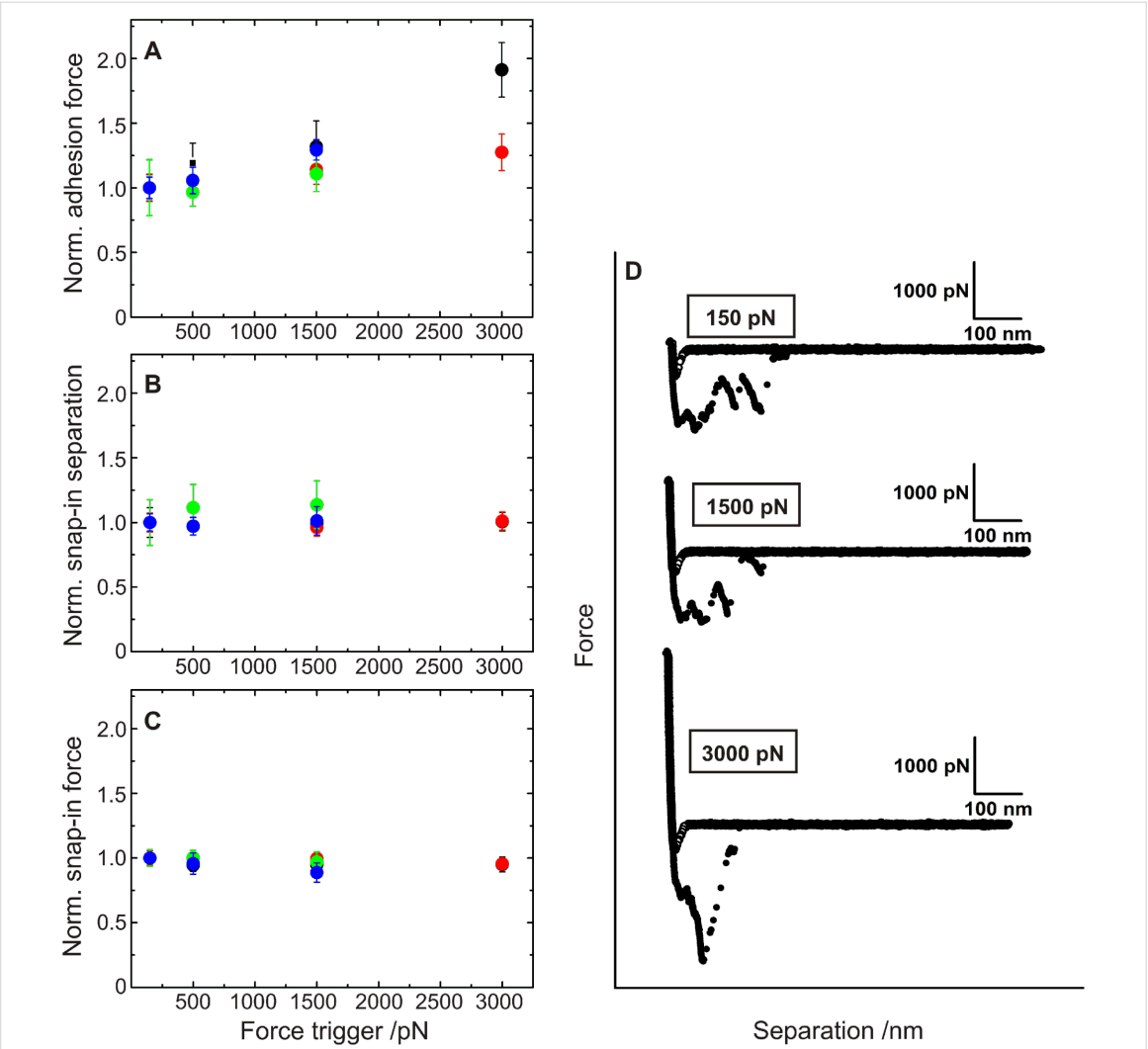

Figure 6: Influence of the force trigger on the adhesion of *S. carnosus*. A–C: For four bacterial probes, values for adhesion force, snap-in force, and snap-in separation are normalized to the value of the measurement with the lowest force trigger (150 pN). D: Exemplary force/distance curves for the exact same bacterial probe for three different force triggers. Different colors represent different bacterial probes.

polymers that can mediate adhesion (adhesins) [28,29]. The form of the retraction part can therefore be explained by a parallel and simultaneous stretching of cell wall proteins tethered to the surface as the piezo retracts [25,30].

Proteins are known to adsorb differently to hydrophilic and hydrophobic surfaces since the hydrophobic interaction can induce intramolecular conformational transitions and change the orientation of hydrophobic side groups of proteins [31-35]. This has also been shown by surface forces apparatus (SFA) experiments [36-38]. The range of the hydrophobic interaction depends on the correlation length of water molecules, which is below 1 nm [39]. Therefore, bacterial surface proteins have to come that close to the OTS surface in order to interact attractively. The SFA studies showed that the more hydrophobic the interacting partners (protein/surface) are, the stronger is the adhesion force.

An influence of further nonproteinaceous cell wall components (like teichoic acids) cannot be excluded and it will depend on the hydrophobicity of these components. However, proteins will play the key role in adhesion to hydrophobic surfaces due to their strong hydrophobic parts. Therefore, we will only talk about cell wall proteins in the following, but are aware of the fact that also other hydrophobic macromolecules may contribute to adhesion. For *S. aureus* for example, teichoic acids

Beilstein J. Nanotechnol. **2014,** *5,* 1501–1512.

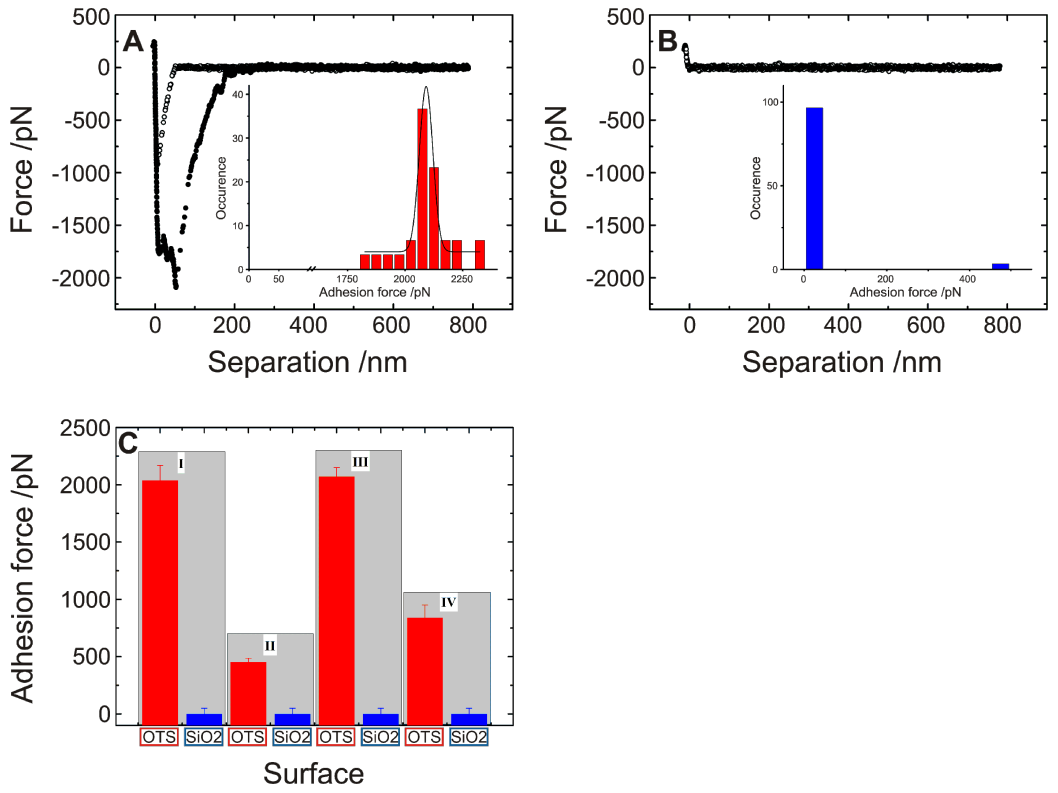

Figure 7: Exemplary force/distance curve taken with a single *S. carnosus* probe on (A) a hydrophobic OTS-covered Si wafer and on (B) a hydrophilic Si wafer. The insets summarize the results of the adhesion force of 30 force/distance curves. (C): Mean adhesion force and standard deviation showing the result of at least 60 force/distance curves of four *S. carnosus* (I–IV) measured on hydrophobic OTS-covered and on hydrophilic Si wafers, covered by a natural SiO_2. Each of the four bars represents measurements of the exact same bacterial probe.

are reported to be strongly hydrophilic [40]. Our model of bacterial adhesion, which will be proposed in the following, however, is not depending on the exact type of adhesive mediator.

Figure 8A summarizes the results of the measured adhesion forces for 30 different bacterial probes. It contains the OTS-wafer data shown in Figure 7C. For an individual *S. carnosus* bacterial probe on an OTS-wafer, the distribution of adhesion forces is rather narrow, the width of the distribution is typically less than 10% of the average adhesion force, as depicted in the inset of Figure 7A. Comparing different *S. carnosus* probes as shown in Figure 8A, the adhesion forces vary between 400 pN and 3000 pN, with the average at 1500(800) pN (solid line).

Inspecting the approach curve, it is noticeable that also the "snap-in" is an extended event rather than a sudden jump-to-contact (a jump-in or -out can be recorded whenever the gradient of the force exceeds the gradient of the restoring force of the cantilever (i.e., the spring constant) [24]). A closer look at the snap-in events reveals that the snap-in force is proportional to the snap-in separation (Figure 8B) and that the form of the curves greatly resemble each other. Moreover, since the adhesion force is also proportional to both, the snap-in force and -separation, see Figure 8C and Figure 8D, we deduce that the involved mechanisms are identical. Hence also upon approach, cell-wall polymers are involved in establishing the contact to the hydrophobic Si wafer. The snap-in separation reaches values up to 50 nm on hydrophobic surfaces, and can hence serve as an estimate for the hydrodynamic radius of the bacterial cell-wall proteins.

Based on the recently published genome sequence of *S. carnosus* strain TM300 (deposited in the EMBL nucleotide database under accession number AM295250), 19 putative cell-wall anchored proteins harboring LPXTG motifs are predicted, including homologues of well-studied *S. aureus* adhesins such as clumping factor A and B, fibronectin binding protein, and

Beilstein J. Nanotechnol. **2014,** *5*, 1501–1512.

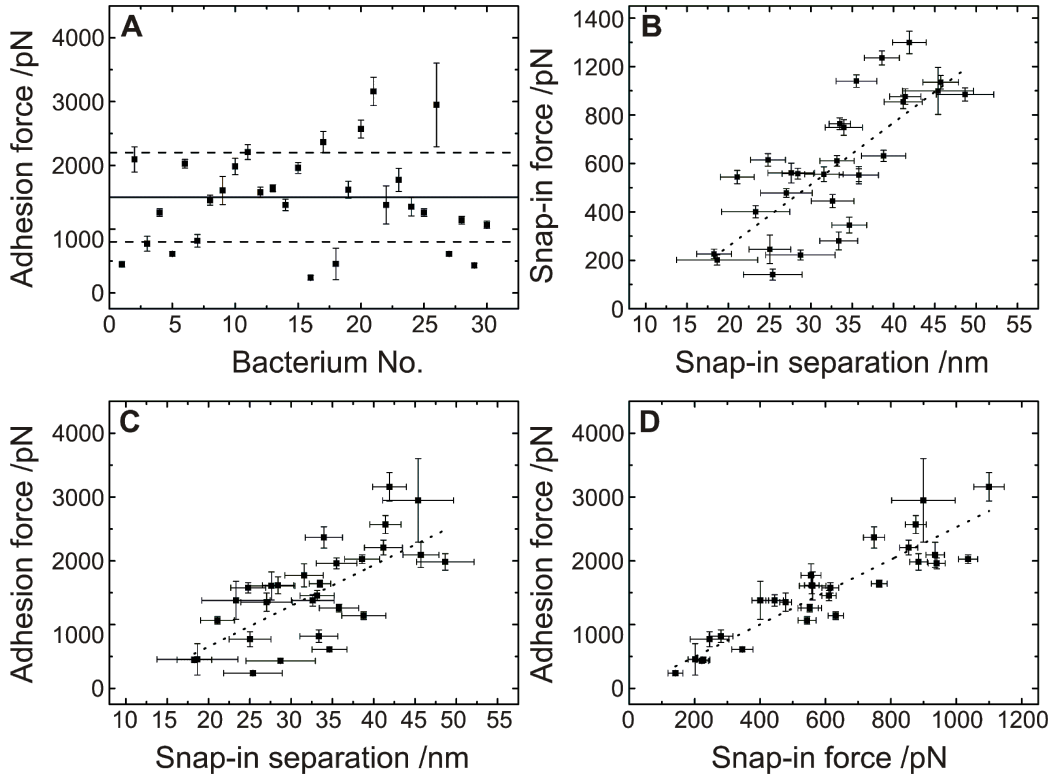

Figure 8: Results of 30 different single cell force spectroscopy experiments on OTS with *S. carnosus* bacterial probes, each data point consists of 30 force/distance curves with a force trigger of 150 pN and a tip velocity of 800 nm/s. A: Solid line: average adhesion force, dashed lines: range of the standard deviation. B–D: Dotted lines: linear fit to the data.

elastin binding protein (cf. [5]). However, nothing is known about the structures and the lengths (e.g., hydrodynamic radius under in vivo conditions) of these putitative cell-wall proteins, making it difficult to correlate the measured adhesion phenomena to specific proteins.

We can now revisit the presented results on the influence of the tip velocity (Figure 5) and the force trigger (Figure 6) to the adhesion process: The long cell-wall polymers need time to come into contact with the surface. The search for contact is a stochastic process; a higher tip velocity thereby results theoretically in a smaller snap-in separation because the residence time in each separation, and therefore the probability that a protein comes into contact in a certain distance, is smaller. Moreover, the polymer needs also time to perform conformational changes in the vicinity of the surface. Both time windows are reduced at higher tip speeds and, hence, the distance at which the cantilever starts to deflect, the snap-in separation, is reduced. The snap-in force is reduced, since the deflection of the cantilever is smaller at the lowest point of the approach curve.

Upon retraction, a variation of the tip velocity probes the rheological properties of the involved group of (stretched) macromolecules, which may also interact collaboratively [41]. Since for the group of cell-wall proteins, no rheological data is available, a prediction for the tip-velocity-dependent behavior is not possible. We find that the adhesion force is constant within the applied variation of tip velocities; moreover, snap-in and snap-off events are highly reproducible. Both together strongly indicate that at these speeds, the macromolecules act elastically. These findings are also in accordance with the study of Alsteens et al. [25], in which “protein nanosprings” are one model description of microbial adhesins.

According to our model of *S. carnosus* adhesion, a higher force trigger should provoke a larger contact area, a closer contact and involve additional cell- wall polymers to tether. All of which should result in a higher adhesion force and a different form of the retraction curve. The snap-in event, however, should not be affected. The experiments reveal that indeed snap-in separation and force are independent of force trigger, c.f. Figure 6B and Figure 6C and the adhesion force is

Beilstein J. Nanotechnol. **2014,** *5,* 1501–1512.

increasing as expected Figure 6A. Also, for each force trigger (as well as for each *S. carnosus* bacterial probe), a characteristic set of force/distance curve can be recorded (Figure 6D).

Merging all experimental results, we propose the model sketched in Figure 9: Upon approach, Figure 9A, the cell-wall proteins interact with the surrounding medium (1) and, if at reach, with the surface (2). If an attractive surface is in the vicinity, parts of the proteins can tether (unspecifically in our case) to the surface. Tethering can start at distances below 50 nm, c.f. Figure 8B and Figure 8C. The experiments show that this is the case for hydrophobic wafers. The distance of 50 nm can, hence, serve us as an upper estimate for the coil size of the protein in solution. A further approach gives more proteins the opportunity to tether (3) until a point is reached, at which the maximum attractive force is reached (4). From now on, the proteins start to act as elastic springs that are compressed by the force exerted by the cantilever through the piezo drive. Nevertheless, also in this phase, additional proteins may tether. Approach is stopped shortly after zero force has been reached (5).

Upon retraction, Figure 9B, first, the elastic springs are released (6), achieving the same slope in the curve as during approach. It indicates a reversible fold-and-stretch mechanism of multiple chains. Then, some of the springs start to be stretched against the steric repulsion of the coil (7) [36], followed by a loss of contact of single macromolecules, each of which gives rise to a sudden jump in the force/distance curve (8) and (9) until the entire bacterium has lost contact (10). Depending on type and number of the involved proteins, the retraction curve looks different for every bacterial probe, a fact that has been found earlier in non-bacterial systems involving macromolecules [30,36-38]. For the exact same bacterial probe and the identical contact area (realized by an identical force trigger) and even if 30 approach/retraction cycles have been performed on a different surface, the form of the force/distance curve is characteristic and can be taken as a "fingerprint" for the individual cell.

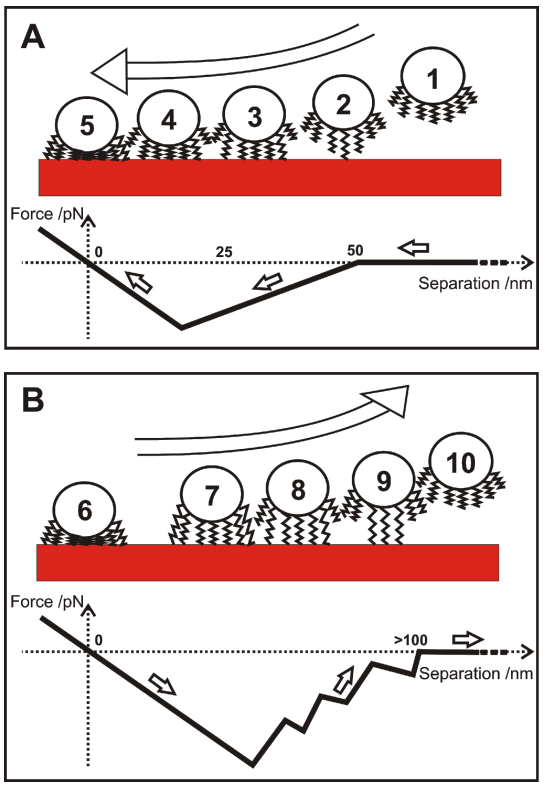

Figure 9: Sketch of approach (A) and retraction (B) of a single bacterial probe and respective force/distance curves. For clarity, neither the AFM cantilever nor the macromolecules that are not involved in adhesion are drawn.

Conclusion

To conclude, our experiments strongly corroborate the model that the unspecific adhesion of *S. carnosus* is mainly governed by number, properties and arrangement of the bacterial cell-wall proteins. Through this, the proteins are subject to van der Waals and electrostatic forces as well as forces due to hydrophobic interaction. Comparing hydrophilic and hydrophobic Si wafers (in our case differing only in a monomolecular OTS layer), we find for the exact same bacterial probe strong adhesion of *S. carnosus* to the hydrophobic wafers (up to about 3000 pN) and low adhesion (close to the experimental resolution, about 30–50 pN) to the hydrophilic ones. From that we infer that the hydrophobic interaction is responsible for the strong adhesion on the hydrophobic wafers, exceeding the forces exerted by electrostatic and van der Waals forces by at least an order of magnitude.

The main observations are (i) the form of the force/distance curves is characteristic for each bacterium, (ii) this form is independent of the "adhesive history" and (iii) the retraction curves (including the adhesion forces) are unaffected by the tip velocities probed. These observations lead us to the conclusion that cell-wall proteins act as elastic springs. Since the separation at which the cantilever starts to deflect, the snap-in separation, reaches values up to 50 nm on hydrophobic surfaces, we can estimate the extension of the cell-wall proteins.

Aiming at understanding the detailed form of the force/distance curves, it is inevitable to shed more light onto the "real" molecular composition of the bacterial surface, possibly with the help of atomistic simulations. For future studies, single-cell force

spectroscopy can additionally be combined with genetic tools that enable us to specifically modify the composition of the cell-wall proteins. That way, the responsible adhesins can be identified for each of the bacterial species.

Acknowledgements

This work was supported by the Deutsche Forschungsgemeinschaft (DFG) within the collaborative research center SFB 1027 and the research training group GRK 1276 (N.T.). P.J. and M.B. were supported by grants of the German Ministry for Education and Research 01Kl1014B and 01Kl1301B.

References

1. Rosenstein, R.; Götz, F. *Curr. Top. Microbiol. Immunol.* **2013,** *358,* 33–89. doi:10.1007/82_2012_286
2. Schleifer, K. H.; Fischer, U. *Int. J. Syst. Bacteriol.* **1982,** *32,* 153–156. doi:10.1099/00207713-32-2-153
3. Barrière, C.; Leroy-Sétrin, S.; Talon, R. *J. Appl. Microbiol.* **2001,** *91,* 514–519. doi:10.1046/j.1365-2672.2001.01411.x
4. Rosenstein, R.; Nerz, C.; Biswas, L.; Resch, A.; Raddatz, G.; Schuster, S. C.; Götz, F. *Appl. Environ. Microbiol.* **2009,** *75,* 811–822. doi:10.1128/AEM.01982-08
5. Rosenstein, R.; Götz, F. *Int. J. Med. Microbiol.* **2010,** *300,* 104–108. doi:10.1016/j.ijmm.2009.08.014
6. Fey, P. D.; Ulphani, J. S.; Götz, F.; Heilmann, C.; Mack, D.; Rupp, M. E. *J. Infect. Dis.* **1999,** *179,* 1561–1564. doi:10.1086/314762
7. Giese, B.; Dittmann, S.; Paprotka, K.; Levin, K.; Weltrowski, A.; Biehler, D.; Lâm, T.-T.; Sinha, B.; Fraunholz, M. J. *Infect. Immun.* **2009,** *77,* 3611–3625. doi:10.1128/IAI.01478-08
8. Gerke, C.; Kraft, A.; Süßmuth, R.; Schweitzer, O.; Götz, F. *J. Biol. Chem.* **1998,** *273,* 18586–18593. doi:10.1074/jbc.273.29.18586
9. Cramton, S. E.; Gerke, C.; Schnell, N. F.; Nichols, W. W.; Götz, F. *Infect. Immun.* **1999,** *67,* 5427–5433.
10. Møretrø, T.; Hermansen, L.; Holck, A. L.; Sidhu, M. S.; Rudi, K.; Langsrud, S. *Appl. Environ. Microbiol.* **2003,** *69,* 5648–5655. doi:10.1128/AEM.69.9.5648-5655.2003
11. Camesano, T. A.; Liu, Y.; Datta, M. *Adv. Water Resour.* **2007,** *30,* 1470–1491. doi:10.1016/j.advwatres.2006.05.023
12. Busscher, H. J.; Weerkamp, A. H. *FEMS Microbiol. Lett.* **1987,** *46,* 165–173. doi:10.1111/j.1574-6968.1987.tb02457.x
13. Loskill, P.; Hähl, H.; Thewes, N.; Kreis, C. T.; Bischoff, M.; Herrmann, M.; Jacobs, K. *Langmuir* **2012,** *28,* 7242–7248. doi:10.1021/la3004323
14. Planchon, S.; Gaillard-Martinie, B.; Leroy, S.; Bellon-Fontaine, M. N.; Fadda, S.; Talon, R. *Food Microbiol.* **2007,** *24,* 44–51. doi:10.1016/j.fm.2006.03.010
15. Harraghy, N.; Seiler, S.; Jacobs, K.; Hannig, M.; Menger, M. D.; Herrmann, M. *Int. J. Artif. Organs* **2006,** *29,* 368–378.
16. Binnig, G.; Quate, C. F.; Gerber, C. *Phys. Rev. Lett.* **1986,** *56,* 930–933. doi:10.1103/PhysRevLett.56.930
17. Helenius, J.; Heisenberg, C.-P.; Gaub, H. E.; Müller, D. J. *J. Cell Sci.* **2008,** *121,* 1785–1791. doi:10.1242/jcs.030999
18. Müller, D. J.; Dufrêne, Y. F. *Nat. Nanotechnol.* **2008,** *3,* 261–269. doi:10.1038/nnano.2008.100
19. Beaussart, A.; El-Kirat-Chatel, S.; Herman, P.; Alsteens, D.; Mahillon, J.; Hols, P.; Dufrêne, Y. F. *Biophys. J.* **2013,** *104,* 1886–1892. doi:10.1016/j.bpj.2013.03.046
20. Brzoska, J. B.; Azouz, I. B.; Rondelez, F. *Langmuir* **1994,** *10,* 4367–4373. doi:10.1021/la00023a072
21. Lessel, M.; Bäumchen, O.; Klos, M.; Hähl, H.; Fetzer, R.; Seemann, R.; Jacobs, K. *arXiv:1212.0998 [cond-mat.mtrl-sci]* **2012**.
22. Bellion, M.; Santen, L.; Mantz, H.; Hähl, H.; Quinn, A.; Nagel, A.; Gilow, C.; Weitenberg, C.; Schmitt, Y.; Jacobs, K. *J. Phys.: Condens. Matter* **2008,** *20,* 404226. doi:10.1088/0953-8984/20/40/404226
23. Hutter, J. L.; Bechhoefer, J. *Rev. Sci. Instrum.* **1993,** *64,* 1868–1873. doi:10.1063/1.1143970
24. Bushan, B., Ed. *Handbook of Nanotechnology;* Springer: Berlin Heidelberg New York, 2007.
25. Alsteens, D.; Beaussart, A.; El-Kirat-Chatel, S.; Sullan, R.-M. A.; Dufrêne, Y. F. *PLoS Pathog.* **2013,** *9,* e1003516. doi:10.1371/journal.ppat.1003516
26. Israelachvili, J. N. *Intermolecular and surface forces;* Elsevier Inc., 2011.
27. Loskill, P.; Puthoff, J.; Wilkinson, M.; Mecke, K.; Jacobs, K.; Autumn, K. *J. R. Soc., Interface* **2013,** *10,* 20120587. doi:10.1098/rsif.2012.0587
28. Linke, D.; Goldman, A., Eds. *Bacterial Adhesion;* Springer: Dordrecht Heidelberg London New York, 2011.
29. Koebnik, R.; Locher, K. P.; Van Gelder, P. *Mol. Microbiol.* **2000,** *37,* 239–253. doi:10.1046/j.1365-2958.2000.01983.x
30. Florin, E.-L.; Moy, V. T.; Gaub, H. E. *Science* **1994,** *264,* 415–417. doi:10.1126/science.8153628
31. Hähl, H.; Evers, F.; Grandthyll, S.; Paulus, M.; Sternemann, C.; Loskill, P.; Lessel, M.; Hüsecken, A. K.; Brenner, T.; Tolan, M.; Jacobs, K. *Langmuir* **2012,** *28,* 7747–7756. doi:10.1021/la300850g
32. Norde, W. *Colloids Surf., B* **2008,** *61,* 1–9. doi:10.1016/j.colsurfb.2007.09.029
33. Czeslik, C. *Z. Phys. Chem.* **2004,** *218,* 771–801. doi:10.1524/zpch.218.7.771.35722
34. Wahlgren, M.; Arnebrant, T. *Trends Biotechnol.* **1991,** *9,* 201–208. doi:10.1016/0167-7799(91)90064-O
35. Malmsten, M., Ed. *Biopolymers at interfaces;* Marcel Dekker: New York, 2003.
36. Wong, J. Y.; Kuhl, T. L.; Israelachvili, J. N.; Mullah, N.; Zalipsky, S. *Science* **1997,** *275,* 820–822. doi:10.1126/science.275.5301.820
37. Leckband, D.; Israelachvili, J. *Q. Rev. Biophys.* **2001,** *34,* 105–267. doi:10.1017/S0033583501003687
38. Helm, C. A.; Israelachvili, J. N.; McGuiggan, P. M. *Biochemistry* **1992,** *31,* 1794–1805. doi:10.1021/bi00121a030
39. van Oss, C. J. *Interfacial forces in aqueous media;* CRC Press, Taylor and Francis Group, 2006.
40. Xia, G.; Kohler, T.; Peschel, A. *Int. J. Med. Microbiol.* **2010,** *300,* 148–154. doi:10.1016/j.ijmm.2009.10.001
41. Bos, M. A.; van Vliet, T. *Adv. Colloid Interface Sci.* **2001,** *91,* 437–471. doi:10.1016/S0001-8686(00)00077-4

Beilstein J. Nanotechnol. **2014,** *5*, 1501–1512.

Addendum IV - Stochastic binding of Staphylococcus aureus to hydrophobic surfaces

Authors: N. Thewes[1], A. Thewes[2] P. Loskill[1], H. Peisker[3], M. Bischoff[3], M. Herrmann[3], L. Santen[2], and K. Jacobs[1]

[1] Department of Experimental Physics, Saarland University, 66041 Saarbrücken, Germany.
[2] Department of Theoretical Physics, Saarland University, 66041 Saarbrücken, Germany [3] The Institute of Medical Microbiology and Hygiene, Saarland University, 66421 Homburg/Saar, Germany.

Reproduced by permission of The Royal Society of Chemistry.
Soft Matter **11**, 8889–9046 (2015).
(`http://dx.doi.org/10.1039/c5sm00963d`)

Author contributions:
Experiments were conceived and designed by N. Thewes and K. Jacobs. AFM experiments were performed by N. Thewes. Modelling was performed by N. Thewes, A. Thewes and K. Jacobs. Simulations were performed by A. Thewes. Data was analyzed by N. Thewes and A. Thewes. The article was mainly written by N. Thewes, A. Thewes, L. Santen and K. Jacobs. Research was mainly directed by L. Santen and K. Jacobs.

Abstract - The adhesion of pathogenic bacteria to surfaces is of immense importance for health care applications. Via a combined experimental and computational approach, we studied the initiation of contact in the adhesion process of the pathogenic bacterium *Staphylococcus aureus*. AFM force spectroscopy with single cell bacterial probes paired with Monte Carlo simulations enabled an unprecedented molecular investigation of the contact formation. Our results reveal that bacteria attach to a surface over distances far beyond the range of classical surface forces via stochastic binding of thermally fluctuating cell wall proteins. Thereby, the bacteria are pulled into close contact with the surface as consecutive proteins of different stiffnesses attach. This mechanism greatly enhances the attachment capability of *S. aureus*. It, however, can be manipulated by enzymatically/chemically modifying the cell wall proteins to block their consecutive binding. Our study furthermore reveals that fluctuations in protein density and structure are much more relevant than the exact form of the binding potential.

Volume 11 | Number 46 | 14 December 2015 | Pages 8889–9046

Soft Matter

www.softmatter.org

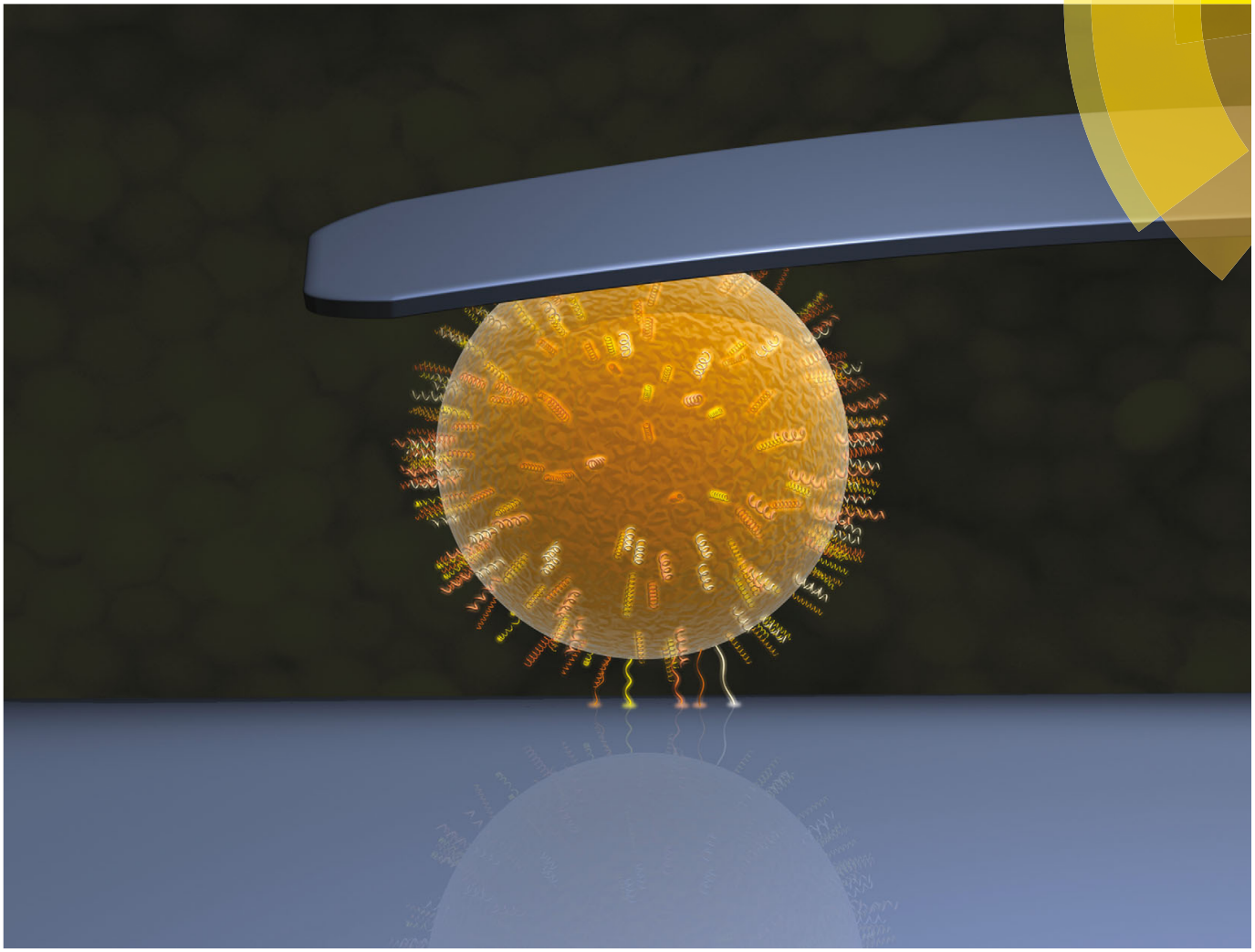

ISSN 1744-683X

ROYAL SOCIETY OF CHEMISTRY

PAPER
Karin Jacobs *et al.*
Stochastic binding of *Staphylococcus aureus* to hydrophobic surfaces

Soft Matter

PAPER

Stochastic binding of *Staphylococcus aureus* to hydrophobic surfaces†

Nicolas Thewes,[a] Alexander Thewes,[b] Peter Loskill,‡[a] Henrik Peisker,[c] Markus Bischoff,[c] Mathias Herrmann,[c] Ludger Santen[b] and Karin Jacobs*[a]

Cite this: *Soft Matter*, 2015, **11**, 8913

Received 22nd April 2015,
Accepted 27th July 2015

DOI: 10.1039/c5sm00963d

www.rsc.org/softmatter

The adhesion of pathogenic bacteria to surfaces is of immense importance for health care applications. *Via* a combined experimental and computational approach, we studied the initiation of contact in the adhesion process of the pathogenic bacterium *Staphylococcus aureus*. AFM force spectroscopy with single cell bacterial probes paired with Monte Carlo simulations enabled an unprecedented molecular investigation of the contact formation. Our results reveal that bacteria attach to a surface over distances far beyond the range of classical surface forces *via* stochastic binding of thermally fluctuating cell wall proteins. Thereby, the bacteria are pulled into close contact with the surface as consecutive proteins of different stiffnesses attach. This mechanism greatly enhances the attachment capability of *S. aureus*. It, however, can be manipulated by enzymatically/chemically modifying the cell wall proteins to block their consecutive binding. Our study furthermore reveals that fluctuations in protein density and structure are much more relevant than the exact form of the binding potential.

The adhesion of bacteria to surfaces plays an important role in many processes in our everyday life: in the clinical setting, it can be the major factor for the transmission of diseases or the starting point of infectious biofilms on implants or catheters.[1,2] The fundamental reason for studying bacterial adhesion is mostly its prevention.[3,4] Yet, the majority of studies concentrate on the detachment process, mainly the adhesion force, which represents the maximum force acting between the bacterium and the colonized surface, in other words, it is studied how to get rid of already attached bacteria.[5–7] In our opinion, the first logical step to prevent bacterial adhesion is to detain a bacterium from attaching and therefore, a fundamental understanding of the contact initiation process of a bacterium to a surface is crucial. In recent years, atomic force microscopy (AFM) was refined to perform force spectroscopy and is now established as a powerful and versatile method to characterise bacterial adhesion; especially the use of 'bacterial probes' allows for a precise and quantitative insight into the involved forces.[6,8–11] 'Bacterial probes' are AFM cantilevers, for which the tip is replaced by a single bacterium or a consortium of bacteria.

Interaction forces that arise in AFM force spectroscopy while the probe is continuously approached to the surface lead to a deflection of the cantilever. The deflection is monitored by a laser beam reflected from the back of the cantilever to a position-sensitive photodiode. Under quasistatic conditions, cantilever deflection is a measure of the force between the tip and the surface. However, a classic force curve features unstable points if, in a certain range, the gradient of the interaction force between the tip and the surface exceeds the cantilever spring constant. This leads to an abrupt change in the cantilever deflection, and the tip/surface separation.[12] Assuming a Lennard-Jones-like interaction potential, one instability occurs during the approach part of the force/distance curve and is called 'jump-to-contact' or 'snap-in'. A detailed analysis is reported by Seo and Jhe.[8] However, recent findings indicate that with a viable bacterial probe, the snap-in can also be a rather extended event (in range and time) than a sudden jump into contact.[13] The phenomenon can be described by a model for bacterial adhesion that involves the consecutive attachment of bacterial cell wall macromolecules to the substratum (for example, due to hydrophobic interactions). It was hypothesised that the form (depth and width) of the snap-in event is characteristic of the adhesive molecules of a bacterium.[13] In this study, we provide experimental evidence for this model, by demonstrating that the form of the snap-in event is defined by the properties of the cell wall proteins. The snap-in process becomes more pronounced as the surface energy of the substratum becomes smaller, therefore we concentrate in this

[a] *Experimental Physics, Saarland University, Campus E2 9, D-66123 Saarbrücken, Germany. E-mail: k.jacobs@physik.uni-saarland.de*
[b] *Theoretical Physics, Saarland University, Campus E2 6, D-66123 Saarbrücken, Germany*
[c] *Institute of Medical Microbiology and Hygiene, Saarland University, D-66421 Homburg/Saar, Germany*

† Electronic supplementary information (ESI) available. See DOI: 10.1039/c5sm00963d

‡ Present address: Department of Bioengineering and California Institute for Quantitative Biosciences (QB3), University of California at Berkeley, Berkeley, California 94720, USA.

study on low-energy surfaces such as hydrophobised silicon (Si) wafers.

We investigated the initiation of contact between exponential phase cells of *S. aureus* strain SA113[14] and the hydrophobic surface of a silanised Si wafer. We additionally performed Monte Carlo (MC) simulations using a simple model for the adhesion of a bacterium to a surface.[13] By comparing experimental and simulated force/distance curves, we gained insights into the molecular mechanisms governing the initial attachment of *S. aureus*. Furthermore, by using bioactive agents that either crosslink or degrade proteins, the properties of the cell wall can be altered in a controlled manner.

1 Material and methods

Preparation of the substratum

As substrates, we used Si wafers since they feature a very low roughness (0.09(2) nm) and are easily available in consistently good quality with a known surface chemistry. Si wafers (Siltronic AG, Burghausen, Germany) have a native silicon oxide layer (d = 1.7(2) nm).§ The wafers were rendered hydrophobic by self-assembly of a CH_3-terminated monolayer of OTS molecules following a standard protocol.[15] The hydrophobised Si wafers have a surface roughness of 0.12(2) nm and an advancing (receding) water contact angle of 111(1)° (107(2)°). Using polar/apolar liquids, the surface energy can be determined to be 24(1) mJ m^{-2},[15] and the streaming potential is −80.0(1) mV at pH 7.3.[10] For the force measurements, hydrophobised silicon wafers are immersed into 6 ml of phosphate-buffered saline (PBS, pH 7.3, ionic strength 0.1728 mol l^{-1} at 20 °C).

Bacterial strain and growth conditions

S. aureus strain SA113 is a cell-invasive and biofilm-positive laboratory strain frequently used to study the functions of cell wall-anchored or -attached molecules of this pathogenic species.[16–19] Exponential growth phase *S. aureus* cells were freshly prepared for each experiment. 40 μl of an overnight culture were transferred into 4 ml of Tryptic soy broth (TSB) medium and cultured at 37 °C and 150 rpm for 2.5 hours. To dilute the bacterial solution, 0.5 ml of the culture and additional 0.5 ml of PBS were inserted into a 1.5 ml microtube. To remove extracellular material, these bacteria were washed four times using 1 ml of PBS each.

Preparation of bacterial probes

Single cell bacterial probes have been prepared following the detailed description of ref. 32: cantilevers were cleaned in an air plasma and vertically immersed for about 50 min into a solution allowing the polymerisation of dopamine, that is 4 mg ml^{-1} of dopamine hydrochloride (99%) in 10 mM Tris-buffer (pH 7.9 at 22 °C), both were provided by Sigma Aldrich, Germany. During polymerisation, the cantilevers are stored in a fridge. Then, cantilevers were carefully rinsed with ultrapure water to remove unbound (poly)dopamine and dried under a laminar flow bench. Cantilever spring constants were determined before attaching a single bacterium using the thermal tune technique.[20] A single bacterium was attached using a micromanipulation system (Narishige Group, Japan) linked to an optical microscope: a droplet (approx. 30 μl) of diluted bacterial solution (see above) was placed on a polystyrene Petri dish, where the bacteria are allowed to sediment. Then, the functionalised cantilever, mounted on the micromanipulator, is dipped into the droplet. By carefully tapping onto a single *S. aureus* cell with the upper end of the polydopamine-coated cantilever, the cell attaches to the cantilever. To safely exclude interactions between the cantilever and the substratum during the force measurements, the single bacterium should get attached as close as possible to the very end of the cantilever (not exceeding a distance of roughly two bacterial diameters). Subsequently, the cantilever is retracted from the droplet of bacterial solution and reintegrated into the AFM to perform force spectroscopy measurements. The inset in Fig. 2b depicts a single bacterial probe. To ensure that our method does not harm the cell, its viability can be checked after completing the measurements, using live/death staining (Life Technologies GmbH, Germany). Thereby, a small amount of live/death stain (20 μl) is added directly onto the bacterial probe and the viability of the bacterium is determined under a fluorescence light microscope (*cf.* ESI†).

Force spectroscopy

All force/distance curves in this study were obtained in PBS at room temperature using a Bioscope Catalyst AFM (Bruker Nano, Santa Barbara, CA). The cantilever was approached (and retracted) over a distance of 800 nm while 1024 data points were recorded for each part. The drive velocity was 400 nm s^{-1} and retraction started immediately after the chosen force trigger was reached on approach. Positive force triggers hereby reflect a net repulsive force, resulting in a 'standard' force distance/curve. Setting a negative force trigger allows us to record 'partitioned' force/distance curves by switching from approach to retraction at the attractive part of the approach curve, as shown below.

2 Results and discussion

Standard force/distance curves

A standard force/distance curve between a single *S. aureus* AFM probe and a hydrophobised Si wafer can be comprehended in terms of the properties of the bacterial cell wall (*cf.* schematic diagram in Fig. 1 and experimental curve in Fig. 2): in the case of *S. aureus*, the cell wall consists of numerous proteinaceous and non-proteinaceous macromolecules.[21,22] According to our model (as recently described for the apathogenic staphylococcal species *S. carnosus*[13]) at a certain distance (called 'snap-in separation') above the wafer surface, the longest and/or most extended macromolecules start to interact with the wafer *via* short-range attractive forces.¶ Once tethered, the extended macromolecules tear the bacterium to the surface at point (1)

§ The number in the parentheses denotes the standard deviation of the last digit.

¶ In electrolyte solution (buffer), screening effects virtually lead to the absence of long-range forces.[23]

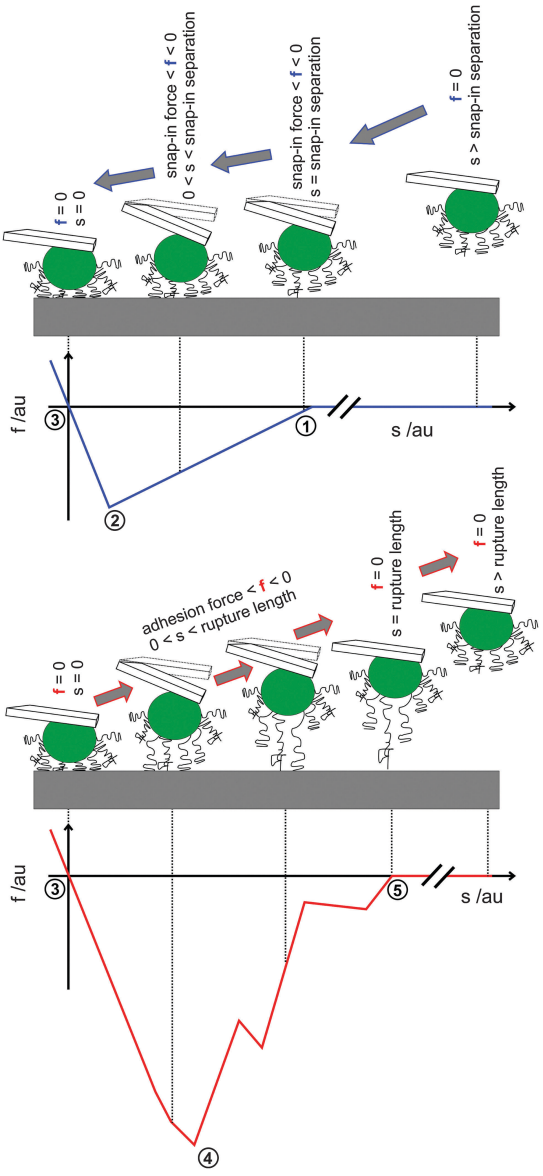

Fig. 1 Schematic diagram showing the bacterial adhesion process according to our model (approach in the upper sketch and retraction in the lower one). An additional sketch of a force/distance curve (with force *f* and separation *s* in arbitrary units au) indicates the link between the model-situation and the respective experimental force/distance signal, approach (retraction) in blue (red). Magnitudes do not reflect real situations.

in Fig. 1, 2a and b. Along with that, more and more macromolecules can tether, yet some of the longest may therefore already be compressed. Fig. 2b demonstrates that the snap-in event is indeed an extended process, since dozens of data points can be recorded. The time between two data points is in the order of 10^{-3} s

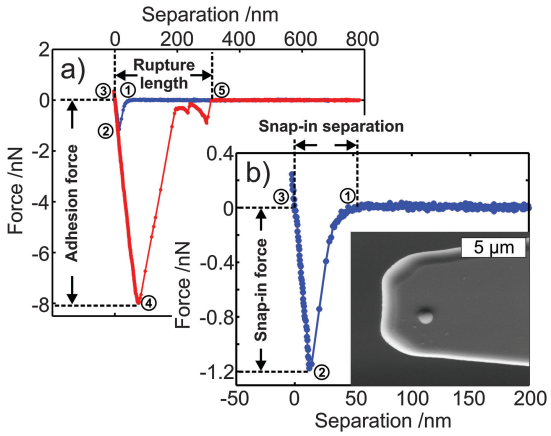

Fig. 2 Exemplary 'standard' force/distance curve recorded with a single *S. aureus* cell on a hydrophobised Si wafer and a positive force trigger of 300 pN (approach is displayed in blue and retraction in red). (a) Entire curve and (b) approach part of (a) in more detail. The inset in (b) shows an electron micrograph of the bacterial probe (radius of the bacterium around 500 nm).

(defined by the force/distance curve parameters, see above). Soon, a point is reached where, with a further approach of the cantilever, more molecules are compressed than new macromolecules tether. Then, the minimum force of the snap-in process (the 'snap-in force') is reached (2) and a further approach mainly compresses the macromolecules. In a standard force/distance curve after crossing zero force (3), approach is stopped once the preset positive force trigger has been reached. Upon retraction, the compressed macromolecules are released, unfolded and/or stretched. Close to the force minimum (reflecting the 'adhesion force'), the slope decreases, since more and more macromolecules start to detach (4). From now on, the number of attached molecules decreases that much that the measured force is more and more reduced. At a certain distance (called the 'rupture length') the bacterium, *viz.* its cell wall macromolecules, detach completely (5). Depending on the types and the number of involved macromolecules, the retraction curve looks different for every individual single cell bacterial probe, a fact that has been found earlier in non-bacterial systems involving macromolecules.[24–27] The four measures of the force/distance curve (snap-in separation, snap-in force, adhesion force and rupture length) are usually very robust for one bacterial cell, as can be seen in an overlay of 20 force/distance curves with the same bacterial probe (*cf.* Fig. 3). For different cells, even of the identical bacterial culture, the four measures can vary markedly. However, by comparing a large number of cells, differences between bacterial species show up. For instance, the adhesion of the facultative pathogenic species *S. aureus* outperforms that of apathogenic *S. carnosus*.[13] In the exemplary curve, the snap-in separation is around 50 nm and the snap-in force is almost 1.2 nN. In the retraction part, discrete steps can frequently be observed which are similar to single molecule force spectroscopy.[28]

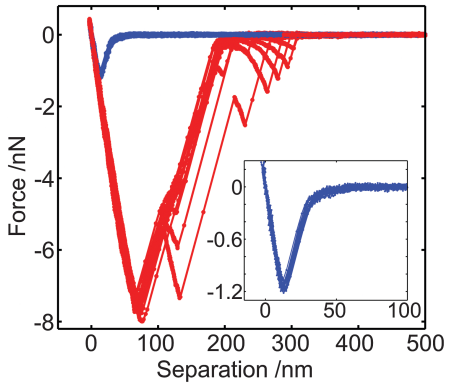

Fig. 3 Overlay of 20 standard force/distance curves showing the adhesion of a single *S. aureus* cell to a hydrophobised Si wafer, force trigger is 300 pN. One of the curves is shown in detail in Fig. 2, approach (retraction) is marked in blue (red). The snap-in process is shown in more detail in the inset.

Partitioned force/distance curves

In order to further explore the initial attachment of a bacterial cell, we focus on the nature of the snap-in event and the above mentioned partitioned force/distance curves. For this purpose, the force trigger is set to a negative value between the snap-in separation (1) and the snap-in force (2) displayed in Fig. 2, using the identical bacterial probe.

Fig. 4a shows an overlay of 20 partitioned force/distance curves with a force trigger of −100 pN. After stopping the approach, the piezo movement is immediately reversed and the bacterial probe is retracted. For −100 pN, the retraction curves did not resemble the ones of the standard force/distance curves shown in Fig. 3, as the adhesion force is greatly reduced. Nevertheless, these retraction curves feature the rupture length of the standard force/distance curve and a gradually reduced force. With decreasing force trigger (negative sign!) and, hence, a reduced distance of the bacterial probe to the surface (*cf.* Fig. 4b–d), the form and the adhesion force of the standard *S. aureus*

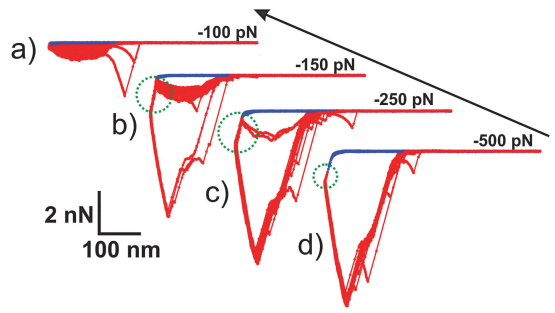

Fig. 4 'Partitioned' force/distance curves of a single *S. aureus* bacterial probe on a hydrophobised Si wafer for four different negative force triggers that allow for a stop of the approach at variable distances above the wafer surface. Each panel displays an overlay of 20 force/distance curves and they were all taken with the exact same bacterium.

force/distance curve are recovered. A closer look reveals that at a force trigger of −150 pN two out of the 20 force/distance curves resembled in their retraction part those of the standard force/distance curve and this ratio increased along with decreasing force trigger (Fig. 4b–d). Three characteristic features are noteworthy:

(i) The retraction curves of the partitioned force/distance curves resemble the 'parallel and simultaneous stretching' of macromolecules independent of the applied negative force trigger.[25]

(ii) With decreasing force trigger (negative sign; getting the bacterium closer to the surface), the adhesion force does not increase gradually: rather, either a low (less than one nN) or the 'standard' adhesion force is obtained. No intermediate force values are observed.

(iii) Even if the piezo already moves the cantilever away from the surface, an increasing adhesive force is recorded, going along with a decreased separation between the probe and the surface (see Fig. 4b–d, the red curve within the dashed green circle), which we term 'pulling regime' in the following. It ends as soon as a minimum separation is reached. Upon further piezo retraction, the standard force/distance curve is recovered. For the low adhesion force, the pulling regime is absent.

These characteristics call for an interpretation in a molecular model: in this model, cell wall macromolecules are responsible for the initial attachment of the bacterium to the hydrophobic surface. A force trigger of only −100 pN (*cf.* Fig. 4a) is apparently insufficient to enable the attachment of a sufficient number and/or the right types of molecules to withstand the restoring force of the cantilever after piezo reversal. Thus, the separation between the surface and the bacterium increases immediately with cantilever retraction and neither a pulling regime nor a standard adhesion force is observed. Rather, this case is accompanied by a low adhesion force. In contrast, at force triggers of −150 pN and less, a pulling regime is observed, so the already attached macromolecules are strong enough to withstand the restoring force of the cantilever after piezo reversal, thereby facilitating the binding of additional macromolecules. Subsequently, the bacterium is pulled closer to the surface against cantilever retraction. The pulling regime ends at the point where the net attractive force of the cell wall macromolecules is outmatched by the restoring force of the cantilever and, thereby, further approach is prevented. Then, the standard retraction curve and adhesion force are recovered.

In Fig. 4b and c, both types of adhesion forces are recorded, which is due to the stochastic nature of the molecular processes involved during contact initiation.[13] In Fig. 4d, no low adhesion force curves were measured, which corroborates the above argument that at larger negative force triggers, more and more molecules are able to tether, giving rise to maximum adhesion.

So far, by applying negative force triggers, we were able to interrupt the 'standard' adhesion process and could show that the snap-in process is (a) a robust and characteristic feature of bacterial adhesion and is (b) mediated by cell wall macromolecules. To corroborate the experimental results and the hypothesised model, we performed Monte Carlo (MC) simulations.

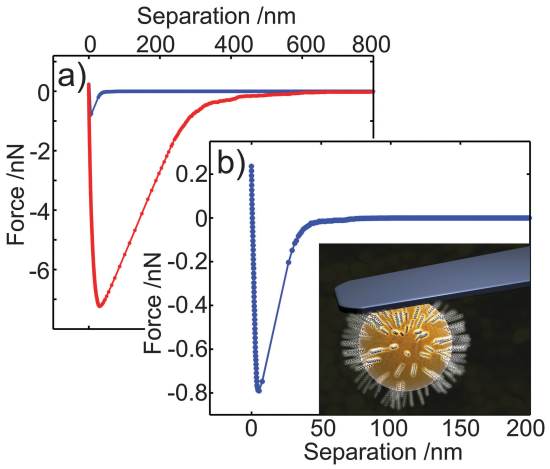

Fig. 5 Monte-Carlo-simulated standard force/distance curve and approach (retract) curve in blue (red). (a) Entire curve and (b) snap-in process of the simulated force/distance curve in more detail. The inset in (b) schematically depicts the MC model where cell wall macromolecules are represented as elastic springs (objects are not to scale).

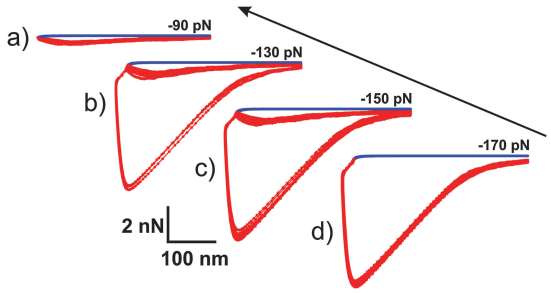

Fig. 6 Monte-Carlo-simulated partitioned force/distance curves for four different negative force triggers. Each panel displays an overlay of 20 simulated force/distance curves.

Monte Carlo simulations

The model for the MC simulations is based on the key assumption that cell wall macromolecules can be described as elastic springs that attach to the substratum (for details of the model *cf.* ESI†). An MC-simulated standard force/distance curve is shown in Fig. 5. Since the density and composition of cell wall macromolecules and their response to external forces are not known, there are many adjustable parameters in the model. However, considering the simplicity of our modeling approach, the agreement between the experiment and MC simulation is remarkable: the snap-in event starts in the simulations (*cf.* Fig. 5b), as well as in the experiment (*cf.* Fig. 2b), with a small gradient which gets larger with decreasing distance until the snap-in force is reached.

Moreover, in the simulations as well, partitioned force/distance curves can be recorded using a negative force trigger (*cf.* Fig. 6). These curves also strikingly resemble the experimental curves, including the above described features, in particular features (ii) and (iii): the simulated curves exhibit a pulling regime, too, and partitioned force distance curves using a force trigger that is located in the low-gradient area only exhibit low adhesion forces like in the experiment (*cf.* experimental curves in Fig. 4a and simulated curves in Fig. 6a). As in the experiment, the number of simulated force/distance curves resembling the simulated standard force/distance curve increases with decreasing force trigger (*cf.* experimental curves in Fig. 4b–d and simulated curves in Fig. 6b–d). The simulated partitioned force/distance curves also show a sudden transition between the low and high adhesion (pulling) regime. In experiments as well as in simulations, this transition occurs at force triggers located in the region where the gradient of the snap-in process in the standard force/distance curve features the strongest increase (*cf.* Fig. 2b and 5b). In other words, from the form of the snap-in event, one is able to predict the partitioned force/distance curves (within the inaccuracy due to the stochastic nature of the process).

Importantly, in the MC model, it is not sufficient to use just one sort of macromolecules (springs) with a given stiffness, rather, a spring constant distribution (*cf.* ESI†) must be implemented for the macromolecules to reproduce the experimental features. The model now allows for a more detailed interpretation of the molecular processes during contact formation.

Due to thermal fluctuations and the structural heterogeneity of the cell wall proteins, a small number of proteins (the softer ones) initiate binding of the bacterium on approach, resulting in a small gradient of the force/distance curve. As the cantilever further reduces the distance to the substratum, more and also stiffer molecules can bind and the gradient of the force/distance curve becomes larger. These findings give rise to the assumption that different sorts of macromolecules with different properties are involved in the adhesion process.

All experimental force/distance curves shown in Fig. 1–3 were obtained with the identical bacterial probe. The described shape of the snap-in event, *i.e.* the increasing gradient for decreasing distances, is indeed characteristic of *S. aureus* single bacterial probes. The exact shape of the snap-in process, however, may vary for different *S. aureus* cells obtained from the same preparation. According to our results, we state that the actual appearance of the snap-in event of a single *S. aureus* bacterial probe is directly linked to the distribution and nature of the contact-forming cell wall macromolecules and that *vice versa* from the shape of the snap-in event it is possible to gather insights into the nature of the contact-forming macromolecules.

Protein-modifying treatment

To further evidence the macromolecular origin of the snap-in event and to explore the nature of cell wall macromolecules involved in the attachment process, we specifically modified the properties of cell wall proteins: we therefore treated the bacterial surface with two different protein-altering compounds, pronase E (Sigma-Aldrich) and glutaraldehyde (25% v/v, Sigma-Aldrich). Pronase E degrades proteins by cutting peptide bonds, whereas glutaraldehyde reacts with several functional groups of proteins

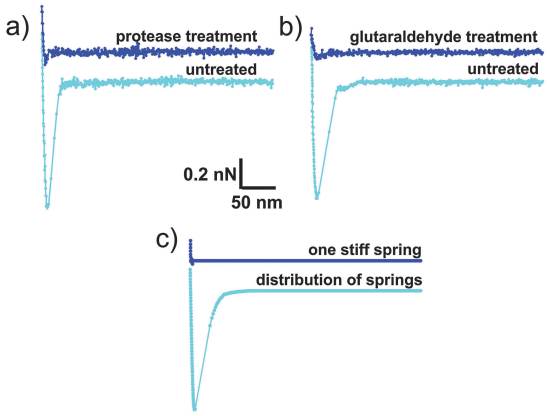

Fig. 7 Influence of enzymatic/chemical treatment on the bacterial snap-in process and its corresponding simulated force/distance curve. Snap-in event of a single *S. aureus* cell adhering to a hydrophobic Si wafer (a) in its native state (cyan curve) and after treating the cell with protease, (b) before (cyan curve) and after treating an *S. aureus* cell with glutaraldehyde. (c) Simulated force/distance curves using a model bacterium covered with a large number of springs with stiffnesses distributed over a certain range (cyan curve) and with only one stiff spring (blue curve). The baselines of the blue curves have been shifted in the *y*-direction by 0.2 nN.

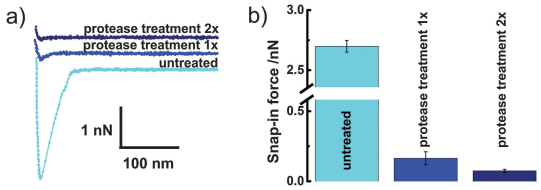

Fig. 8 (a) Influence of two consecutive protease treatments on the bacterial snap-in process of an *S. aureus* cell, the baseline of the blue (dark blue) curve has been shifted in the *y*-direction by 0.4 nN (0.8 nN). (b) Recorded snap-in force for the untreated, and one time and two times with protease treated *S. aureus*.

and crosslinks them that way.[29,30] Thus, if driven by cell wall proteins, both treatments should significantly influence the snap-in process.

For these measurements, bacterial probes were prepared as described before, and prior to the enzymatic or chemical treatment, 20 force/distance curves were recorded on a hydrophobised Si wafer as a reference (Fig. 7a and b each show one reference approach curve for a force trigger of 300 pN). After that, the probe holder with the bacterial probe was removed from the AFM head leaving a droplet of buffer around the tip. With a pipette, 20 μl of 100 μg ml^{-1} solution of protease (or 12.5% glutaraldehyde solution, respectively) was added to the buffer droplet. After 10 min, the droplet around the tip was carefully removed and replaced by a fresh drop of buffer solution. This droplet of buffer was exchanged another three times to remove as much of the protein-modifying compound as possible. Then, a new series of force/distance curves were taken (representative curves are given in Fig. 7a and b).

The protease as well as the glutaraldehyde treatment caused a substantial reduction of the snap-in process: the snap-in distance contracted from more than 30 nm to less than 10 nm and the snap-in force decreased to only a few pN as compared to 800 pN in the reference curves (Fig. 7). By cutting peptide bonds, the non-specific protease mixture should gradually reduce the length of the cell wall-attached proteins, thereby decreasing their hydrodynamic radii which impairs the bacterial snap-in process. To test this, we observed the snap-in event in between and after two consecutive protease treatments that were both applied as described above (*cf.* Fig. 8): indeed, a second treatment with protease caused an additional reduction of the snap-in force (*cf.* Fig. 8b). A similar effect is expected for the protein crosslinker glutaraldehyde, which should affect both the mobility and the flexibility of proteins, thereby suppressing the stochastic process of tethering macromolecules by macromolecules to the surface. To capture the impact of a protein-modifying treatment, a rough model will give insights into the leading processes. As both treatments result in an increased stiffness of the macromolecules[31] and, at least, effectively in a decreased number of springs, we evaluated the force/distance curves of a model bacterium with only one single, stiff spring (spring constant of 1 N m^{-1}), in comparison to the model bacterium covered with a distribution of springs as described above, *cf.* Fig. 7c. The result is a simulated force/distance curve with only a tiny jump-to-contact (blue curve), instead of an extended snap-in process (cyan curve).

The retraction curves (see ESI†) also featured a massive reduction in adhesion force and rupture length due to the enzymatic/chemical treatments, respectively. However, for a detailed discussion of the detachment process, an in-depth knowledge of the molecular composition of the bacterial surface and the impact of the two protein modifying compounds would be needed, which is beyond the scope of this study.

Thus, by interfering with the length and the number or the mobility of cell wall proteins, two important conclusions emerge: (1) cell wall proteins fulfill the major task in bacterial adhesion to hydrophobic surfaces and (2) the consecutive tethering of cell wall proteins features major biological relevance as this mechanism strongly enhances the interaction range and strength between the bacterium and the surface. Simulated force distance curves support these findings.

3 Conclusions

The above results indicate why a general description of bacterial adhesion in the framework of the Derjaguin–Landau–Verwey–Overbeek (DLVO) theory or by the extended DLVO theory (including hydrophobic/hydrophilic interactions) fails if considered between the 'body' of the bacterium and the substratum. Actually, the initiation of bacterial adhesion starts as far as 50 nm (sometimes even 100 nm) above the substratum, a distance, for which DLVO forces between the 'body' of the bacterium and the substratum are negligible.[3] Hence, the extended DLVO theory has to be applied to all cell wall macromolecules involved in the adhesion process.

Our results indicate that on approach of a bacterium to a surface, a simple protein/surface potential allowing the proteins to bind is sufficient, while the number and the distribution of spring constants of the proteins are of importance. In other words, on contact formation, fluctuations in protein density and structure are much more relevant than the exact protein/surface binding potential.

To conclude, we studied and described the fundamental mechanisms of the initiation of contact during the adhesion of *S. aureus*. It has been demonstrated that the approach part of a force/distance curve can be reliably evaluated and characterises the initiation of adhesion comprehensively. MC simulations assuming bacterial cell wall macromolecules as elastic springs of different stiffnesses capture the observed experimental features of force/distance curves. An enzymatic/chemical treatment revealed that cell wall proteins dominate the attachment process and that disrupting the length of these molecules or their mobility causes severe changes in attachment. The proposed model and the resulting adhesion mechanism explain the observed force/distance curves of single cell bacterial probes as well as differences between varying bacterial species. Additional studies, *e.g.* using genetic tools to modify the bacterial cell wall composition, will allow us to distinguish between the contributions of the different components/macromolecules. Applying a similar approach of single cell level experiments accompanied by molecular modeling onto entire force/distance curves, including both the approach and retraction parts, will pave the way for a global understanding of bacterial adhesion.

Acknowledgements

This work was supported by the Deutsche Forschungsgemeinschaft (DFG) within the collaborative research centre SFB 1027 and the research training group GRK 1276 (N.T.). M.B. was supported by grants of the German Ministry for Education and Research 01Kl1014B and 01Kl1301B.

References

1 A. E. Khoury, K. Lam, B. Ellis and J. W. Costerton, *ASAIO J.*, 1992, **38**, 174–178.
2 J. W. Costerton, P. S. Stewart and E. P. Greenberg, *Science*, 1999, **284**, 1318–1322.
3 K. Hori and S. Matsumoto, *Biochem. Eng. J.*, 2010, **48**, 424–434.
4 A. K. Epstein, T.-S. Wong, R. A. Belisle, E. M. Boggs and J. Aizenberg, *Proc. Natl. Acad. Sci. U. S. A.*, 2012, **109**, 13182–13187.
5 P. H. Tsang, G. Li, Y. V. Brun, L. B. Freund and J. X. Tang, *Proc. Natl. Acad. Sci. U. S. A.*, 2006, **103**, 5764–5768.
6 T. Das, B. P. Krom, H. C. van der Mei, H. J. Busscher and P. K. Sharma, *Soft Matter*, 2011, **7**, 2927–2935.
7 R. M. A. Sullan, A. Beaussart, P. Tripathi, S. Derclaye, S. El-Kirat-Chatel, J. K. Li, Y.-J. Schneider, J. Vanderleyden, S. Lebeer and Y. F. Dufrêne, *Nanoscale*, 2014, **6**, 1134–1143.
8 Y. Seo and W. Jhe, *Rep. Prog. Phys.*, 2008, **71**, 016101.
9 S. Kang and M. Elimelech, *Langmuir*, 2009, **25**, 9656–9659.
10 P. Loskill, H. Haehl, N. Thewes, C. T. Kreis, M. Bischoff, M. Herrmann and K. Jacobs, *Langmuir*, 2012, **28**, 7242–7248.
11 A. Beaussart, S. El-Kirat-Chatel, R. M. A. Sullan, D. Alsteens, P. Herman, S. Derclaye and Y. F. Dufrêne, *Nat. Protoc.*, 2014, **9**, 1049–1055.
12 *Handbook of Nanotechnology*, ed. B. Bhushan, Springer, 2004.
13 N. Thewes, P. Loskill, P. Jung, H. Peisker, M. Bischoff, M. Herrmann and K. Jacobs, *Beilstein J. Nanotechnol.*, 2014, **5**, 1501–1512.
14 S. Iordanescu and M. Surdeanu, *J. Gen. Microbiol.*, 1976, **96**, 277–281.
15 M. Lessel, O. Bäumchen, M. Klos, H. Hähl, R. Fetzer, M. Paulus, R. Seemann and K. Jacobs, *Surf. Interface Anal.*, 2015, **47**, 557–564.
16 I. Maxe, C. Ryden, T. Wadström and K. Rubin, *Infect. Immun.*, 1986, **54**, 695–704.
17 A. Peschel, M. Otto, R. W. Jack, H. Kalbacher, G. Jung and F. Götz, *J. Biol. Chem.*, 1999, **274**, 8405–8410.
18 C. Weidenmaier, A. Peschel, Y.-Q. Xiong, S. A. Kristian, K. Dietz, M. R. Yeaman and A. S. Bayer, *J. Infect. Dis.*, 2005, **191**, 1771–1777.
19 S. Bur, K. T. Preissner, M. Herrmann and M. Bischoff, *J. Invest. Dermatol.*, 2013, **133**, 2004–2012.
20 J. L. Hutter and J. Bechhoefer, *Rev. Sci. Instrum.*, 1993, **64**, 1868–1873.
21 C. Heilmann, *Bacterial adhesion*, ed. D. Linke and A. Goldman, Springer, 1st edn, 2011, ch. 7, pp. 105–123.
22 Z. Jaglic, M. Desvaux, A. Weiss, L. L. Nesse, R. L. Meyer, K. Demnerova, H. Schmidt, E. Giaouris, A. Sipailiene and P. Teixeira, *et al.*, *Microbiology*, 2014, **160**, 2561–2582.
23 J. N. Israelachvili, *Intermolecular and Surface Forces*, Academic Press, 3rd edn, 2011.
24 C. A. Helm, J. N. Israelachvili and P. M. McGuiggan, *Biochemistry*, 1992, **31**, 1794–1805.
25 E.-L. Florin, V. T. Moy and H. E. Gaub, *Science*, 1994, **264**, 415–417.
26 J. Y. Wong, T. L. Kuhl, J. N. Israelachvili, N. Mullah and S. Zalipsky, *Science*, 1997, **275**, 820–822.
27 D. Leckband and J. Israelachvili, *Q. Rev. Biophys.*, 2001, **34**, 105–267.
28 M. Rief, F. Oesterhelt, B. Heymann and H. E. Gaub, *Science*, 1997, **275**, 1295–1297.
29 I. Migneault, C. Dartiguenave, M. J. Bertrand and K. C. Waldron, *Biotechniques*, 2004, **37**, 790–806.
30 Y. Wine, N. Cohen-Hadar, A. Freeman and F. Frolow, *Biotechnol. Bioeng.*, 2007, **98**, 711–718.
31 *Polymer Physics*, ed. M. Rubinstein and R. Colby, Oxford University Press, 1st edn, 2003, ch. 2, pp. 49–78.
32 N. Thewes, P. Loskill, C. Spengler, S. Hümbert, M. Bischoff and K. Jacobs, *EPJ E*, 2015, in press.

Soft Matter

Paper - supplementary material

Cite this: DOI: 10.1039/C5SM00963D

Stochastic binding of *Staphylococcus aureus* to hydrophobic surfaces - supplementary material

Nicolas Thewes,[a] Alexander Thewes,[b] Peter Loskill,[a†] Henrik Peisker,[c] Markus Bischoff,[c] Mathias Herrmann,[c] Ludger Santen[b] and Karin Jacobs*[a]

1 Viability of bacterial probe

Fig. S1 depicts a viable bacterial probe (green) manufactured according to the described method and investigated under a fluorescent light microscope using a live/death staining (Life Technologies GmbH, Germany) after a series of force/distance measurements. Random tests of cell viability showed that our whole procedure does not alter the cell viability.

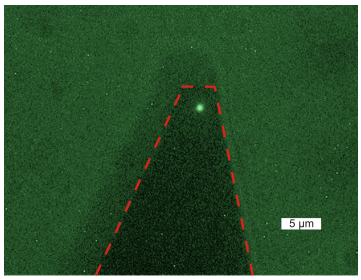

Fig. 1 Fluorescence micrograph (magnification 630x) of a single bacterial probe, after adding a small amount of live/death stain (Life Technologies GmbH, Germany). The cantilever is enframed by dashed red lines to improve visibility.

2 Model details

In our theoretical approach, we implement a reductionist model of the experimental setup.

The cantilever is represented as a linear spring with spring constant k_c and untensioned length $l_0^c = 0$. We model the bacterium as a spherical object with radius R. The cell wall macromolecules are also modelled as linear springs. As a key feature of the model we assign random spring constants k_i and, at least in principle, lengths l_0^i to molecule i. The k_i's are identically distributed random variable chosen from the interval $[k_{min}, k_{max}]$. Such a distribution of k_i's is the only way we found to reproduce the shape of the experimental approach curve. For the simulation results given in the paper the l_0^i is the same for all molecules. We considered a total number of N springs, which may be considerably larger than the actual number of cell wall proteins. The first end of the spring is attached to the cell wall and the second one is pointing towards the substratum. The springs are always parallel to the z-axis.

We considered random spring positions on the cell wall. For the purpose of computational efficiency we decorated only the half of the sphere which is opposite to the substratum, i.e. we restrict the possible z-coordinates of the spring's position at the cell wall to the interval [-R,0] *

In the following we use the coordinate system which is illustrated in Fig. S2: The substratum is located in the x-y-plane at $z = 0$ and the cantilever starts at position $(0, 0, z_c = z_{max})$. The bacterium is attached to the cantilever and its initial distance to the substratum is given by $d = z_{max} - 2R$.

The binding potential between substratum and macromolecules was chosen as a square well potential with a depth of $-14 * k_b * T$ and a range of $3\,nm$. Explicitely, V(z) reads as follows:

$$V(z) = \begin{cases} 0 & z > 3\,nm \\ -14 * k_b * T & 0 < z < 3\,nm \\ \infty & z < 0 \end{cases} \quad (1)$$

According to this, springs that are closer to the substratum than 3nm are considered as bounded, so the energy for a bounded spring is $E_s = \frac{1}{2}(l_i - l_0^i)^2 - 14 k_b T$ and for unbounded springs $E_s = \frac{1}{2}(l_i - l_0^i)^2$, where l_i determines the actual length of spring i.

The following table summarizes the standard parameter setup, which was used for the results in our study.

* Here we give the cell wall position relative to the center of the bacterium.

[a] Experimental Physics, Campus E2 9, Saarland University, D-66123 Saarbrücken, Germany. E-mail: k.jacobs@physik.uni-saarland.de
[b] Theoretical Physics, Campus E2 6, Saarland University, D-66123 Saarbrücken, Germany
[c] Institute of Medical Microbiology and Hygiene, Saarland University, D-66421 Homburg/Saar, Germany
† Present address: Dept. of Bioengineering and California Institute for Quantitative Biosciences (QB3), University of California at Berkeley, Berkeley, California 94720, USA

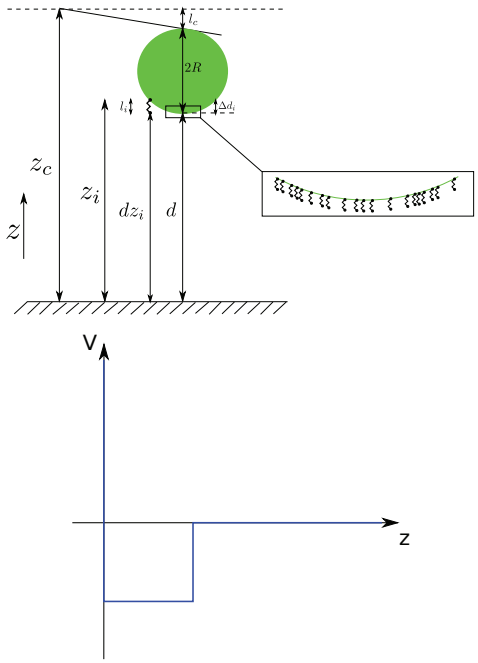

Fig. 2 Upper figure: Schematic picture of the model. Lower figure: Binding potential for the surface macromolecules, the depth of the potential is -14∗k_BT and the width is 3 nm.

Number of proteins N	8000
Untensioned length of proteins l_0^i	30 nm
Maximum spring constant of proteins k_{max}	0.001 nN/nm
Minimum spring constant of proteins k_{min}	$5*10^{-6}$ nN/nm
Untensioned length of the cantilever l_0^c	0 nm
Spring constant of the cantilever	0.03 nN/nm
Radius of the bacterium	500 nm
Range of binding potential	3 nm
Depth of binding potential	$-14*k_b*T$

These values were chosen since they give a good agreement between experiment and simulations.
We carefully checked the influence of changes in the parameters on the simulation results. We found that variations of the parameters only result in quantitative changes of the received curves, the principle shape was preserved. For example, a higher number of proteins or a deeper potential lead to a larger adhesion force, decreasing the untensioned length of proteins results in a smaller snap-in separation.

Given that n springs are bound to the substratum, the equilibrium position of the bacterium, which determines the extension of the bound springs, can be calculated analytically.
The total energy of the system consists of two parts, the bending energy of the cantilever and the energy of the stretched springs:

$$E = \frac{1}{2}\sum k_i(l_i - l_0^i)^2 + \frac{1}{2}k_c(l_c - l_0^c)^2 \tag{2}$$

where the sum runs over all bounded springs.
We suppressed the contribution from the binding potential since this is constant for bounded springs and plays no role when calculating the equilibrium position.

By considering the boundary conditions of the model, one can rewrite the energy as a function of a single variable, which we chose to be the distance of the bacterium to the substratum d.
The position z_c of the cantilever is given by

$$z_c = l_c + 2R + d \tag{3}$$

with l_c = actual deflection of the cantilever. The z-coordinate z_i of the first end of spring i is

$$d + \Delta d_i = z_i = dz_i + l_i \tag{4}$$

with dz_i = distance of the second end of the spring to the substratum, Δd_i = distance of the first end of the i-th spring to the plane $z = d$.
The latter quantity is given by

$$\Delta d_i = R - \sqrt{R^2 - (x_i^2 + y_i^2)} \tag{5}$$

with x_i, y_i = x,y-coordinate of the first end of the i-th spring.

Putting all this together we can write the energy of the system as follows:

$$E = \frac{1}{2}\sum k_i(d + \Delta d_i - dz_i - l_0^i)^2 + \frac{1}{2}k_c(z_c - d - 2R - l_0^c)^2 \tag{6}$$

This form contains only a single variable d, all other quantities are given parameters of the system configuration. Therefore, the equilibrium distance d of the bacterium to the substratum for a given cantilever position and configuration of bound springs reads as:

$$d_E = \frac{k_c(z_c - 2R - l_0^c) - \sum k_i(\Delta d_i - dz_i - l_0^i)}{k_c + \sum k_i} \tag{7}$$

All in all we have three different kinds of degrees of freedom in the model. First, the position of the cantilever, which is updated following the given experimental protocol. Second, the position of the bacterium, which we consider as the equilibrium position for a given configuration of bound springs and position of the cantilever, and, third, the stochastic simulation of the springs, which we carry out at room temperature using standard Metropolis algorithm.

Precisely, our simulation approach, which is closely related to the experimental setup consists of the following steps:

1. Move the cantilever by an amplitude which corresponds to one hundredth of the step length in experiment.

2. Perform 200 MC-sweeps for the springs and the bacterium,

where a sweep is given by

(a) N spring-updates:

i. Chose a spring i and a random displacement r.

ii. Move the second head of spring i by distance r.

iii. If allowed, meaning $dz_i > 0$ and $l_i > 0$, accept the move according to Metropolis algorithm.

iv. Go back to (i) until N spring-updated are completed

(b) Update of the bacterium position

3. Go back to one, after every hundredth step of the cantilever, read out the configuration of the system

Retraction starts if the given force trigger is reached.

3 Protein-modifying treatment

Supplementary material to Fig. 6

To evaluate the macromolecular origin of bacterial adhesion, bacteria have been treated by pronase E and glutaraldehyde. In Fig. S3 force/distance curves of approach (blue) and retraction part (red) are shown, whereas in Fig. 6 only the approach parts have been depicted for clarity. Experimental parameters were optimized to study the approach process. Therefore, relatively soft cantilevers were used. Curves a) and c) are before treatment, curve b) is recorded after pronase E application and curve d) is taken after glutaraldehyde action. For the cases shown, the maximum adhesion forces of the two bacteria of the reference curves are that large that they cannot be evaluated in detail. However, the order of magnitude can roughly be estimated by the extrapolation of the gradients of the retraction curves: For both, it is in the range between -20 nN and -30 nN. Clearly, after any of the protein-modifying treatments, the maximum adhesion force is greatly reduced.

The same holds true for the simulated force/distance curve using the rough model, with only one stiff spring, for describing the effect of the protein-modifying treatment (cf. Fig. S4). Also in the simulated force/distance curve the adhesion force is greatly reduced by using only one stiff spring (Fig. S4b) as compared to a distribution of soft springs (Fig. S4a).

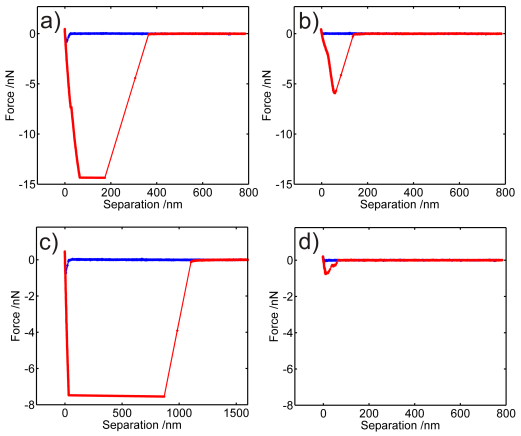

Fig. 3 Force/distance curves of approach (blue) and retraction (red) parts of two individual bacterial probes for testing the influence of enzymatic/chemical treatment on the bacterial adhesion process. Curves in a) and c) each depict the native state, the curve in b) shows the adhesion after pronase E treatment and curve d) after glutaraldehyde action.

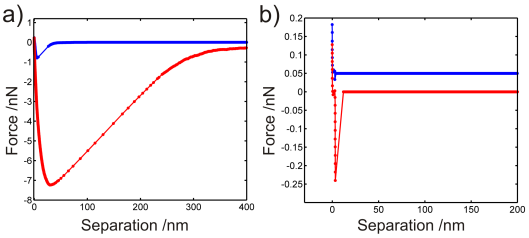

Fig. 4 Simulated force/distance curve with approach (blue) and retraction (red) part. a) MC model force/distance curve using the parameter setup described above and b) simulated force/distance curve that reflects the protein-modifying treatment by using only one stiff spring (for clarity, the blue curve has been shifted by +0.05 nN).

Addendum V - Adhesion of *Staphylococcus aureus* to abiotic surfaces

Authors: N. Thewes[1], A. Thewes[2], A. Peschel[3], M. Bischoff[4], and K. Jacobs[1]

[1] Department of Experimental Physics, Saarland University, 66041 Saarbrücken, Germany.
[2] Department of Theoretical Physics, Saarland University, 66041 Saarbrücken, Germany [3] Cellular and Molecular Microbiology Division, Interfaculty Institute of Microbiology and Infection Medicine, University of Tübingen, Tübingen 72076, Germany [4] The Institute of Medical Microbiology and Hygiene, Saarland University, 66421 Homburg/Saar, Germany.

in preparation

Author contributions:
Experiments were conceived and designed by N. Thewes and K. Jacobs. AFM experiments were performed by N. Thewes. Simulations were performed by N. Thewes. Simulations were directed by A. Thewes. Data was analyzed by N. Thewes. The article was written by N. Thewes, and K. Jacobs. A. Peschel provided the mutant cells. Research was directed by M. Bischoff and K. Jacobs.

Abstract - The adhesion of *Staphylococcus aureus* to abiotic surfaces is crucial for the spreading of infectious diseases. This study provides unique insights into the adhesion process of pathogenic *S. aureus* to abiotic substrates by combining high throughput single cell force spectroscopy measurements with genetically modified *S. aureus* cells and computer simulations of a model describing bacterial adhesion. A comparison between simulated and experimental force/distance curves reveals that bacterial adhesion on abiotic substrates solely relies on tethering of bacterial surface polymers. On hydrophobic substrates, adhesion is dominated by the excessive binding of proteins via the hydrophobic interaction, while on hydrophilic substrates, adhesion is much weaker and mediated by only few but strongly bound bacterial surface polymers. Single cell force spectroscopy revealed that pathogenic *S. aureus* adheres much stronger on abiotic substrates than apathogenic *S. carnosus* and that different bacterial cells even of one and the same culture may exhibit strongly varying adhesion properties. This 'individuality' is a result of the cell wall polymer composition that is unique for each individual cell. Furthermore, our results show that proteins that are covalently bound to the bacterial cell wall strongly interact with hydrophobic substrates, while their contribution to the overall adhesion force is small on hydrophilic substrates.

1 Introduction

Staphylococcus aureus is an opportunistic pathogen associated with different community and hospital acquired infections [Low1998]. The organism is a major cause of implant related infections [Cha2001, Myl2001, Dar2004]. One reason for the high infectivity is the ability of *S. aureus* to adhere strongly to various types of surfaces [Hal2004, Yon2007, Lin2011, The2015b]. AFM force spectroscopy with single bacterial probes ('single cell force spectroscopy') is the state-of-the-art method in quantitative bacterial adhesion research [Kan2009, The2014, Duf2015, Agu2015b, The2015b]. Different force spectroscopy studies investigated the adhesion properties of *S. aureus* focusing on the interaction to protein covered, conditioned surfaces [Mit2008, Ovc2012, Her2015]. In this study, we present an analysis of the fundamental binding properties of *S. aureus* on abiotic substrates, i.e. substrates without any surface conditioning layer. Our research is based on single cell force spectroscopy with *S. aureus* mutants exhibiting changes in surface adhesin properties and computer simulations of the force spectroscopy process. Adhesion forces were investigated on very hydrophilic and strongly hydrophobic, Si wafer-based substrates with an unprecedented high sample size of more than 150 single bacterial cells. In a reverse engineering approach, the fundamental properties of *S. aureus* adhesion were captured in numerical simulations to reveal basic binding mechanisms.

2 Experimental

2.1 Preparation of the substrates

Si wafers are the basis of the hydrophilic as well as the hydrophobic substrates used in this study. The Si substrates feature a native silicon oxide layer of 1.7(2) nm (the number in parentheses denotes the error of the last digit) and a rms surface roughness of 0.09(2) nm [Bel2008]. Cleaning the Si wafers thoroughly results in a hydrophilic substrate with an advancing water contact angle of 5(2)°, a surface energy 64(1) mJ m^{-2} and a zeta-potential of -104.4(1) mV at pH 7.3 [Bel2008]. The hydrophobic substrate is prepared by covering Si wafers with a self-assembled monolayer of octadecyltrichlorosilane (OTS) according to a standard protocol [Les2015]. The result is a CH_3-terminated substrate with an advancing (receding) water contact angle of 111(1)° (107(2)°), a surface energy of 24(1) mJ m^{-2} [Les2015] and a zeta-potential of -80.0(1) mV [Bel2008]. In depth information about the substrate preparation can be found in ref. [The2014].
Both substrates were immersed into phosphate-buffered saline (PBS, pH 7.3, ionic strength 0.1728 mol/l at 20 °C) and were glued next to each other in order to enable force spectroscopy experiments with the same living bacterial cell on both substrates. That way, changes in adhesion behavior can be linked directly to changes in substrate chemistry.

2.2 Bacterial strains and growth conditions

Adhesion studies were performed with *Staphylococcus aureus* strain SA113. This biofilm-positive laboratory strain is a common platform to study cell wall macromolecules of *S. aureus* [Max1986, Pes1999, Wei2005, Bur2013]. For an in-depth analysis of the cell wall polymer contribution to the staphyloccocal adhesion process, the adhesion of SA113 wild type cells on abiotic substrates was compared to mutant cells featuring the following changes in cell wall polymer properties:

- *S. aureus* SA113 Δdlt: whose lipo- and wall teichoic acids lack d-alanin sidegroups [Pes1999].
- *S. aureus* SA113 ΔtagO: lacking the cell wall anchored wall-teichoic acids [Wei2005].
- *S. aureus* SA113 ΔsrtA: deficient in the enzyme sortase that catalyzes the covalent linkage of proteins to the cell wall [Wei2008].

As an additional comparison, adhesion measurements with apathogenic *Staphylococcus carnosus* cells were performed [Sch1982, Goe1990, The2014].
All bacterial cultures were prepared the same way starting the day before the force spectroscopy experiments: An overnight culture was prepared in 5 ml tryptic soy broth (TSB) medium and incubated at 37 °C. The next day, 40 μl of the overnight culture were transferred into 4 ml of fresh TSB medium and incubated for another 2.5 hours to obtain exponential phase cells. Subsequently, 0.5 ml bacterial solution were diluted 1:1 with PBS and washed four times, using 1 ml PBS each, to remove extracellular material.

2.3 Single cell force spectroscopy

Single bacterial probes were prepared according to a recently published protocol [The2015a]. Briefly, tipless cantilevers (MLCT-O, Bruker, Billerica, MA, USA) were covered with a thin layer of polydopamin by polymerization of dopamine hydrochloride (99%, Sigma-Aldrich). Single bacterial probes were manufactured by attaching a single viable cell to a functionalized cantilever using a micromanipulator, care was taken that cells never dry out during preparation or force measurements.
Force spectroscopy measurements with single bacterial probes were conducted under ambient conditions in PBS using a Bioscope Catalyst (Bruker, Billerica, MA, USA). Force/distance curves were performed using parameter values that correspond to similar studies [Bea2013a, Zen2014, The2014, Her2014]. The ramp size was set to 800 nm, the force trigger was 300 pN and retraction speed was 800 nm/s. Approach speed was 800 nm/s for force/distance measurements without surface delay and 100 nm/s if a surface delay of 5 s was applied. Surface delay times of a few seconds are a common choice to study the influence of the contact time on bacterial adhesion processes [Bea2013a, Zen2014, Her2014]. Measurements without surface delay yield a contact time below 0.5 s [Bea2013a, The2014]. Two types of force spectroscopy experiments were done and accordingly, this study is divided into two parts:

- **Part 1** Measurements with one and the same *S. aureus* wild type cell on a hydrophilic and a hydrophobic substrate with surface delay times of zero and five seconds.

- **Part 2** Measurements with different cells of one species (*S. carnosus*, *S. aureus* wild type and mutant cells) on either the hydrophilic or the hydrophobic substrate. On hydrophilic substrates contact times of zero and five seconds were applied.

The series of measurements in **Part 1** enable the investigation of the influence of the surface hydrophobicity on the adhesion mechanisms of *S. aureus*. In **Part 2**, the series of measurements were conducted to identify differences between different bacterial species by comparing a large number of single bacterial probes. Thereby, per bacterial probe and parameter set at least 50 force/distance curves were recorded.

3 Results and discussion

Part 1

Adhesion without surface delay. Consecutive force/distance measurements with one and the same bacterial probe were performed on hydrophilic and hydrophobized Si wafers. On both substrates, the retraction curves indicate the consecutive stretching and rupturing of tethered macromolecules [Hel2008, Hor2010], i.e. on both substrates, bacterial adhesion relies on the binding of bacterial surface polymers, see fig 1.

Adhesion forces differ by two orders of magnitude between hydrophilic (F_{adh}=0.23(30) nN) and hydrophobic (F_{adh}=35.2(9) nN) substrates, fig. 1. Van der Waals and electrostatic properties differ only slightly between both subtrates. Hence, the hydrophobic interaction strongly influences the adhesion of *S. aureus*. Similar results have been presented for different bacterial species, including *S. carnosus* an apathogenic relative of *S. aureus* [Bea2013a, The2014, Sul2015]. The strong adhesion to hydrophobic substrates is caused by the extensive binding of bacterial surface proteins via hydrophobic sidegroups [Bea2013a, The2014]. In contrast, on hydrophilic substrates, tethering of macromolecules relies on electrostatic and van der Waals forces or on directional hydrogen-bonds [Juc1997, Lec2001].

The shapes of the force/distance curves also exhibit strong differences on hydrophilic and hydrophobic substrates, see fig 1: i) Individual force/distance curves of one bacterial probe on the hydrophobic substrate all look nearly the same, see fig. 1B. On the hydrophilic substrate, however, the shapes of force/distance curves fluctuate strongly between different curves of one bacterial probe, see fig. 1A. ii) Force/distance curves on hydrophilic substrates have a 'spiky' shape and show distinct peaks that correspond to the stretching and rupturing of surface polymers [Low2001, ElK2014]. These peaks are well described by the worm-like chain (WLC) model [Mar1995, Rub2003], see fig. 1A first curve. In contrast, on hydrophobic substrates force/distance curves are very smooth and feature a linear increase in force upon retracting the bacterium from the surface, see fig. 1B. Close to the maximum force value, the gradient of the force/distance

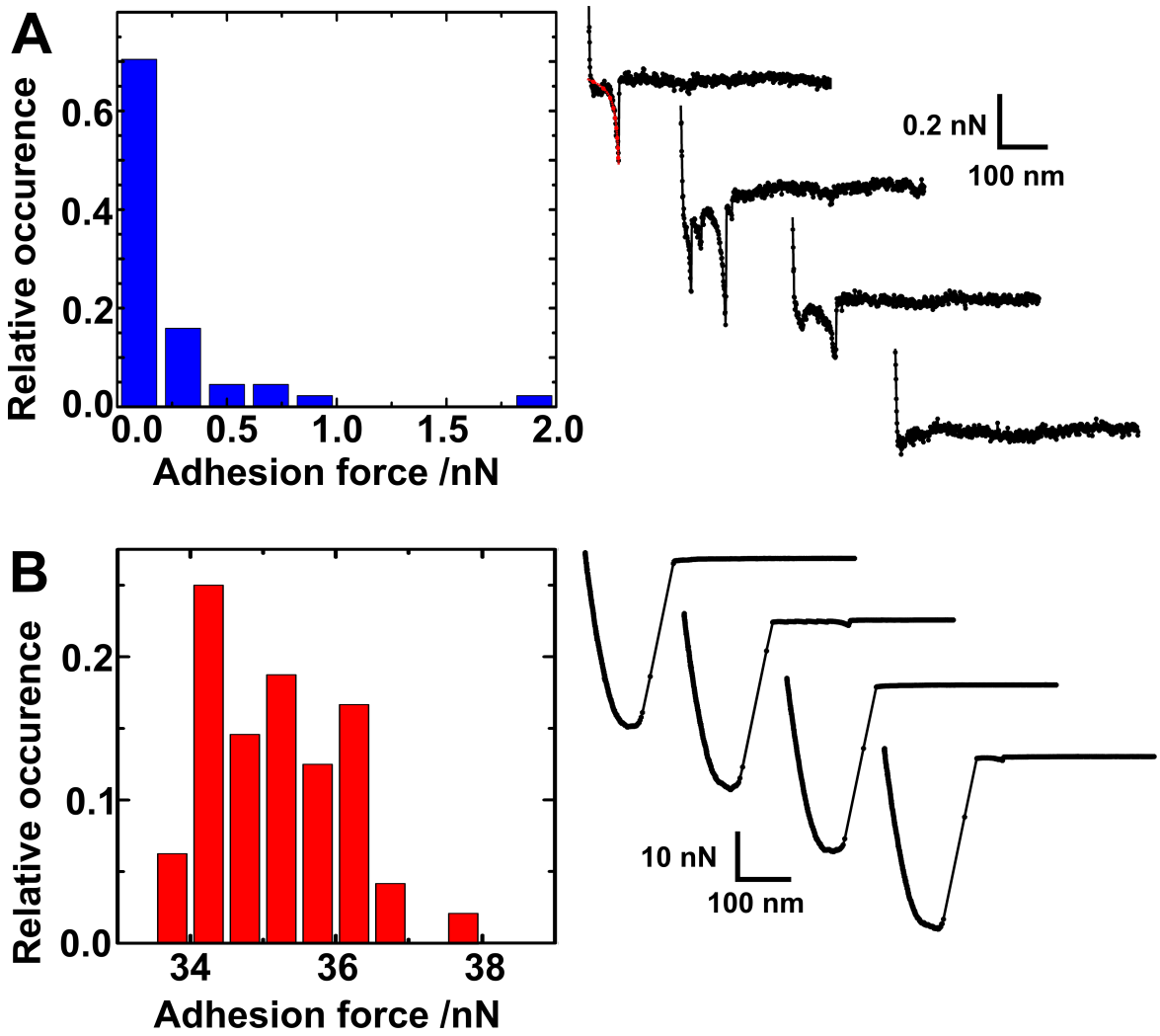

Figure 1: Adhesion of *S. aureus* on abiotic surfaces (without surface delay). One and the same bacterial probe was used to perform 50 force/distance curves each on a hydrophilic A) and a hydrophobic substrate B). The figures depict the distribution of adhesion forces (left) as well as 4 exemplary retraction curves (right) for each substrate. The dashed red line in the first exemplary curve in A) shows a fit of the worm-like chain model [Mar1995] to the experimental data. The fit yielded a Kuhn length of 0.2 nm and a contour length of 79 nm. Note the different force axis scales in A) and B). Forces are displayed as absolute values.

curves decreases and around the maximum force, a force plateau may be observed. On hydrophobic substrates, polymer stretching signals are only frequently observed in the back of the force/distance curves.

Adhesion with 5 s surface delay. Bacterial adhesion forces increase for prolonged contact, in the range of a few seconds, between bacterial cells and substrates [Bea2013a, Her2013, Zen2014, The2014, Agu2015a]. In order to investigate the adhesion of *S. aureus* to abiotic surfaces in more detail, we studied the effect of the contact time on the adhesion of *S. aureus* on hydrophilic and hydrophobic substrates. Therefor, we used the same bacterial cell as in fig. 1 and applied an additional surface contact time of 5 s.

The relative increase of adhesion forces was much more pronounced on the hydrophilic compared to the hydrophobic substrate, see fig. 2. Force/distance measurements with 5 s of surface delay revealed, that the mean adhesion force on the hydrophilic substrate increased, by a factor of 5.5 to 1.26(66) nN, while on the hydrophobic substrate the mean adhesion force increased to 47.4(16) nN, which yields a factor of only 1.3 compared to zero seconds surface delay.

The basic characteristics concerning the shape of the force/distance curves do not change. The shapes of the force/distance curves on hydrophilic and hydrophobic substrates described for zero seconds of surface delay hold true for 5 s of surface delay. Only, on the hydrophilic substrate more characteristic polymer stretching signals and peaks occur in the force/distance curves with 5 s of surface delay.

Summary of the present results. To deepen the understanding of the above results and to detail *S. aureus* adhesion to abiotic surfaces, we tried to capture the fundamental characteristics of the experimental force/distance curves in simulated force/distance curves using a simple model to describe the bacterial adhesion process. We start with a recapitulation of the experimental results in part 1 of our study:

- Roughly two orders of magnitude higher adhesion forces on hydrophobic surfaces compared to hydrophilic ones.
- The shape of the force/distance curves on hydrophobic substrates is very smooth and characteristic in depth and width. The form is very reproducible for each individual bacterial probe.
- The shape of the force/distance curves on hydrophilic substrates is very spiky due to the presence of individual characteristic polymer stretching signals. Consecutive force/distance curves exhibit strong fluctuations in number and depth of individual peaks.
- Adhesion on hydrophilic substrates depends strongly on the surface contact time.

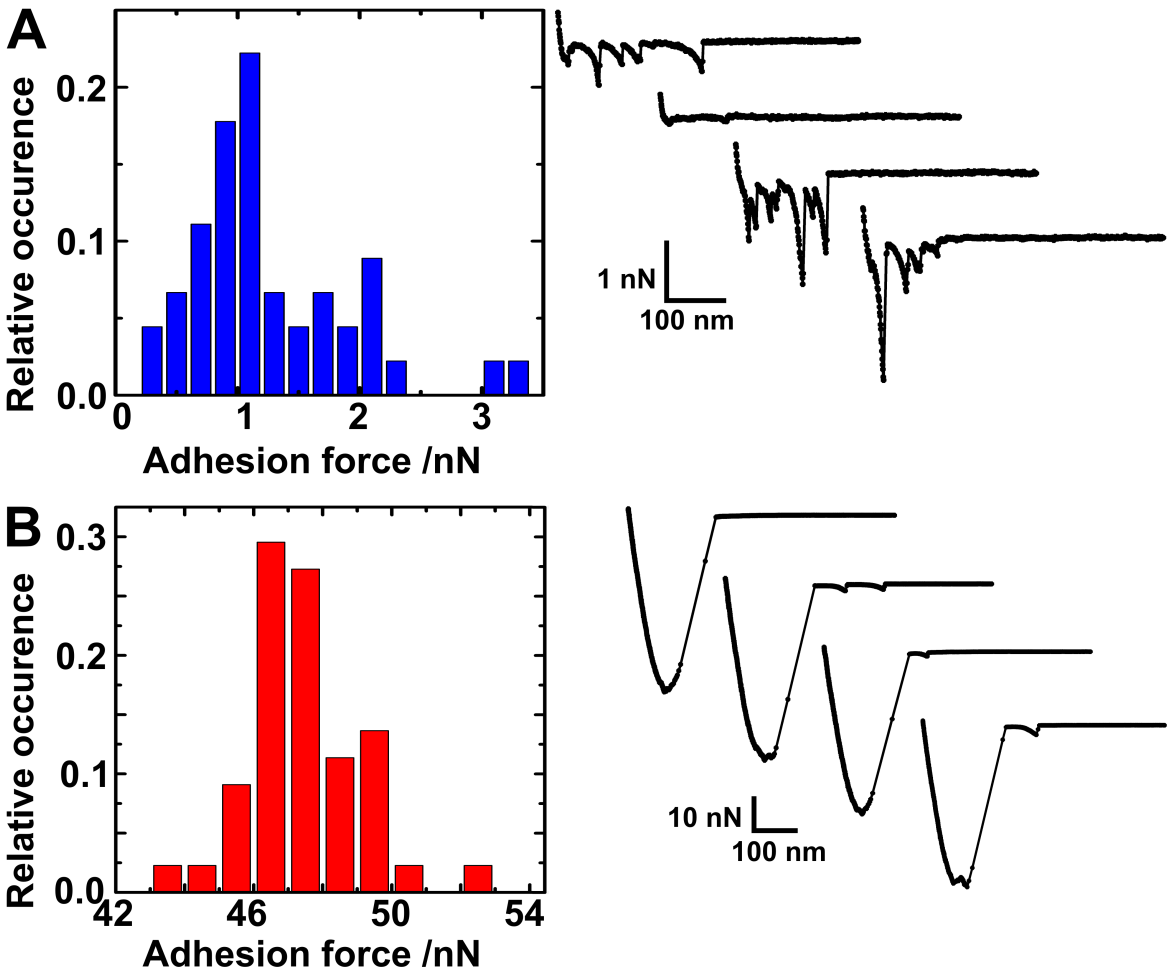

Figure 2: Adhesion of *S. aureus* on abiotic surfaces with a surface delay of 5 s. One and the same bacterial probe was used to perform 50 force/distance curves each on a hydrophilic A) and a hydrophobic substrate B). The figures depict the distribution of adhesion forces (left) as well as 4 exemplary retraction curves (right) for each substrate. Note the different force axis scales in A) and B). Forces are displayed as absolute values.

Model and Simulation

The model. The presented force/distance curves indicated that cell wall polymers exhibit major influence in bacterial adhesion and in order to identify basic mechanisms of *S. aureus* adhesion, we developed a idealized model of the bacterial adhesion process. In our model a bacterium is an undeformable sphere that is uniformly covered with elastic polymers [The2014, The2015b]. The behavior of polymer chains is well documented (e.g. see [Rub2003]). In a good solvent, as assumed for cell wall macromolecules in PBS buffer, polymers may be described by the worm-like chain (WLC) model [Rub2003]. The polymers are subject to thermal fluctuations and coming in reach of a surface, they may attach to the surface - in our model - via a square potential. To account for the spatial extend of real cell wall polymers, a minimum length l_0 is defined, below that, a polymer chain causes repulsion according to Hooke's law (see eq. 1). If the polymer is stretched above the threshold length l_0, the potential energy is calculated according to the WLC approach [Mar1995]:

$$w_{polymer}(l) = \begin{cases} \frac{(l-l_0)^2}{b}\left(\frac{1}{M} + \frac{1}{2(M-(l-l_0))}\right) & \text{if } l \geq l_0 \\ \frac{3}{2Mb}(l-l_0)^2 & \text{if } l < l_0 \end{cases}, \tag{1}$$

where the energy of the polymer is in units of k_bT with Boltzmann constant k_b and temperature T. The contour length of the polymer is denoted as M and b is the *Kuhn length* of the polymer. The spring constant in the Hooke regime is calculated according to the Gaussian approximation for small extensions of ideal polymers [Rub2003]. Note that this energy function as well as its derivative are continuous functions.
The described model is analyzed using a Monte Carlo algorithm. The equilibrium position of the cantilever/bacterium/surface system is calculated using the bisection method. The bisection algorithm is a common numerical method to approximate the zero of a function. Thereby, the zero is approached by consecutively decreasing the length of the interval that contains the zero of the respective function.
Free parameters of our model are the mechanical properties of the polymers, i.e. M and b, as well as the polymer surface density and the depth of the square binding potential. The threshold length l_0 is chosen to be $2 \cdot \sqrt{b \cdot M/6}$, which is twice radius of gyration of an ideal linear polymer [Rub2003]. This choice is a reasonable approach for a threshold size below that a polymer acts against further compression.
According to the 'ideal chain' model characterizing basic properties of linear polymer chains, we term our model 'ideal cell' model, since we make use of spherically and uniformly distributed ideal polymers to describe the adhesion process of bacterial cells.

The parameters of the simulation. To achieve an optimal match between experimental and simulated force/distance curves, we extracted the mechanical properties of polymer stretching signals from experimental force/distance curves using the WLC model [Mar1995]. Nevertheless, a perfect match between experimental and simulated curves is fairly possible, as mechanical and physical properties of bacterial cells and its surface polymers stay largely unknown to date. However, the fundamental shape of the experimental force curves is reproducible in simulated force curves using the described model and polymer densities of $2.2 \cdot 10^{-5}\,\mathrm{nm}^{-2}$ and $3.2 \cdot 10^{-2}\,\mathrm{nm}^{-2}$. That is, one polymer per $4.5 \cdot 10^4\,\mathrm{nm}^2$ respectively $31.3\,\mathrm{nm}^2$. We choose contour lengths uniformly distributed

between 60 nm and 300 nm as well as Kuhn lengths uniformly distributed between 0.072 nm and 0.36 nm. The binding potential had a depth of -18 k_bT respectively -54 k_bT and a range of 3 nm. The radius of the simulated bacterium was 500 nm.

Experimental and simulated force/distance curves. Figure 3A opposes experimental and simulated force/distance curves. Using a protein density of $2.2 \cdot 10^{-5}\,\mathrm{nm}^{-2}$ and a square potential of -54 k_bT results in the effective binding of less than ten surface polymers. The result is a simulated force/distance curve with an adhesion force of roughly 0.4 nN that exhibits a very spiky shape where distinct WLC profiles are visible. By increasing the protein density to $3.2 \cdot 10^{-2}\,\mathrm{nm}^{-2}$ and decreasing the potential to -18 k_bT the adhesion force rises to roughly 33 nN and the corresponding force/distance curve exhibits a very smooth shape with a decreasing gradient towards the maximum force.
Figure 3B shows simulated force/distance curves for different depths of the square binding potential and a protein density of $3.2 \cdot 10^{-2}\,\mathrm{nm}^{-2}$. The adhesion force decreases for decreasing absolute values of the potential energy. However, the shape of the force/distance curves does not change much, rather the curves exhibit a certain self-similarity.

Different numbers of tethering cell wall polymers reproduce the experimental results. Our model is able to reproduce the basic shapes and differences of the experimental force/distance curves, see fig. 3A. The transition between high adhesion on hydrophobic and low adhesion on hydrophilic substrates was modeled by decreasing the polymer density from $3.2 \cdot 10^{-2}\,\mathrm{nm}^{-2}$ to $2.2 \cdot 10^{-5}\,\mathrm{nm}^{-2}$ and at the same time increasing the potential from -18 k_bT to -54 k_bT. The simulated low adhesion curves that reflect adhesion on hydrophilic substrates, also show the spiky shape of the experimental force/distance curves. These spikes are a result of the stretching of polymer chains that are anchored on the bacterium with one end and bound to the surface with the other end.
In contrast, the simulated high adhesion force curves that illustrates adhesion on hydrophobic substrates, reproduce the smooth shape of the experimental force distance curves, as well as the force plateau around the maximum force value. The smooth shape is a result of the large number of bound polymers, that suppresses the stretching signals of individual polymers. Towards the maximum force, more and more polymers detach from the surface, which causes the gradient of the force/distance curve to decrease. In the region of the maximum force, the load of detaching polymers is shared among the still attached polymer chains in such a way, that the overall force between cell and substrate is almost unchanged (force plateau).

Smaller polymer binding potentials are not able to reproduce the experimental results. In principle, smaller adhesion forces may also correspond to lower binding potentials between bacterial cell wall polymers and a surface, while the protein density stays constant. Hence, to exclude that a smaller binding potential causes different adhesion forces on hydrophilic and hydrophobic substrates, we simulated force/distance curves using the high protein density ($3.2 \cdot 10^{-2}\,\mathrm{nm}^{-2}$) and different depths of the square potential, see fig. 3B. Although, it is possible to reproduce the small adhesion forces of bacterial cells on hydrophilic substrates using this approach, it is not possible to reproduce the spiky shape of the experimental force/distance curves. The other way around, it is also not possible to produce simulated force/distance curves with high adhesion forces and very smooth shapes by using the small protein density ($2.2 \cdot 10^{-5}\,\mathrm{nm}^{-2}$) and increasing the binding potential (data not shown).

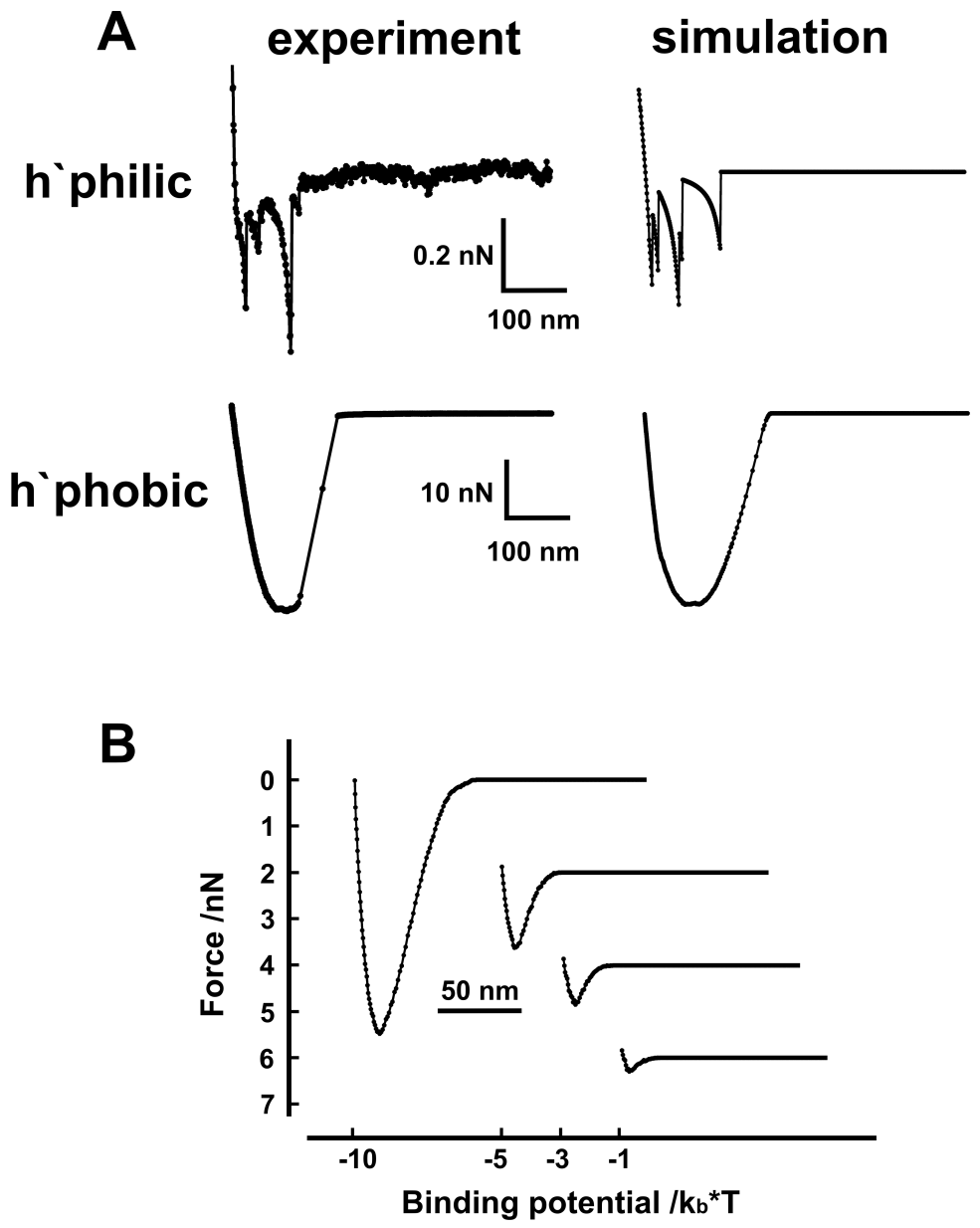

Figure 3: Retraction part of representative experimental force/distance curves and simulated force/distance curves of the described model. The experimental force/distance curves are the second curve (h'philic) and the first curve (h'phobic) of fig. 1A and B. Simulated force/distance curves were calculated using two different polymer densities of $2.2 \cdot 10^{-5}\,\mathrm{nm}^{-2}$ (h'philic) and $3.2 \cdot 10^{-2}\,\mathrm{nm}^{-2}$ (h'phobic) as well as different square potentials of -54 k_bT (-18 k_bT) for the hydrophilic (hydrophobic) case. A comparision between experimental and simulated force/distance curves is shown in A). Simulated force/distance curves with different binding potentials and a fixed protein density ($3.2 \cdot 10^{-2}\,\mathrm{nm}^{-2}$) are shown in B). Force values are in absolute numbers.

Adhesion of *S. aureus* to abiotic substrates; what did we learned so far? Differences in the adhesion of *S. aureus* on hydrophilic and hydrophobic substrates are mainly caused by different numbers of tethering bacterial surface polymers. That way, the experimental results concerning adhesion forces and curve shapes may be explained with regard to the simulations: i) Large adhesion forces correspond to large amounts of tethered surface polymers. A high number of tethering surface polymers decreases the load on each polymer, thus decreases the probability for each polymer to detach from the surface. The result is a high adhesion force. Vice versa, small adhesion forces correspond to low numbers of tethered polymers. ii) At the same time, a high number of tethering surface polymers suppresses stochastic fluctuations and causes a very reproducible and smooth curve shapes without characteristic polymer stretching signals. In contrast, a low number of tethering polymers on hydrophilic substrates produces force/distance curves where individual polymer stretching is visible and where curve shapes (number and depths of individual peaks) fluctuate strongly.

What causes different amounts of tethering surface polymers? On hydrophobic substrates polymer (protein) tethering is mediated by the hydrophobic interaction [VanOss2006, Isr2011, Bea2013a, The2014]. Van der Waals and electrostatic interactions are usually at least one order of magnitude weaker than the hydrophobic interaction [VanOss2006, Isr2011]. Hence, regarding the high potential in the simulations that was necessary to reproduce the experimental low adhesion force/distance curves, polymer binding on the hydrophilic substrates is most likely a result of hydrogen bond formation. A single hydrogen bond has a typical strength of 5-10 k_bT [Juc1998, Isr2011], therefore, it might be speculated that several hydrogen bonds per polymer cause tethering on hydrophilic substrates.
The low amount of tethering polymers on the hydrophilic substrate, that causes low adhesion forces, may have two reasons: i) The bacterial surface polymers that mediate adhesion to hydrophilic substrates and the bacterial surface polymers that mediate adhesion to hydrophobic substrates are not the same. Then, the polymers that cause adhesion to hydrophilic substrates could be less numerous (smaller density) on the bacterial surface. ii) The formation of hydrogen bonds between bacterial surface polymers and hydrophilic substrates is less likely than the tethering of proteins via the hydrophobic interaction.
A combination of the two reasons is possible and further improvements of our model will help to distinguish between both. It should be mentioned that the large increase of adhesion forces on hydrophilic substrates with prolonged contact time is a hint towards reason ii) because obviously, a reservoir of additional bacterial surface polymers that may bind to hydrophilic substrates exists.

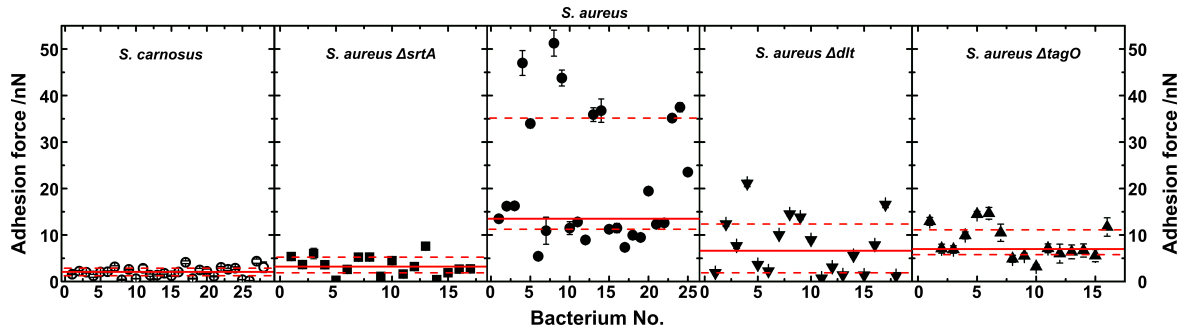

Figure 4: Adhesion forces of individual *S. carnosus* cells as well as *S. aureus* wild type and mutant cells to hydrophobized Si wafers. Each point in the figure depicts the mean adhesion force and the standard deviation of an individual cell with at least 50 (*S. aureus* strains) or at least 30 (*S. carnosus*) force/distance curves. The red lines show the median (solid line) as well as the first and the third quartiles (dashed lines) of the mean adhesion forces. *S. carnosus* data taken from ref. [The2014].

Part 2

In the second part of this study, we investigate the adhesion of *S. aureus* to abiotic substrates by comparing the adhesion of wild type cells to the adhesion of apathogenic *S. carnosus* cells and to *S. aureus* mutant cells exhibiting changes in surface polymer properties. To identify differences between the strains, we compare the adhesion of a large number of single cells on hydrophilic and hydrophobized Si wafers. On both substrates, we use a surface contact time of zero seconds and additionally, 5 s of surface delay on hydrophilic substrates due to the strong dependence of adhesion forces to hydrophilic substrates on the contact time.

S. aureus adhesion to hydrophobic substrates. Figure 4 depicts the adhesion forces of 25 *S. aureus* wild type cells compared to 28 *S. carnosus* cells, 17 *S. aureus* ΔsrtA cells, 16 *S. aureus* ΔtagO cells and 18 *S. aureus* Δdlt cells to OTS substrates.
Obviously, adhesion forces of different cells of one and the same strain vary significantly. For instance *S. aureus* wild type cells seem to divide into cells that adhere with a force between 5 nN and 25 nN to hydrophobized Si wafers and cells that exhibit higher adhesion forces between 35 nN and 50 nN. Strong variation between adhesion forces of different cells of the same strain have been described earlier and might be called 'individuality' of bacterial cells [Bea2013b, The2014, Van2015]. However, by comparing a relatively large number of individual cells, distinct differences can be identified, see fig. 4: i) On hydrophobic substrates pathogenic *S. aureus* cells (median at 13.5 nN) adhere way stronger than apathogenic *S. carnosus* cells (median at 2 nN). ii) Also *S. aureus* ΔsrtA cells (median at 3.2 nN) exhibit a decreased adhesion capability and adhere only slightly stronger than apathogenic *S. carnosus* cells. iii) TagO (median at 7 nN) and dlt (median at 6.6 nN) mutant cells exhibit similar binding strengths to hydrophobic surfaces, yet adhere significantly weaker as compared to wild type strain cells.

***S. aureus* wild type cells on hydrophobized Si wafers.** *S. aureus* wild type cells adhering to hydrophobized Si wafers cover a huge range of adhesion forces and the force values seem to exhibit

a bimodal distribution. At the moment we are not able to distinguish if this distribution emerges in our measurements by chance and vanishes for larger sample sizes or if the bimodal distribution has a biological reason. From a biological point of view, a possible explanation might be that some cells form a polysaccharides capsule. Several *S. aureus* strains are able to produce capsular polysaccharides and capsules may influence adhesion properties [Wil1983, O'R2004]. However, the capsule is usually produced in late growth phase and as we are using predominantly exponential growth phase cells an influence of capsule polysaccharides in our measurements is highly speculative at the moment. Therefore, further research will be necessary at this point.

***S. aureus* wild type vs *S. aureus* ΔsrtA.** *S. aureus* ΔsrtA cells lack the cell wall anchored proteins, thus features a reduced protein surface density. By assuming that a decreased polymer density results in a decreased number of tethering polymers during the adhesion process (which is reasonable), the smaller adhesion force of *S. aureus* ΔsrtA nicely corroborates the results of part 1 by evidencing the importance of the pure number of tethered polymers for the adhesive strength.

***S. aureus* wild type vs *S. carnosus*.** Two reason may explain the weaker adhesion of apathogenic *S. carnosus* compared to *S. aureus* cells. The smaller adhesion forces may be a result of a smaller density of surface adhesins or the surface polymers of *S. carnosus* are not specialized to adhere on hydrophobic substrates. It is known that *S. carnosus* does not produce a lot of surface adhesins found in *S. aureus* [Goe1990]. However, as hydrophobic sidegroups are a general property of proteins, the smaller adhesion capability of *S. carnosus* is most likely a result of a smaller protein surface density.

***S. aureus* wild type vs *S. aureus* ΔtagO.** *S. aureus* ΔtagO cells lack the wall teichoic acids [Pes1999, Wei2005]. Wall teichoic acids are responsible for the overall negative surface charge of bacterial cells. The hydrophobized Si wafers also feature a negative surface potential [Bel2008]. Hence, a positive effect on adhesion forces due to removal of the wall teichoic acids would agree with considerations concerning simple electrostatics. However, the results point towards an opposite effect: *S. aureus* ΔtagO cells exhibit decreased adhesion forces compared to wild type cells. Bacterial adhesion is stronger influenced by the hydrophobicity of a substrates than by charges [Li2004, The2014] and bacterial adhesion to hydrophobic substrates relies on the binding of surface proteins [Bea2013a, The2014]. Therefore, the different adhesion forces of ΔtagO and wild type cells might implicate that the lacking wall teichoic acids negatively influence the surface density of proteinaceous adhesins which would cause smaller adhesion forces. Another possible reason is that wall teichoic acids directly contribute to the adhesion of *S. aureus* cells to hydrophobic substrates by tethering to the surface.

***S. aureus* wild type vs *S. aureus* Δdlt.** *S. aureus* Δdlt mutant cells lack the positively charged d-alanin groups linked to teichoic acids [Pes1999, Wei2005]. Therefore, dlt mutant cells carry a higher negative surface charge compared to wild type cells. However, as the tagO mutant cells did not show an increased adhesion capability, it is very unlikely that the decreased adhesion of dlt mutants is of electrostatic origin. Rather, if wall teichoic acids can tether to the negatively charged OTS surface (as was proposed in the preceding paragraph to explain the decreased adhesion forces of ΔtagO cells), the positively charged d-alanin groups may play an important role by inducing locally attractive electrostatic interactions. Thus, a direct influence of wall teichoic acids on *S. aureus* adhesion to hydrophobic substrates may explain the decreased adhesion of Δdlt cells (less teichoic acids tether due to a decreased electrostatic attraction) and ΔtagO mutant cells (no wall

teichoic acids at all).
Additionally, if wall teichoic acids are able to tether directly to the OTS substrate, this might explain the bimodal distribution of adhesion forces of *S. aureus* wild type cells to hydrophobic substrates: Perhaps, the weakly adhering wild type cells lack wall teichoic acids (by chance) and, thus, feature adhesion forces in the same range as compared to ΔdIt and ΔtagO cells, see fig. 4.

Finally, the experimental results concerning the influence of teichoic acids on *S. aureus* adhesion to OTS substrates nicely corroborate the results of part 1 by showing that bacterial adhesion can not be explained by looking at simple DLVO interactions between the entire cell and a substrate. Rather, it is necessary to inspect molecular details of the bacterium/surface contact to explain bacterial adhesion.

S. aureus adhesion on hydrophilic substrates. Figure 5 depicts adhesion forces of more than 15 cells of each of the described strains on hydrophilic Si wafers with surface delay times of 0 s and 5 s. With 50 force/distance curves per bacterial probe and surface delay time, at least 750 single adhesion force values condense in each histogram.
Also on hydrophilic Si wafers *S. aureus* wild type cells adhere stronger than apathogenic *S. carnosus* cells no matter of the applied contact time. *S. carnosus* cells do not show any adhesion in more than 60% of the force curves for zero seconds additional contact time. *S. aureus* ΔsrtA cells adhere only slightly weaker to hydrophilic substrates than wild type cells, especially for a surface delay of 5 s. In particular, the difference in adhesion forces between ΔsrtA and wild type cells is significantly smaller compared to hydrophobic substrates, see fig. 5 and fig. 4. *S. aureus* ΔdIt cells adhere weaker than wild type cells to hydrophilic Si substrates and exhibit a similar binding capability as apathogenic *S. carnosus* to hydrophilic substrates. Interestingly, tagO mutant cells show significantly higher adhesion forces, for 0 s and 5 s surface delay, to hydrophilic substrates as compared to *S. aureus* wild type cells.

***S. aureus* wild type vs *S. carnosus*.** The force spectroscopy data may be again interpreted in light of the results of part 1 of the study. Comparing adhesion forces of pathogenic *S. aureus* and apathogenic *S. carnosus* on hydrophilic Si wafers, the large difference may, again, attributed to a smaller polymer density in general or at least a smaller density of polymers specialized to attach to abiotic substrates in the case of *S. carnosus* [Goe1990].

***S. aureus* wild type vs *S. aureus* ΔsrtA.** All the more interesting is the result of the comparison between wild type cells and ΔsrtA cells of *S. aureus* (that lack covalently bound cell wall proteins). On hydrophilic substrates the difference in adhesion forces between both organisms is much smaller compared to hydrophobic substrates. In part 1 of our study we speculated about the origin of the smaller number of tethering bacterial surface polymers on hydrophilic substrates. The latest result is a clear hint that, at least partially, different bacterial surface polymers mediate adhesion to hydrophilic and hydrophobic substrates. Furthermore, our results reveal that surface proteins, covalently linked to the bacterial cell wall, are much less important for the adhesion to hydrophilic substrates than to hydrophobic substrates. This might be an important result for application scenarios.

***S. aureus* wild type vs *S. aureus* ΔdIt & ΔtagO.** The mutant cells without d-alanin residues on teichoic acids (ΔdIt) respectively without wall teichoic acids (ΔtagO) enable the investigation of the influence of charges on the adhesion of *S. aureus*. In contrast to hydrophobic substrates,

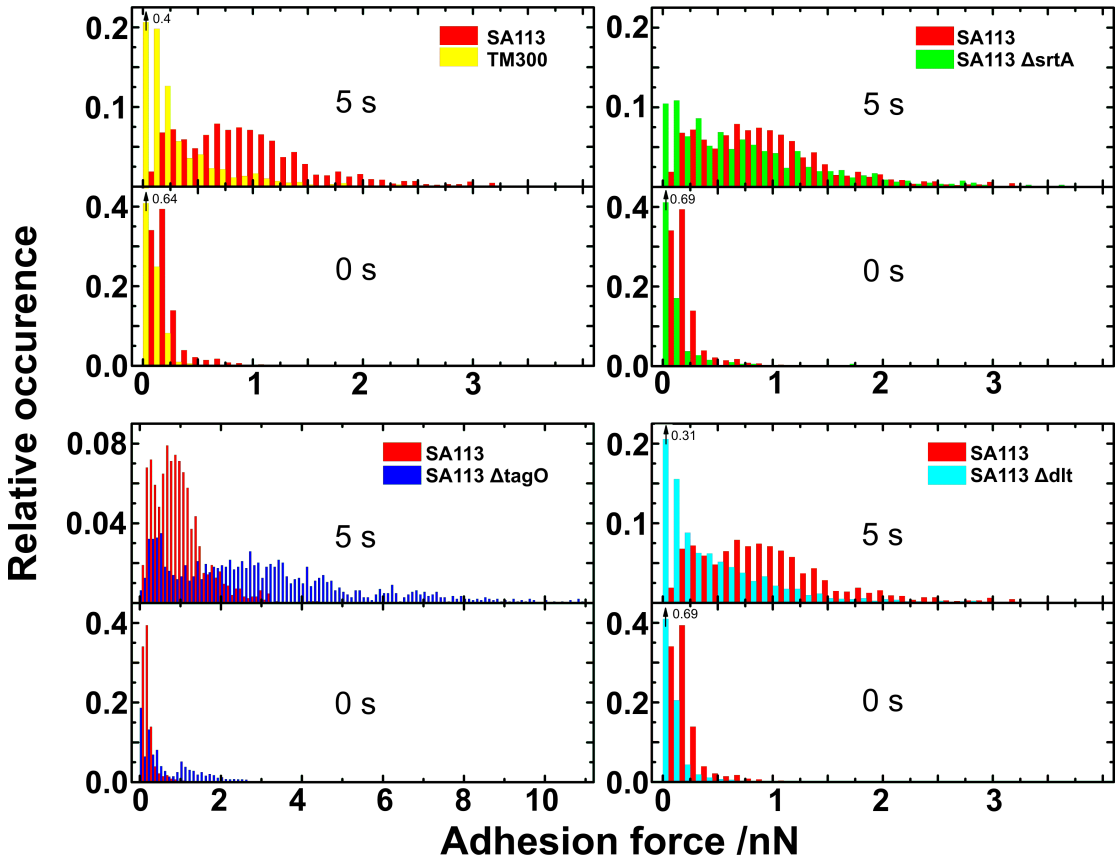

Figure 5: Adhesion forces of *S. aureus* wild type and mutant cells as well as *S. carnosus* cells adhering to hydrophilic Si wafers with a surface delay of 0 s and 5 s, respectively. Each histogram contains data of at least 15 different cells with 50 force/distance curves per contact time and cell.

we find an influence of the bacterial surface charge on the adhesion of *S. aureus* to hydrophilic substrates.
Adhesion forces of dlt mutant cells are smaller compared to wild type cells. This result agrees with the increased negative surface charge of these mutant cells and the consequently stronger electrostatic repulsion between mutant cells and substrate. Yet, adhesion forces of tagO mutant cells on hydrophilic substrates strongly increased compared to wild type cells. This result also agrees with the decreased electrostatic repulsion between ΔtagO cells and hydrophilic substrates. Furthermore, this result reveals that wall teichoic acids do not contribute directly to the adhesion of *S. aureus* to abiotic hydrophilic substrates. At the moment, we are not able to explain the molecular origin of this result. The reason may be that especially the formation of hydrogen bonds, that governs the adhesion to hydrophilic substrates, is influenced by changed electrostatic interactions.

4 Conclusion and outlook

We investigated the adhesion process of *S. aureus* to abiotic substrates by combining AFM single cell force spectroscopy with genetic modification tools and computer simulations of the 'ideal cell' model. That way, we were able to reveal fundamental properties of *S. aureus* adhesion and finally, we might draw a quite complete picture of *S. aureus* adhesion to abiotic surfaces:

On abiotic substrates bacterial adhesion is solely governed by the binding of bacterial surface polymers. The process of contact formation is governed by thermally fluctuating surface proteins, that attach a surface and pull the bacterium into close contact, as has been shown in a preceding study [The2015b]. The snap-in is the more pronounced, the higher the substrate hydrophobicity is.
In this study, we investigated the accomplishment of the adhesion force of *S. aureus* in presence and absence of the hydrophobic interaction. We found that adhesion mechanisms differ markedly depending on the available surface forces.
On hydrophobic substrates, the hydrophobic interaction leads to a fast tethering of a large number of bacterial surface proteins. The result is a high adhesion force and a very stable (in terms of reproducibility) adhesion process. This result nicely corroborates, that the snap-in process, that relies on fast tethering of bacterial surface proteins, predominantly shows up on hydrophobic substrates.
In contrast, on hydrophilic substrates the number of tethering bacterial surface polymers is very low which causes small adhesion forces and strongly fluctuating force/distance curve shapes. However, the binding potential between each polymer and a hydrophilic surface is high compared to hydrophobic substrates. Thus, polymer tethering on hydrophilic substrates relies on the formation of (multiple) hydrogen bonds between bacterial surface polymers and a hydrophilic substrate.

The investigation of adhesion forces of different *S. aureus* mutants on hydrophilic and hydrophobic substrates revealed that i) bacterial surface polymers mediating adhesion differ, at least partially, on both substrates. ii) Covalently bound cell wall proteins largely contribute to the adhesion on hydrophobic substrates and much less on hydrophilic substrates. iii) On hydrophilic substrates, adhesion forces are influenced by the cell surface charge and iv) on the hydrophobic substrates, wall teichoic acids seem to contribute directly to the adhesion of *S. aureus*.

Furthermore, our study may explain the individuality of bacterial cells: Number and nature of bacterial surface polymers define the adhesion capability of an individual bacterial cell. Hence, variations in the surface polymer composition cause bacterial cell individuality.

Finally, the fundamental mechanisms of *S. aureus* adhesion to abiotic surfaces revealed in this study, may be translated to other bacterial species as bacterial adhesion in general relies on the binding of surface polymers. Furthermore, the ideal cell model may be extended to capture the adhesion on biotic, conditioned substrates.

Acknowledgement

This work was supported by the Deutsche Forschungsgemeinschaft (DFG) within the collaborative research center SFB 1027 and the research training group GRK 1276 (N.T.). M.B. was supported by the grant of the German Ministry for Education and Research 01Kl1301B.

References

[Agu2015a] S. Aguayo, N. Donos, D. Spratt, and L. Bozec, *Nanoadhesion of Staphylococcus aureus onto Titanium Implant Surfaces*, Journal of dental research **94** (2015) 1078–1084.

[Agu2015b] S. Aguayo, N. Donos, D. Spratt, and L. Bozec, *Single-bacterium nanomechanics in biomedicine: unravelling the dynamics of bacterial cells*, Nanotechnology **26** (2015) 062001.

[Bea2013a] A. Beaussart, S. El-Kirat-Chatel, P. Herman, D. Alsteens, J. Mahillon, P. Hols, and Y. F. Dufrêne, *Single-cell force spectroscopy of probiotic bacteria*, Biophysical journal **104** (2013) 1886–1892.

[Bea2013b] A. Beaussart, P. Herman, S. El-Kirat-Chatel, P. N. Lipke, S. Kucharíková, P. Van Dijck, and Y. F. Dufrêne, *Single-cell force spectroscopy of the medically important Staphylococcus epidermidis–Candida albicans interaction*, Nanoscale **5** (2013) 10894–10900.

[Bel2008] M. Bellion, L. Santen, H. Mantz, H. Hhl, A. Quinn, A. Nagel, C. Gilow, C. Weitenberg, Y. Schmitt, and K. Jacobs, *Protein adsorption on tailored substrates: long-range forces and conformational changes*, Journal of Physics: Condensed Matter **20** (2008) 404226.

[Bur2013] S. Bur, K. T. Preissner, M. Herrmann, and M. Bischoff, *The Staphylococcus aureus extracellular adherence protein promotes bacterial internalization by keratinocytes independent of fibronectin-binding proteins*, Journal of Investigative Dermatology **133** (2013) 2004–2012.

[Cha2001] A. L. Chamis, G. E. Peterson, C. H. Cabell, G. R. Corey, R. A. Sorrentino, R. A. Greenfield, T. Ryan, L. B. Reller, and V. G. Fowler, *Staphylococcus aureus bacteremia in patients with permanent pacemakers or implantable cardioverter-defibrillators*, Circulation **104** (2001) 1029–1033.

[Dar2004] R. O. Darouiche, *Treatment of infections associated with surgical implants*, New England Journal of Medicine **350** (2004) 1422–1429.

[Duf2015] Y. F. Dufrene, *Sticky microbes: forces in microbial cell adhesion*, Trends in microbiology (2015).

[ElK2014] S. El-Kirat-Chatel, C. D. Boyd, G. A. OToole, and Y. F. Dufrêne, *Single-molecule analysis of Pseudomonas fluorescens footprints*, ACS nano **8** (2014) 1690–1698.

[Goe1990] F. Goetz, *Staphylococcus carnosus: a new host organism for gene cloning and protein production*, Journal of Applied Microbiology **69** (1990) 49S–53S.

[Her2015] P. Herman-Bausier, S. El-Kirat-Chatel, T. J. Foster, J. A. Geoghegan, and Y. F. Dufrêne, *Staphylococcus aureus Fibronectin-Binding Protein A Mediates Cell-Cell Adhesion through Low-Affinity Homophilic Bonds*, mBio **6** (2015) e00413–15.

[Hel2008] J. Helenius, C.-P. Heisenberg, H. E. Gaub, and D. J. Muller, *Single-cell force spectroscopy*, Journal of Cell Science **121** (2008) 1785–1791.

[Her2013] P. Herman, S. El-Kirat-Chatel, A. Beaussart, J. A. Geoghegan, T. Vanzieleghem, T. J. Foster, P. Hols, J. Mahillon, and Y. F. Dufre ne, *Forces driving the attachment of Staphylococcus epidermidis to fibrinogen-coated surfaces*, Langmuir **29** (2013) 13018–13022.

[Her2014] P. Herman, S. El-Kirat-Chatel, A. Beaussart, J. A. Geoghegan, T. J. Foster, and Y. F. Dufrêne, *The binding force of the staphylococcal adhesin SdrG is remarkably strong*, Molecular microbiology **93** (2014) 356–368.

[Hor2010] K. Hori and S. Matsumoto, *Bacterial adhesion: From mechanism to control*, Biochemical Engineering Journal **48** (2010) 424 –434.

[Hal2004] L. Hall-Stoodley, J. W. Costerton, and P. Stoodley, *Bacterial biofilms: from the Natural environment to infectious diseases*, Nat Rev Micro **2** (2004) 95–108.

[Isr2011] J. N. Israelachvili, *Intermolecular and surface forces* (J. N. Israelachvili, Hrsg.), Academic Press, 2011.

[Juc1997] B. Jucker, H. Harms, S. Hug, and A. Zehnder, *Adsorption of bacterial surface polysaccharides on mineral oxides is mediated by hydrogen bonds*, Colloids and Surfaces B: Biointerfaces **9** (1997) 331–343.

[Juc1998] B. A. Jucker, A. J. Zehnder, and H. Harms, *Quantification of polymer interactions in bacterial adhesion*, Environmental science & technology **32** (1998) 2909–2915.

[Kan2009] S. Kang and M. Elimelech, *Bioinspired Single Bacterial Cell Force Spectroscopy*, Langmuir **25** (2009) 9656–9659.

[Lec2001] D. Leckband and J. Israelachvili, *Intermolecular forces in biology*, Quarterly reviews of biophysics **34** (2001) 105–267.

[Les2015] M. Lessel, O. Bäumchen, M. Klos, H. Hähl, R. Fetzer, M. Paulus, R. Seemann, and K. Jacobs, *Self-assembled silane monolayers: an efficient step-by-step recipe for high-quality, low energy surfaces*, Surface and Interface Analysis **47** (2015) 557–564.

[Li2004] B. Li and B. E. Logan, *Bacterial adhesion to glass and metal-oxide surfaces*, Colloids and Surfaces B: Biointerfaces **36** (2004) 81–90.

[Lin2011] D. Linke and A. Goldman (Hrsg.), *Bacterial adhesion*, Springer, 2011.

[Low1998] F. D. Lowy, *Staphylococcus aureus infections*, New England Journal of Medicine **339** (1998) 520–532.

[Low2001] S. K. Lower, M. F. Hochella, and T. J. Beveridge, *Bacterial Recognition of Mineral Surfaces: Nanoscale Interactions Between Shewanella and FeOOH*, Science **292** (2001) 1360–1363.

[Mar1995] J. F. Marko and E. D. Siggia, *Stretching dna*, Macromolecules **28** (1995) 8759–8770.

[Max1986] I. Maxe, C. Ryden, T. Wadström, and K. Rubin, *Specific attachment of Staphylococcus aureus to immobilized fibronectin.*, Infection and immunity **54** (1986) 695–704.

[Mit2008] G. Mitchell, C.-A. Lamontagne, E. Brouillette, G. Grondin, B. G. Talbot, M. Grandbois, and F. Malouin, *Staphylococcus aureus SigB activity promotes a strong fibronectin–bacterium interaction which may sustain host tissue colonization by small-colony variants isolated from cystic fibrosis patients*, Molecular microbiology **70** (2008) 1540–1555.

[Myl2001] E. Mylonakis and S. B. Calderwood, *Infective endocarditis in adults*, New England Journal of Medicine **345** (2001) 1318–1330.

[O'R2004] K. O'Riordan and J. C. Lee, *Staphylococcus aureus capsular polysaccharides*, Clinical microbiology reviews **17** (2004) 218–234.

[Ovc2012] E. S. Ovchinnikova, B. P. Krom, H. J. Busscher, and H. C. van der Mei, *Evaluation of adhesion forces of Staphylococcus aureus along the length of Candida albicans hyphae*, BMC Microbiology **12** (2012).

[Pes1999] A. Peschel, M. Otto, R. W. Jack, H. Kalbacher, G. Jung, and F. Götz, *Inactivation of the dlt Operon in Staphylococcus aureus Confers Sensitivity to Defensins, Protegrins, and Other Antimicrobial Peptides*, Journal of Biological Chemistry **274** (1999) 8405–8410.

[Rub2003] M. Rubinstein and R. H. Colby, *Polymer physics*, OUP Oxford, 2003.

[Sch1982] K. H. Schleifer and U. Fischer, *Description of a New Species of the Genus Staphylococcus: Staphylococcus carnosus*, International Journal of Systematic Bacteriology **32** (1982) 153–156.

[Sul2015] R. M. A. Sullan, J. K. Li, P. J. Crowley, L. J. Brady, and Y. F. Dufrêne, *Binding Forces of Streptococcus mutans P1 Adhesin*, ACS nano **9** (2015) 1448–1460.

[The2014] N. Thewes, P. Loskill, P. Jung, H. Peisker, M. Bischoff, M. Herrmann, and K. Jacobs, *Hydrophobic interaction governs unspecific adhesion of staphylococci: a single cell force spectroscopy study*, Beilstein journal of nanotechnology **5** (2014) 1501–1512.

[The2015a] N. Thewes, P. Loskill, C. Spengler, S. Hümbert, M. Bischoff, and K. Jacobs, *A detailed guideline for the fabrication of single bacterial probes used for atomic force spectroscopy*, The European Physical Journal E **38** (2015) 1–9.

[The2015b] N. Thewes, A. Thewes, P. Loskill, H. Peisker, M. Bischoff, M. Herrmann, L. Santen, and K. Jacobs, *Stochastic binding of Staphylococcus aureus to hydrophobic surfaces*, Soft matter **11** (2015) 8913–8919.

[Van2015] T. Vanzieleghem, P. Herman-Bausier, Y. F. Dufrene, and J. Mahillon, *Staphylococcus epidermidis Affinity for Fibrinogen-Coated Surfaces Correlates with the Abundance of the SdrG Adhesin on the Cell Surface*, Langmuir **31** (2015) 4713–4721.

[VanOss2006] C. J. Van Oss, *Interfacial forces in aqueous media*, CRC press, 2006.

[Wei2005] C. Weidenmaier, A. Peschel, Y.-Q. Xiong, S. A. Kristian, K. Dietz, M. R. Yeaman, and A. S. Bayer, *Lack of wall teichoic acids in Staphylococcus aureus leads to reduced interactions with endothelial cells*

and to attenuated virulence in a rabbit model of endocarditis, Journal of infectious diseases **191** (2005) 1771–1777.

[Wei2008] C. Weidenmaier, J. F. Kokai-Kun, E. Kulauzovic, T. Kohler, G. Thumm, H. Stoll, F. Götz, and A. Peschel, *Differential roles of sortase-anchored surface proteins and wall teichoic acid in Staphylococcus aureus nasal colonization*, International Journal of Medical Microbiology **298** (2008) 505–513.

[Wil1983] B. J. Wilkinson, *Staphylococcal capsules and slime*, Staphylococci and staphylococcal infections **2** (1983) 481–523.

[Yon2007] R. Yongsunthon, V. G. Fowler, B. H. Lower, F. P. Vellano, E. Alexander, L. B. Reller, G. R. Corey, and S. K. Lower, *Correlation between fundamental binding forces and clinical prognosis of Staphylococcus aureus infections of medical implants*, Langmuir **23** (2007) 2289–2292.

[Zen2014] G. Zeng, T. Mu ller, and R. L. Meyer, *Single-cell force spectroscopy of bacteria enabled by naturally derived proteins*, Langmuir **30** (2014) 4019–4025.

Addendum VI - Direct measurement of the contact radius of cocci bacteria

Authors: C. Spengler[1], N. Thewes[1] A. Thewes[2], and K. Jacobs[1]

[1] Department of Experimental Physics, Saarland University, 66041 Saarbrücken, Germany.
[2] Department of Theoretical Physics, Saarland University, 66041 Saarbrücken, Germany

in preparation

Author contributions:
C. Spengler and N. Thewes contributed equally to this work. Experiments were conceived and designed by N. Thewes, C. Spengler. AFM experiments and substrate preparation were performed by C. Spengler. Simulations were performed by N. Thewes. Simulations were directed by A. Thewes. Data was analyzed by N. Thewes and C. Spengler. The manuscript was written by N. Thewes, C. Spengler and K. Jacobs. Research was directed by K. Jacobs.

Abstract - Bacterial adhesion is a crucial step during the formation of biofilms. Fundamental research of bacterial adhesion mechanisms is, hence, of utmost importance. In this study, we present a single cell force spectroscopy-based method to investigate the contact area between single bacterial cells and a solid substrates. The technique relies on the strong influence of the hydrophobic interaction on bacterial adhesion: By crossing a very sharp hydrophilic/hydrophobic edge while performing force/distance curves with a single bacterial probe, a direct measurement of the bacterial contact radius is possible. In this study, we present a 'proof of concept' by showing that we are able to measure the contact radius of single *Staphylococcus carnosus* cells.

1 Introduction

Bacterial adhesion to solid substrates is of utmost importance concerning the formation of biofilms [Cos1999, Hal2004, Shi2009]. A fundamental understanding of the bacterial adhesion process can help to control or prevent the attachment of bacterial cells [Hor2010]. AFM force spectroscopy with bacterial probes lead to an unprecedented expansion of the knowledge of bacterial adhesion mechanisms [Agu2015, Duf2015]. Most AFM studies concentrate on bacterial adhesion properties like adhesion forces, rupture length or protein mechanics [Ovc2012, Zen2015, Hei2015]. All these publications, however, lack the information about the extent of the contact area between bacterial cells and a substrate. This gap will be filled by our study.
Typical cocci species like *Staphylococci* exhibit a cell diameter of roughly 1 μm. Hence, investigating the bacterial contact area by classical optical microscopy is challenging. Therefore, contact mechanical modeling was the only way to investigate the contact area of bacterial cells. However, bacterial adhesion to substrates is governed by the binding of bacterial surface polymers [The2014, The2015b, Her2015]. Hence, classical contact models, like the *Hertz model*, are most likely not appropriate to model the complex adhesion mechanics of a bacterial cell [Her1882, Mau1992, Bar2008]. A promising modeling approach was developed by Chen et al., however also this model does not consider the complexity of the bacterial adhesion process [Che2012].

In this study, we introduce an atomic force microscopy (AFM) based technique to measure the contact radius of spherical bacterial by using single bacterial probes [The2015a].
The *conditio sine qua non* of our method is that the bacterial cell to be probed adheres much stronger to a material B than to a material A and that the transition zone between material A and B is sufficiently sharp (and exhibits a negligible height difference).
On a straight pathway crossing the transition zone, subsequent force/distance curves recorded by AFM, such that the contact zone of the bacterial cell gradually probes first only material A, then variable parts of both materials and finally only material B, enable for the evaluation of the contact zone.
Bacterial cells, such as *Staphylococcus carnosus*, bind much stronger to hydrophobic than to hydrophilic substrates [Bea2013a, The2014, The2015b]. This is a consequence of the excessive binding of bacterial surface proteins on hydrophobic substrates via the hydrophobic interaction [VanOss2006, Bea2013a, The2014, The2015b]. In contrast, on hydrophilic substrates, macromolecular tethering is much less likely. Thus, in the case of bacteria, material A is a hydrophilic and material B a hydrophobic surface.

We prepared a substrate with a sharp transition (width of transition zone less than 20 nm) between a strong hydrophobic and very hydrophilic surface and performed single cell force spectroscopy experiments with consecutive force/distance curves on slightly varying positions while crossing the hydrophilic/hydrophobic transition zone. The experimental procedure will cause the behavior sketched in fig. 1: Almost no binding will occur on the hydrophilic surface resulting in small adhesion forces as well as small adhesion energies. By approaching the hydrophobicity transition zone, first macromolecules reaching the surface on the hydrophobic part, likely attach the surface. This causes an increase in adhesion force and energy. In the following, the larger the part of the cell body is that is placed above the hydrophobic part of the surface, the more macromolecules attach and the stronger is the adhesion. Adhesion force and energy reach a plateau value if the whole contact area, that means all macromolecules reaching the bottom, are positioned over the hydrophobic surface.

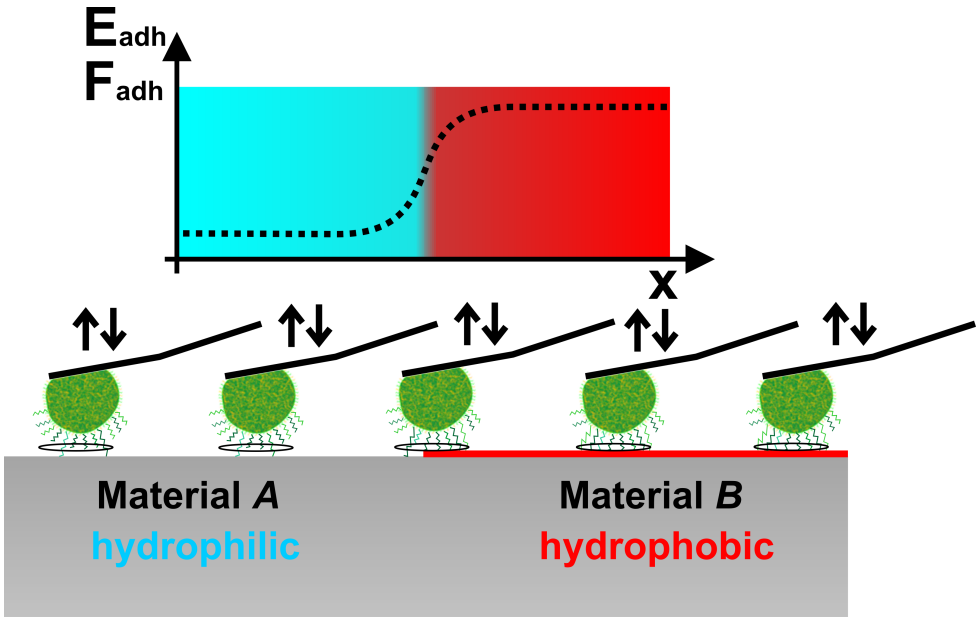

Figure 1: Illustration of the experimental setup to measure the contact radius of a spherical bacterial cell. The contact area is indicated by the black circle. A substrate with an extremely sharp transition zone between a very hydrophilic and a strongly hydrophobic surface is produced. Consecutive force/distance measurements with single bacterial probes on slightly varying x-positions enable for the investigation of the bacterial contact radius. Adhesion on the hydrophilic surface is weak due to a low number of tethering macromolecules, the higher the portion of the cell above the hydrophobic surface is, the more macromolecules (proteins) bind to the surface and the higher is the measured adhesion strength. Adhesion reaches a maximum, as soon as the entire contact area is positioned above the hydrophobic surface. Finally, the progression of adhesion force and energy is a function of the bacterial 'interaction radius'.

By plotting adhesion forces or adhesion energies against the horizontal position of bacterial probe the radius of the contact zone or rather, of the 'interaction zone' can be evaluated.

To deepen the understanding of the experimental results, we modeled the experimental approach. Thereby, a bacterial cell is assumed to be an inelastic sphere that is covered with elastic polymers. The polymers represent bacterial surface macromolecules that enable for the adhesion on substrates. The interaction between bacterial surface polymers and substrates is modeled via square potentials. Subsequently, the experimental procedure is modeled by simulating force/distance curves for a bacterial cell that crosses the transition between two surfaces with different polymer/surface interactions.

2 Experimental

2.1 Bacteria and bacterial probes

For the experiments, freshly prepared *Staphylococcus carnosus* (strain TM300) cells in exponential growth phase were used [Sch1982, Goe1990]. The bacteria were cultured on blood agar plates. The day before each experiment one colony was transferred into 5 ml TSB medium and cultured at 37 °C overnight. Before the experiments, 40 µl of the overnight culture were transferred into 4 ml of fresh TSB medium and cultured for another 2.5 hours. Then, bacteria were washed three times using phosphate buffered saline (PBS, pH 7.3, ionic strength 0.1728 mol/l at 20 °C) to remove extracellular material. Subsequently, a single bacterial cell was attached to a polydopamin coated tipless AFM cantilever (MLCT-0 from Bruker-Nano, nominal spring constant of 0.03 N/m) using a micromanipulator (Narishige Group, Tokyo, Japan) according to a protocol published elsewhere [The2015a].

2.2 Substrate preparation

Silicon (Si) wafers (Siltronic AG, Burghausen, Germany) with a native oxide layer (d=1.7(2) nm) were partially covered with a self-assembling monolayer of CH_3-terminated octadecyltrichlorosilane molecules (OTS, Sigma-Aldrich, St. Louis, MO, USA) in the following way:
An area of the wafer was masked with a thin polymer film exhibiting a very distinct edge. Then, the uncovered area of the wafer was silanized according to a standard protocol [Les2015]. Subsequently, the polymer film was removed by thoroughly rinsing the wafer with another solvent (e. g. toluene, chloroform).

2.3 Measuring procedure and data fitting

We investigated the quality of the hydrophilic/hydrophobic edge, by scanning the wafer surfaces with an atomic force mircoscope (Bioscope Catalyst, Bruker-Nano, Santa Barbara, CA) using

different scan sizes and PeakForce QNM mode^{TM}. The surface hydrophobicities were studied by water contact angle measurements using a costume-made setup.

Subsequently, to reveal the interaction radius of single bacterial cells, force/distance curves were recorded in PBS at room temperature using a Bioscope Catalyst and single bacterial probes of *S. carnosus* cells. In the first step, the surface was covered with approx. 8 ml of PBS and placed under the AFM in such a way that the interface between bare silicon and OTS was in the middle of the scan area. Then, the cantilever holder for measurements in liquid was mounted on the AFM and the cantilever carrying a single bacterial probe was approached towards the surface. Subsequently, consecutive force/distance curves were recorded starting on the hydrophilic surface. The x-position of the cantilever (i.e. the bacterium) was changed by 10 nm in between each two force/distance curves and force measurements were carried out until the whole bacterium was placed above the hydrophobic substrate. At every position, one force/distance curve with a ramp size of 800 nm and a ramp velocity of 800 nm/s was recorded. In one passage, 200 force/distance curves were recorded, hence, the total movement in x-direction was 2 µm. To guarantee for high lateral precision, the cantilever must not be withdrawn during this procedure.

For each force/distance curve, adhesion force as well as adhesion energy were calculated as described before [The2015a]. These values were plotted against the x-position of the bacterial probe and fitted using function 1. Fitting procedure was implemented with a Matlab script (MathWorks, Natick, MA, USA) using a non-linear least square fit with a trust-region algorithm.

$$F_{fit}(x) = \begin{cases} F_{min} \quad \textbf{for } x \leq x_0 - r \\ \left(r^2 \cdot \arccos\left(1 - \frac{r+(x-x_0)}{r}\right) - (x-x_0) \cdot \sqrt{2 \cdot r \cdot (r+(x-x_0)) - (r+(x-x_0))^2}\right) \cdot \frac{F_{max}-F_{min}}{r^2} \\ +F_{min} \quad \textbf{for } x_0 - r < x \leq x_0 \\ \left(\pi \cdot r^2 - \left(r^2 \cdot \arccos\left(1 - \frac{r-(x-x_0)}{r}\right) - (-(x-x_0)) \cdot \sqrt{2 \cdot r \cdot (r-(x-x_0)) - (r-(x-x_0))^2}\right)\right) \cdot \frac{F_{max}-F_{min}}{r^2} \\ +F_{min} \quad \textbf{for } x_0 < x \leq x_0 + r \\ F_{max} \quad \textbf{for } x > x_0 + r \end{cases} \tag{1}$$

The fundamental idea of equation 1 is a circle of radius r crossing a straight line (in the experiment represented by the transition between bare Si and OTS) at position x_0 in positive x-direction. The function gives the fraction of the circular area that has crossed the line as a function of the movement x. Thereby, the fraction of the area before crossing the line is weighted with F_{min}, whereas the fraction after crossing the line is weighted with F_{max}.

The fitting parameters are the minimal force of adhesion F_{min} (present on the hydrophilic Si surface), the maximum adhesion force F_{max} (on the hydrophobic OTS surface), the position of the interface x_0 and the radius r of the interaction area (that is assumed to be circular).

To account for the exact orientation of the hydrophilic/hydrophobic transition zone, we performed the described procedure two times (i.e. the hydrophilic/hydrophobic edge was crossed two times), while the pathway in both series were perpendicular to each other, see fig. 2. If the bacterial cell crosses the transition by an angle θ, the measured interaction radius is larger than the 'real' radius. Using the values of two series, r_1 and r_2 (with $\theta_1 + \theta_2 = 90°$), it is $\tan(\theta_1) = r_1/r_2$ and

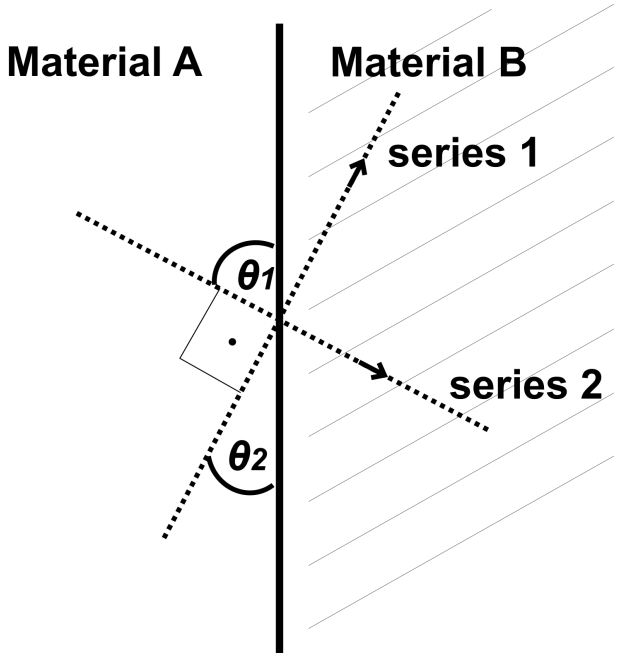

Figure 2: Sketch of the experimental procedure. Two series of measurements are performed perpendicular to each other. The angles θ_1 and θ_2 depict the angle between each pathway and the hydrophilic/hydrophobic transition.

the 'real' radius r_0 of the bacterial interaction area then reads to $r_0 = r_1/\sin(\theta_1)$. Note that these calculations base on an assumed circular-shaped interaction area.

3 Results and Discussion

3.1 The hydrophilic/hydrophobic substrate

AFM images of the Si based substrate revealed a transition zone of 30 nm between the hydrophilic and the hydrophobic part of the substrate, see fig. 3C. By taking into account that the AFM tip used to scan the surface (scanasyst-air, Bruker-Nano, Santa Barbara, CA) has a nominal radius of 2 nm and a maximum radius of 12 nm, the transition zone features a 'real' width d of less than 26 nm. The difference in height between the lower hydrophilic and the higher hydrophobic part was 1.8 nm. Water contact angle measurements revealed an advancing water contact angle of 112(3)° on the hydrophobic part of the surface and 8(2)° on the hydrophilic part. Surface roughness (rms) was determined to 0.09(2) nm on the Si surface and 0.12(2) nm on the OTS surface, thus the 'half and half' wafer features the same surface characteristics as a native Si wafer or a fully covered OTS wafer [Les2015]. The hydrophilic/hydrophobic transition zone is straight on length scales of 10 µm, see fig 3A. Figure 3B shows a 1x1 µm scan of the edge, representing the 'view' of a *S. carnosus* cell, that features a typical cell diameter of 1 µm.
In the transition zone, the surface hydrophobicity may not rise to its maximum (OTS) value

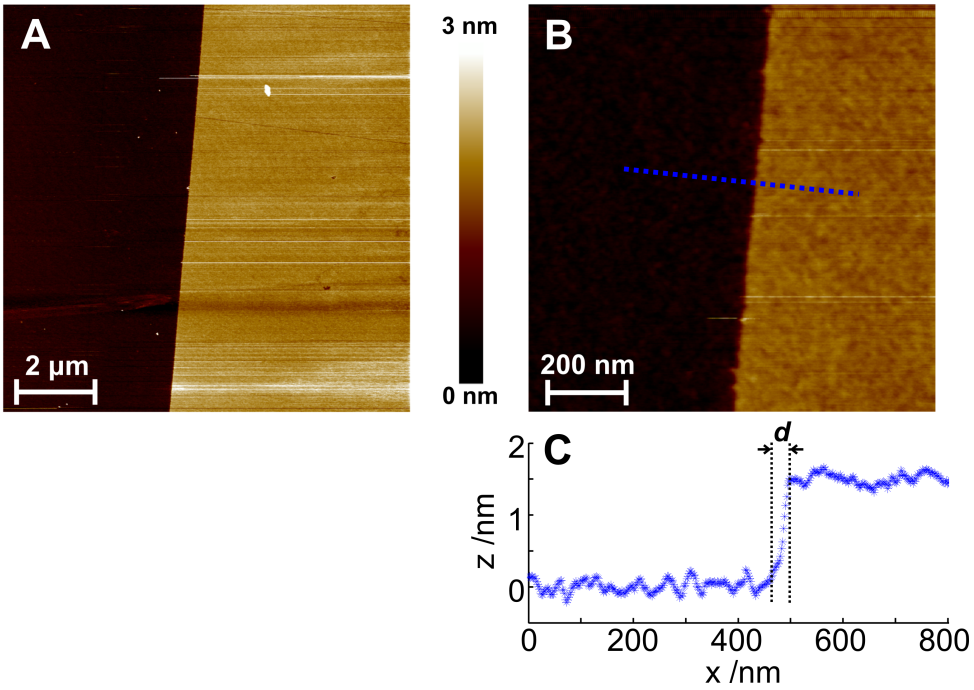

Figure 3: AFM images of the hydrophilic/hydrophobic transition zone taken with PeakForce QNM mode^{TM}. Images were recorded with a scan size of 10 µm and a scan rate of 0.33 Hz A) as well as 1 µm and 0.65 Hz B). C) Scan line perpendicular to the hydrophilic/hydrophobic edge indicating the width of the transition zone $d \approx 26$ nm.

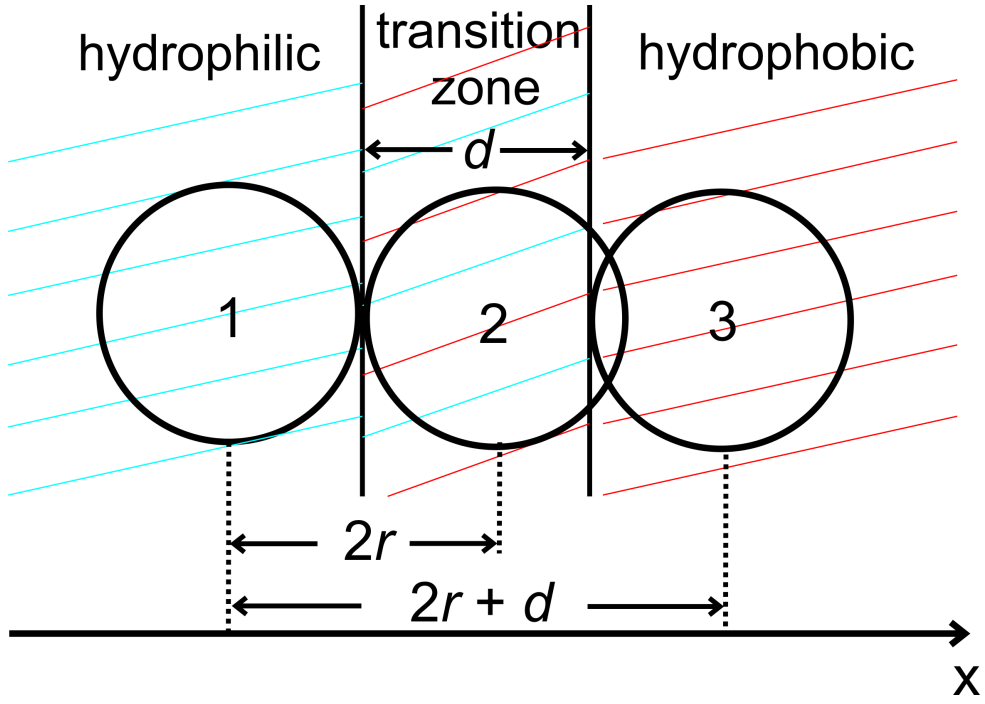

Figure 4: Sketch to illustrate the influence of the width d of the transition zone on the measurement of the bacterial contact radius r. The circles denote different position of the bacterial contact area while crossing the hydrophilic/hydrophobic transition zone. Transition zone and bacterial contact area are not to scale.

instantaneously. Rather, intermediate hydrophobicities might be present. Therefore, the width of the transition zone may lead to an overestimation of the bacterial interaction radius, see fig. 4: The adhesion force of a bacterium with a contact radius r that crosses the hydrophilic/hydrophobic transition zone starts to rise as soon as its contact area hits the transition zone (circle 1). After the contact area (respectively the bacterium) was moved by a distance of $2r$, the bacterium does not touch the hydrophilic part of the substrate anymore (circle 2). However, because the surface hydrophobicity may not reach its maximum yet (due to the transition zone), further movement of the bacterium in x direction may results in a further increase of the adhesion force. The adhesion force reaches its maximum as soon as the entire bacterial contact area probes only the hydrophobic part of the substrate (circle 3), i.e. after a distance of $2r + d$ (circle 3 relative to circle 1). This distance reflects the diameter of the bacterial contact area measured according to our method. Hence, the radius of the bacterial contact area may be overestimated by half of the width of the transition zone (up to 13 nm in our case).

3.2 Direct investigation of the bacterial interaction zone

Figure 5A depicts a typical measurement of adhesion forces against x-position of a bacterial probe during the transition from the hydrophilic to the hydrophobic substrate area. Adhesion forces clearly show the expected trend: Almost no adhesion occurs on the hydrophilic part of the sub-

strate, then adhesion forces rise while the bacterial cell crosses the hydrophilic/hydrophobic transition zone and reach a saturation value as soon as the cell only probes the hydrophobic part of the surface. Thereby, on hydrophobic substrates adhesion forces are roughly an order of magnitude higher compared to the ones on hydrophilic substrates [Bea2013a, The2014, ElK2015].
For every bacterial probe, the hydrophilic/hydrophobic transition zone was crossed two times on pathways that are perpendicular to each other. *S. carnosus* features robust adhesion mechanisms that withstand multiple adhesion events probed by AFM force spectroscopy [The2014]. Nevertheless, if adhesion forces changed significantly between the first and the second pathway, the respective bacterial probe was discarded.
The interaction radii (r_1 and r_2) determined for each of the two pathways vary depending on the exact orientation of the hydrophilic/hydrophobic transition (i.e. on θ_1 and θ_2, see fig. 2). However, according to describes procedure, we are able to calculate the 'real' contact radius r_0 of a single bacterial cell.
Figure 5B shows the interaction radii of nine different bacterial cells. The values were calculated by using adhesion force data as well as adhesion energy values. The errors of the radii are defined by the 95% confident interval of the respective fit. Note that all radii might be overestimated by up to 13 nm as described in the preceding paragraph.

We find interaction radii that differ strongly between different cells. This in accordance with results concerning adhesion force measurements, that revealed an individual adhesion behavior of bacterial cells [Bea2013b, The2014, Van2015]. Different adhesion behavior were attributed to differences in amount and nature of bacterial surface polymers [The2014]. The same explanation may be applied to explain the varying interaction radii of bacterial cell. Thus, our results match the general assumption, that bacterial adhesion is mediated solely by bacterial surface polymers.
A comparison between the contact radius values determined using adhesion forces and adhesion energies reveals two possible outcomes within the experimental error: i) The interaction radii are equal, ii) the contact radius defined by the adhesion energy exceeds the radius of the adhesion force. Both cases may be understood in terms of the polymeric nature of bacterial adhesion: In case i) the bacterial surface polymers that contribute to the overall adhesion force contribute equally to the adhesion energy. In the second case, bacterial surface polymers exist, that contribute to the adhesion energy, but not to the adhesion force. This can be explained by some long or very soft polymers that start contributing to the overall force between bacterium and surface after the maximum force value (taken as adhesion force) was reached.
The measured contact radii exhibit values between 20 nm and 300 nm. Thus, the contact radii determined with our method are in the same range as compared to values according to the 'elastic deformation model' [Che2012].

4 Simulation

Bacterial adhesion is based on the binding of surface macromolecules [Hor2010, Bea2013a, The2014, The2015b]. Hence, a simple, but reasonable model treats a bacterium as a sphere covered by ideal polymers [The2014, The2015b]. In this model, the potential energy of the polymers is calculated according to the worm-like chain model above a certain threshold and according to an entropic

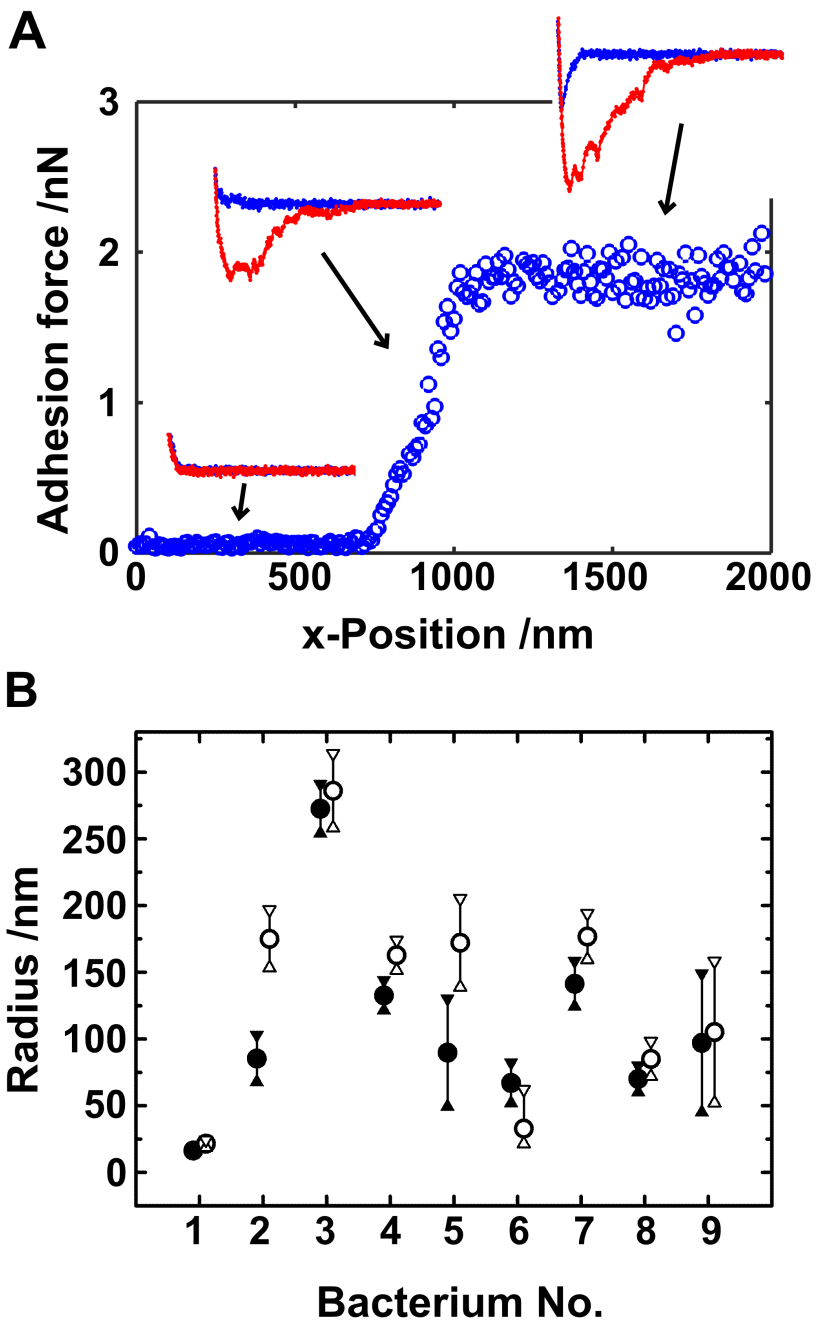

Figure 5: A) Adhesion forces as function of position crossing the hydrophilic/hydrophobic transition zone. Insets depict representative force/distance curves (blue: approach part, red: retraction part). B) Interaction radii of nine different bacterial cells calculated using adhesion forces (closed symbols) and adhesion energies (open symbols). The error bars of the radii depict the limits of the 95% confidence bands of the fits. Note that all radii might be overestimated by up to 13 nm.

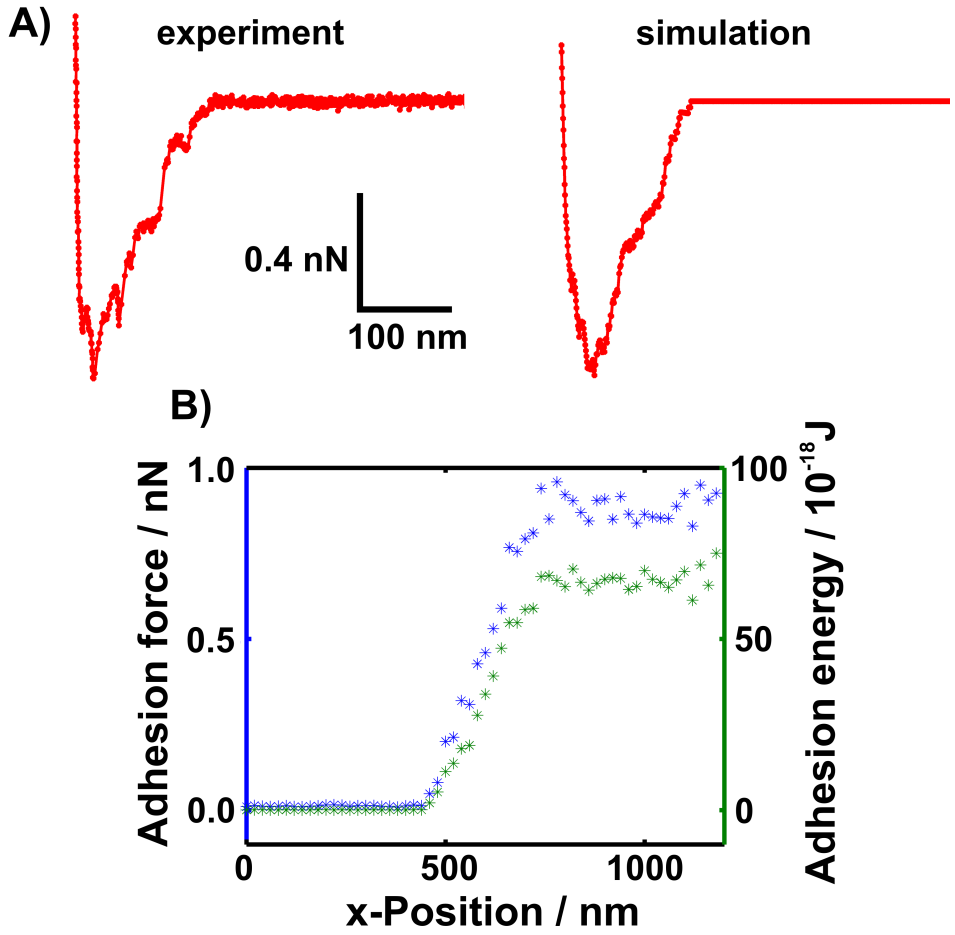

Figure 6: Experimental procedure adapted in numerical simulations. Comparison between an exemplary experimental and simulated force/distance curve A). Progression of adhesion forces and energies of simulated force/distance curves during the transition from low to high adhesion area B).

spring below [Mar1995, Rub2003]. The threshold length accounts for the spatial expansion of polymers and is, in our model, taken as twice the radius of gyration of an ideal linear polymer. The polymers can bind to a surface in close proximity via a square potential. To reproduce the experimental situation, different adhesion forces are incorporated by two different depths of the square potential. In the simulation, the transition between low and high adhesion area is assumed to change instantaneously. The model is analyzed using a Monte Carlo algorithm.

In order to understand the experimental results in more detail, we tried to remodel the experimental approach for one specific cell. Figure 6A shows a comparison between an experimental and a simulated force/distance curve. Our model is able to reproduce the basic shape of the experimental force/distance curves as well as the fundamental magnitudes adhesion force and rupture length. We used the configuration of the simulated force/distance curve in fig. 6A to adapt the experimental procedure and simulate force/distance curves for a bacterium that crosses a transition between an

area with low and high adhesion forces, see fig. 6B.

By fitting eq. 1 to the progression of the adhesion forces of the simulated force/distance curves we find an interaction radius of 151(12) nm for the simulated bacterial cell. The corresponding real cell to the mimicked force/distance curves exhibited an interactions radius of only 90 nm (bacterium number 9 in fig. 5B). In the simulation, the bacterial surface polymers are equally distributed on the cell surface. Hence, a possible explanation for the difference between experiment and simulation is, that in the natural system adhesion polymers are not equally distributed. This could mean, that the bacterial surface polymers form cluster on the cell wall. Cluster formation of surface adhesins has been described for different microbial organisms [Dup2010]. This could also account for the very small interaction radius of cell no. 1 in the experimental data, see fig. 5B.

5 Conclusion and Outlook

Our study describes a method to determine the interaction radius of a single bacterial cell. We find large differences between different, individual bacterial cells, even of one and the same culture. We attribute the differences to individual properties (spatial distribution, mechanical properties, density) of bacterial surface polymers. However, the interpretation of the experimental results is not straightforward, in general. Also, the experimental setup needs further improvement. For instance, the angle of the hydrophilic/hydrophobic transition zone should be adjusted in a controlled manner. That way, the assumption of a circular shaped interaction radius (that might not be a hundred percent true for bacterial cells) would be obsolete and, furthermore, by turning the hydrophilic/hydrophobic edge relative to the bacterial cell, the interaction zone could be gauged in different directions. Finally, by performing further measurements accompanied by computer simulations, our technique can open a window into the molecular world of bacterial surface contact.

References

[Agu2015] S. Aguayo, N. Donos, D. Spratt, and L. Bozec, *Single-bacterium nanomechanics in biomedicine: unravelling the dynamics of bacterial cells*, Nanotechnology **26** (2015) 062001.

[Bar2008] E. Barthel, *Adhesive elastic contacts: JKR and more*, Journal of Physics D: Applied Physics **41** (2008) 163001.

[Bea2013a] A. Beaussart, S. El-Kirat-Chatel, P. Herman, D. Alsteens, J. Mahillon, P. Hols, and Y. F. Dufrêne, *Single-cell force spectroscopy of probiotic bacteria*, Biophysical journal **104** (2013) 1886–1892.

[Bea2013b] A. Beaussart, P. Herman, S. El-Kirat-Chatel, P. N. Lipke, S. Kucharíková, P. Van Dijck, and Y. F. Dufrêne, *Single-cell force spectroscopy of the medically important Staphylococcus epidermidis–Candida albicans interaction*, Nanoscale **5** (2013) 10894–10900.

[Che2012] Y. Chen, W. Norde, H. C. van der Mei, and H. J. Busscher, *Bacterial Cell Surface Deformation under External Loading*, mBio **3** (2012) 00378–12.

[Cos1999] J. W. Costerton, P. S. Stewart, and E. P. Greenberg, *Bacterial Biofilms: A Common Cause of Persistent Infections*, Science **284** (1999) 1318–1322.

[Duf2015] Y. F. Dufrene, *Sticky microbes: forces in microbial cell adhesion*, Trends in microbiology (2015).

[Dup2010] V. Dupres, D. Alsteens, G. Andre, and Y. F. Dufrne, *Microbial nanoscopy: a closer look at microbial cell surfaces*, Trends in Microbiology **18** (2010) 397 –405.

[ElK2015] S. El-Kirat-Chatel, A. Beaussart, S. Derclaye, D. Alsteens, S. Kucharikova, P. Van Dijck, and Y. F. Dufrêne, *Force nanoscopy of hydrophobic interactions in the fungal pathogen Candida glabrata*, ACS nano **9** (2015) 1648–1655.

[Goe1990] F. Goetz, *Staphylococcus carnosus: a new host organism for gene cloning and protein production*, Journal of Applied Microbiology **69** (1990) 49S–53S.

[Her2015] P. Herman-Bausier, S. El-Kirat-Chatel, T. J. Foster, J. A. Geoghegan, and Y. F. Dufrêne, *Staphylococcus aureus Fibronectin-Binding Protein A Mediates Cell-Cell Adhesion through Low-Affinity Homophilic Bonds*, mBio **6** (2015) e00413–15.

[Hei2015] K. P. Heim, R. M. A. Sullan, P. J. Crowley, S. El-Kirat-Chatel, A. Beaussart, W. Tang, R. Besingi, Y. F. Dufrene, and L. J. Brady, *Identification of a Supramolecular Functional Architecture of Streptococcus mutans Adhesin P1 on the Bacterial Cell Surface*, Journal of Biological Chemistry **290** (2015) 9002–9019.

[Her1882] H. H. Hertz, *ber die Berhrung fester elastischer Krper*, Journal fr die reine und angewandte Mathematik (1882).

[Hor2010] K. Hori and S. Matsumoto, *Bacterial adhesion: From mechanism to control*, Biochemical Engineering Journal **48** (2010) 424 –434.

[Hal2004] L. Hall-Stoodley, J. W. Costerton, and P. Stoodley, *Bacterial biofilms: from the Natural environment to infectious diseases*, Nat Rev Micro **2** (2004) 95–108.

[Les2015] M. Lessel, O. Bäumchen, M. Klos, H. Hähl, R. Fetzer, M. Paulus, R. Seemann, and K. Jacobs, *Self-assembled silane monolayers: an efficient step-by-step recipe for high-quality, low energy surfaces*, Surface and Interface Analysis **47** (2015) 557–564.

[Mar1995] J. F. Marko and E. D. Siggia, *Stretching dna*, Macromolecules **28** (1995) 8759–8770.

[Mau1992] D. Maugis, *Adhesion of spheres: the JKR-DMT transition using a Dugdale model*, Journal of colloid and interface science **150** (1992) 243–269.

[Ovc2012] E. S. Ovchinnikova, B. P. Krom, H. J. Busscher, and H. C. van der Mei, *Evaluation of adhesion forces of Staphylococcus aureus along the length of Candida albicans hyphae*, BMC Microbiology **12** (2012).

[Rub2003] M. Rubinstein and R. H. Colby, *Polymer physics*, OUP Oxford, 2003.

[Sch1982] K. H. Schleifer and U. Fischer, *Description of a New Species of the Genus Staphylococcus: Staphylococcus carnosus*, International Journal of Systematic Bacteriology **32** (1982) 153–156.

[Shi2009] X. Shi and X. Zhu, *Biofilm formation and food safety in food industries*, Trends in Food Science & Technology **20** (2009) 407–413.

[The2014] N. Thewes, P. Loskill, P. Jung, H. Peisker, M. Bischoff, M. Herrmann, and K. Jacobs, *Hydrophobic interaction governs unspecific adhesion of staphylococci: a single cell force spectroscopy study*, Beilstein journal of nanotechnology **5** (2014) 1501–1512.

[The2015a] N. Thewes, P. Loskill, C. Spengler, S. Hümbert, M. Bischoff, and K. Jacobs, *A detailed guideline for the fabrication of single bacterial probes used for atomic force spectroscopy*, The European Physical Journal E **38** (2015) 1–9.

[The2015b] N. Thewes, A. Thewes, P. Loskill, H. Peisker, M. Bischoff, M. Herrmann, L. Santen, and K. Jacobs, *Stochastic binding of Staphylococcus aureus to hydrophobic surfaces*, Soft matter **11** (2015) 8913–8919.

[Van2015] T. Vanzieleghem, P. Herman-Bausier, Y. F. Dufrene, and J. Mahillon, *Staphylococcus epidermidis Affinity for Fibrinogen-Coated Surfaces Correlates with the Abundance of the SdrG Adhesin on the Cell Surface*, Langmuir **31** (2015) 4713–4721.

[VanOss2006] C. J. Van Oss, *Interfacial forces in aqueous media*, CRC press, 2006.

[Zen2015] G. Zeng, R. Ogaki, and R. L. Meyer, *Non-proteinaceous bacterial adhesins challenge the antifouling properties of polymer brush coatings*, Acta biomaterialia (2015).

Erklärung

Hiermit versichere ich an Eides statt, dass ich die vorliegende Arbeit selbstständig und ohne Benutzung anderer als der angegebenen Hilfsmittel angefertigt habe. Die aus anderen Quellen oder indirekt übernommenen Daten und Konzepte sind unter Angabe der Quelle gekennzeichnet. Die Arbeit wurde bisher weder im In- noch im Ausland in gleicher oder ähnlicher Form in einem Verfahren zur Erlangung eines akademischen Grades vorgelegt.

Saarbrücken, den 24. März 2016

Nicolas Thewes